Metalloproteins Containing Cytochrome, Iron-sulfur or Copper Redox Centers

Jing Liu,[†,||] Saumen Chakraborty,[†,||] Parisa Hosseinzadeh, [‡,||] Yang Yu,[§, ||]
Shiliang Tian,[†] Igor Petrik,[†] Ambika Bhagi[†] and Yi Lu[†,‡,§,*]
[†]*Department of Chemistry,* [‡]*Biochemistry, and* [§]*Center for Biophysics and Computational Biology, University of Illinois at Urbana-Champaign, Urbana, IL 61801*

Contents

1. Introduction

Redox reactions play important roles in almost all biological processes, including photosynthesis and respiration, which are two essential energy processes that sustain all life on Earth. It is thus not surprising that biology employs redox-active metal ions in these processes. It is largely the redox activity that makes metal ions uniquely qualified as biological cofactors and makes bioinorganic enzymology both fun to explore and challenging to study.

Even though most metal ions are redox active, biology employs a surprisingly limited number of them for electron transfer (ET) processes. Prominent members of redox centers involved in ET processes include cytochromes, iron-sulfur clusters, and cupredoxins. Together these centers cover the whole range of reduction potentials in biology (Figure 1). Because of their importance, general reviews about redox centers,[1-77] and specific reviews about cytochrome,[8,24,78-90] iron-sulfur proteins,[91-93] and cupredoxins[94-104] have appeared in the literature. In this review, we provide classification and description of each member of the above redox centers, including both native and designed proteins, as well as those proteins that contain a combination of these redox centers. Through this review, we examine structural features responsible for their redox properties, including knowledge gained from recent progress in fine-tuning the redox centers. Computational studies like DFT calculations become more

and more important in understanding the structure-function relationship, and facilitating the fine-tuning of the electron transfer properties and reduction potentials of metallocofactors in proteins. Since this aspect has been reviewed extensively before,[105-110] and by other reviews in this theme issue, it will not be covered here.

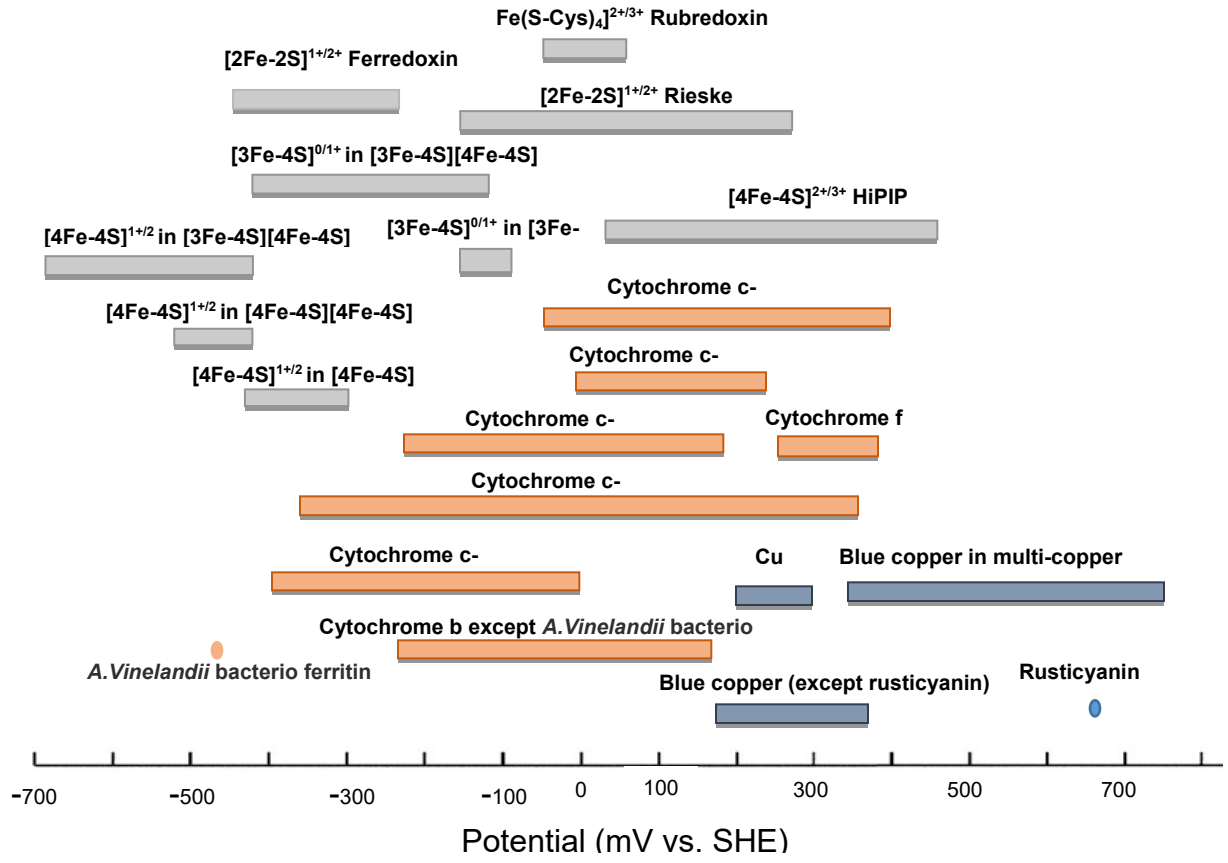

Figure 1. Reduction potential range of redox centers in electron transfer processes.

2. Cytochromes in Electron Transfer Processes

2.1. Introduction to Cytochromes

Cytochromes (cyts) are a major class of heme-containing electron transfer (ET) proteins found ubiquitously in biology. They were first described in 1884 as respiratory pigments (called myohematin or histohematin) to explain colored substances in cells.[81,111] These colored substances were later rediscovered in 1920, and named as "cytochromes," or cellular pigments.[112] The intense red color combined with relatively

high thermodynamic stability makes cyts easy to observe and to purify. As of today, more than 70,000 cytochromes have been discovered.[78] In addition, due to their small size, high solubility, well-folded helical structure, and the presence of the heme chromophore, cyts are one of the most extensively studied class of proteins spanning several decades.[79]

Cytochromes are present mostly in the inner mitochondrial membrane of eukaryotic organisms, and are also found in a wide variety of both Gram-positive and Gram-negative bacteria.[113,114] Cytochromes play crucial roles in a number of biological ET processes associated with many different energy metabolisms. Additionally, cyts are involved in apoptosis in mammalian cells.[115] Further description of the latter role of cyts is beyond the scope of this review, which is solely on the role of cyts in electron transfer. For a similar reason, another family of cytochromes, the cyts P450 (CYP), which catalyze the oxidation of various organic substrates such as metabolites (lipids, hormones etc.) and xenobiotic substances (drugs, toxic chemicals) will not be covered in this review, either.

A number of books and reviews have appeared in the literature describing cytochromes as ET proteins.[8,24,78-90] Here we summarize studies on both native and designed cytochromes and their roles in biological ET processes.

2.2. Classification of Cytochromes

Cytochromes are classified based on the electronic absorption maxima of the heme macrocycle, such as *a, b, c, d, f,* and *o*. More specifically, these letter names represent characteristic absorbance maxima in the UV-visible electronic absorption spectrum when the heme iron is coordinated with pyridine in its reduced (ferrous) state, designated as the “pyridine hemochrome” spectrum (Figure 2).

Table 1 shows the maximum peak positions and their corresponding extinction coefficients of the “pyridine-hemochrome” spectra of various classes of cytochromes. These differences arise from different substituents at the β-pyrrole positions on the periphery of the heme.

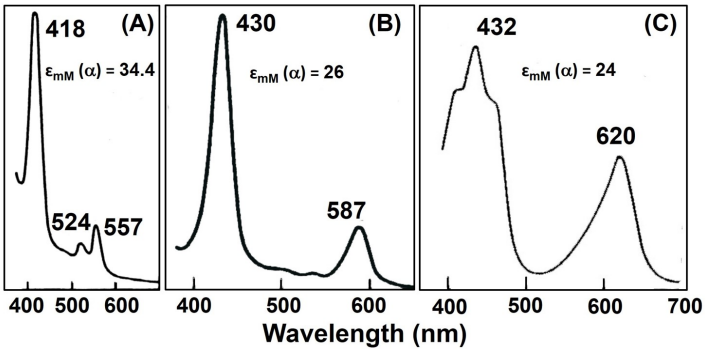

Figure 2. Representative pyridine hemochromogen spectra of hemin cofactor (A) heme *b* (B) heme *a* (C) heme d_1. The spectra of pyridine ferrohemochrome *c* is similar to that of heme *b*. Reprinted with permission from ref [116]. Copyright 1992 Springer-Verlag.

The word "heme" specifically describes the ferrous complex of the tetrapyrrole macrocyclic ligand called protoporphyrin IX (Figure 3).[81] It is the precursor to various types of cytochromes through different peripheral substitutions. Figure 3 shows a schematic of these various types of hemes.

Table 1. UV-vis spectral parameters of "pyridine-hemochrome" spectra of various types of cytochromes.

Heme	**Pyridine Hemochromogen**		**α peak (nm) of reduced protein**	**Examples**	**Ref.**
	Position of α peak (nm)	**ε_{mM} (at α peak)**			
Protoheme IX (*b*)	557	34.4	557-563	Cyt b_6f complex	[117]
Heme *c*	550	29.1	549-561	Cyt *c*	[118]
Heme *a*	587	26	587-611	Cyt aa_3 oxidase	[117]
Heme *d*	613		630-635	Cyt *bd* oxidase	[116]
Heme d_1	620	24	625	Cyt cd_1 nitrite	[116]

			reductase	
Heme *o*	553	560	Cyt bo_3 oxidase	[119]

Adapted with permission from ref 116. Copyright 1992 Springer-Verlag.

The b-type cytochromes have four methyl substitutions at positions 1, 3, 5, and 8, two vinyl groups in positions 2 and 4, and two propionate groups at positions 6 and 7, resulting in a 22 π electron porphyrin. Hemes *a* and *c* are biosynthesized as derivatives of heme *b*. In heme *a,* the vinyl group at position 2 of the porphyrin ring of heme *b* is replaced by a hydroxyethylfarnesyl side chain while the methyl group at position 8 is oxidized to a formyl group. These substituents make heme *a* more hydrophobic as well as more electron-withdrawing than heme *b* due to the presence of farnesyl and formyl groups, respectively. Covalent cross-linking of the vinyl groups at β-pyrrole positions 2 and 4 of heme *b* with Cys residues from a protein yields heme *c,* where the vinyl groups of heme *b* are replaced by thioether bonds.

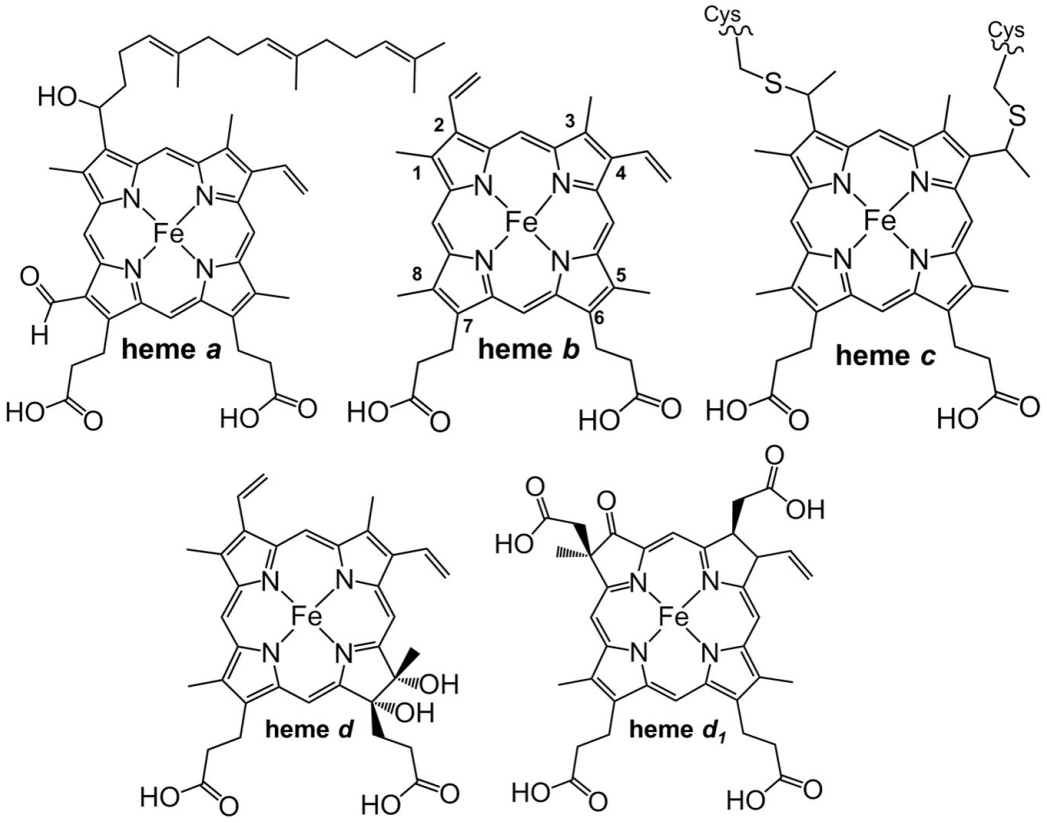

Figure 3. Different types of heme structures found in cytochromes.

The covalent cross linking of the two Cys residues from the protein to the porphyrin ring occurs at highly conserved -Cys-Xxx-Xxx-Cys-His- sequences. This cross-linking covalently attaches the heme *c* to the protein. The histidine residue in the conserved sequence serves as an axial ligand to the heme iron. In heme *d,* two *cis* hydroxyl groups are inserted at positions 5 and 6 on the β-pyrrole, which renders heme *d* as a 20 π-electron chlorin. Heme *d1* contains two ketone groups in place of the vinyl groups at positions 2 and 4, while two acetate groups are added to positions 1 and 3 of the tetrapyrrole macrocycle, resulting in 18 π electron isobacteriochlorins. The hemes in cyts *f* are the same as heme *c*, but differences in the ligands that coordinate to the heme iron at the axial position (called axial ligands) make hemes *c* and *f* spectroscopically distinct.

Common axial ligands found in cytochromes are shown in Figure 4. With the exception of cyts *c',* all cytochromes with ET function contain 6-coordinate low spin (6cLS) hemes axially ligated to amino acids such as His or an N-terminal amine group. Two axial His residues act as ligands to the heme iron in *b*-type cytochromes. The only example of bis-Met axial coordination to heme *b* is observed in the iron storage protein bacterioferritin.[120,121] A common axial His ligand is found in all cyts *c*, where the axial His is a part of the conserved -Cys-Xxx-Xxx-Cys-His- sequence, through which the heme is covalently attached to the protein. The most commonly encountered second axial ligand in *c*-type cytochromes is the side chain of Met with the exception of multi-heme *c*-type cytochromes, which generally display bis-His axial ligation of the heme iron (section 2.3.6).[80] In most cases, the His ligands are coordinated to the heme iron by their N^{ε} atom. However, an example of N^{δ} coordination has been reported.[122] The *f*-type cytochromes contain the same type of heme with one axial His ligand, as in cyts *c*; the only exception is in the nature of the second axial ligation in that the second axial ligand is the NH_2 group of an N-terminal tyrosine instead of the most commonly found Met or His as the second axial ligand.[123] Not surprisingly, the variation in the axial ligation makes each heme type electronically unique resulting in different out-of-plane

distortions of the heme iron from the heme plane (Figure 4) as well as different spectroscopic features (Figure 1).

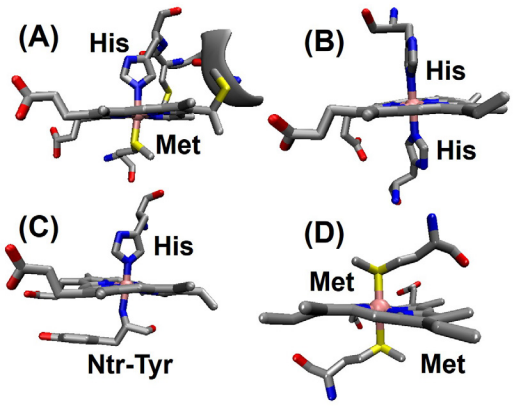

Figure 4. Commonly found heme axial ligands in various cytochromes. a) Class I cyts *c* (PDB ID 3CYT) with His/Met axial ligation. b) Cyts *b* and multi-heme cyts *c* contain bis-His ligation (bovine liver cyt b_5: PDB ID 1CYO). c) Unusual His/amine ligation is found only in cyt *f* (PDB ID 1HCZ). d) Bis-Met ligation is encountered in bacterioferritin (PDB ID 1BCF). For *c*-type cytochromes the conserved -Cys-Xxx-Xxx-Cys-His- ligation and its covalent linkage to the heme via Cys residues are shown.

2.3. Native Cytochromes *c*

2.3.1. Functions of Cytochromes *c*

Cytochromes *c* are involved in biological ET processes in both aerobic and anaerobic respiratory chains. In aerobic respiration, they are involved in the mitochondrial respiratory chain to produce the energy currency ATP by transferring electrons from the transmembrane bc_1 complex to cyt *c* oxidase.[85,86] In addition, cyts *c* have also been recently discovered to play a crucial role in programmed cell death (apoptosis), where they activate the protease involved in cell death, caspase 3.[124-126] Other examples where *c*-type cytochromes are involved in ET include the reduction of sulfate to hydrogen sulfide, conversion of nitrogen to ammonia in nitrogen fixation, reduction of nitrate to dinitrogen in denitrification, phototrophes that use light energy to carry out various cellular processes, and methylotrophes that use methane or methanol as the carbon source for their growth. Detailed descriptions of the roles of cyts *c* in these cases will be discussed in the following sections.

As cyts *c* are involved in numerous crucial biological processes, they have been used extensively as a hallmark system to study biological electron transfer by site-directed mutagenesis studies, which have elucidated the regions of the protein that are critical for their ET properties as well as fine tuning the reduction potentials.[87,127-131] In addition, various inorganic redox couples have been covalently appended to surface sites of cyts *c* to study intra-protein ET pathways.[24,132,133] Various complexes of cyts *c* with other protein partners have also been prepared to study inter-protein electron transfer pathways.[134-149]

2.3.2. Classifications of Cytochromes *c*

Cytochromes *c* generally contain ~100-120 amino acids. Biosynthesis of cyts *c* involves the formation of two thioether bonds between two Cys residues and the two vinyl groups of heme *b* by post-translational modification.[150,151] Primary amino acid sequence alignment shows that the residue identity of cyts *c* is 45-100% among eukaryotes. The electronic spectra of cyts *c* are dominated by the allowed porphyrin $\pi \rightarrow \pi^*$ transitions that are mixed together with interelectronic repulsions that give rise to an intense band at ~410 nm (called the Soret or γ band) and two weaker signals in the 500-600 nm range (the α and β bands). The reduced form of the protein shows a Soret band at 413 nm, and sharp α and β bands at 550 nm (ε = 29.1 $mM^{-1}cm^{-1}$), and 521 nm (ε = 15.5 $mM^{-1}cm^{-1}$), respectively, with a ratio of α/β bands of 1.87 (Table 1). The electronic spectra of cyts *c* from other sources are very similar to that of horse heart cyt *c.* Originally classified by Ambler,[89,152] cyts *c* have been divided into four major classes based on the number of hemes, position and identity of the axial iron ligands, and reduction potentials (Table 2).

Table 2. Axial ligand types and reduction potentials of various cytochromes**.**

Cytochromes	**Axial ligand**	**Class**	**E (mV)**	**Mutants**	**E (mV)**	
Nitrosomonas europaea Di-heme cyt *c* Peroxidase	His-Met	Class I (c)	450			[153,154]

Rhodocyclus tenuis THRC cyt *c*		Class IV (c)	420			[155]
HP1	His-Met		420			
HP2	His-Met		110			
LP1	Bis-His		60			
LP2	His-Met					
Rhodopseudomonas Viridis THRC cyt *c*		Class IV (c)	380			[156,157] Class IV (c)
H1(c_{559})	His-Met		330			
H3(c_{556})	His-Met		20			
H2(c_{552})	Bis-His		-60			
H4(c_{554})	His-Met					
Rhodobacter Capsulatas cyt c_2	His-Met	Class I (c)	373	Gly29Ser	330	[158-160]
				Pro30Ala	258	
				Tyr67Cys	348	
				Tyr67Phe	308	
Chlamydomonas reinhardtii cyt *f*	His-Nte(Tyr)	Cyt *f*	370	Tyr1Phe	369	[161]
				Tyr1Ser	313	
				Val3Phe	373	
				Phe4Leu	348	
				Phe4Trp	336	
				Tyr1Phe/Phe4Tyr	370	
				Tyr1Ser/Phe4Leu	289	
				Val3Phe/Phe4Trp	342	
Rhodospirillum rubrum cyt c_2	His-Met	Class I (c)	324			[156]
Pseudomonas aeruginosa	His-Met	Class I (c)	310			[162]

cyt *c* Nitric Oxide Reductase						
	Bis-His	Cyt *b*	345			
P. aeruginosa cyt *c* Peroxidase	His-Met	Class I (c)	320			163
Arthrospira maxima cyt c_6	His-Met	Class I(c)	314			164
Saccharomyces cerevisiae iso-2 cyt *c*	His-Met	Class I(c)	288	Asn52Ile	243	130
S. cerevisiae iso-1 cyt *c*	His-Met	Class I(c)	272	Arg38Lys	249	131,165 -173
			285	Arg38His	245	
			290	Arg38Gln	242	
				Arg38Asn	238	
				Arg38Leu	231	
				Arg38Ala	225	
				Asn52Ala	257	
				Asn52Ile	231	
				Tyr67Phe	234	
				Phe82Leu	286	
				Phe82Tyr	280	
				Phe82Ile	273	
				Phe82Trp	266	
				Phe82Ala	260	
				Phe82Ser	255	
				Phe82Gly	247	
P. aeruginosa cyt c_{551}	His-Met	Class I(c)	276			156
Horse cyt *c*	His-Met	Class I(c)	262	Met80Ala	82	158,174
				Met80His	41	
				Met80Leu	-42	

				Met80Cys	-390	
Rat cyt *c*	His-Met	Class I(c)	260	Pro30Ala	258	
				Pro30Val	261	
				Tyr67Phe	224	
Rps. palustris cyt c_{556}	His-Met	Class II	230			[80]
E. Coli cyt b_{562}	His-Met	Cyt *b*	168	Phe61Gly	90	[175,176]
		(Class II)				
				Phe65Val	173	
				Phe61Ile/Phe65Tyr	68	
				His102Met	240	
				Arg98Cys/His102Met	440	
Alicycliphilus denitrificans cyt *c*'	His-Met	Class II	132			[80]
Rps. palustris cyt *c'*	His-Met	Class II	102			[80]
Cytochrome b_5	His-His	Cyt *b*		Form A	80	[177]
				Form B	-26	
Desulfovibrio vulgaris cyt c_{553}	His-Met	Class I	37	Met23Cys	29	[156,178]
			20±5	Gly51Cys	28	
				Met23Cys/Met23Cys	88	
				Gly51Cys/Gly51Cys	105	
Bovine liver microsomal cyt b_5	Bis-His	Cyt *b*	3	Protoheme IX Dimethyl ester	70	[179]
S. cerevisiae cyt b_2	Bis-His	Cyt *b*	-3			[156]

Chromatium vinosum cyt *c'*	His-	Class II (c)	-5			[80]
Rat liver microsomal cyt b_5	His-His	Cyt *b*	-7±1			[129,180]
R. rubrum cyt *c'*	His-Met	Class I (c)	-8			[80]
Tryptic bovine hepatic cyt b_5	His-Met	Class I (c)	-10±3	Val61Lys	17	[181]
				Val61His	11	
				Val61Glu	-25	
				Val61Tyr	-33	
Allochromatium Vinosum triheme cyt *c*	Bis-His	Class III (c)	-20			[182]
	His-Met		-200			
	His-Cys/Met		-220			
R. Sphaeroides cyt *c'*	His-Asn	Cyt *c*	-22			[183]
Cytochrome b_6f complex	Bis-His	Cyt *b*	-45			[184]
			-150			
Thermosynechococcus elongates PS cyt c_{550}	His-Met	Class I (c)	-80	In absence of mediators	200	[185]
MamP Magnetochrome	His-Met	Class I (c)	-76			[186]
Rat liver OM cyt b_5	His-His	Cyt *b*	-102	His63Met	110	[187,188]
				Val45Leu/Val61Leu	-148	
				Protoheme IX Dimethyl ester	-36	
D. Desulfuricans Norway cyt c_3	His-His	Class III (c)	-132			
	His-His		-255			
	His-His		-320			
	His-His		-360			
Chlorella Nitrate reductase	His-His	Cyt *b*	-164			[189,190]

cyt b_{557}				
Ectothiorhodospira Shaposhnikovii cyt b_{558}	His-His	Cyt *b*	-210	[191]
Azotobacter Vinelandii bacterioferritin	His-His	Cyt *b*	-225	[192]
(in presence of non heme iron core)			-475	
D. vulgaris	His-His	Class III (c)	-280	[192,193]
Hildenborrough cyt c_3	His-His		-320	
	His-His		-350	
	His-His		-380	
Synechocystis Sp. cyt c_{549}	His-His		-250	
A. maxima cyt c_{549}	His-Met		-260	[164]

Adapted from ref [78]. Copyright 2004 Elsevier.

The class I cyts *c* include small (8-120 kDa) soluble proteins containing a single 6cLS heme moiety and display a range of reduction potential from -390 to +450 mV (Table 2).[78] Based on sequence and structural alignments, class I cyts *c* have further been partitioned into sixteen different subclasses.[88] The majority of the subclasses include mitochondrial cyts *c* and purple bacterial cyt *c.* Examples of other subclasses represent a wide variety of different sources including cyts c_{551}, cyts c_4, cyts c_5, cyts c_6 (cyts c_{553} in algae) from *Pseudomonas*, *Chlorobium* cyt c_{555}, *Desulfovibrio* cyts c_{553}, c_{550} from cyanobacteria and algae, *Ectothiorhodospira* cyts c_{551}, flavocytochromes *c*, methanol dehydrogenase-associated cyt c_{550} or c_L, cyt cd_1 nitrite reductase, cyt subunit associated with alcohol dehydrogenase, nitrite reductase associated cyt *c* from *Pseudomonas*, and cyt *c* oxidase subunit II from *Bacillus*.[78]

Class I cyt *c* domains are characterized by their signature cyt *c* fold and the presence of an N-terminal conserved -Cys-Xxx-Xxx-Cys-His- sequence containing cysteines for covalent cross-linking of the heme to the protein and the His which acts as the axial ligand to the heme iron. Class I Cyt *c* fold is recognized as having a total of five α-helices arranged in a unique tertiary structure. There are two helices, one each at the

N- and C-termini, represented as α1 and α5, respectively. In between, there is a small helix α3, (also called the 50's helix in mitochondrial cyts *c*) followed by two other helices, α4, and α5 which are known as the 60's helix and 70's helix, respectively, in mitochondrial cyts *c.* The 70's helix precedes a loop towards the C-terminus that contains the second axial ligand Met to the heme iron. There are examples where the second axial ligand is a residue other than Met, e.g. Asn, His, or even absent.[79] In many cases, this core cyt *c* domain can be found fused to other membrane proteins. General features of class I cyt *c* fold are shown in Figure 5.

The class II cyts *c* consist of a *c*-type heme covalently attached to the highly conserved C-terminal -Cys-Xxx-Xxx-Cys-His- sequence, as in class I cyts *c*, with the Cys residues, and the His as one of the axial ligands.[80] Four α-helices and a left-hand twisted overall structure represent this subclass of cyts *c* (Figure 5). The second axial ligand to the heme iron is variable.[194,195] The subclass cyt *c'* is axially coordinated to a single His imidazole ligand and lacks the second axial ligand, and has a relatively small range of reduction potentials ranging from approx. -200 to +200 mV (Table 2).[8,90] Members from this subclass represent a wide range of sources that include photosynthetic, denitrifying, nitrogen fixing, methanotrophic, and sulfur oxidizing bacteria. This class has two subclasses based on the distinct spin states displayed by the heme. The subclass IIa of cyt *c'* displays a HS ferrous [Fe(II), S=2] electronic configurations, while the ferric form shows either a HS S=5/2 or S=3/2, S=5/2 mixture of spin states.[196-202] The subclass IIa proteins, isolated from *Rhodopseudomonas palustris (Rp. Palustris)*, *Rhodobacter capsulatus* (*Rb*. *capsulatus*), and *Chromatium* V*inosum* (*Ch*. V*inosum*) display a large value of S=3/2 ground state in the spin-state admixture, ranging from 40-57% as determined from EPR simulations.[196,201,203] The second subclass, IIb, includes cyt c_{556} from *Rp*. *palustris*,[204] *Rb. sulfidophilus*,[205] *Agrobacterium tumefaciens*,[80] and cyt c_{554} from *Rb*. *sphaeroides*[206], which contain heme in the LS configuration. This subclass of proteins has a second axial ligand to the heme iron which is a Met residue located close to the N-terminus. Class II cyts display reduction potentials ranging from −5 to +230 mV (Table 2).

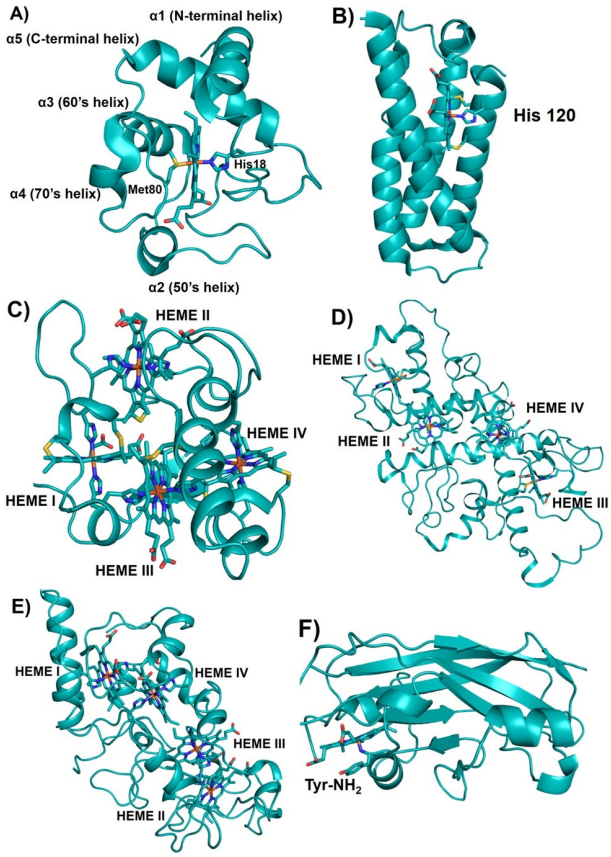

Figure 5. Schematic representations of various classes of cyts *c*. A) Class I cyt *c* fold with His/Met heme axial ligands (PDB ID 3CYT). Mitochondrial designation of the helices is also shown. B) Four-helix bundle Cyt *c'* belongs to class II cyt *c* having a 5c heme with His 120 as the sole axial ligand (PDB ID 1E83). C) Tetraheme cyt c_3 belongs to class III cyt *c* with bis-His ligation to all four hemes (PDB ID 1UP9). Hemes I and III are attached to the protein via the highly conserved -Cys-Xxx-Xxx-Cys-His- sequence whereas hemes II and IV are covalently bound to the protein by a -Cys-Xxx-Xxx-Xxx-Xxx-Cys-His- motif. In A), B), and C) the covalent attachment of the heme to the protein via Cys residues is shown. D) Tetraheme cyt *c* from photosynthetic reaction center (RC) belongs to class IV of cyt *c*. Hemes I, II, and III have His/Met axial ligands while heme IV has bis-His axial ligation to the heme iron (PDB ID 2JBL). E) Cyt c_{554} from *N. europaea* belongs to a class of its own. Hemes I, III, and IV have bis-His ligated heme iron whereas heme II is 5c with His as the only axial ligand (PDB ID 1BVB). Heme numbering in C), D), and E) is according to their attachment occurring along the protein's primary sequence. F) Cyt *f* from chloroplast is unique from all other classes of cytochromes in that it mostly contains β-sheets and the heme is 6c with a His and N-terminal backbone NH_2 group of a Tyr residue (PDB ID 1HCZ). It has been included as a subclass of cyt *c* because the

heme is covalently bound to the protein via the highly conserved -Cys-Xxx-Xxx-Cys-His- signature motif for heme attachment ubiquitously found in *c*-type cytochromes.

Class III cyts *c* include proteins containing multiple hemes with bis-histidine ligation and display reduction potentials in the range of 0 to -400 mV (Table 2).[80,88,152,207-212] In some cases this class of cytochromes have up to 16 heme cofactors and display no structural similarity with other classes of cyts *c.* They are found as terminal electron donors in bacteria involved in sulfur metabolism. [213] These bacteria utilize sulfur or oxidized sulfur compounds as terminal electron acceptors in their respiratory chain. One of the best studied proteins in this class is cyt c_3 (~13 kDa) (Figure 5) from *Desulfovibrio* which acts as a natural electron acceptor and donor in hydrogenases and ferredoxins.[214] The overall protein fold containing two β-sheets and 3-5 α-helices is conserved among the known structures of cyts c_3 as well as the orientation of the four hemes which are located in close proximity to each other with each of the heme planes being nearly perpendicular to the others.[88] Each of the hemes displays a distinct reduction potential spanning a range from -200 to -400 mV.[215-219] Cyt $c_{555.1}$, also known as cyt c_7 (~9 kDa, 70 amino acids) from *Desulfuromonas acetoxidans* is another class III cyt *c* that contains three hemes, the structure of which has been determined.[220] These proteins have been proposed to be involved in electron transfer to elemental sulfur as well as in the coupled oxidation of acetate and dissimilatory reduction of Fe(III) and Mn(IV) as an energy source in these bacteria.[221] In cyt c_7 two of the hemes have a reduction potential of −177 mV, and the third heme has a reduction potential of −102 mV.[222]

Class IV cyts *c* fall in the category of large molecular weight (~35-40 kDa) cytochromes that contain other prosthetic groups in addition to *c*-type hemes such as flavocytochromes *c* and cyts *cd*.[152] One example of class IV cyts *c* is revealed by the X-ray structure of photosynthetic reaction center (RC) from *Rp. viridis* where light energy is harvested and converted to chemically useful energy. The cyt *c* in the RC consists of four *c*-type heme moieties covalently bound to the subunit C of the RC. Three of the hemes have His/Met axial ligation while the fourth heme is bis-His ligated. The four hemes are oriented in two types of pairs. The porphyrin planes of hemes I/III and II/IV

are orientated parallel to each other, while the porphyrin planes of each pair of hemes are perpendicular to each pair's porphyrin planes (Figure 5).[223]

Cyt c_{554} is another tetraheme cytochrome that is involved in the ET pathway of the biological nitrogen cycle in the oxidation of ammonia in *Nitrosomonas europaea (N. europaea).*[122,224] This family of cyts does not fall into either class III or class IV cyts and has been proposed to belong to a class of its own. A pair of electrons is passed from hydroxylamine oxidoreductase (HAO) to two molecules of cyt c_{554} upon oxidation of hydroxylamine to nitrite. One of the hemes is HS, and the other three are 6cLS with reduction potentials of +47, +47, -147, and -276 mV, respectively. Porphyrin planes of hemes III and IV are oriented almost perpendicular to each other while the heme pairs I/III and II/IV have parallel orientation (Figure 5). The sets of parallel hemes overlap at an edge, and such heme orientation has been observed in HAO and cyt *c* nitrite reductase.

Cyt *f* is a high potential (Table 2) electron acceptor of the chloroplast cyt b_6f complex involved in oxygenic photosynthesis by passing electrons from photosystem II to photosystem I of the RC.[123,225] Cyt *f* accepts electrons from a Rieske-type iron-sulfur cluster and passes electrons to the copper protein plastocyanin. Cyt *f* consists of two domains primarily of β-sheets and is anchored to the membrane by a transmembrane segment while most of the protein is located on the lumen side of the thylakoid membrane. The heme is also located on the lumen side at the interface of the two domains and is covalently attached to the protein via the signature sequence of cyts *c,* -Cys-Xxx-Xxx-Cys-His-. The β-sheet fold has not been observed in any other families of cytochromes and is thus unique to cyts *f.* Intriguingly, this family of cytochromes also contains an unusual second axial ligation to the heme iron, an N-terminal $–NH_2$ group of a Tyr residue (Figure 5).

Quite uniquely, the only exception to the bis-Cys covalent attachment of the *c*-type hemes via the conserved -Cys-Xxx-Xxx-Cys-His- motif in cyt *c* is found in eukaryotes from the phylum Euglenozoa, including trypanosome and *Leishmania* parasites. In the mitochondrial cyt *c* of these organisms the heme is attached to the protein via a single Cys residue from the heme binding motif -Ala(Ala/Gly)-Gln-Cys-His-[226-228]

2.3.3. Conformational Changes in Class I Cytochromes *c* Induced by Changes in Heme Oxidation State

Many structural studies have been undertaken to determine whether there is any effect on the protein structure associated with different oxidation state of the heme iron. These studies include X-ray and NMR structures of oxidized and reduced cyts *c* from various sources,[229-235] which indicate that the oxidation state of the heme iron has minimal effect on the tertiary structures of the proteins (Figure 6). The major changes are observed in the conformation of some amino acid residues located close to the heme pocket. Among these residues, Asn52, Tyr67, Thr78, and a conserved water (wat166) molecule show maximal changes in conformations depending on the oxidation state of the heme iron. These conserved residues,[236] along with the conserved water molecule, the axial ligand Met80, and the heme propionate 7 form a hydrogen bonding network around the heme site. High resolution X-ray structure of yeast iso-1-cytochrome *c* shows that in the reduced state the heme is significantly distorted from planarity, into a saddle shape. The degree of heme distortion in the oxidized state is even more pronounced compared to the reduced state, suggesting that the planarity of the heme group is dependent on the oxidation state of the iron. The major change in the bond length of the heme iron ligands is observed in the case of axial Met80, which increases from 2.35 Å to 2.43 Å in going from reduced to oxidized state. On the contrary, the other axial ligand, His18 shows a minute change of 0.02 Å, from 1.99 Å to 2.01 Å.[230]

In the reduced state of *iso*-1-cytochrome *c,* the conserved water molecule is hydrogen bonded to Asn52, Tyr67, and Thr78 (Figure 6). Upon oxidation the wat166 undergoes a 1.7 Å displacement towards the heme, which results in the loss of hydrogen bond to Asn52, but interactions with Tyr67 and Thr78 are retained. Figure 6 shows an overlay of the residues near the heme pocket between reduced and oxidized states of *iso*-1-cytochrome *c.*[87]

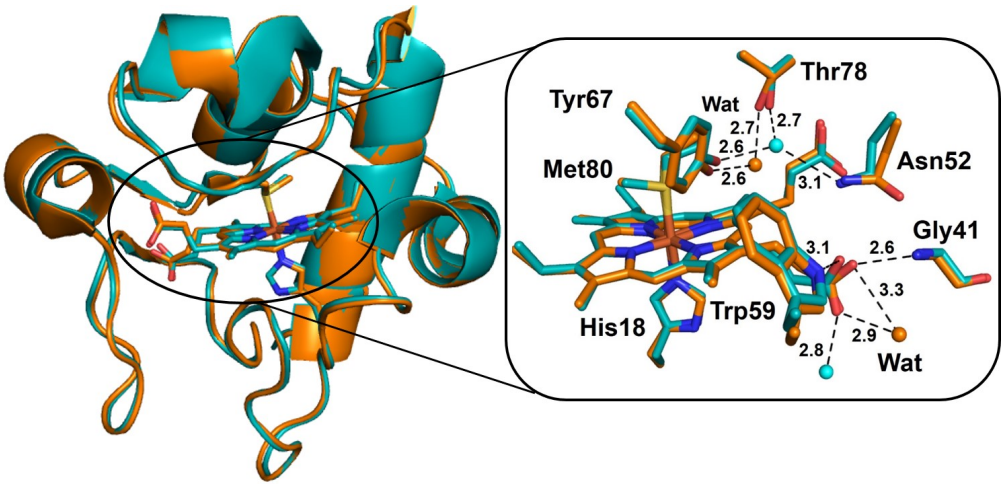

Figure 6. Overall structural overlay of the reduced (cyan, PDB ID 1YCC), and oxidized (orange, PDB ID 2YCC) *iso*-1-cyt *c* (left). A close look at the heme site and the nearby residues is shown on the right along with some hydrogen bond interactions.

Further analysis suggested that the wat166 plays a key role in stabilizing both oxidation states of the heme iron by reorienting the dipole moment, changing the heme iron-wat166 distance, and variations in the nearby hydrogen bonding network. Another noticeable change is observed in the hydrogen bonding between a conserved water, wat121, and the heme propionate 7. In the reduced state, wat121, and Trp59 are hydrogen bonded to the O1A, and O2A oxygen of propionate 7, respectively. In the oxidized state, interaction between Trp59 and O2A of heme propionate weakens, while that of O2A and the conserved Gly41 increases. Additionally, wat121 moves by 0.5 Å and causes a bifurcated hydrogen bond between both O1A and O2A of the propionate.[230] Thus, it appears that there are three major regions that show significant changes in conformation between the two oxidation states: the heme propionate 7, wat166, and Met80. A conserved region that does not show mobility between oxidation states is the region encompassing the residues 73-80 in *iso*-1-cytochrome *c* which is linked to the three major regions of conformation change through Thr78. Based on this observation it has been suggested that the region 73-80 acts as a contact point with redox partners and triggers the necessary conformational changes in other parts of the protein that is required to stabilize both oxidation states of cyt *c*.[230] A contrasting observation from NMR studies is that the wat166 moves 3.7 Å away from the heme iron

when going from reduced to oxidized state, rather than moving towards the heme iron.[237,238]

Similar to the changes of heme propionate observed in eukaryotes, cyts c_2[160,239-242] and c_6[220,243,244] from some prokaryotes also display conformational changes in the heme propionate between reduced and oxidized states of the protein. In the cases of cyt c_H (reduces methanol oxidase in methylotropic bacteria) from *Methylobacterium extorquens*, and cyt c_{552} [245-247] (electron donor to a ba_3-cytochrome *c* oxidase) from *Thermus thermophilus (T. thermophilus)*, there is no conserved water molecule in the heme pocket, suggesting that the water mediated hydrogen bonding network is not a critical requirement for electron transfer.[248-250]

2.3.4. Cytochromes *c* as Redox Partners to Other Enzymes

In the following sections we summarize some specific examples of native enzymes use cyts *c* as the native electron donor for performing various biochemical processes.

2.3.4.1. Cytochrome c as a Redox Partner to Cytochrome c Peroxidases (CcP)

Cytochrome *c* Peroxidases (C*c*Ps) are a family of enzymes that catalyze the conversion of H_2O_2 to water and are found in both eukaryotes and prokaryotes. Eukaryotic C*c*Ps are located in the inner mitochondrial membrane and contain a single heme cofactor, heme *b*, while prokaryotic C*c*Ps are located in the periplasmic space and contain two covalently bound *c*-type hemes,[251,252] one of which is a low potential (lp) heme and another is a high potential (hp) heme. In general, the physiological electron donors to bacterial C*c*Ps are mono-heme cyts *c,* although other donors such as azurin or pseudo-azurin have also been found in some bacteria.[253] The hp heme is located at the C-terminal domain and has a more positive reduction potential than cyt *c* as it accepts electrons from cyt *c*. The reduction potential for the hp heme varies depending on the organism, e.g. *Pseudomonas aeruginosa (P. aeruginosa)* C*c*P hp site has a reduction potential of +320mV,[163] *R. capsulatus* of +270mV,[254] and *N. europaea* has a value of +130mV.[154] The electrons are then transferred from the hp heme to the lp heme of C*c*P. In some organisms e.g. *P. aeruginosa* and *R. capsulatus* the hp heme

should be in ferrous state in order for the enzyme to be active,[254,255] whereas in other cases the enzyme is fully functional even with the ferric state of the hp heme, e.g. in *N. europaea*.[154] The axial ligands for the hp heme are a His and a Met, similar to most *c*-type cytochromes. The lp heme is the site for H_2O_2 reduction. It is located at the N-terminal domain and has two His as axial ligands. The lp heme also displays a wide range of reduction potential from as low as -330 mV in *P. aeruginosa*[163] to as high as +70 mV in *N. europaea* C*c*P.[154] Electron transfer between the hp and lp hemes, which are 10 Å apart from one another, is thought to occur through tunneling.[255]

Cyts *c* interact with C*c*P at a small surface patch of the enzyme which has a hydrophobic center and a charged periphery.[256] The small size of the surface patch suggests that the interaction of the enzyme with the electron donor is transient, but at the same time is highly specific which ensures complex formation due to desolvation of the surface waters and binding of cyt *c*. The charged periphery has been shown to be important to guide the donor towards the surface site, but it does not increase the specificity of the interactions or the ET rate.[257] Mutagenesis studies in *R. capsulatus* C*c*P have shown that the interface at which the enzyme interacts with its electron donor cyt c_2 involves non-specific salt bridge interactions, as the extent of the interaction is dependent on the ionic strength of the solution.[258] In contrast, in *P. nautica* C*c*P, the interaction surface between the enzyme and the electron donor cyt *c* is highly hydrophobic based on studies which showed that the enzyme was active across a wide range of ionic strength of the solution.[259] Studies from *P. denitrificans* C*c*P have shown that two molecules of horse heart cyt *c* are able to bind to the enzyme surface.[260] Binding of an 'active' and 'waiting' cyt *c* in a ternary complex with the enzyme has been proposed to improve the electron transfer rate. Structural studies of *P. denitrificans* C*c*P with the monoheme cyt *c* has shown that the heme of the donor binds above the hp heme of C*c*P, while the two molecules of horse heart cyts *c* bind in between the two hemes of the enzyme.[261]

2.3.4.2. Cytochrome c as a Redox Partner to Denitrifying Enzymes: Nitrite, Nitric Oxide, and Nitrous Oxide Reductases

Denitrification is a stepwise process in biological nitrogen cycle where nitrogen oxides act as electron acceptors, and are sequentially reduced from nitrate to nitrite, nitrite to nitric oxide, nitric oxide to nitrous oxide, and finally nitrous oxide to nitrogen. These four steps of the nitrogen cycle are catalyzed by a diverse family of enzymes *viz.* nitrate reductase, nitrite reductase, nitric oxide reductase, and nitrous oxide reductase, all of which are induced under anoxic conditions.[262-264] Various cyts *c* domains act as electron donors in the denitrification process. Reduction of nitrite to nitric oxide is catalyzed by one of the two structurally diverse enzymes that also have different catalytic sites, a) cytochrome cd_1 nitrite reductase (cyt-cd_1 NiR)[265,266] and b) multi-copper nitrite reductase (CuNiR).[267,268] Cyt-cd_1 NiRs are periplasmic, soluble heterodimeric enzymes containing an electron transfer cyt *c* domain and a catalytic cyt d_1 domain in each subunit, while multi-copper nitrite reductases are homotrimeric enzymes containing T1Cu as electron transfer sites and T2Cu as catalytic sites. Cyts c_{552} are the putative electron donors of cyt cd_1.[269] Multi-copper nitrite reductases have cupredoxin-like folds and use azurins and pseudo-azurins as their biological redox partner, and as such are unexpected to have cyt *c* domains. Contrary to this expectation, two instances have been found where a fusion of multi-copper nitrite reductase and cyt *c* domains were discovered in the genomes of *Chromobacterium violaceum* and *Bdellovibrio bacteriovorus* where in both cases, the cytochrome *c* domain is present at the end of an ~ 500 residue long sequence.[79] These cyt *c* sequences are similar to those of the caa_3 oxidases sequences.

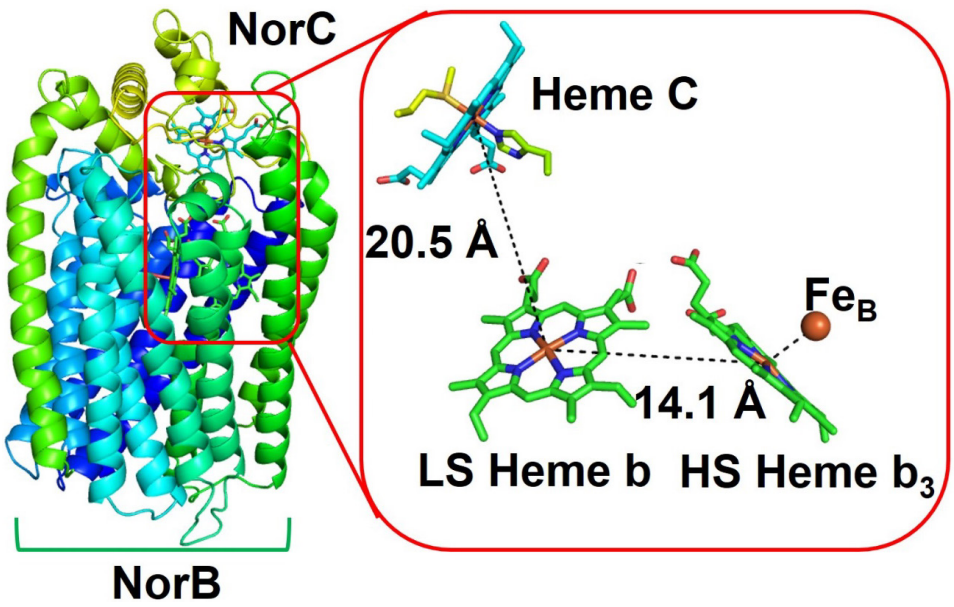

Figure 7. X-ray structure of cyt *c* dependent NOR (cNOR) (PDB ID 3O0R) from *P. aeruginosa*.

Nitric oxide reductases (NORs) are integral membrane proteins that catalyze the two electron reduction of nitric oxide to nitrous reductase.[270,271] A recent x-ray structure of the Gram-negative bacterium *P. aeruginosa* cyt *c*-dependent NOR (cNOR) (Figure 7) show that the enzyme consists of two subunits.[272] The NorB subunit is the transmembrane subunit and contains the binuclear active site consisting of a HS heme b_3 and a non-heme iron (Fe_B) site. It also houses a LS electron transfer cofactor heme *b*. The NorC is a membrane-anchored cyt *c* and contains a *c*-type heme. Electrons are received from cyt c_{552} or azurin to the heme *c,* which then passes the electrons to LS heme *b* to the catalytic binuclear active site. The reduction potentials are +310 mV, +345 mV, +60 mV, and +320 mV for heme *c,* heme *b,* heme b_3 and the Fe_B sites, respectively.[162]

2.3.4.3. Cytochromes c as a Redox Partner to Molybdenum-Containing Enzymes

Mononuclear molybdenum containing enzymes constitute a group of enzymes that catalyze a diverse set of reactions and are found in both eukaryotes and prokaryotes.[273,274] The general function of these groups of enzymes is to catalytically transfer an oxygen atom to and from a biological donor or acceptor molecule, and these enzymes are thus referred to as molybdenum oxotransferases. These enzymes

possess a Mo=O unit at their active site and an unusual pterin cofactor which coordinates to the metal via its dithiolene ligand moiety. These Mo-containing enzymes are generally classified into three families depending on their structures and the reactions that they catalyze. The first one is xanthine oxidase from cow's milk which has a $LMo^{VI}OS(OH)$ (L=pterin) catalytic core and generally catalyzes the hydroxylation of carbon centers. The second family includes sulfite oxidase from avian or mammalian liver with a core coordination consisting of a $LMo^{VI}O_2$(S–Cys) moiety that catalyzes the transfer of an oxygen atom to or from the substrate's lone pair of electrons. The third family of oxotransferases shows diversity in both structure and functions and uses two pterin ligands instead of only one used by the first two classes. The reaction occurs at the active site core containing $L_2Mo^{VI}O(X)$, where X could be a Ser as in DMSO reductase or Cys as in assimilatory nitrate reductase.

Xanthine oxidases have been reported to be co-expressed with three cyt *c* domains in *Bradyrhizobium japonicum*, *Bordetella bronchiseptica*, *P. aeruginosa*, and *Ps. putida,* however the exact cause for this association is not well understood as these enzymes use flavins as their redox partners.[79] Sulfite oxidase catalyzes the oxidation of sulfite to sulfate using two equivalents of oxidized cyt *c* as physiological oxidizing substrates (Scheme 1).[273] The molybdenum is reduced from

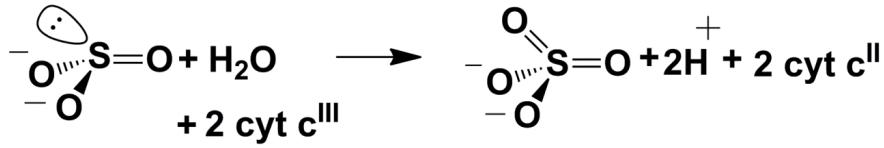

Scheme 1. Scheme showing the oxidation of sulfite to sulfate by cyt *c* in sulfite oxidase. Reprinted with permission from ref [273]. Copyright 1996 American Chemical Society.

VI to IV oxidation state, and the reducing equivalents are then transferred sequentially to the cyt *c* in the oxidative half reaction. The assimilatory nitrate reductases (NRs) are found in algae, bacteria and higher plants which uptake and utilize nitrate.[273] These enzymes contain a cyt b_{557} and FAD in addition to the Mo center. Electrons flow from FAD to cyt b_{557} to the Mo center under physiological conditions. The midpoint reduction potentials for FAD, and cyt b_{557} from *chlorella* NR have been determined to be -288 mV,

and -164 mV, respectively.[189,190,275] The Mo center displays reduction potentials of +15 mV for the $Mo^{VI/V}$ couple and -25 mV for $Mo^{V/IV}$ couple. These reduction potentials indicate that the physiological direction of electron flow is thermodynamically favorable. The cyt b_{557} domain of NR is homologous to the mammalian cyt b_5, yeast flavo-cyt b_2 and the cyt *b* domain of sulfite oxidase.[276]

The DMSO reductase family consists of a number of enzymes from bacterial and archaeal sources that display remarkable sequence similarity. Respiratory DMSO reductases are periplasmic and use membrane-anchored multi-heme cyts *c* as electron donors that transfer electrons from the quinine pool to the periplasmic space. These cyts are about 400 amino acids long and are encoded in the same operon as the enzyme. In some γ-proteobacteria, the tetra-heme cyts *c* occur as a fusion to the C-terminal cyt *c*-binding domain of the enzyme. On the other hand, in some ε-proteobacteria single-domain cyts *c* have been co-expressed with the DMSO reductase that act as electron donors to the enzyme. Nonetheless, the cyts *c* sequences from both types of proteobacteria are clustered together suggesting that even though the mechanism of electron transfer is different, they are functionally similar.[79] Even though these electron transfer proteins in DMSO reductases are referred to as cyts *c* because they contain *c*-type hemes, their structural folds do not fall on the uniquely defined category of cyt *c* fold as mentioned in section 2.3.2.

2.3.4.4. Cytochrome *c as a Redox Partner to Alcohol Dehydrogenase*

The type II quinohemoprotein alcohol dehydrogenases are periplasmic enzymes that catalyze the oxidation of alcohols to aldehydes and transfer electrons from substrate alcohols first to the pyrroloquinoline quinone (PQQ) cofactor which subsequently transfers electrons to an internal heme group that is found in a cyt *c* domain.[277] This cyt *c* domain of about 100 residues contains three α-helices in the core cytochrome domain and is similar to the cyt *c* domain in *p*-cresol methylhydroxylase (PCMH) from *P. putida*[278] and the cyt c_{551i} from *P. denitrificans*.[279]

2.3.4.5. Involvement of Cytochromes c in Photosynthetic Systems

Photosynthesis involves the conversion of light energy to useful chemical forms of energy which is accomplished by two large membrane protein complexes photosystem I (PSI) and photosystem II (PSII).[280] The catalytic cores of the two PSs are referred to as the reaction centers (RC), which have Fe_4S_4 clusters and quinines as terminal electron acceptors for the PSI and PSII, respectively. Like algae and higher plants, cyanobacteria also use PSI and PSII to convert light energy to chemical forms by producing oxygen from water oxidation. Even though cyanobacteria have bis-His coordinated PS-$_{C550}$ cyt subunit in their PSII, apparently there is no redox role of this cytochrome.[281,282] Being located at the lumenal surface of the enzyme, PS-$_{C550}$ cytochrome acts as an insulator of the catalytic core from reductive attack and contributes to structural stabilization of the complex.[283,284] The low midpoint reduction potentials of the soluble protein from -250 to -314 mV exclude any redox role of this class of cyts.[285-288] When complexed with PSII, more positive values of reduction potentials have been determined.[288,289] A reduction potential of +200 mV in PS-$_{C550}$ cytochrome from *Thermosynechococcus elongates* has recently been reported,[185] which suggest a possible role of this cytochrome in electron transfer in PSII, despite a long distance (~22 Å) between PS-$_{C550}$ cytochrome and its nearest redox center, the Mn_4Ca cluster.[290]

In cyanobacteria, cyt c_6 is known to act interchangeably with the copper protein plastocyanin as electron donor to PSI, depending on the availability of copper,[291-293] while in higher plants plastocyanin is the exclusive electron donor. Based on this observation it has been proposed that cyt c_6 is the older ancestor which has been replaced by plastocyanin during evolution due to the shortage of iron in the environment.[294]

Another cytochrome, cyt c_M, is found exclusively in cyanobacteria but its role is ambiguous. It has been shown to be expressed under stress-induced conditions such as intense light or cold temperatures where the expression of both cyt c_6 and plastocyanin are suppressed.[295] Thus it would be tempting to believe that cyt c_M is a third electron donor to PSI in cyanobacteria under stress conditions, but experimental evidence goes against this hypothesis.[296]

2.3.4.6. Cytochrome c as a Single Domain Oxygen Binding Protein

Sphaeroides heme protein (SHP) is an unusual *c*-type cytochrome which was discovered in *Rb. sphaeroides.*[183] SHP (~12 kDa) has a single HS heme with a reduction potential of -22 mV and an unusual His/Asn axial heme coordination in the oxidized form. SHP is spectroscopically distinct from cyts *c'* which also have HS heme. SHP was shown to bind oxygen transiently during slow auto-oxidation of the heme. The Asn axial ligand was shown to swing away upon reduction of the heme or binding of small molecules such as cyanide or nitric oxide. The distal pocket of SHP shows marked resemblance to other heme proteins that bind gaseous molecules.[297] It has been suggested that SHP could be involved as a terminal electron acceptor in an electron transfer pathway to reduce small ligands such as peroxide or hydroxylamine.[297]

2.3.5. Cytochromes *c* Domains in Magnetotactic Bacteria

Magnetotactic bacteria consist of a group of taxonomically and physiologically diverse family of bacteria that can align themselves with the geomagnetic field.[298] The unique property of these bacteria is due to the presence of iron-rich crystals inside their lipid vesicles forming an organelle, referred to as the magnetosome. From sequence analysis, three proteins, MamE, MamP and MamT in the Gram-negative bacterium *Magnetospirillum magneticum* AMB-1 that contribute to the formation of the magnetosome have been discovered to contain a double -Cys-Xxx-Xxx-Cys-His- motif, characteristic of cyts *c*.[186] All three proteins were expressed and purified in *E. coli.* Subsequent characterization of these proteins confirmed that MamE, MamP and MamT indeed belong to *c*-type cytochromes, and have been designated as 'magnetochromes'. Midpoint reduction potentials were determined to be -76 and -32 mV for MamP and MamE, respectively. The presence of cyts *c* proteins in magnetotactic bacteria is intriguing and suggests that these proteins take part in electron transfer, although the exact nature of their electron transfer partners are not known. It has been hypothesized that the magnetochromes can either donate electrons to Fe(III) and participate in magnetite [mixture of Fe(III) and Fe(II)] formation, or accept electrons from magnetite to maintain a redox balance or they can act as redox buffers to maintain a proper ratio of maghaemite (all ferric irons) and magnetite.

2.3.6. Multi-Heme Cytochromes *c*

Multi-heme cyts *c* occur as both soluble, and membrane-anchored electron transfer proteins in many enzymes across diverse functionalities.[79,299] Tri-heme Cys c_7 from *Geobacter sulfurreducens,* and *Desulfuromonas acetoxidans* are involved in electron transfer for Fe(III) respiration[207,300-303] although their exact roles are not known. These proteins have conserved secondary structural elements consisting of double-stranded β-sheet at the N-terminus followed by several α-helices. The protein displays a miniaturized version of cyt c_3 fold where heme II and the surrounding protein environment are missing (Figure 8). The arrangement of hemes is conserved in cyts c_7 in terms of the distances between heme-iron atoms and the angles between heme planes. Hemes I and IV are almost parallel to each other, and are mutually perpendicular to heme III which is in close contact with hemes I and IV. NMR and docking experiments suggest that heme IV is the region of interaction with similar physiological partners, while the other interacting partner would most likely interact through the region near hemes I and III. Such differences in interaction surfaces might play a role in choosing the right redox partners to perform different physiological functions.

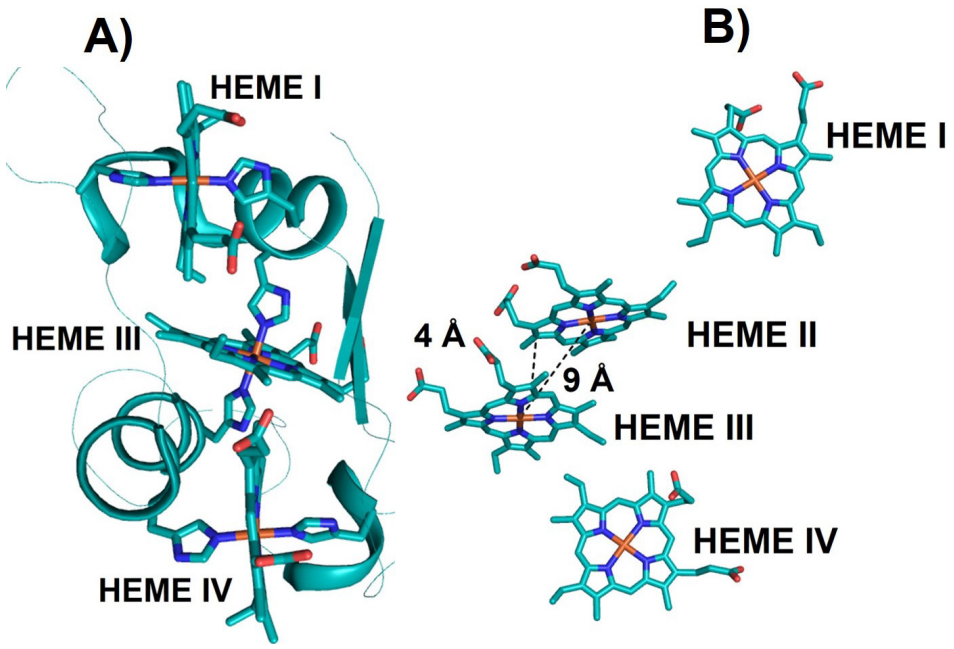

Figure 8. A) X-ray structure of tri-heme cyt c_7 (PDB ID 1HH5). All the hemes are bis-His ligated. Cyt c_7 is a minimized version of cyt c_3 where heme II is missing. B) Spatial arrangement of the four hemes in flavocytochrome c_3 fumarate reductase (PDB ID IQO8). The heme irons of the heme pair II and III are in close proximity at 9Å from each other and the heme edges are only at 4 Å away.

An unusual triheme cyt *c* is DsrJ from the purple sulfur bacterium *Allochromatium vinosum* that is a part of a complex involved in sulfur metabolism.[182,304] Sequence analysis suggested the presence of three distinct *c*-type hemes containing bis-His, His/Met, and a very unusual His/Cys axial ligation, respectively. Subsequent cloning and expression of DsrJ in *E. coli* indeed confirmed the presence of three hemes, and EPR data showed the presence of partial His/Cys coordination to one of the hemes (His/Met is another possibility). From redox titrations, reduction potentials of the hemes were determined to be -20, -200, and -220 mV, respectively. Although the exact role of DsrJ is still unknown, its involvement in catalytic functions rather than in ET have been hypothesized.[182]

Other examples of multi-heme cyts *c* include, a tetra-heme cyt *c* (NapC) involved in nitrate reductase from *Paracoccus denitrificans (P. denitrificans)*,[305] an Fe(III)-induced tetra-heme flavocytochrome c_3 (Ifc_3)[306] in fumarate reductase (Fcc_3) from *Shewanella frigidimarina*, in hydroxylamine oxidation in *N. europaea* by a hydroxylamine oxidoreductase (HAO) containing eight heme groups,[307] and a penta-heme nitrite reductase (NrfA) for nitrite reduction in *Sulfurospirillum deleyianum*.[308,309] A periplasmic flavocytochrome c_3 which is an isozyme of the soluble Fcc_3 is also induced by Fe(III).[310-312] X-ray structure of this protein shows that the tetra-heme arrangement in Fcc_3 includes an intriguing heme pair where the two irons are only 9 Å from one another and the closest heme edges are within 4 Å (Figure 8).

The four hemes from Ifc_3 and Fcc_3 can be superimposed on four of the eight hemes in HAO.[307] All four hemes of Ifc_3 overlay on four of the hemes from the penta-heme NrfA,[308] and all five hemes from NrfA overlay on five of the HAO hemes. Lastly, two hemes from Ifc_3 overlay on two of the four hemes from of cyt c_{554},[122] from *N. europaea,* all four hemes of which overlay on four hemes from HAO. Despite such similarities in heme arrangement there is no resemblance in the primary structure of

these enzymes. Nevertheless, such similar heme arrangements in these proteins suggest that they share a common ancestor, but have evolved divergently to perform four different reactions *viz.* Fe(III)-reduction, fumarate reduction, hydroxylamine reduction, and nitrite reduction.[313] Some membrane-bound multi-heme cytochromes, belonging to NapC/NirT family, contain four heme binding sequences that have evolved due to gene duplication of di-heme domains.[314] In NapC and CymA all four hemes are 6cLS with bis-His axial ligation and display a reduction potential of +10 mV and -235 mV, respectively.[305,313]

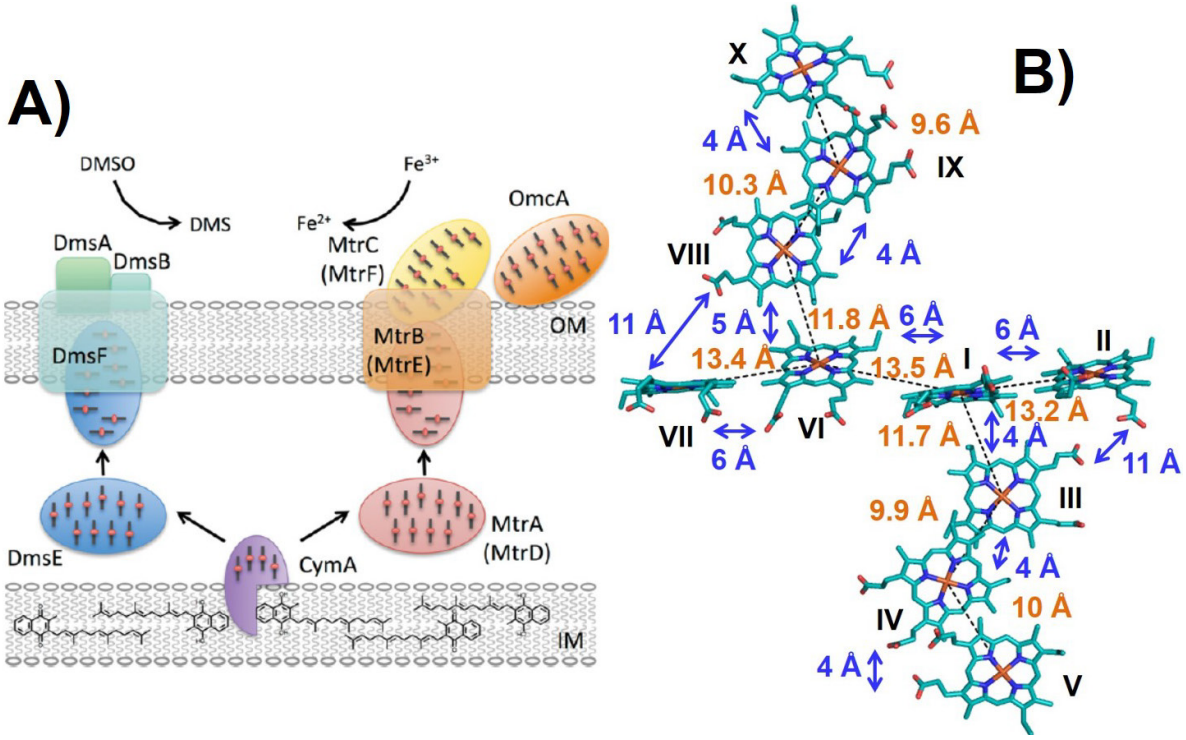

Figure 9. A) A schematic model for DMSO reduction by DmsEFAB and iron reduction by MtrABC(DEF). Flows of electrons are shown with arrows. DmsE and MtrA(D) are proposed to accept electrons from the menaquinone pool via CymA. Multi-heme groups in CymA, MtrACDF and DmsE are shown. IM = inner membrane; OM = outer membrane. B) "Staggered-cross" orientation of the hemes in outer membrane decaheme MtrF (PDB ID 3PMQ). Heme numbering is shown in Roman numerals, heme-iron distances in orange, and distances between heme edges are shown in blue. A is reproduced with permission from ref[315]. Copyright 2012 the Biochemical Society. B is adapted from ref [316]. Copyright 2011 National Academy of Sciences, USA.

Shewanella oneidensis MR-1 is a facultative anaerobe that is capable of using many terminal electron acceptors such as DMSO or metal oxides such as ferrihydrite and manganese dioxide outside the outer cell membrane, accepting electrons from the quinol pool and the tetra-heme protein CymA.[317-325] Electron transfer in *Shewanella oneidensis* MR-1 is facilitated by two periplasmic decaheme cyts *c*, DmsE which supplies electrons to DMSO), and MtrA, which is involved in electron transfer to metal oxides (Figure 9). Both of these decaheme proteins have been proposed to be involved in a long range electron transfer across a ~300 Å 'gap'[326] (~230 Å periplasmic gap, and ~40-70 Å thick outer membrane). Using protein film voltammetry, a potential window between -90 and -360 mV and an ET rate of ~122 mV s^{-1} was measured for DmsE at pH 6.[315] The measured reduction potential window for DmsE is shifted ~100 mV lower than what was observed in MtrA,[327-329] although the rate of electron transfer is similar in both proteins. Although the MtrA and DmsE families of decaheme proteins facilitate long range electron transfer in *Shewanella oneidensis*, it is not clear how electron transfer is feasible across a 300 Å gap, especially given the fact that MtrA spans only 105 Å in length.[330] Clearly the arrangement of hemes must play a crucial role; however, the exact mechanism of this electron transfer process is yet to be known. A recent NMR study proposes the presence of two independent redox pathways by which the electron transfer occurs from cytoplasm to electron acceptors on the cell surface across the periplasmic gap in MtrA,[331] one involving small tetra-heme cyt *c* (STC), and another involving FccA (flavocytochrome *c*). Both of these proteins interact with their redox partners CymA (donor), and MtrA (acceptor) through a single heme and show a large dissociation constant for protein-protein complex formation. Together, these facts suggest that stable multi-protein redox complex spanning the periplasmic space does not exist. Instead, electron transfer across the periplasmic gap is facilitated through the formation of transient protein-protein redox complexes.

MtrF is a decaheme *c*-type cytochrome found in the outer membrane of *Shewanella oneidensis* MR-1 (Figure 9) which has been proposed to transfer electrons to solid substrates through the outer membrane, like its homologue MtrC, with the help of periplasmic MtrA and a membrane barrel protein MtrE that facilitates electron transfer

by forming contact between MtrA and MtrF.[332,333] A recent crystal structure of MtrF shows that the protein consists of four domains, domains I and III containing β-sheets and domains II and IV being α-helices.[316] The arrangement of the ten bis-His ligated hemes is like a “staggered cross” where four hemes (I,II,VI,VII) are almost coplanar with each other and are almost perpendicular to a pair of three hemes (III,IV,V and VIII,IX,X) that are parallel to each other (Figure 9).

The reduction potentials of the hemes in MtrF lie in the range of 0 to -312 mV as determined by both solvated and protein film voltammetry. Unfortunately, reduction potentials of individual hemes have not been possible to assign due to their similar chemical nature. Molecular dynamics simulations show an almost symmetrical free energy profile for electron transfer. Additionally, the computed reorganization energies range of 0.75 to 1.1 eV, is consistent for partially solvent exposed heme cofactors capable of overcoming the energy barrier for electron transfer.[334,335] Further molecular details of electron transfer in MtrF are unknown.

Multi-heme cyts *c* also act as electron transfer agents in the Fe(III)-respiring genus *Shewanella.*[299] However, due to the fact that Fe(III) is soluble only at pH<2, these organisms face the problem of moving electrons from the cytoplasm across two cell membranes to the extracellular space to reduce the insoluble extracellular species. It has been proposed that these organisms circumvent this problem by employing a number of tetra-heme and decaheme cyts *c* which act as “wires” to transfer electrons between the inner and outer membranes.[313,336]

For tetraheme cyts c_3, hemes I and III are covalently attached to the protein segment by a conserved -Cys-Xxx-Xxx-Cys-His- sequence, while hemes II and IV are linked to the protein with the two Cys occurring in the sequence -Cys-Xxx-Xxx-Xxx-Xxx-Cys-His-.[337,338] Although the overall orientation of hemes is conserved, the order of heme oxidation varies from source to source.[217,339,340] The hemes in cyts c_3 display redox cooperativity, such that the reduction potential of one heme is dependent on the oxidation state of other hemes. The reduction potentials of the hemes in cyts c_3 are also dependent on pH, called the redox-Bohr effect,[340-342] due to the interactions of the heme propionates in hydrogen bonding network and/or with electrostatic interactions with the residues in the vicinity.[341,343-345]

Type I cyts c_3 are soluble, periplasmic proteins, and contain a patch of positively charged residues close to heme IV which have been proposed to interact with its partners.[346] This class of cyts c_3 mediates electron transfer between periplasmic hydrogenases and transmembrane electron transfer complexes where the electron acceptor is thought to be type II cyts c_3. Type II cyts c_3 are structurally similar to those of type I, but lack the lysine patch.[347] It was proposed that type I cyts c_3 receive electrons from hydrogenase and deliver them to type II cyts c_3. Recent experimental evidence shows that these two types of cyts c_3 form complex with each other and are indeed physiological partners, but type I cyts c_3 transfer only one electron to type II cyts c_3 in solution.[348,349]

2.3.7. Cytochromes b_5

Cyts b_5 are ET hemoproteins containing bis-His ligated *b*-type hemes, and are found ubiquitously in bacteria, fungi, plants, and animals. Cyts b_5 display reduction potentials that span a range of ~400 mV.[350-353] Mitochondrial and microsomal cyts b_5 are membrane-bound while those from bacteria and erythrocytes are soluble. In addition, there are various cyt b_5-like proteins that act as redox partners in various enzymes such as flavocytochrome b_2 (L-lactate dehydrogenase), sulfite oxidase, assimilatory nitrate reductase, and cyt b_5/acyl lipid desaturase fusion proteins. The structures of cyts b_5 from various sources reveal that there are two hydrophobic cores on each side of a beta sheet and belong to the α+β class (Figure 10).[350] The larger hydrophobic core contains the heme-binding crevice while the smaller hydrophobic core is proposed to have only a structural role. About 3% of deoxy hemoglobin in adults is oxidized to inactive methemoglobin.[354] Soluble cyts b_5 in erythrocytes reduce methemoglobin to functionally reduced deoxy form that binds oxygen. For this reaction electrons are transferred from NADH to methemoglobin via NADH cyt b_5 reductase and cyt b_5.[355] Microsomal cyts b_5 are found in the membranes of endoplasmic reticulum anchored to the membrane by a stretch of 22 hydrophobic residues.[353] Microsomal cyts b_5 and are known to function by transferring electrons in fatty acid desaturation, cholesterol biosynthesis, and hydroxylation reactions involving cyts P450.[356]

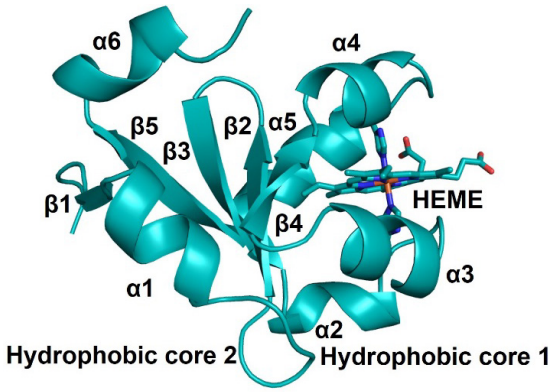

Figure 10. Schematic representation of the x-ray structure of bovine cyt b_5 that belongs to α+β class (PDB ID 1CYO). Two hydrophobic core domains, 6 α-helices, 5 β-strands, and 6c bis-His ligated heme are shown. Adapted with permission from ref [357]. Copyright 2011 American Chemical Society.

Two different forms of cyt b_5 have been detected in rat hepatocyte; one is associated with the membrane of the endoplasmic reticulum (microsomal, or Mc, cyt b_5) while the other is anchored to the outer membrane of liver mitochondria (OM cyt b_5).[358-362] These two types of cyt b_5 display a reduction potential difference of 100 mV (-107 mV for OM cyt b_5,[187,363] -7 for Mc cyt b_5).[180] The rat OM cyt b_5 is involved in the reduction of cytosolic ascorbate radical using NADH as the electron source.[364,365] The mammalian OM cyt b_5 and Mc cyt b_5 have three different domains, an N-terminal hydrophilic domain that binds the heme, an intermediate hydrophobic domain and a C-terminal hydrophilic domain. The N-terminal heme binding domains for both types of cyts b_5 have very similar structural folds consisting of six α-helices and four β-strands. The heme is bound in a pocket formed by four α-helices and a β-sheet formed by two of the β-strands.[141,366] Studies relating to the complex formation and electron transfer rates between cyts b_5 and its redox partners suggest that the nature of interactions between two proteins is primarily electrostatic in nature and the heme edge of cyts b_5 make contacts with electron donors and acceptors.[350] Within this general area, there are multiple overlapping sites with which cyts b_5 interact with its various partners.

A gene encoding a cyt b_5-type heme from the protozoan intestinal parasite *Giardia lamblia* was recently cloned into *E. coli* as a soluble protein.[367] Spectroscopic properties of this cloned cyt b_5 are similar to those of the microsomal cyts b_5 and

homology modeling suggests the presence of bis-His ligated heme. Residues near heme binding core from *Gialdia* cyt b_5 are comprised of charge amino acids and differ from other families of cyt b_5. The reduction potential of the heme was determined to be -165 mV.

2.3.7.1. Heme Orientation Isomers in Cytochromes b_5

Solution NMR studies of the soluble fragment of cyt b_5 suggested the coexistence of two different species that contained two orientation isomers (forms A and B, Figure 11) of heme that are related by a 180° rotation about an axis through the heme α,γ-meso carbon atoms.[368-372]

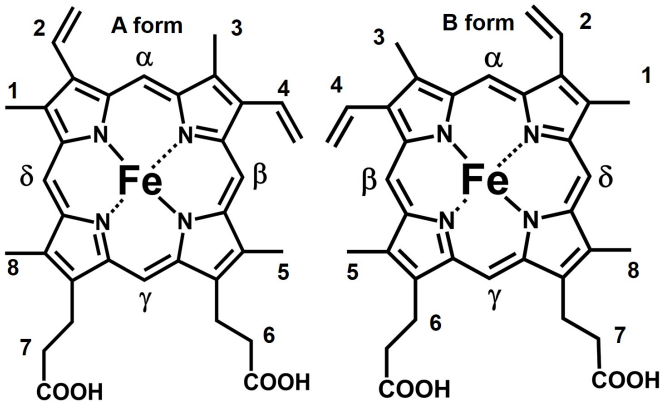

Figure 11. Two orientation isomers (A and B forms) of heme observed in solution studies of the soluble fragment of cyt b_5. The two isomers are related by a 180° rotation around the α,γ meso carbon atoms.

The relative population of the two isoforms A and B varies from species to species. In bovine and rabbit, the A/B ratio is ~10/1,[177,368,370,373] 20/1 in chicken cyt b_5,[374] 6/4 in rat Mc cyt b_5,[374] and 1/1 in the OM cyt b_5.[375] Even though reconstitution of apo cyt b_5 with heme resulted in the initial formation of 1:1 ratio of species A and B, they converted back to the proportion found in the thermodynamically stable native state after some time.[370,373] Reduction potentials of +0.8 mV and -26.2 mV were calculated for the isoforms A, and B, respectively, from spectroelectrochemical titrations.[177] Interaction between 2-vinyl group and side chains of residues 23 and 25 was initially thought to be the driving factor that dictated the heme orientation isomers.[368,374,376] This

theory was disputed in later studies.[375] It is now generally accepted that the heme itself can adapt to the surrounding environment by a rotation of the porphyrin plane around an axis perpendicular to the iron which is proposed to be the determining factors that caused the different heme orientation in species A and B.[376-378] Several studies have indicated that residue H39 is the major determining factor of the electronic state that orients the molecular orbitals for easy electron transfer through the exposed pyrrole ring III and meso-carbon heme edge.[370,379,380]

2.3.8. Cytochrome b_{562}

Cyt b_{562} is a 106-residue monomeric heme protein of unknown function found the periplasm of *E. coli* It is a four-helix bundle protein where the helices are oriented anti-parallel to each other (Figure 12).[381,382]

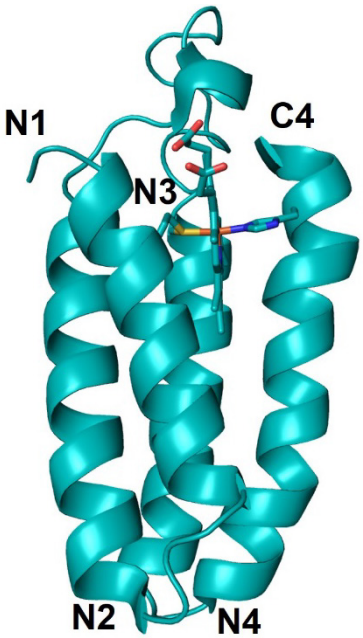

Figure 12. NMR structure of the anti-parallel four-helix bundle cyt b_{562} (PDB ID 1QPU). His/Met axial coordination to the heme iron is shown.

The protein has a noncovalently bound 6cLS heme with His102 and Met7 axial ligands, even though this protein is structurally homologous to cyt *c'* that contains a covalently bound 5cHS *c*-type heme. In the oxidized unfolded state, the heme of cyt b_{562}

is converted to 5cHS with His102 as the only axial ligand.[383] The folding properties of this protein are highly dependent on pH. At pH 7 the reduction potential of the heme in the folded state is 189 mV, while that of the unfolded state is -150 mV suggesting that the reduced state has a greater driving force for folding than the oxidized state.[176,384-387] Unfolding of the oxidized state of the protein occurs reversibly with a midpoint GuHCl concentration of 1.8 M, while the reduced state shows irreversible unfolding at >5 M GuHCl due to heme dissociation. Folding of the reduced state has been shown to be triggered by photo-induced electron transfer to the oxidized form of the protein under 2-3 M GuHCl concentrations. A folding rate of 5 μs was extrapolated in the absence of denaturant, which is similar to the intrachain diffusion time scale of the polypeptide.[388]

2.4. Designed Cytochromes

In addition to studying native systems by a top-down approach, in recent decades, many groups have adopted a bottom-up approach of building minimal functional proteins that mimic natural ones. The theoretical simplicity and ubiquity of cytochromes has made them appealing targets for design, and a number of artificial cytochrome-mimicking proteins have been engineered, with varying levels of sophistication. In this issue of Chemical Reviews, Pecoraro and coworkers give a thorough review of protein design strategies and successes, including designed heme electron transfer proteins. Here, we give a brief account focusing on the redox properties of designed six-coordinate heme proteins mimicking electron transfer cytochromes.

2.4.1. Designed cyts in De novo designed protein scaffolds

Two *de novo* heme proteins called $VAVH_{25}$(S-S) and retro(S-S)[389] were designed to bind heme in a bis-His coordination, by strategically engineering His residues into the *de novo* cystine-crosslinked, homodimeric four helix bundle called α_2, originally designed by the DeGrado lab.[390-392] Both sequences yielded artificial cytochromes with dissociation constants for heme in the sub-micromolar range, and spectroscopic properties of these proteins were consistent with low-spin bis-imidazole ligated heme, with reduction potentials of -170 mV and -220 mV for each of the proteins. Although

these potentials are nearly unchanged from the potentials of bis-imidazole heme in aqueous solution, presumed to be due to the “molten globular” state of the protein, the success of incorporation demonstrated the power of rational *de novo* design and set the stage for rapid development of more complex and native-like structures. Using an alternative tetrameric protein scaffold, consisting of two pairs of disulfide linked alpha-helices, a series of proteins mimicking the heme-b domain of cytochrome bc_1 were also designed by strategic placement of histidine residues. The designed proteins incorporated either two or four hemes per bundle,[393] with potentials of the individual sites reported to range from -230 mV to -80 mV in the tetra-heme construct. More impressively, the sites showed cooperative redox properties, with the presence of a second ferric heme site proposed to raise the potential of the first ~115 mV through electrostatic interactions (*vide infra*).[393,394] In a systematic study of the electronic properties of this scaffold, varying the heme, pH, and local charge, could achieve a potential range of 435 mV (-265 mV to +170 mV),[395] over half the 800 mV range covered by native cytochromes. Interestingly, investigation of the more natural mutation of one of the His ligands with a Met resulted in only a 30 mV increase in reduction potential, and substitution of heme *b* with heme *c* gave no significant change.[396] Rational mutagenesis of several core residues, as well as incorporation of helix-turn-helix and asymmetric disulfide bonds further improved the structural rigidity and uniqueness of the designed scaffolds.[397,398] Subsequently, this maquette system was extended in a variety of ways to achieve coupling to electrode surfaces,[399] incorporation of non-natural amino acid ligands,[400] and binding two different hemes – which mimics the structure of ba_3 oxidases.[401] Particularly exciting is the demonstration of coupling of electron transfer and protonation of carboxylate residues on the protein,[402-404] which is relevant for understanding and engineering proton pumping.

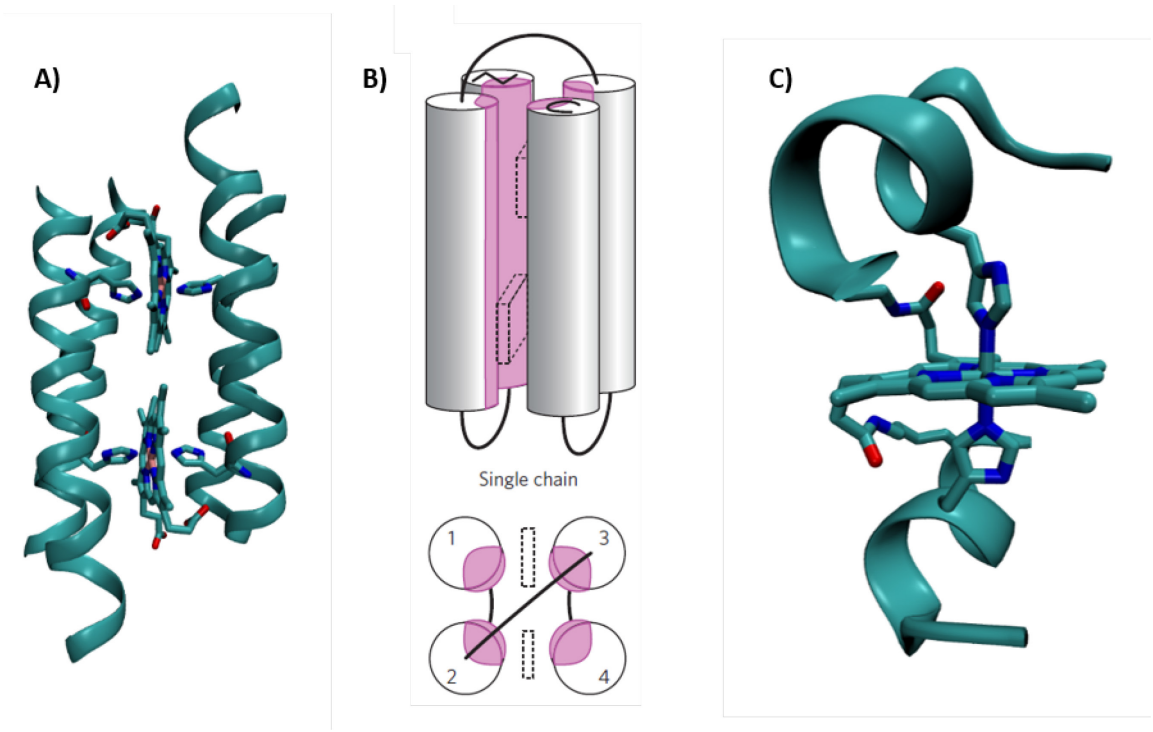

Figure 13. Structural models of designed cytochrome models in de novo scaffolds. (A) A design model for a homodimeric four-helix tetraheme binding protein inspired by cyt. bc_1. Remade from coordinates courtesy of G. Ghirlanda and W. F. DeGrado.[405] (B) Schematic representation of monomeric 4-α-helix maquettes used to mimic electron transfer cytochromes. **Reprinted by permission from Macmillan Publishers Ltd: [Nature Chemical Biology] [406], copyright (2013).** (C) Crystal structure of Co(II) mimichrome IV (PDB 1PYZ).[407]

Based on recent developments in structural understanding of cytochrome bc_1 and improvements in computational modeling, Ghirlanda et al. investigated designing a more structurally unique mimic of the bc_1 complex. The structure of the heme-b binding portion of bc_1 was modeled as a coiled-coil, and secondary coordination sphere interactions to the coordinating histidines, such as conserved Gly, Thr, and Ala residues, were added to stabilize the orientation of the His ligand and tune its electronic properties (Figure 13A).[405] The potentials were measured by CV as -76 and -124 mV in the oxidative and reductive directions at pH 8, significantly higher than the potential of aqueous bis-imidazole heme and earlier bis-His ligated designed proteins. The hysteresis in the potentials is attributed to conformational reorganization of the ligating His residues between the oxidized and reduced forms. The model was further improved

by linking and expression as a single chain for more efficient structure determination studies,[408] as well as incorporation into a membrane.[409]

Most recently, Dutton and co-workers have reported the design and thorough characterization of a monomeric, single-chain 4-α-helix bundle maquette protein, which can bind up to two hemes (Figure 13B). It is particularly noteworthy for the subject of this review that the redox properties of this scaffold as a function of charge distribution were systematically analyzed. By raising the total charge uniformly from -16 to +11, the reduction potential of both hemes changed from -290 mV to -150 mV, as expected. Furthermore, the potentials of the hemes could be changed individually, by only increasing the charge at one end of the protein; the potentials of the individual hemes were -240 and -150 mV. Finally, it was demonstrated that the reduced negatively charged protein could transfer an electron to native cytochrome c with rate constants approaching those of in native photosynthetic and respiratory electron transport chains. Such a single-chain 4-helix bundle was also used to build an artificial oxygen-binding cytochrome *c* with an intramolecular B-type electron transfer heme with a 60 mV lower reduction potential, mimicking a natural electron transfer chain.[410]

More rational computational protein design algorithms have also been brought to bear on the *de novo* design of artificial cytochromes. Xu and Farid used the algorithm named CORE[411] to design a native-like four (27 amino acid) helix bundle that binds two to four hemes in a bis-His fashion.[412] The alpha-helical character was confirmed by CD and the binding affinity for the first two equivalents was determined to be in the micromolar range, while due to negative cooperativity, the remaining sites had K_d >3 mM. The measured potentials for the di-heme and tetraheme protein were -133 to -91 and -190 to -0110 mV, respectively.

While the rationally guided design strategies described above have been very successful, the lack of *a priori* knowledge about the necessary structural features for design of functional metalloproteins limits the scope of sequence and structure space that is probed by the strategy. As a complementary approach, Hecht and coworkers have utilized a semi-rational “binary code” library generation method to produce fifteen 74-residue sequences that formed helical bundles and bound heme,[413] one with sub-

micromolar affinity, although the complexes adopted poorly ordered, “molten-globular” structures. Extending this scaffold further produced five 102-residue sequences with higher stabilities and more “native-like” structures.[414] Analysis of a handful of these proteins revealed spectroscopic features typical of low-spin heme proteins and reduction potentials ranging from -112 to -176 mV.[415] Furthermore, it was demonstrated that at least one construct was electrically competent on an electrode.[416] A similar semi-rational combinatorial approach was utilized by Haehnel and coworkers, who combined it with template-assisted synthetic protein (TASP) methods, in which two sets of anti-parallel helices are template onto a polypeptide ring, to design and screen an impressive library of 399 cytochrome *b* mimicking four-helix bundles.[417,418] Using a colorimetric screen, the potentials were estimated to range from -170 to -90 mV. It was also demonstrated that the proteins could be incorporated onto electrodes[419,420] and achieved estimated electron transfer rate constants comparable to native cytochromes.

A number of smaller, water-soluble peptide-based cytochrome mimics have also been developed, utilizing one or two short alpha-helical peptides. Two groups independently developed heme compounds with covalently attached, short alpha-helix-forming peptides, with His ligands. In one case, peptide sandwiched mesoheme (PSM) compounds were prepared by covalently attaching a 12-mer peptide to each of the two propionate groups of the heme via amide bonds with lysine groups on the peptide.[421] Although the helicity of the free peptide was low, upon ligating the heme, the helicity was seen by CD to increase to ~50% and the electronic spectra were consistent with bis-His heme ligation, similar to *b*-type cytochromes.[421,422] Further work suggested that aromatic sidechain interaction with the heme, such as Phe and Trp improve helix stability and heme binding,[423] and covalent linkage of the peptide termini via disulfide bonds resulted in further stabilization. [424] Studies of the redox properties of a PSM and a mutant with an Ala to Trp mutation, PSM^{W}, highlight the importance of stability in determining reduction potential, with more stable helix binding in PSM^{W} lowering the reduction potential 56 mV (-281 mV to -337 mV), due to the increased ability of the His ligands to stabilize the Fe(III) state.[425] The authors propose that this effect may also explain the difference in potential between mitochondrial and microsomal cyts b_5.

Similarly, short alpha-helical peptides, based on the heme binding peptide fragment of myoglobin, have been covalently attached to deuteroheme by a similar amide-bond attachment strategy, yielding compounds known as mimochromes.[426] It is noteworthy that the peptides retained their alpha-helical character even in the absence of heme binding.[426,427]. The stability of the model was further improved in later revisions by enhancing the intramolecular interpeptide interactions by extending the peptide (mimochrome II),[428] or rational mutagenesis (mimochrome IV).[429] A crystal structure of the Co(II) derivative of mimochrome IV has been obtained and substantiates the designed structure (Figure 13C).[407] The reduction potential of Fe-mimochrome (IV) at pH 7 is -80 mV, though it exhibits strong pH dependence over the range of pH 2 to 10 (~+30 to -170 mV).[429] The low pH dependence is attributed to the His ligands unbinding from the heme, while the high pH transition is proposed to be caused by deprotonation of a nearby arginine, however this is surprising due to the 4 orders of magnitude higher apparent acidity and requires further investigation to be proven. Still, it is exciting that this simple mimic is well folded enough to be crystallized and has a potential in the range of native cytochromes.

Intermediate between these covalently attached heme-peptide models and full polyhelical bundles described above, heme protein complexes consisting of heme ligated by designed short peptides that are not covalently attached have also been developed.[430-434] Studies on the binding of a variety 15-mer peptides showed a strong correlation between peptide-heme affinity and reduction potential (-304 mV to -218 mV), with lower potentials for more stable complexes, consistent with the results of studies on PSMs.[425,431] The overall low potential was attributed to the inability of the small peptides to reduce the strong dielectric constant of the solvent, as native proteins do (*vide infra*). In order to further improve the stability, two peptides were covalently linked at both ends by disulfide ligands, resulting in a series of cyclic dipeptide heme binding motifs, with reduction potentials ranging from -215 to -252 mV.[433]

Interestingly, in a step away from the helix bundle paradigm, Isogai and coworkers were able to rationally design a series of *de novo* proteins that would fold into a globin fold, but with only ~25% sequence identity to sperm whale myoglobin. [435,436] Although the proteins were designed for a 5-coordinate myoglobin-like heme binding

site, the resulting proteins were consistent 6-coordinate bis-His ligated heme. In these scaffolds, the reduction potential was in the range of -170 to -200 mV, similar to aqueous bis-Im heme, which was attributed to higher solvent access to the heme due to the molten-globular state of the proteins. This was further supported by the re-engineering of a non-heme globin protein, phycocyanin, into a heme-binding protein (*vide infra*), which had a more unique, hydrophobic, and native-like core structure, and 50 mV higher reduction potential.[437]

2.4.2. Designed cytochromes in natural scaffolds

As suggested above, in addition to designing scaffolds for cytochromes *de novo*, an appealing alternative strategy is to make use of the diversity of natural proteins as scaffolds. One of the most straightforward approaches is to convert a non-cytochrome heme-protein into a cytochrome by site directed mutagenesis. Along these lines, various myoglobins have also been redesigned into bis-His cytochrome-like proteins, similar to b_5, by mutating the near-by valine at position E11 to histidine (Figure 14A).[438-440] The spectroscopic features of reduced and oxidized forms of these mutants are consistent with low spin bis-Histidine ligated heme and the crystal structure confirms the ligation.[440] The mutations result in a 170 mV decrease in reduction potential of myoglobin, from ~60 mV to ~-110 mV.

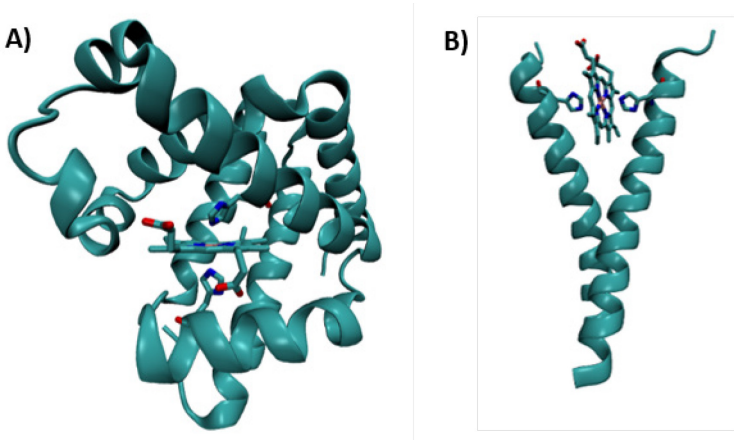

Figure 14. Structural models of designed cytochrome models in native scaffolds. (A) X-ray crystallographic model of a pig-myoglobin designed to have cytochrome-like bis-His ligation (1MNI).[440] (B) Molecular dynamics model of a histidine mutant of the membrane protein, glycophorin A, designed to bind heme in a cytochrome-like manner.[441] Coordinates provided courtesy of G. Ghirlanda.

Similarly, natural non-heme proteins can also be designed to bind heme in a manner consistent with the cytochrome-binding motif. As briefly mentioned above, Isogai and coworkers introduced two histidines into the natural non-heme plant globin phycocyanin[437] to generate a heme binding site, Although the protein was designed as a myoglobin mimic, the spectral features were consistent with low-spin bis-His coordination, similar to cytochromes *b*, with a one electron reduction potential of -120 mV.

Heme binding sites have also similarly been designed into native alpha-helical bundle proteins that do not have native heme binding sites. Starting with the DNA binding protein, rop, a specific bis-His heme binding protein was designed by removing surface histidines and introducing two internal histidine residues.[442] An alternative His-Met binding mode was also investigated. [443] Both proteins displayed electronic spectra characteristic of low spin heme, with reduction potentials of -155 mV and -88, respectively. A cytochrome-like heme binding site was also designed into the transmembrane protein Glycophorin A by Ghirlanda and coworkers (Figure 14B).[441,444] Each of the proteins bound heme with sub-micromolar affinity, and the presence of aromatic phenylalanine residues near the heme lowered the reduction potential from -128 to -172 mV.

2.4.3. Conversion of one cytochrome type to another

In addition to designing cytochrome sites in non-cytochrome proteins, several groups have investigated the conversion of one type of cytochrome into another.[445-449] Conversion of c-type to b-type cytochrome has been achieved in cytochrome c_{552}, by removing the Cys residues in the -Cys-Xxx-Xxx-Cys-His- heme binding motif with the C11A/C14A double mutation.[447] CD and NMR spectra confirmed that the structure of the protein and heme site was maintained. [447,450] However, it was found that the

removal of the c-type heme-binding motif destabilized the protein toward chemical and thermal denaturation. While electron withdrawing potential of the vinyl groups of heme b relative to the thioether groups of heme c would be expected to raise the potential[80], the resulting protein had a reduction potential of 170 mV, 75 mV lower than wild type, suggesting that the electronic structure of the porphyrin is not the major determinant of the reduction potential difference between cytochromes *c* and *b*.

Conversion from cyt b_{562} to c-type heme has been achieved by introducing the conserved -Cys-Xxx-Xxx-Cys-His- motif into the wild type protein by means of two mutations (Arg98Cys and Tyr101Cys).[449,451] The resulting *c*-type cytochrome displayed enhanced stability towards chemical denaturants, maintaining the same protein fold and axial His ligation. C-type heme attachment has also been achieved in cytochrome b_5 by introducing a surface cysteine residue with the Asn57Cys mutation.[448] The resulting holo protein was isolated in four forms, with distinct forms of heme, one of which, contained covalently attached heme and a hemochrome α-band at 553 nm, intermediate between that of b-type (556 nm) and c-type (551) heme, suggesting the presence of a single c-type thioether linkage. NMR further confirmed the stereochemical nature of this linkage and the protein displayed a reduction potential of -19 mV, 23 mV lower than wild type b_5.

2.5. Features controlling redox chemistry of cytochromes

Being involved in distinct electron transfer pathways, each cytochrome has evolved its electron transfer properties to match its redox partners. Therefore, reduction potentials of cytochromes span a range of almost 1V, from -475 mV in bacterioferritin from *A. Vinelandii*[192,452] to +450 mV in the heme c of di-heme cytochrome *c* peroxidase of *N. Europaea*[153,154] vs. SHE.[453] Through a variety of studies, many properties have been found to be important in determining the redox properties of heme proteins. As expected, the molecules in the first coordination sphere of the iron, namely the four pyrrole groups of the porphyrin and the axially coordinating residues, are important in determining the baseline reduction potential, as they interact directly with the iron center. These interactions are also fine-tuned by the secondary coordination sphere – chemical moieties that interact with the primary coordination sphere ligands and adjust their

properties. Secondary coordination sphere interactions with the amino acid residue ligands, such as hydrogen bonding can cause strengthening or weakening of ligand-metal interactions. The overall charge as well as the electrostatic environment of the metal center, which is determined by the surrounding charge, dipole distribution, and solvent accessibility, also critically modulates the redox properties.

2.5.1. Role of heme type

It is known that *c*-type hemes tend to be found in cytochromes with more extreme potentials (much lower or much higher) relative to *b*-type, however it is unclear whether a direct causative relationship exists. One way to probe the role of the heme type in a way that is less dependent on other factors is to replace the heme in one protein with another. In studies of the *de novo* designed four-helix bundles, the strongest effect on reduction potential was attributed to the nature of the heme,[395] though unnatural hemes were used in the study. In the more natural protein cases, several groups have interconverted between b- and c-type hemes.[445-449] It has been found, however, that this interconversion shows little inherent effect on reduction potential[447,448] with no clear trend. For instance, it was found that converting the *c*-type heme in cyt c_{552} into a *b*-type heme by mutating away the conserved Cys residues lowered the reduction potential by 75 mV.[447] On the other hand, Barker, et al. showed that introducing a thioether bond between heme in cytochrome b_5 and the protein, and therefore converting the b-type heme into a c-type heme, also lowered the potential by 23 mV.[448] It is clear that the choice of heme c over heme b has little effect on reduction potential, and other effects, such as structural changes or solvent accessibility, may play a bigger role.

If the choice of heme *c* or heme *b* does not play a significant role in determining the reduction potentials of cytochromes, one may wonder why organisms invest in the energetically expensive process of synthesizing *c*-type linkages. Though the exact reason that Nature has chosen *c*-type hemes in certain proteins remains to be fully understood, several hypotheses have been proposed.[454-456] It is suggested that multi-heme cytochromes, such as c_3, with largely exposed hemes in close proximity may utilize heme anchoring as a strategy to ensure stable heme binding in the absence of well-defined hydrophobic interactions.[457] Similarly, the high-potential cyts *c*, with His-

Met coordination, may use covalent anchoring as a strategy to prevent heme dissociation due to the relatively weaker binding of methionine to ferric heme.[457] Alternatively, it is proposed that covalent heme attachment may help in protein folding and stability,[454,456] or may strengthen the Fe-His bond and help maintain a low-spin state.[456] Regardless, the choice of heme *c* over heme *b* likely does not itself directly tune the reduction potential in a significant or consistent way, but may allow the protein greater flexibility in achieving other functionality and tuning the potential by other means, such as solvent accessibility.

In addition to hemes *b* and *c*, heme *a* is a unique heme used for electron transfer in proteins such as HCOs. The heme incorporates two unique peripheral structural features, namely a hydroxyethylfarnesyl group and a formyl group, and these have been suggested to play a role in tuning the reduction potential of the heme. While heme *a* has been replaced with other hemes in a native system,[458] detailed studies of how this substitution affects the redox chemistry of the protein have not been reported. Using their *de novo* designed scaffold (*vide supra*), Gibney and coworkers,[459] have studied the redox properties of hemes *a* and *b*, as well as diacetyl heme and found that the electron withdrawing acyl groups increased the potential by ~160 mV. This effect can be fully accounted for by the 200-fold lower affinity of the ligands for the oxidized form over the reduced form of the heme and it is proposed that the hydrophobic farnesyl group serves to anchor the heme stably in the protein,[460] to compensate for the lower affinity of the ferric state.

2.5.2. Role of ligands

In addition to the heme type, the identity of the axial ligands sets the baseline potential for the reduction potential of cytochrome.[457] Between the two most common ligands (His and Met), it has been found that Met ligation generally raises the potential of the heme by ~100-150 mV, relative to His ligation.[461-463] However, contrary to this, early work by Sligar and coworkers found that redesigning bis-His cyt b_5 into a His-Met cyt *lowered* the reduction potential by ~240 mV. This opposite change in the reduction potential was attributed to the change in spin state of the heme, from low-spin bis-His to high-spin His-Met cyt.[464] More consistent with theory, it was demonstrated that

conversion of bis-His to His-Met ligation in cyts c_3 results in a reduction potential increase of 160-180 mV.[192] Similarly, using a proteolytic fragment of cyt *c*, it was found that methionine ligation in cyts *c* contributes 130 mV to the energy.[386] Conversely, a 105 mV drop in the reduction potential was observed when the methionine in cytochrome c_{551} was replaced with a histidine.[463] Interestingly, Hay and Wydrzynski[462] observed a 260 mV decrease in reduction potential when they substituted the native Met ligand in cyt b_{562} with His, yielding a typical bis-His cyt. This decrease is greater than the ~150 mV and the authors attribute it to destabilization of the fold and increased solvent exposure, which is known to significantly lower potential (*vide infra*). In contrast, an Arg98Cys and His102Met double mutant of the same protein, cyt b_{562}, shows 6cLS bis-Met axial ligation at low pH, with a reduction potential of +440 mV, ~180 mV higher than native His-Met cyt b_{562}.[465] The authors note that the effect of bis-Met ligation is likely to be slightly higher at ~200 mV, as they expect the *c*-type thioether heme linkage to lower the potential. The stereochemical alignment of the axial methionine ligands results in an almost axial symmetry of the heme, caused by a 110° change in the torsion angle between the sulfur lone pairs.[466] The reduction potential of this protein is 665 mV higher than that of the only other known bis-Met axial ligated heme system in bacterioferritin (-225 mV)[176] in which the ground state of the oxidized form of the heme is highly rhombic in nature.[120,121,467] Therefore, factors other than the differences in the ligand coordination are most likely to be involved to account for the reduction potential difference.[78] In general, all else being equal, the preference of soft methionine thioether for the softer ferrous heme over the harder ferric heme contributes to a ~100-200 mV increase in reduction potential over His ligation.

2.5.3. Role of protein environment

2.5.3.1. Solvent exposure

Consistently, one of the most important factors in raising the reduction potentials of the cyts is the extent of heme burial in the protein, or alternatively, the extent of solvent exposure of the heme.[178,187,386,457,468-473] The basis for this effect lies in the lower dielectric constant of proteins relative to aqueous solution, which significantly

destabilizes the charged ferric site over the neutral ferrous state of the heme. For instance, Tezkan et al. estimated that solvent exclusion accounts for ~240 mV of the potential increase in cyt *c*.[386] Similarly, a thorough computational study of heme proteins spanning an 800 mV range of potentials, Zheng and Gunner identified that heme solvent exclusion accounts for ~20% of the reduction potential difference between proteins.[457] Interestingly, the same study, found less correlation between the reduction potentials and the remaining individual factors or energy terms, yet the computation was able to faithfully reproduce and account for heme protein potentials over an 800 mV range. This study elegantly demonstrates that the reduction potential is determined by an intricate balance of numerous factors of comparable energy.

2.5.3.2. Secondary coordination sphere of ligand

Although the nature of the ligand itself determines primary interaction energies with the heme, and therefore is the primary determinant of the reduction potential, the electronic character of the ligand can be further modulated by secondary non-covalent interactions, such as hydrogen bonds. These so-called secondary coordination sphere effects have been shown to be influential in determining the potentials of a number of heme proteins, including cytochromes.[230,472,474-477] For instance, in cyt *c* in particular, Bowman et al. demonstrated that strengthening the hydrogen bond between the proximal His ligand and a backbone carbonyl through peripheral mutations resulted in an almost 100 mV decrease in the reduction potential, attributable to increased imidazolate character.[474] Similarly, Berguis et al. show in three different mutants of yeast iso-1-cyt *c* that a disruption of the hydrogen bond from a tyrosine 67 to the methionine ligand consistently decreases the potential by 56 mV, due to an increase in electron density on the Met sulfur stabilizing the ferric form of the heme,[230,476], and Ye, et al., found that the presence of hydrogen bonds between Gln64 and the axial Met ligand in *P. aeruginosa* and *H. thermophilus* cyt c lowered the potential by 15-30 mV.[477] In addition, aromatic interactions with the axial ligand have also been implicated in tuning the heme reduction potentials. For instance, it was shown that Tyr43, which interacts with the π system of His 34, and contributed a ~35-45 mV decrease in reduction potential.[478] Therefore, although the identity of the ligand is a primary

determinant of reduction potential of the heme, the secondary coordination sphere interactions to it also play a role of similar magnitude in determining reduction potential.

2.5.3.3. Local charges and electrostatics

Another important means by which cytochromes have been found to modulate their reduction potentials is through the judicious use of charge and electrostatic interactions. For instance, by comparison and selective mutagenesis of the structurally homologous cyts c_6 and c_{6A}, it was demonstrated that the interaction of the positive dipole of the amide group of a carefully positioned glutamine (residue 52 in c_6 and 51 in c_{6A}) with the heme is a strategy used by Nature to raise the reduction potential by ~100 mV.[479] Similarly, Lett et al. observed an increase in the reduction potential of cytochrome *c* by 117 mV through the Tyr48Lys mutation.[480] The Tyr48 is involved in a hydrogen bonding interaction with a heme propionate and it is likely that introduction of lysine at this position stabilizes the propionate negative charge and destabilizes the ferric heme state. It has also been shown that replacement of a neutral residue in contact with the heme in myoglobin with a polar or negatively charged residue can reduce the potential by up to 200 mV.[481] Furthermore, a library screen of cytochrome b_{562} mutants at four residues near the heme-binding site identified mutations that could gradually tune the potential over a 160 mV range.[482] Even relatively distant surface electrostatic interactions have been shown to control redox function of cytochromes.[483] These reports demonstrate the critical role of local charge in determining the reduction potential of the heme. In general, negative local charges stabilize the ferric state and lower the reduction potential, and the magnitude of this effect can be comparable to ligand substitution or ligand secondary coordination sphere effects.

In addition to charge interactions, more subtle effects such as electrostatic interactions can also play an important role in determining redox properties. As discussed in section 3.3.9 above, a conserved aromatic residue in cyt b_6f is found to be in contact with the heme *f* at position 4, and the identity of the aromatic residue differs between cyanobacteria and algae. Interconversion between Phe and Trp at this position accounts for about half of the 70 mV difference between these proteins.[161] The origin of this effect is attributed to differential interaction of the side-chain electrostatic potentials

with the porphyrin π system and the Fe orbitals. A similar effect has also been reported in cyt c_3, where a phenylalanine in contact with heme I is proposed to maintain its low potential by a π-π interaction with the porphyrin π system.[484]

Since many charged residues around the heme, such as Glu, Asp, Lys and Arg, as well as the heme propionate group itself, can be protonated or deprotonated depending on the pK_as of the residues and pH of the solution, protonation states of these groups will affect the reduction potential of the heme by preferentially stabilizing one redox state over the other. Therefore, the pH of the solution can have significant effects on the reduction potentials in various cytochromes.[342,485-490] For example, protonation of a heme propionate in cyt *c* contributed an increase of 65 mV to the reduction potential. [485] Similar effects of 60 mV and 75 mV have been reported in cyt c_{551}[491,492] and in cyt b_{559},[490] respectively. In cyt c_2, pH dependent reduction potentials covered a range of ~150 mV, between pH 4 and 10.[493] In their *de novo* designed maquette, Dutton and coworkers observed a 210 mV range of reduction potentials over a pH range of 3.5 to 10, and such a change was attributed to the involvement of Glu residues near the heme site.[494] Furthermore, the role of the propionate charge has been investigated specifically by studies in which the carboxylate groups have been neutralized to their ester form. An increase of reduction potential by ~60 mV was reported,[495,496] consistent with those obtained from the described studies above.

A special case of the effect of local charges on reduction potential is the cooperativity between near-by hemes in multi-heme cytochromes. [497] It is known that the presence of multiple hemes in various oxidation states greatly affects the macroscopic or observable reduction potentials of the hemes. For instance, it has been demonstrated in multi-heme cyt c_3 that interaction energy between hemes can shift the reduction potential by 50-60 mV.[498-500] It is suggested that this effect may be mediated by electrostatic interactions also involving local aromatic groups.[484] The cooperativity between hemes in multi-heme cytochromes is proposed to be a major factor in their reduction potential regulation.

In the cyt c_3, the redox-Bohr effect can result in pK_a differences of up to 2.8 pH units, and the coupling between protonation has been linked to cooperativity between the hemes, resulting in concerted two electron transfer steps.[340,501,502] On the other

hand, the pH dependent reduction potential difference, over a range of 10 pH units, can be ~200 mV.[503] In this organism, this property is crucial for proper charge separation to generate a promotive force that drives ATP synthesis.[343,504] Similarly, this coupling of proton and electron transfer plays a key role in the proton pumping mechanism of cytochrome *c* oxidase. Although there are several proposed mechanisms, they share the common theme that proton uptake to the heme sites and release into the P-side of the membrane is driven by charge compensation during electron transfer events from the low-spin to high-spin heme.[505-507] It is clear that local electrostatic interactions at heme redox centers are of immense physiological importance.

2.5.3.4. Heme distortion/ruffling

Another significant contributor to heme redox properties is the plasticity of the heme. It is now well known that heme distortion or ruffling plays an important role in the electronics of the porphyrins,[508,509] due to decreased delocalization of the π electrons.[510-516] While the phenomenon has been described in many heme proteins, including cytochromes,[512,513,515,517,518] thorough investigation of how it affects redox properties is limited. Recently, Marletta and coworkers demonstrated that protein induced heme-distortion can account for up to a 170 mV increase in potential in the heme nitric oxide/oxygen binding protein.[513] Furthermore, a basic computational model was implemented by Senge and coworkers and it was estimated that porphyrin distortion can account for 54 mV of the difference between hemes in a bacterial tetraheme cytochrome.[519] Further investigation is needed to gain a more detailed understanding of the role of heme distortion in the redox properties of typical cytochromes.

3. Fe-S redox centers in electron transfer processes

3.1. Introduction to Fe-S redox centers

Iron-sulfur proteins are among the oldest metalloproteins on earth. The early atmosphere, under which both sulfur and iron were abundant, enabled the spontaneous assembly of these two elements into clusters, mainly containing 4 iron and 4 sulfur atoms.[91,520] Early life took advantage of the redox properties of these clusters and used them as electron transfer and redox centers. Despite the later shift to a more oxidizing

environment on earth, the established Fe-S proteins continued to be used as electron carriers. Thus, these proteins are found ubiquitously throughout all kingdoms of life and play roles in crucial processes such as photosynthesis and respiration. The wide range of reduction potentials these proteins can accommodate, and their diverse structural motifs allow them to interact with different redox partners, acting as electron carriers in a variety of biological processes.[91-93]

The Fe-S proteins were first discovered in 1960s based on their unique g = 1.9 EPR signal that appears upon reduction and wasn't observed before for any metalloproteins. This discovery was aided by the abundance of these proteins, their unique spectral features, and often highly charged nature of the proteins, which made them easier to purify and analyze. Studies of these proteins were further facilitated by advances in molecular biology and recombinant protein expression, allowing the use of site-directed mutagenesis to unravel important features of these proteins and their function.

While Fe-S proteins are well known for their function as electron carriers, they are also known to be involved in the active sites of many enzymes, performing several functions[521] such as reduction of disulfide bonds and initiation of radical chain reactions,[522-526] or serving as Lewis acids.[525-528] In addition, Fe-S centers can simply function as structural elements that stabilize the protein or another active site in the protein.[529] Furthermore, the sensitivity of Fe-S proteins to an oxidative environment and their range of redox states make them good candidates for sensing oxidative and metal stress, and balancing the oxidative homeostasis of the cells.[93,525,530-533] Functions in DNA repair have also been reported for several Fe-S proteins.[532,534]. Finally it has been shown that Fe-S proteins can be used as a storage for sulfur or iron.[532] This review focuses exclusively on the ET function of the Fe-S proteins.

3.2. Classification of Fe-S redox centers and their general features

Fe-S clusters are often classified based on the number of iron and sulfur atoms in the cluster, as suggested by the Nomenclature Committee of the International Union of Biochemistry (IUB) in 1989[535]. In this convention, the elements of the core cluster (iron and inorganic sulfur atoms) are placed in a bracket with the oxidized level of the

core cluster shown as a superscript outside the bracket (e.g. $[2Fe\text{-}2S]^{2+}$). A comma or a slash in the superscript can show multiple possible oxidation states. A more expanded notation can be used to show the ligands and the overall charge of the whole cluster, including those ligands. Another common classification of Fe-S clusters, which is used in this review, is based on the protein type. This scheme classifies Fe-S sites not only based on the number of iron and sulfur atoms but also certain structural motifs and spectroscopic and electrochemical properties. In this classification, the Fe-S proteins are divided into major groups as follows: rubredoxins ([1Fe-4S]), ferredoxins (low potential [2Fe-2S], [4Fe-4S], [3Fe-4S], [3Fe-4S][4Fe-4S], and [4Fe-4S][4Fe-4S]), Rieske proteins (which are high potential [2Fe-2S] proteins), and high potential iron-sulfur proteins (HiPIP, which are high potential [4Fe-4S] proteins). In addition, we will also describe more complex Fe-S proteins that contain multiple Fe-S cofactors or Fe-S cofactors coupled with other cofactors, such as heme (Table 3).[92,93,523,526,529,536-540]

Though certain structural elements may differ between them, members of each class of Fe-S proteins usually consists of a common structural motif. Between classes the overall structure is distinct. Despite these overall structural differences, however, the geometries of the Fe-S clusters are quite similar, especially within each cluster class. The iron cofactor has a distorted tetrahedral geometry in almost all the Fe-S proteins. In case of proteins with more than one iron, the distance between S-S is usually 1.3 times longer than the Fe-Fe distance.[523,540] Each iron atom is coordinated by a total of four ligands, typically cysteine or inorganic sulfurs, although other ligands have been observed. For instance, in Rieske proteins two cysteine ligands have been replaced with histidine. In some [3Fe-4S] clusters, an aspartate serves as a ligand to iron. In certain enzymes such as aconitase, a hydroxyl group from solvent is shown to be one of the ligands. CO and CN^- have also been found to serve as ligands to the catalytic Fe-S cluster in enzymes with hydrogenase activity.[541]

Table 3 Classification of Fe-S proteins

Cluster	Class	Structure	Redox state	UV-vis (nm)	Transition	Total Spin (mms^{-1})	d
1Fe	Rubredoxin		$Fe^{2+/3+}$	311, 331, reduced *Cp*Rd; 350, 380, oxidized *Cp*Rd; 490 , 570, 750, oxidized *D. gigas* Rd;	Fe^{2+}	0.7	2
					Fe^{3+}	0.32	5/2
2Fe-2S	Ferredoxin	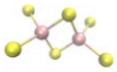	$[2Fe\text{-}2S]^{1+/2+}$	330,420, 436, 560,oxidized	$Fe^{3+}Fe^{2+}$	0.35, 0.65	1/2
				312, 350,390,540, oxidized	$2Fe^{3+}$	0.27	0
	Rieske	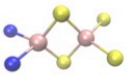	$[2Fe\text{-}2S]^{1+/2+}$	325, 458, shoulder at 560 -580 (oxidized)	$Fe^{3+}Fe^{2+}$	0.35, 0.65	1/2
				380-383, 425-433,505-550 (reduced)	$2Fe^{3+}$	0.27	0
3Fe-4S	Ferredoxin	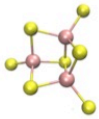	$[3Fe\text{-}4S]^{0/1+}$	Broad absorption at 380-400	$2Fe^{2.5+}1Fe^{3+}$	0.46.0.32	2
					$3Fe^{3+}$	0.27	1/2
4Fe-4S	Ferredoxin		$[4Fe\text{-}4S]^{1+/2+}$	Broad absorption at 380-400	$2Fe^{2+}2Fe^{2.5+}$	3/2, 0.5, 0.58	1/2
					$4Fe^{2.5+}$	0.42	0
	HiPIP		$[4Fe\text{-}4S]^{2+/3+}$	388, shoulder at 450 and 735	$4Fe^{2.5+}$	0.42	0
					$2Fe^{2.5+}2Fe^{3+}$	0.4, 0.29	1/2

While the geometry of Fe and its coordinating cysteine/sulfur ligands is very similar in all Fe-S proteins, the amino acid sequences and peptide motifs that accommodate these clusters differ significantly even in a given class, resulting in further categorization of each group. Interestingly, the ligands of Fe-S proteins usually reside within loop regions. This structural flexibility is important in accommodating the geometric requirement of the Fe-S clusters and thus minimizing reorganization energy required for rapid electron transfer. The iron site has large spin-polarization effects, strong Fe-S covalency, and spin coupling through inorganic sulfurs. The strong covalency and the delocalization features of Fe-S proteins result in low reorganization energy, mostly by lowering the inner sphere effects. Gas phase DFT calculations give the following reorganization energies for different Fe-S proteins: 0.41 eV (1Fe, Rd) < 0.45 eV(4Fe HIPIP) < 0.64 eV(4Fe Fd) < 0.83 eV (2Fe Fd).[542]

The sulfur atom has several advantages over other ligands for coordinating Fe: it can occupy 3d orbitals of the iron while the effects of its nuclear charge are not significant, and as a weak ligand, it can keep iron in a high spin state.[543] However, it imparts an intrinsic instability to the cluster, as sulfur is subject to oxidation. As a result, the iron-sulfur clusters are usually very sensitive to oxidation, hydroxylation, and other chemical modifications. In fact, one of the characteristic features of Fe-S clusters is their being “acid-labile”.[1] The protein provides a protective, hydrophobic environment around the Fe-S clusters, excluding solvent and improving stability.[523]

The Fe-S proteins have long been the focus of bioinorganic studies due to their rich electronic structure and magnetism. Presence of iron as the core redox active center provides researchers with a wealth of techniques to investigate this site, which are not easily applicable to most other redox active metals. A very intriguing feature of Fe-S proteins is the presence of mixed valence species, and these have been the subjects of extensive investigations. All common bioinorganic methods have been applied to study Fe-S proteins including EPR, ENDOR/ESEEM, 1D and 2D NMR, XAS analysis, X-ray crystallography, Mössbauer, and CD/MCD. Information can be deducted even with simple electronic absorption spectroscopy techniques.[537,538,540]

3.3. Biosynthesis of Fe-S proteins:

In vitro studies have shown that Fe-S proteins can be reconstituted by addition of $FeCl_3$ and Na_2S in a reductive environment.[539,544-546] The presence of iron and sulfur in the solution is sufficient for formation of [4Fe-4S] cluster.[91] Despite the straightforward *in vitro* assembly, the assembly of Fe-S clusters *in vivo* is a more precise and complex process. Multiple experiments have been performed with the aim of elucidating the exact mechanism of assembly of different Fe-S clusters and every year, new discoveries are made in this field. Nif, Isc, and Suf cluster binding systems are the most common systems involved in *in vivo* assembly of Fe-S proteins. These systems are abundant in different organisms and many organisms have more than one of them. Briefly, all of these systems require a cysteine desulfurase to produce sulfur from L-cysteine, a scaffold that plays the role of a carrier for the formation of the cluster, and a carrier to transfer the cluster to the final protein. The source of iron remains to be

definitively elucidated. The Nif system is dedicated to maturation of nitrogenase and was first found in *Azotobacter vinelandii*. Isc and Suf systems, in contrast, are more general and homologues of these systems are found in mitochondria and chloroplast respectively. The two systems are conserved between bacteria and eukaryotes. The Isc system utilizes 5 proteins: IscU that acts as scaffold, IscS that generates sulfur from cysteine, HscA/B that facilitates the transfer of cluster to the protein, and the ferredoxin. Suf system composed of two subcomplexes: 1) SufBCD that can bind to and transfer [4Fe-4S] cluster to proteins. In this sub-complex, SufB acts as scaffold, SufD is important for iron entry, and SufC is an essential ATPase. 2) The SufSE sub-complex that acts as a heterodimer and donates sulfur to the cluster. SufS is the major component with cysteine desulfurase activity and SufE enhances its activity. Several classes of proteins are important in transferring the cluster to the apoprotein, but the so-called A type proteins are the most common among these. Recently, members of CIA machinery have been found as main components of Fe-S biogenesis in cytosol. Fe-S biogenesis is tightly regulated and correlated to oxidative and metal stresses. [520,547-554]

3.4. Native Fe-S proteins

3.4.1. Rubredoxin

3.4.1.1. Structural aspects

Rubredoxin (Rd) is the simplest among Fe-S proteins. It is a robust small protein usually composed of 45-54 amino acids with molecular weight of 6~7 kDa mainly found in bacteria, archaea, and anaerobes. It contains a mono iron center, coordinated by four cysteines from two C-X_2-C-G segments, with a distorted tetrahedral geometry (Figure 15a).[555,556] Sequence alignment reveals that the four cysteine residues are conserved in rubredoxins from different sources. Moreover, nearby glycine and proline residues, several aromatic residues like tyrosine, tryptophan, and phenylalanine, and two charged lysine residues are conserved as well. However, a novel rubredoxin has been identified in several members of the *Desulfovibrio* genus, possessing an N-terminal C-X_4-C segment.[557]

Rubredoxin from mesophilic *Clostridium pasteurianum* (*Cp*Rd) is among the most well studied members of the family,[556] and rubredoxin from hyperthermophilic archaeon *Pyrococcus furiosus* (*Pf*Rd) is one of the most thermal stable proteins with a melting temperature of 200°C. [558] The overall fold of rubredoxin is composed of a three-strand antiparallel β sheet with a hydrophobic core and two loops containing the coordinating cysteines with pseudo two-fold symmetry (Figure 15b). The loop carrying ligands Cys6 and Cys39 (numbering of *Cp*Rd), buried inside the protein, is more constrained by the rigid aromatic core of the protein. In combination with a bulky aliphatic residue (Ile/Leu/Val33), these conserved aromatic residues contribute to the stabilization of the overall three-dimensional structure as well as exclusion of water from the metal center.[559,560] Charged residues, mainly glutamate and aspartate, are distributed over the surface, and result in high solubility and a very acidic isoelectric point of about 4. The metal binding site is close to the protein surface, between the two binding-loops, and metal incorporation contributes to stabilization of the protein as well.

The two coordinating loops exhibit a pseudo-2-fold symmetry about the [Fe(Cys)$_4$] center with six NH…S H-bonds in a range of 3.5-3.9 Å. The Fe-S bond distances to the buried Cys6 and Cys39 ligands are slightly longer (2.28-2.30 Å based on three different rubredoxins) than those of Cys9 and Cys42, which are close to the surface (2.25-2.26 Å). This is possibly because Cys6 and Cys39 are involved in two H-bonds with the backbone amide of Thr7/Val8 and Pro40/Leu41, respectively, while Cys9 and Cys42 have only one H-bond donor each, from the backbone amide of Tyr11 and Val44, respectively (numbering of *Cp*Rd, Figure 15b).[561,562] Nine sp^3-hybridized C-H…S weak hypervalent interactions are identified by ^{13}C NMR in *Cp*Rd, which contribute to stabilization of the protein as well.[563,564] X-ray absorption near-edge spectral (XANES) fitting of the oxidized forms of recombinant *Cp*Rd at pH 8.0 give a bond length of 2.27(1) Å for Fe(III)-S,[562] comparable to the average bond length of 2.26(3) Å from crystal structures.[556]

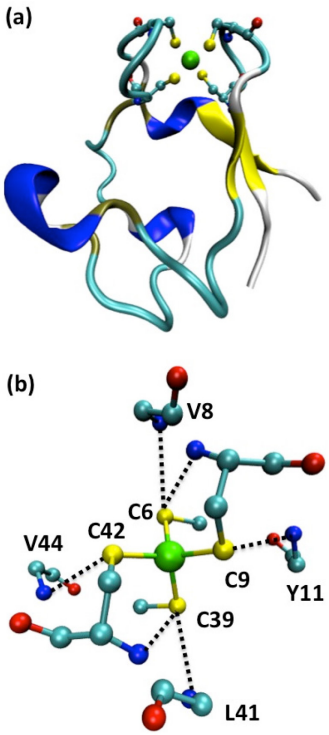

Figure 15. Crystal structure of *Cp*Rd, PDB code: 1IRO, at 1.1 Å resolution. (a) The overall fold of chain A of *Cp*Rd. The $Fe(Cys)_4$ center is displayed as a ball-and-stick representation. (b) The NH…S H-bond interactions around $Fe(Cys)_4$ center of *Cp*Rd. The side chain of C6, C39, V8, Y11, L41 and V44 are omitted for clarity. Color code: Fe, green; C, cyan; S, yellow, O, red; N, blue.

3.4.1.2. Function

The electron rich iron center of rubredoxin is redox active, and its Fe(II)/Fe(III) couple is involved in a variety of biological electron transfer processes.[565] No significant structural changes are observed by NMR and crystallographic studies when the ferric center is reduced. Slight lengthening of the Fe-S bonds by an average of 0.096 Å (*Cp*Rd),[566] 0.033 Å (*Pf*Rd),[555] or 0.012 Å (Leu41Ala *Cp*Rd)[567], as well as shortening of the cysteine involved H-bonds has been observed, consistent with the valence change of the metal center. DFT calculations reveal that the Fe-S center of Rd from *Desulfovibrio vulgaris* has low reorganization energy during oxidation due to high Fe-S bond covalency and large electronic relaxation, which makes it well suited for fast electron transfer.[568]

Rubredoxin from *Pseudomonas oleovorans* (*Po*Rd) forms an electron transfer complex with rubredoxin reductase (RR) in its physiological environment, and provides

a good system for studies of inter-protein electron transfer. *Po*Rd transfers electrons from RR to a membrane bound ω-hydroxylase for aliphatic and aromatic hydrocarbon oxidation. The electron transfer from NADH to Rd is gated by a rate limiting adiabatic step preceding the electron transfer step.[569-572]

Similarly, rubredoxin from *P. aeruginosa* is involved in alkane oxidation by transferring electrons from NAD(P)H via NAD(P)H:rubredoxin reductase to the terminal electron acceptor.[573] FAD-dependent NAD(P)H:rubredoxin reductase has been co-crystallized with RubA2(PA5350), an AlkG2-type rubredoxin from *P.* aeruginosa closely related to *Pf*Rd,[574] and diffracted to 2.45 Å. The shortest distance between redox centers has been determined to be 6.2 Å, which leads to an estimated maximum electron transfer rate in nanosecond range.[575,576]

Rubredoxin from *Desulfobrio gigas* is important in the oxidative stress defense system in anaerobic organisms, by functioning as the redox partner of NADH-rubredoxin oxidoreductase and rubredoxin-dioxygen oxidoreductase,[561,577-579] and transferring electrons from ferredoxin:NADP+ oxidoreductase to superoxide reductase to reduce O_2 or reactive oxygen species (ROS).[580-582] It also donates electrons to rubrerythrin or diiron SORs (i.e. rubredoxin oxidoreductase or desulfoferrodoxin, see section 3.4.2.4) to reduce hydrogen peroxide or superoxide respectively in *Desulfovibrio vulgaris*.[583]

Rubredoxin is an electron acceptor of carbon monoxide dehydrogenase and pyruvate ferredoxin oxidoreductase in *Chlorobium tepidum*,[584] and intracellular lactase dehydrogenase in *D. vulgaris Miyazaki F*.[585] Furthermore, nucleomorph-encoded rubredoxin has been discovered to associate with photosystem II (PSII), and proposed to branch electrons from PSII to plastid membrane-located pathways or replace some of the electron transfer proteins in photosynthesis machinery under certain circumstances.[586]

Rubredoxin also exhibits high electron self-exchange rates. For example, the k_{ese} of *Cp*Rd has been determined to be 3×10^5 $M^{-1}s^{-1}$ at 30 °C in 50 mM potassium phosphate at pH 7.[587] DFT calculations reveal that pathways through the two surface cysteines dominate in electron self-exchange process, and surface-accessible amides H-bonded to the cysteines play an important role as well.[568]

3.4.1.3. Important structural features

The reduction potential of the metal cofactor in a protein is generally determined by its ionization energy, electronic structure, reorganization energy and solvent accessibility during the redox process.[588] Specifically in the case of rubredoxin, the NH…S H-bonding interactions and water solvation of the active site are proposed to have significant influence on the reduction potential of the iron center. The reduction potentials of rubredoxins vary in the range of -100 to +50 mV vs. NHE (those of the model complexes are around -1V vs. SHE),[92,588-590] and can be divided into two categories by the residue at position 44 (Table 4).[590] Rubredoxins like mesophilic *Cp*Rd with lower reduction potentials have a Val residue at position 44 followed by Gly 45, while those like hyperthermophilic *Pf*Rd with higher reduction potentials (~50 mV difference) have an Ala residue at position 44 followed by Pro 45. Mutating Ala44 of *Cp*Rd to Val increases the reduction potential, and Val44 of *Pf*Rd to Ala decreases the reduction potential (Table 4). The short peptide Ala44Pro45 has higher backbone stability, and consequently, higher probability of orienting the backbone dipole towards the redox center.[591-595] No correlation between reduction potential and Fe-S bond covalency of *Cp*Rd and *Pf*Rd has been observed by sulfur K-edge XAS studies.[596]

Table 4 Reduction potentials for simple rubredoxins[a]

Class	*Source*	E_m, mV
I (V44)	*Clostridium pasteurianum*	- 77, - 53
	Chlorobium limicola[2]	- 61
	Butyribacterium methyltrophicum	- 40
	Heliobacillus mobilis	- 46
	Pyrococcus furiosus A44V	- 58
	Cp Pf chimeras[3]	- 46 to - 67
II (A44)	*Clostridium pasteurianum V44A*	- 24, + 31
	Pyrococcus furiosus	0 to + 31
	DesuEfovibrio vulgaris H[4]	0
	Desulfovibrio vulgaris M[5]	+ 5
	Desulfovibrio gigas	+ 6
	Megasphaera elsdenii	+ 23
	Cp Pf chimeras[3]	+ 63 to + 69

[1]*versus NHE.*
[2]f. sp. Thiosulfatophylum
[3]constructions of fused domains from *Clostridium pasteurianum and Pyrococcus furiosus*
[4]strain Hilden borough
[5]strain Miyazaki

[a]Reproduced from ref. [590], with permission from The Royal Society of Chemistry.

The reduction potential of rubredoxin is pH independent in the pH range of 5-10, but pressure and temperature dependent. The reduction potential of *Cp*Rd and *Pf*Rd have been reported to linearly decrease with increase of temperature (-1.6 mV/^{o}C and -1.8 mV/^{o}C, respectively) and decrease of pressure (0.028 mV/atm and 0.033 mV/atm, respectively).[597] The phenomena could be rationalized by the dielectric constant change of a solvent like water, which is lower at higher temperature and lower pressure, and consequently less efficient in protein solvation. Since the stability of a protein oxidation state is dependent on the solvent-solute interactions to neutralize the excess charge, the oxidized state of Rd with less net charge is more stable at high temperatures and low pressures.[598]

Replacement of one of the surface cysteines with serine in *Cp*Rd resulted in significant decrease of reduction potential by up to 200 mV, while for internal cysteines only a 100 mV decrease was observed (Table 5). Sulfur K-edge XAS studies of wild type *Cp*Rd and the four Ser mutants revealed an increase in the pre-edge energy of the Cys for all four mutants compared to wild type, indicating higher d orbital energy for the mutants, arising from the more electronegative olate serine ligand, which will lower the reduction potential as observed experimentally. Consistent with the pre-edge data, EXAFS fitting shows longer average Fe-S bonds for the four mutants. DFT calculations also indicate that alkoxide ligand stabilizes Fe(III) better than a thiolate ligand. Changes of solvent accessibility, H-bonding, electrostatic field around the site are other factors possibly involved.[599,600] The Ser mutants display strong pH dependence, possibly arising from the protonation of coordinating oxygen of Ser following reduction at neutral or low pH.[601-603]

Mutations of the secondary sphere residues have been conducted mainly on the conserved residues, and potential changes of 100 mV in both directions have been achieved (Table 5).[604,605] In recombinant *Cp*Rd, Gly43Ala eliminates the Val44-NH…S-Cys42 H-bonding interactions, and a Gly10Val mutation significantly perturbs the overall structure of C9 containing loop by increasing steric hindrance. Replacement by Val decreases the reduction potential more than Ala, and the mutations lower reduction potentials up to -86 mV.[604,606,607] Side chain variation of the surface residue 44 of *Cp*Rd

also could influence the reduction potential of the metal center. Three mutants V44I, V44A, V44G increase the reduction potential to -53, -24, and 0 mV, respectively, from -77 mV of wild type. The increasing of E^o is well correlated with decreasing of NH…S H-bond distance determined by ^{15}N NMR. A possible explanation of the trend is that the shortening of H-bonds might lead to increased capacity for electron delocalization or decreased electron donation from the sulfur ligands, and finally to higher reduction potential of the metal center.[608,609] Similarly, quantum mechanical calculations reveal that shortening of H-bonds would decrease the energy of the reduced state faster than that of oxidized state, and result in increased reduction potential.[610]

Table 5 Reduction potentials for CpRds[a]

Protein	E^o, mV	protein	E^o, mV	protein	E^o, mV
native	-76	G43A	-93	V44G	0
recombinant	-77	G43V	-123	V44A	-24
C6S	-170	G10V/G43A	-134	V44I	-53
C39S	~-190	G10V/G43V	-163	V8G/V44G	+39
C9S	-284	V8G	-7	V8I/V44I	-13
C42S	-273	V8A	-44	V44I/V44I	-55
G10A	-104	V8L	-82	V44L	-87
G10V	-119	V8I	-81		

[a] Square wave voltammetry data, *vs* SHE.

Electrostatic effects of the charged residues make important contributions to the reduction potential of iron center as well. Two neutral surface residues Val8 and Leu41 of *Cp*Rd close to the iron center were replaced by positively charged Arg, and the resulting mutants display increased reduction potentials as expected. However, mutants Val8Asp and Leu41Asp, in which two negatively charged residues were incorporated, also gave higher reduction potentials. The mutations might have also changed the solvent accessibility, and consequently the dielectric constant around the metal center,

leading to complicated effects difficult to predict and explain simply by Coulomb's law.[611,612]

A series of unnatural analogues of tyrosine have been incorporated into the Tyr10 position of *Pf*Rd close to sulfur of Cys38 (3.95 Å at the closest point) by native chemical ligation methods, and the reduction potentials of the resulting proteins are linearly correlated with the Hammett σ_p of the para substituent of the phenyl ring. Electron donating groups shift E^o to more negative values (Tyr10 *Pf*Rd, -78.0 mV; Phe10 *Pf*Rd, -69.5 mV; 4-F Phe10 *Pf*Rd, -61.5 mV vs. NHE), and electron-withdrawing groups shift E^o to more positive values (4-NO_2 F10 *Pf*Rd, -49.5 mV; 4-CN F10 *Pf*Rd, -43.5 mV vs. NHE).[613] The trend is not well correlated with the dipole movement of the side chain,[614] and is proposed to arise from either electrostatic interaction[615,616] or modulation of the H-bond strength between the sulfur of Cys38 and residue 10.[617-619]

3.4.1.4.Spectroscopic features

Ferrous rubredoxin is colorless, with weak absorptions centered at 311 and 331 nm. On the other hand, ferric rubredoxin displays strong absorption peaks at 350, 380, 490, and 570 nm from LMCT of the σ orbital and a weak peak at 750 nm from π orbital of the cysteinyl sulfur to the metal center (Figure 16a). Mutating one of the Cys to Ser still gives LMCT bands in ferric form, but with the peaks shifted to higher energy together with some changes of intensity, consistent with a decreased S to Fe(III) LMCT contribution.[562] CD spectra of rubredoxins display minima at 202 and 226 nm from β-sheet structures in the protein.[620-622]

Mössbauer spectra of ferrous rubredoxin as purified give parameters of an S = 2 Hamiltonian with D = 5.7(3) cm^{-1}, E/D = 0.25(2), δ = 0.70(3) mm/s and ΔE_Q = -3.25(2) mm/s (Figure 16b).[623] Consistent with the Mössbauer studies, experiments using Broad-Band Quasi-Optical HF-EPR reveal a D value of 4.8 ± 0.2 cm^{-1} and E/D of 0.25 ± 0.01.[624] The ferric form is high spin as well, as determined by EPR spectroscopy, with a set of signals arising from an S = 5/2 spin state, including g= 4.3 from the middle Kramers doublet, and g = 9.5 from the lowest Kramers doublet (Figure 16c). The Mössbauer spectrum of the oxidized form of *Cp*Rd shows δ = 0.24 ± 0.01 mm/s at 4.2 K.[603,625]

The Fe-S covalency has also been probed using single molecule AFM by measuring the mechanical stabilities of Fe(III)-thiolate bonds. The rupture forces of interior Fe-S bonds of *Pf*Rd are greater than those of surface Fe-S bonds, consistent with other experimental observations.[626] The mechanical stability of Fe-S bonds also shows good correlation with the NH…S H-bond strength reflected by the reduction potential.[627]

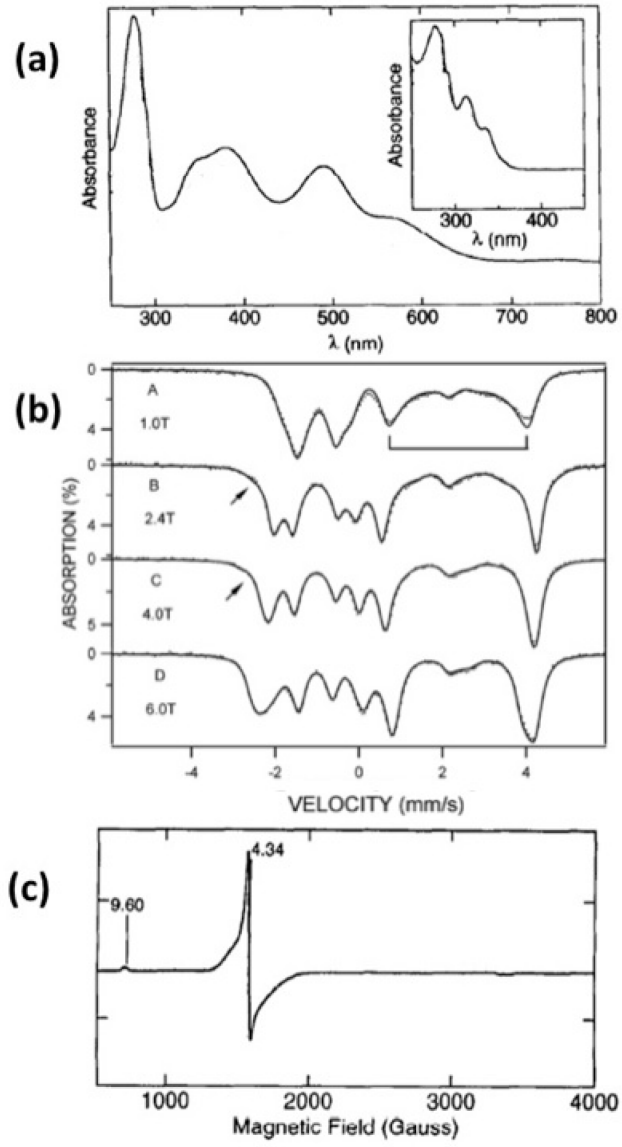

Figure 16. Representative spectra of rubredoxins. (a) UV-Vis spectra of ferric and ascorbate reduced ferrous (inset) *Cp*Rd (b) Mössbauer spectra of dithionite reduced ferrous *Cp*Rd measured at 4.2 K under magnetic field applied parallel to the γ rays. Reprinted with permission

from ref [623]. Copyright 2002 American Chemical Society. (c) EPR spectra of *Cp*Rd. Reprinted from ref [611]. Copyright 1996, with permission from Elsevier.

The dynamic properties of the redox iron center are important for the redox properties of a protein. ^{57}Fe nuclear resonance vibrational spectroscopy (NRVS) of the oxidized form of *Pf*Rd, which is sensitive to all normal modes involving the Fe center, shows bands around 70, 150, and 364 cm^{-1}. The 70 cm^{-1} signal is from collective motion of some or all of the coordinating cysteines with respect to the iron center. The ~150 cm^{-1} signal mostly involves S-Fe-S bending motion composed of a doubly degenerate E mode (v_2) and a mixed T2 v_4 mode of Td symmetry. The strong signal between 355 and 375 cm^{-1} is mainly from an asymmetric Fe-S stretch mode v_3 of Td symmetry, consistent with average value of 362 cm^{-1} from Raman spectra of *Desulfovibrio gigas* (*Dg*) Rd. In the case of reduced form, the asymmetric Fe-S stretching modes shift to 300-320 cm^{-1}, bending modes shift slightly lower, and collective motion modes at ~70 cm^{-1} do not change substantially. Derived force constants of both stretching and bending modes are higher in the oxidized form than in the reduced form.[614,628].

The rR spectra of oxidized Rd display the strongest band at ~315 cm^{-1}, from totally symmetric Fe-S_4 breathing modes.[614] The force constant of the v_3 frequency is lower than in synthetic models, probably because of the H-bonding to the S of the cysteines in the protein scaffold.[589]

^{1}H NMR has been utilized to study the magnetic properties of ferrous rubredoxin. Broadening and shifting of signals are observed due to the presence of iron. To avoid the strong paramagnetism of iron, other metals such as Zn, Cd, and Hg were used as a surrogate of Fe(II) for structural studies. Paramagnetic contact shifts in ^{1}H, ^{2}H, ^{13}C, and ^{15}N nuclei of oxidized *Cp*Rd have been measured experimentally, and the data are consistent with high-level all-electron density functional calculations based on high-resolution crystal structures. Computational studies reveal that the experimental hyperfine shifts are mainly from Fermi contact interactions.[629,630] NMR has also been applied in measuring the magnetic susceptibility anisotropies of both oxidized and reduced *Cp*Rd, demonstrating that pseudocontact has negligible contributions to hyperfine shifts.[631]

3.4.2. Rubredoxin-like proteins

3.4.2.1. Flavorubredoxin

Flavorubredoxin is a type of protein containing a rubredoxin-like domain coupled to a flavodiiron protein and a flavodoxin domain binding one flavin mononucleotide.[632,633] It has been isolated from *E. coli* and *Moorella thermoacetica*, and discovered to be involved in electron transfer pathways in reduction of nitric oxide and conversion of CO_2 to acetate.[634-637] The reduction potential of flavorubredoxins from *E. coli* have been determined to be -140 ± 20 mV at pH 7.6[635] and -120 ± 20 mV at pH 7.5.[636] Reduction potential of flavorubredoxin from *Moorella thermoacetica* is -30 ± 10 mV at pH 7.0.[638,639]

3.4.2.2. Diiron-rubredoxins

Diiron-rubredoxin is composed of two [$FeCys_4$] domains connected by a 70-80 amino acid linker.[570,640] It can be readily prepared from corresponding monoiron rubredoxin by precipitation and resolubilization, and is proposed to be the physiological form of rubredoxin. Though less stable, it can transfer electrons from reduced spinach ferredoxin reductase to cytochrome *c* just as the monoiron form. The midpoint reduction potential of both of the two-electron reduction process is -10 mV vs. NHE at pH 7.0, similar to that of mono-iron rubredoxins.[641].

3.4.2.3. Desulforedoxin

Desulforedoxin (Dx), isolated from sulfate reducing bacterium *Desulfovibrio gigas*, is an α_2 dimer with 36 amino acids for each subunit. Each dimer contains a four-stranded antiparallel β-sheet and several turns and inter-chain short β-sheets. Each monomer has a high spin rubredoxin-like [$Fe(Cys)_4$] center. The iron center is near the protein surface, coordinated by four cysteine residues C9-X-X-C12 and C28-C29. Unlike rubredoxin, two of the four coordinating cysteines are consecutive, making the tetrahedral coordination geometry distorted (Figure 17).[642,643] In addition, Dx only has one aromatic residue, while Rd has up to six. The Fe-S bond lengths of Dx range from 2.25 to 2.36 Å, and the S-Fe-S angles vary from 102^o to 119^o.

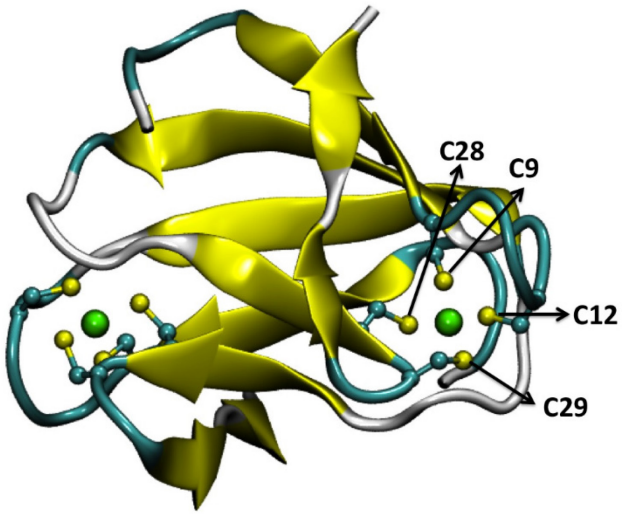

Figure 17. Crystal structure of desulforedoxin from *D. gigas*. PDB code: 1DXG. The [$FeCys_4$] centers are displayed as ball-and-stick mode and denoted. The Backbones of coordinating cysteines are omitted for clarity. Color code for the ball-and-stick mode: cyan, carbon; green, iron; yellow: sulfur.

Oxidized Dx displays three major UV-Vis absorptions centered at 278, 370 and 507 nm. The 370 and 507 nm absorptions arise from the sulfur to iron charge transfer, and the extinction coefficient of the 507 nm absorption is 4580 M^{-1} cm^{-1} per monomer, falling in the normal range of Fe-S proteins.

Unlike the nearly rhombic EPR features of oxidized Rd (E/D = 0.28),[644] the EPR spectra of oxidized Dx displays an S = 5/2 site with near axial symmetry, with *g* = 4.1, 7.7, and 1.8 from the ground Kramers doublet, and g = 5.7 from the middle Kramers doublet.[645] This difference reflects different geometric and electronic structures of the two iron sites. D = 2.2 ± 0.3 cm^{-1}, ΔE_Q = -0.75 mm/s, and δ = 0.25 mm/s are obtained by Mössbauer studies of oxidized Dx. The parameters of reduced Dx from Mössbauer studies are D = -6 cm^{-1}, E/D = 0.19, ΔE_Q = 3.55 mm/s and δ = 0.70 mm/s. The positive ΔE_Q value of reduced Dx indicates that the ground state orbital is mainly $d_{x^2-y^2}$, while the ΔE_Q value of reduced Rd is correlated to pure d_{z^2} as the ground state orbital.[642]

Insertion of a Gly residue or Pro-Val residues between Cys28-Cys29 makes the ferric center of Dx nearly spectroscopically identical to that of Rd, However both mutations are detrimental to the protein stability.[646]

Similar to Rd, Dx associates with other metal centers in biological systems. For example, Desulfoferredoxin (Dfx) possesses a binding motif for Dx-type [$FeCys_4$] center associated with another non-heme mono iron center with N/O ligands[647] (see section3.4.2.4. Desulfoferrodoxin). Moreover, Dx in *D. gigas* is reported to transfer electrons to SOR more efficiently than Rd.[648]

3.4.2.4. Desulfoferrodoxin

Desulfoferrodoxin (Dfx) is an α_2 dimer with molecular weight of ~28 kDa, belonging to the diiron superoxide reductase family.[649,650] Each monomer contains a [$FeCys_4$] center (center I) and a non-heme iron center coordinated by a 4-His-1-Cys motif (center II).[651] The 1.9 Å resolution crystal structure reveals that center I is structurally similar to the metal center of Dx.[652] The mid-point reduction potential of center I is around 0 mV, falling in the range of [$FeCys_4$] centers in Dx and Rd.[647,653-656]

Replacement of Cys13 of Dfx from *D. vulgaris (Hildenborough)* with serine results in a [1Fe-3Cys-1Ser] center instead of the Rd/Dx like center. Redox titration reveals no influence on reduction potential of center II by such a mutation, indicating the independence of the two cofactors.[657] On the other hand, reduction potentials of Dfx from hyperthermophilic archaeon *A. fulgidus* are +60 mV for center I, and +370 mV for center II,[649] while the E^o is +230 mV for mono-Fe SOR containing only center II cofactor from the same genome.[658] The difference of E^o implies possible involvement of center I of Dfx in facilitating the reduction of center II.[654]

3.4.2.5. Rubrerythrins

Rubrerythrin (Rr), an α_2 dimer, is a non-heme iron protein with peroxidase and *in vitro* ferroxidase activity.[583,659] Each monomer contains a diiron-oxo site in the middle of a four-helix bundle, and a [$FeCys_4$] center at the C terminus.[660,661] The [$FeCys_4$] center is structurally very similar to Rd, yet the midpoint reduction potentials are estimated to be +230 mV at pH 8.6 and +281 mV at pH 7.0, much higher than the normal value of around 0 mV for Rd centers.[662,663] The crystal structure reveals the dramatic potential increase and pH dependent behavior might be due to the polar and solvent exposed environment around the iron center created by nearby residues, including Asn160,

His179 and Ala176, which are not conserved in Rd.[660,664] Replacement of the iron in the Rd-like domain with zinc inhibits the peroxidase activity of the protein, indicating the essential role of the Rd domain in the electron transfer process.[665]

Desulforubrerythrin, a unique member of rubrerythrin family, has been isolated recently from *Campylobacter jejuni*. It is an α_4 protein and each 24 kDa monomer is composed of three domains: Dx-like N-terminal domain, a four-helix bundle domain containing a μ-oxo bridged diiron site, and a Rd-like C-terminal domain. The reduction potentials of the [$FeCys_4$] centers in the N-terminal and C-terminal domains are +240 ± 30 mV and +185 ± 30 mV, respectively, at pH.7.0 vs. SHE.[666]

Nigerythrin is an α_2 dimer containing one diiron-oxo center and a [$FeCys_4$] center, very similar to rubrerythrin. The reduction potential of the Rd-like center in nigerythrin from *D. vulgaris* is +280 mV vs. NHE at pH 7.5, comparable to that of Rr as well.[663,667,668]

3.4.3. Ferredoxins:

3.4.3.1. Introduction:

The term ferredoxin refers to a wide range of small, low molecular weight Fe-S proteins that function solely as electron carriers in different biological pathways including photosynthesis and respiration.[669] Ferredoxins first were observed based on their distinct rhombic EPR feature with g = 1.9. EPR studies with ^{57}Fe later confirmed that the signal is from a non-heme iron.[670] Evolution of H_2S gas upon acid treatment was an indicator of the presence of inorganic sulfur in this protein.[1,671] All ferredoxins share some common features: They are all low molecular weight, highly acidic proteins that contain iron and inorganic or “acid-labile” sulfurs.[1] The Fe-S cluster resides in a hydrophobic patch within the protein and gives the proteins a distinctive reddish-brown color. All ferredoxins go through partial decrease in absorbance upon reduction. Reduction can be achieved through chemical treatment by sodium hydrosulfite or enzymatic treatment with H_2 gas and hydrogenase. The pattern of reduction is dependent on the method and extent of reduction. After reduction, a rhombic EPR signal appears with g<2 (exact value depending on cluster type). Ferredoxins usually have low reduction potentials with an average of -400 mV and spanning a range of 800

mV depending on cluster type, protein structure, H-bonding network, water solubility of the cluster, and ligands to the iron. This wide range enables ferredoxins to serve as redox partners to a variety of molecules in a number of important biological reactions. Due to the high acidity, these proteins usually have high affinity for DEAE Sepharose and can be easily purified by acetone precipitation and DEAE-facilitated separation. It has been shown that the proteins can usually be reconstituted by treatment with iron and Na_2S under reducing conditions (in presence of B-mercaptoethanol).[539,546,672-674]

All of the low reduction potential ferredoxins seem to have evolved from a common 27 residue ancestral polypeptide.[91] Despite different types, CD and ORD studies show that all ferredoxins have a very similar polar active-site environment around the cluster in which the iron assumes tetrahedral coordination geometry. The similarity of extinction coefficients of their electronic absorption bands, mainly due to metal to ligand charge transfer, also indicates a similar bonding pattern of iron.[539] Despite somewhat surface exposed iron, the reaction of proteins with iron chelators is usually slow, unless denaturing conditions are applied.[675,676] Ferredoxins are further divided into sub-categories based on the number of iron molecules present in the cluster:

3.4.3.2. 2Fe-2S clusters:

3.4.3.2.1. Structural aspects:

As their name suggests, 2Fe-2S clusters are a class of one-electron transport ferredoxins containing two iron atoms that are coordinated in a distorted tetrahedral geometry by two inorganic sulfurs and four cysteine thiolates from the protein. The 2Fe-2S cluster is not completely planar having a small tilt in the plane of first and second iron. Three of the four cysteines come from one loop in the structure of the protein, with the other one being at the tip of a β-strand in a different loop (3+1 arrangement). The cluster is positioned close to the surface of the protein, surrounded by hydrophobic residues. Aside from the vicinity of the cluster, the surface of 2Fe-2S ferredoxins is highly acidic, covered with a large number of Asp and Glu residues. This acidic patch is used to interact with the basic surface of the redox partner. After initial alignment through these electrostatic interactions, hydrophobic interactions between the two

surfaces and water exclusion further facilitate the electron transfer between the proteins.[540,677] A role for orientation of redox partners has been proposed in electron transfer rates.[678] Lack of complete complementarity between the two surfaces ensures the separation of oxidized ferredoxin and initiation of a new cycle.[540] There are several NH…S H-bonds from backbone amides to the sulfurs of the cluster, with sulfur ligands of FeI (the iron closer to the surface) being involved in more H-bonds than those of FeII. It appears that the Fe-Fe and Fe-S_γ bonds lengthen upon reduction while the H-bonds strengthen and shorten, consistent with increased negative charge on S.

Despite these similar features, 2Fe-2S ferredoxins can be further divided into three subcategories based on differences in sequence and structural alignments and in the ligand Cys motifs (Figure 18). The details about each category are briefly explained below[677]:

Plant-type clusters: The archetype of plant-type ferredoxins is chloroplast ferredoxin I (FdI). The members of this family share a common β-grasp structural motif, which consists of three to five β-strands, with one to three adjacent α-helices, and some additional secondary structures and loops.[91] Three of four coordinating Cys are in a loop with a conserved C-X_4-C-X_2-C motif and the fourth Cys is 29 amino acids away. The cluster is usually buried at one end of the protein in a hydrophobic environment. Although plant-type ferredoxins have high sequence homology, there are multiple isoforms of them in each organism, which suggests different roles of the isoforms in different evolutionary and physiological conditions. Acidic residues are usually distributed in an asymmetric fashion resulting in a dipole with its negative end near Fe-S cluster. This dipole is shown to be important in docking of the ferredoxin into its redox partner.[679-681] Proteins from acidophilic organisms, however, have a more uniform acidic charge distribution on the surface. Several H-bonds anchor the cluster to the protein and are known to be important in fine-tuning the reduction potential of the protein. A water channel with five water molecules connects the solvent to the proximity of the cluster in the C-terminal region of protein.[677,682-686]

Mammalian/mitochondrial cluster: Also known as hydroxylating ferredoxins, these clusters include mammalian 2Fe-2S proteins as well as some bacterial 2Fe-2S proteins. The archetypes of this class are adrenodoxin and bacterial putiredoxin. The

overall fold and structure of this class is very similar to plant-type clusters with the exception that they have an additional interaction loop,[91] a large hydrophobic domain that is used as an interacting domain with the redox partner. The conserved ligating motif of this class is C-X_5-C-X_2-C, with the fourth cysteine 35 to 37 residues away from the third ligand, further away than in plant-type structures. This group has a very flexible C-terminal which is very difficult to crystallize, but can be captured in the presence of its redox partner. It also has a compact α+β structure, characteristic of ferredoxins. Interestingly the same fold has been observed in enzymes containing Fe-S clusters as well as some unrelated proteins that are void of Fe-S clusters. There has been evidence of structural changes upon reduction in some loops as well as the C-terminus. The solvent channel is shorter in mammalian-type ferredoxins compared to plant-types.[677,681,682]

Thioredoxin-like clusters: These proteins are only reported in bacteria, mostly in proteobacteria and cyanobacteria. They were first discovered in *Clostridium pasteurianum*[687] and *Azotobacter vanidilii*[670] due to their spectroscopic features, which are distinct from common 2Fe-2S ferredoxins. Their sequence as well as positioning of the cysteine ligands differs significantly from other ferredoxins.[688] These differences were further confirmed by analyzing vibrational bands in resonance Raman studies. Two features in the structure of this class are known to cause these differences: a distortion of the loop containing the Cys ligands, and an H-bond between two cysteine residues. Proteins of this class function as a dimer, each monomer having a thioredoxin-like fold, despite low sequence homology (~7%). Two regions are notably distinct between these proteins and thioredoxins: a protruding surface loop that has been shown to have no significant function, and an α-helix in one subunit and a short helix in the other subunit that are important in interaction[689] between two subunits. The cluster lies within two loop regions in the periphery of subunits in a conserved motif of C-$X_{10\text{-}12}$-C-$X_{29\text{-}34}$-C-X_3-Cys. The fourth cysteine is placed in a protruding loop, which is absent in other ferredoxins. Several studies showed that the position of this Cys is flexible and that it can be moved to other positions in the loop.[690,691] Some members of this class contain five cysteines instead of four. ESEEM studies and mutational analyses showed that loss of one of these cysteine residues can be compensated by

the other four.[690] There are a small number of conserved residues in the family, including the four cysteine ligands and some cysteines in the dimer interface. The overall common structure has five β strands, two long α-helices, and an additional short helix. The Cys ligands of the more buried iron are provided by the loop that is longer. The cluster itself shows some deviation from other ferredoxins with 2 irons. One is a more compressed angle with Fe^{2+}, and the other is a longer distance between one of the Cys and Fe2 than other Fe-S distances. The cluster is more surface-exposed in this class than the other two classes of 2Fe-2S ferredoxins.[91,682,689,692,693]

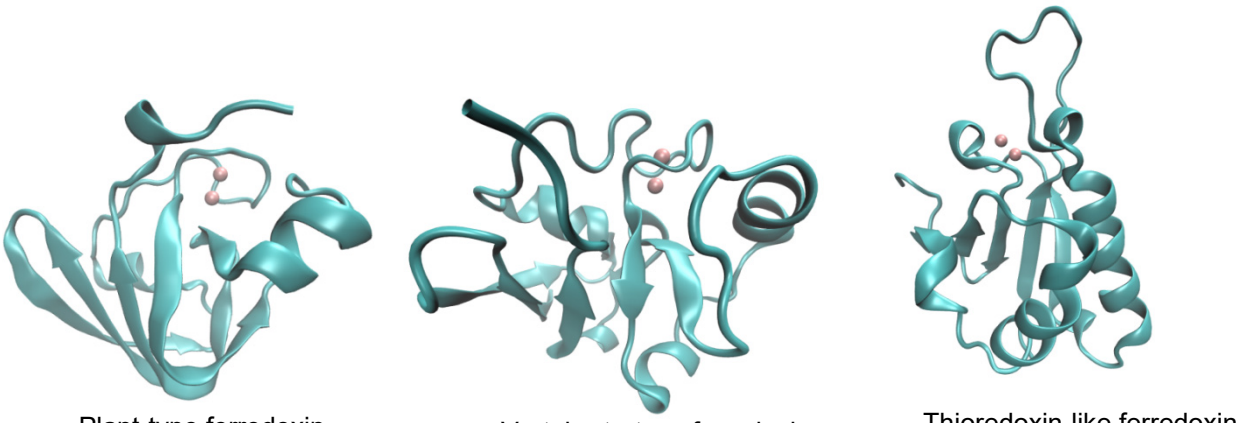

Figure 18. Structures of three classes of 2Fe-2S ferredoxins. Notice that in their physiological form, Thioredoxin like ferredoxins function as a dimer.

3.4.3.2.2. Function:

3.4.3.2.2.1. Plant-type ferredoxins

Plant-type ferredoxins can usually be found in the stroma of chloroplast of higher plants and algae as well as cytoplasm of cyanobacteria. Ferredoxins play a role as the first electron acceptor in the stromal side of chloroplast and function mainly as electron distributors in photosynthesis. They are also involved in a variety of other functions such as sulfur and nitrogen assimilation, biosynthesis of several compounds such as chlorophyll, and redox homeostasis of the cell.[538]

The most important and well-studied function of these proteins is the transfer of two electrons in two consecutive steps from photo-reduced photosystem I (PSI) to

ferredoxin:NADP oxidoreductase (FNR), which finally will result in CO_2 assimilation.[538] FNR binds two molecules of ferredoxin, with negative binding cooperativity between oxidized ferredoxin and NADP. However, the affinity of FNR for ferredoxin increases 30-fold upon reduction of ferredoxin. In organs that produce NADPH by the pentose phosphate cycle, FNR acts in the reverse direction, reducing ferredoxin.[677]

Ferredoxin also distributes electrons from photoreduced PSI to ferredoxin-dependent enzymes such as nitrite reductase, glutamate synthase, and ferredoxin: thioredoxin reductase (FTR), for nitrogen and sulfur assimilation. Cyanobacteria have a vegetative ferredoxin that functions in photosynthesis, and a heterocyst ferredoxin that transfers electrons to nitrogenase. Ferredoxin from halobacteria can function as electron carrier in α-keto acid decarboxylation or in nitrite reduction.[669,694]

One of the most studied realms in the field of ferredoxins is their interaction patterns with their redox partners. These complexes have been studied using several techniques such as cross-linking, NMR, ITC, and site directed mutagenesis; however, it is not completely understood whether ferredoxin uses the same surface, partially overlapping surfaces, or totally different surfaces for interacting with different redox partners. The most likely hypothesis is that ferredoxin acts as a mobile electron carrier between PSI and other redox partners.[677]

3.4.3.2.2.1.1 Interactions with other proteins

Interaction with ferredoxin:NADP+ reductase (FNR)

The most well-known partner of plant-type ferredoxins is FNR. It has been shown that ferredoxin and FNR has very tight binding with K_d in range of 10^{-8}-10^{-9} M. As discussed previously, several surface amino acid residues are conserved in ferredoxins, and mutation of these amino acids revealed important factors in interaction between these redox partners. Laser flash photolysis is one of the techniques that have been used to analyze the reactivity of several ferredoxin mutants from *Anabaena*. Among the conserved residues, Phe65 was the only one essential for tight binding between ferredoxin and FNR.[684,695-697] Ser47, Glu94, and Phe65 were also shown to be important in the rapid ET between the two partners, though conservative mutations to other similar residues were tolerated. Interestingly mutating residues adjacent to these three had

much lower effect on the activity.[677] Mutational studies of Glu92 in spinach Fd, which is analogous to Glu94 in *Anabaena*, resulted in decreased activity, but much less significant than that of the former. More interestingly, this mutation resulted in an increase in reduction potential and stimulation of NADPH-cytochrome *c* reductase activity catalyzed by FNR. These mutants were more efficient in transferring electrons in the direction opposite to the physiological ET pathway. Although several studies have shown significant correlation between ET and reduction potential, ET changes are thought to be more likely a result of changes in protein orientation and transient state configuration rather than a consequence of reduction potential changes. A thorough study of the mutants with laser flash photolysis showed very similar effects of Glu92/94 mutation in both spinach and *Anabaena* variants, hence suggesting a difference between these results and previous NAD^+ photoreduction results.[677] ITC studies suggested entropy as the main driving force of complex formation, meaning that hydrophobic interactions are the major forces governing the efficient interaction between the two partners. The proposed binding surfaces of many Fds are covered with water, so the binding of the partners will release water molecules and favor the reaction entropically.[698]

Several models of complexes between ferredoxins and FNRs have been made based on experimental evidence coming from chemical modification, cross-linking, partial proteolysis, and mutational studies, as well as homology models. These models predicted the binding site between ferredoxin and FNR to be a large hollow surface near dimethylbenzyl ring edge of the flavin in FNR. The binding will bring the Fe-S cluster and the flavin close, so that they can transfer electrons. While Fd has an excess of positive charge on the binding surface, FNR has a net negative charge on its binding surface. The specific orientations of dipoles in the two proteins have been shown to be important in recognition between two partners. Another model proposes that electrostatic potential complementation plays an important role. The two models differ in the orientation of the ferredoxin molecule about the axis perpendicular to the protein-protein surface.[677,679,680] Cross-linking experiments have been done to study the complex between ferredoxin and FNR. The cross-linked molecule showed oligomer states in crystal structure that might be relevant to *in vivo* interactions.[699]

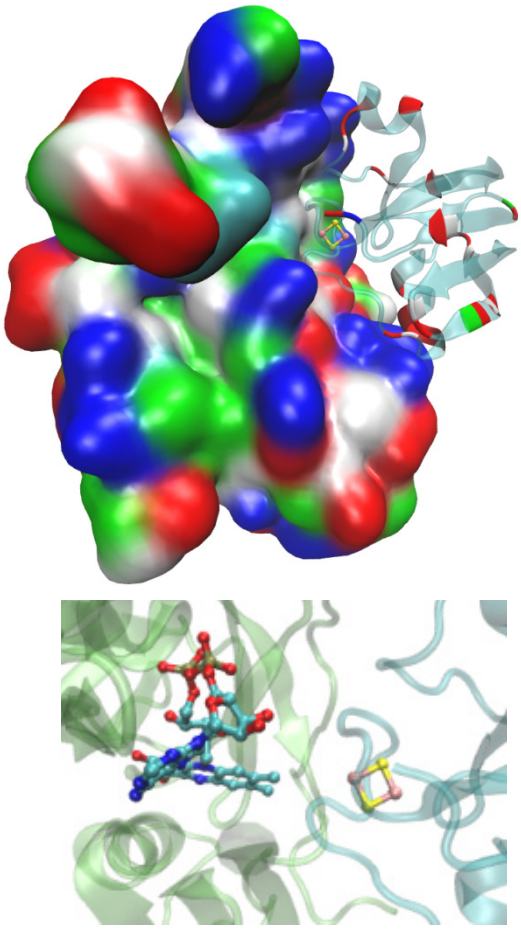

Figure 19. Structure of Fd (right) cross-linked to FNR (left); PDB: 3W5U. As shown, red acidic patches of ferredoxin are positioned in contact with blue basic residues of FNR. An enlargement of the cofactors (Fe-S and FAD) is shown on the bottom.

Interaction with ferredoxin:thioredoxin reductase, nitrite and sulfite reductase, glutamate synthase

Reduced ferredoxin donates electrons to ferredoxin:thioredoxin reductase (FTR) to reduce thioredoxin, which is involved in multiple steps of the Krebs carbon cycle. FTR is found only in oxygenic photosynthetic organisms. Chemical modification of acidic residues on the surface showed that the Glu92-94 acidic patch is important for the interaction between the two partners. A model has been proposed based on the crystal structures of the two partners. In this model, ferredoxin docks into the opposite site of the flat, disk-like structure of FTR in such a way as to position itself close to the 4Fe-4S cluster and the redox active disulfide bond[700]. In this ternary complex, two successive one-electron transfer reactions take place. The complex between ferredoxin and FTR has very high affinity, with both electrostatic and hydrophobic interactions being involved.

Site-directed mutagenesis and chemical modification studies suggest that the same site of Fd is responsible for interacting with nitrite reductase, sulfite reductase, and glutamate synthase.[701,702] The surface is formed in low ionic strength, indicating a role for electrostatic interactions in formation of the complex. Another site has also been proposed for sulfite reductase (SiR).[703,704] While less is known for SiR, NMR analyses of the contact shifts between the presumed complex confirmed the important role of acidic surface residues on complex formation.

Nitrate reductase is found in cyanobacteria and performs two-electron reduction of nitrate to nitrite. It has been shown that there is only one ferredoxin binding site in nitrate reductase, so the reduction proceeds in two separate consecutive steps.[704]

Nitrite reductase performs 6-electron reduction of nitrite to ammonia. As with nitrate reductase, only one binding site exists for ferredoxin. A conserved Trp residue has been shown to play an important role in electron transfer between the two partners.[704]

A loop close to the [3Fe-4S] cluster of glutamate synthase is responsible for binding of ferredoxin. CD analyses showed that neither of the two proteins undergoes significant conformational changes upon binding.[704]

Interaction with photosystem I

Photosystem I (PSI) is an essential part of the photosynthetic electron transfer pathway in cyanobacteria and plants. This multi-subunit complex is a membrane bound system that harvests light and helps convert it into a chemical potential. The complex consists of multiple chlorophylls, carotenoids, phylloquinones, bound lipids, and 4Fe-4S clusters. Three subunits at stromal site of PSI are involved in docking and reducing of FdI: PsaC (with 4Fe-4S clusters F_A and F_B), PsaD, and PsaE. F_A, F_B, and F_X are three low potential 4Fe-4S clusters that lie in stromal side of the PSI complex. F_A and F_B are bound to PsaC and F_B functions as a terminal electron acceptor (figure 20). F_x is an inter-polypeptide cluster, positioned between PsaA and PsaB and has the most negative reduction potential reported so far for a 4Fe-4S cluster (-705 mV).[705]

In vitro studies and cross-linking experiments revealed PsaD as the main docking site for FdI. A binding site for PsaC has been also proposed based on mutational studies. It has been shown that PsaD and FNR compete with each other in binding to Fd; yet no ternary complex has been observed.[705]

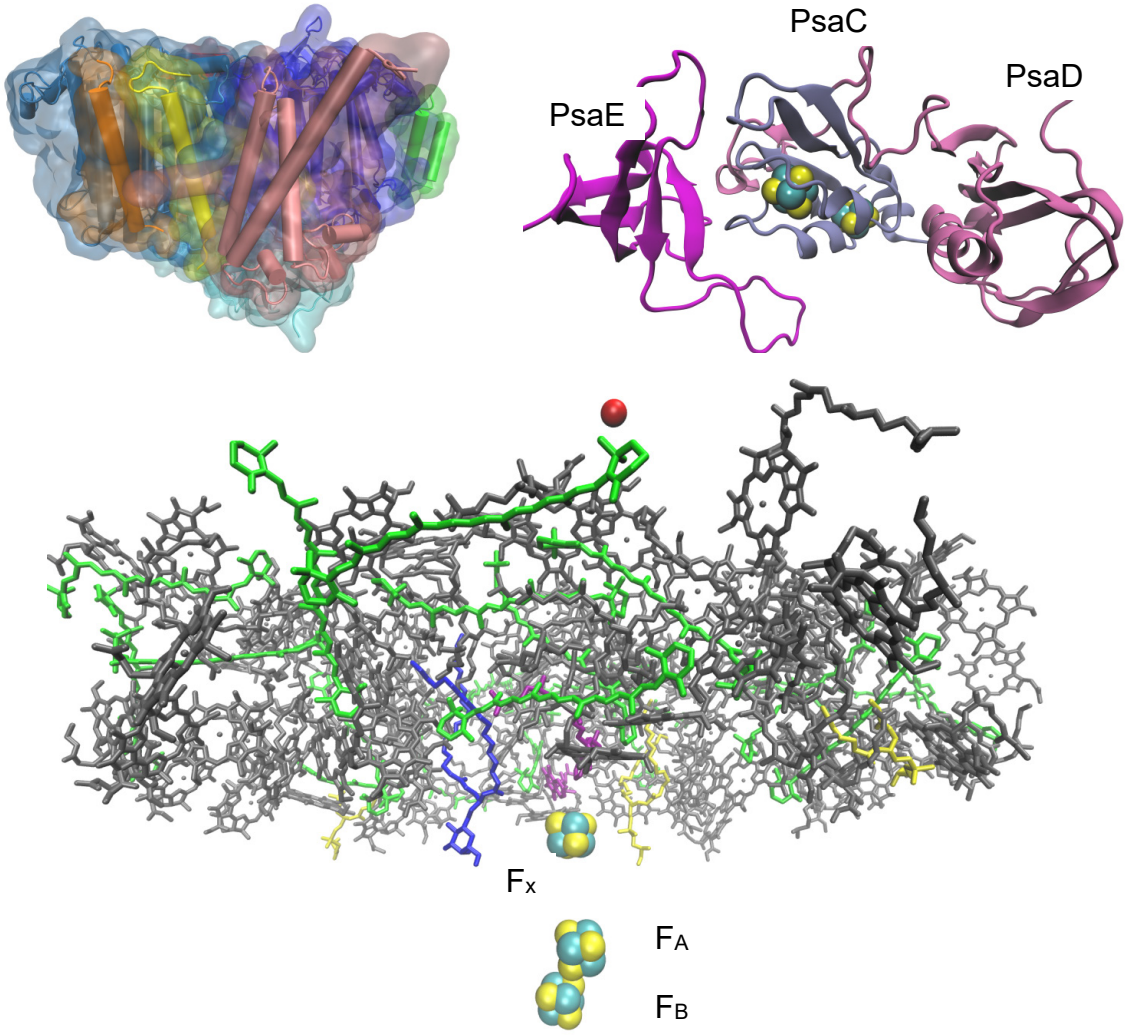

Figure 20. Structure of Photosystem I (PSI) (PDB: 1JB0). The top left figure shows the overall structure and the bottom figure shows all the cofactors in the system. The top right figure is showing PSaC/D/E site with F_A and F_B. Ferredoxin binds in the cleft that is made by the three proteins.

3.4.3.2.2.2. Mammalian-type and thioredoxin-like ferredoxins:

The main function of mammalian-type ferredoxins is electron transfer in the mitochondrial electron transfer chain, electron transfer to P450s, and Fe-S biosynthesis. It has been shown that Adrenodoxin has very tight binding to both adrenodoxin reductase and cytochrome P450, in the order of 10^{-7}-10^{-8} M.[706] As with ferredoxin, Adrenodoxin interacts with its redox partners through an acidic surface, with Asp76 and Asp79 being essential for the binding. The overlapping interaction surface supports a

mobile carrier hypothesis for the Adrenodoxin. A model based on the crystal structures of the partners suggests that Adrenodoxin binds in the cleft between two domains of adrenodoxin reductase, resulting in a distance of 16 Å between Fe-S cluster and isoalloxazine ring of the FAD in the reductase.[707,708] A specific electron transfer path between the two has also been proposed.[708] Several studies on Putiredoxin have shown the same overlapping surface for reductase and P450 interaction. The crystal structure of the complex between Adrenodoxin and Adrenodoxin reductase further confirmed the importance of charged Asp and Glu residues on the surface of ferredoxin in the formation of the complex (Figure 21).[709]

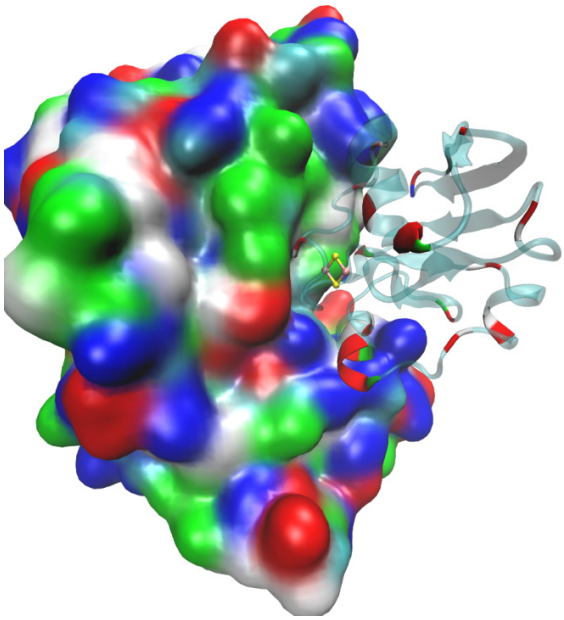

Figure 21. Structure of Adrenodoxin (right) in complex with Adrenodoxin reductase (left); PDB: 1E6E. As shown, red acidic patched of Adrenodoxin are positioned against blue basic residues of Adrenodoxin reductase. A zoom in of the cofactors (Fe-S and FAD) is shown on the bottom.

No certain function has been determined for thioredoxin-like ferredoxins yet. However, their abundance in nitrogen fixing bacteria suggests a role in nitrogen metabolism. Some molecular dynamics and docking studies have shown an interaction surface with this class of proteins and MoFe protein of nitrogenase, suggesting a role as electron carrier to this complex.[692 689,710]

To analyze electron transfer activity of 2Fe-2S ferredoxins, a simple spectroscopic assay can be performed using cytochrome *c* as the final electron acceptor. A wealth of mutational studies showed the importance of entropy as the main driving force in this interaction. While positive surface charges are important in bringing the two proteins into proximity, hydrophobic interactions are the major players in stabilizing the complex.[694]

3.4.3.2.3. Important structural features:

The reduction potentials of ferredoxins from plants and mammals are between -460 to -300 mV.[694] On average, mammalian ferredoxins have higher reduction potentials than plant-type ferredoxins, due to different patterns of electron delocalization, as observed by NMR.[711] Interestingly, mammalian ferredoxins show a pH-dependent redox behavior.[712] The average reduction potential for the thioredoxin-like class is around -300 mV.[682] Multiple methods have been used to measure reduction potentials of ferredoxins, including lipid bilayer modified gold electrode[713], direct protein film voltammetry[714,715], and spectrochemical titration [714]. While the normal transition is from $[2Fe\text{-}2S]^{2+}$ to $[2Fe\text{-}2S]^{1+}$, a hyper-reduced state has been observed during direct voltammetry analysis.[716]

Several factors have been reported to be important in fine-tuning the reduction potentials of ferredoxins. Overall protein fold and solvent accessibility of the cluster are known to be important in giving a low reduction potential range to ferredoxins compared to Rieske centers that also have a 2Fe-2S cluster core. These factors are discussed in more detail in the Rieske center section.

Models of 2Fe-2S proteins have been used to analyze the reduction potential properties. These analyses have shown the nature of peptide to be important in reduction potential determination and behavior.[717] Other factors such as H-bonding network from backbone amides to sulfurs and overall charge of protein are reported to play a role in determining the reduction potential value within 2Fe-2S ferredoxin classes. In all the classes, there is a conserved H-boding network, with sulfurs ligating the higher potential iron being involved in more H-bonds (Figure 22). It has been shown that the number of these bonds and more importantly the overall dipole around the cluster plays an essential role in reduction potential.[718,719]

Point mutations near the active site that change the charge resulted in a 100 mV change in reduction potential.[720] Three kinds of mutations were found to influence the reduction potential in thioredoxin-like ferredoxins the most: replacing Cys ligands, swapping ligands or changing the loop containing them, and changing the charge in the vicinity of the cluster.[720] Interestingly, changing the loop (either insertion or deletion) resulted in a reduction potential correlated with the sum of the charged residues left in the loop. Cys → Ser mutations caused a decrease in reduction potential.[690,721] A 100 mV change in reduction potential was observed upon mutating one of the Cys in thioredoxin-like ferredoxins that has five Cys.[690] Mutations of Glu94 and Ser47 of *Anabaena* Fd showed a significant increase in the reduction potential of this protein mostly due to rearrangement of the H-bonding network as well as removal of a negative charge close to the cluster.[678]

3.4.3.2.4. Spectroscopic features

All [2Fe-2S] ferredoxins share very similar UV-Vis spectra with a protein peak at 280, a near ultra-violate peak at 330 nm, and visible region absorptions at 420 and 463 nm, with a shoulder at 560 nm in oxidized form. The relative intensities of 420 and 460 bands are inverted in thioredoxin-like ferredoxins compared with the other two groups. Depending on the hydrophobicity and H-bonding pattern around iron atoms, one of them, usually the one closest to the surface, is reduced more easily. After reduction, the spectral intensity decreases to about 50% of that of the oxidized form and the band positions were altered to a maximum at 540, with small peaks at 460, 390, 350, and 312

nm.[538,539] These proteins show similar CD and ORD spectra. A red shift was observed in the spectra after Selenium substitution. Strong positive bands between 420 and 460 nm in the oxidized form dominate CD spectra. The reduced state has negative bands at 440 and 510 nm. From these CD analyses, bands from $d_{z2} \rightarrow d_{xz}$ and $d_{z2} \rightarrow d_{yz}$ have been assigned.[539]

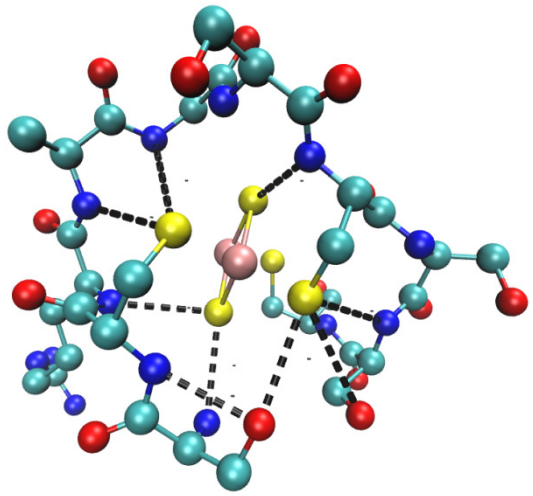

Figure 22. H-bonding network in plant-type ferredoxins.

Ferredoxins were first identified through their unique EPR signal in the reduced state. The two iron atoms in the oxidized state each have a spin of S = 5/2, and are antiferromagentically coupled, resulting in a final diamagnetic EPR silent species. Upon reduction of one of the iron ions, the net spin will change to 1/2 and a rhombic EPR signal at g = 1.94 is observable at temperatures below 100 K. When the iron in the protein is replaced with ^{57}Fe, the samples showed a broader or split EPR signature, proving that the signal is from iron.[670] Multiple studies showed that part of the g = 1.94 signal comes from the inorganic sulfurs.[722,723] ENDOR experiments were performed and provided complimentary information to EPR that is required for computer simulation of Mössbauer data. These studies showed two nonequivalent iron sites in the reduced form, consistent with Mössbauer results. They also revealed some protons that are coupled to irons in the cluster.[539] While all studies are consistent with a localized electronic structure of the irons in the reduced state, a Cys → Ser mutant of a

thioredoxin like ferredoxin showed a valence-delocalized S = 9/2 feature in EPR, which was further confirmed by Mössbauer.[724]

Due to the centrosymmetric core of [2Fe-2S] ferredoxins (D_{2d}-oxidized or C_{2v}-reduced), the ungerade vibrations are Raman-inactive and the protein has fewer features than its counterpart Rieske centers. They show a characteristic Bt_{3u} at around 283-291 cm^{-1} region, which shifts to 263-273 in reduced form. Other features are an A_gt peak at 329-338 cm^{-1}, a B_{1u}t at 350-357 cm^{-1} (mostly Fe-S_t stretching mode), and an A_gb peak at 387-400 cm^{-1} in the oxidized form. These peaks appear at 307-314, 319-328, and 370-385 cm^{-1} in the reduced form, respectively. RR spectra of thioredoxin-like ferredoxins are substantially different from the other two categories due to different cluster environment. The main peaks are observed at 208, 290, 313, 335, 353, 366, 387, and 404 cm^{-1} in the oxidized form and at 267, 280, 310, 328, 370, and 390 cm^{-1} in the reduced form.[725]

It was first shown by Mössbauer that upon reduction one of the irons changes to Fe^{2+}. Mössbauer of the oxidized state shows a narrow quadruple doublet with d = 0.27 mm/s relative to iron and a splitting of 0.6 mm/s. the doublet position is temperature independent and the splitting show slight decrease at temperatures higher than 200 K. In presence of an external field, a diamagnetic species forms. The spectrum in the reduced form is temperature dependent and more complex, primarily because of magnetic hyperfine interactions and quadruple interactions. The reduced state shows d = 0.55-0.59 mm/s at 200 K. The A tensor of these proteins is more symmetric along the z-axis. In the reduced state, Mössbauer of ferredoxins reveals two quadruple doublets, one at d = 0.30 mm/s and the other at d = 0.72 mm/s, indicating two localized irons.[529,539,726]

NMR studies show that in the reduced state, the protein has a mixed valence Fe^{2+}/Fe^{3+} state with the iron closer to the surface being in the Fe^{2+} form. Solvent exchange studies by NMR suggested that reduction of the cluster might increase accessibility of protons to the cluster. NMR studies were used to analyze the interaction of ferredoxins with their redox partners to find their contact points. Chemical shift changes upon reduction have been assigned. NMR has also been extensively used for structure assignment. NMR studies showed differences between plant-type and

mammalian-type ferredoxins. While plant-type proteins show a downfield shift of Cys ligands in the reduced state, with the ligands of Fe^{3+} showing Curie-type behavior and Fe^{2+} ligands showing anti-Curie behavior, vertebrate type proteins have both upfield and downfield signals of cysteine ligands in their reduced state and all show Curie-type behavior.[539,727]

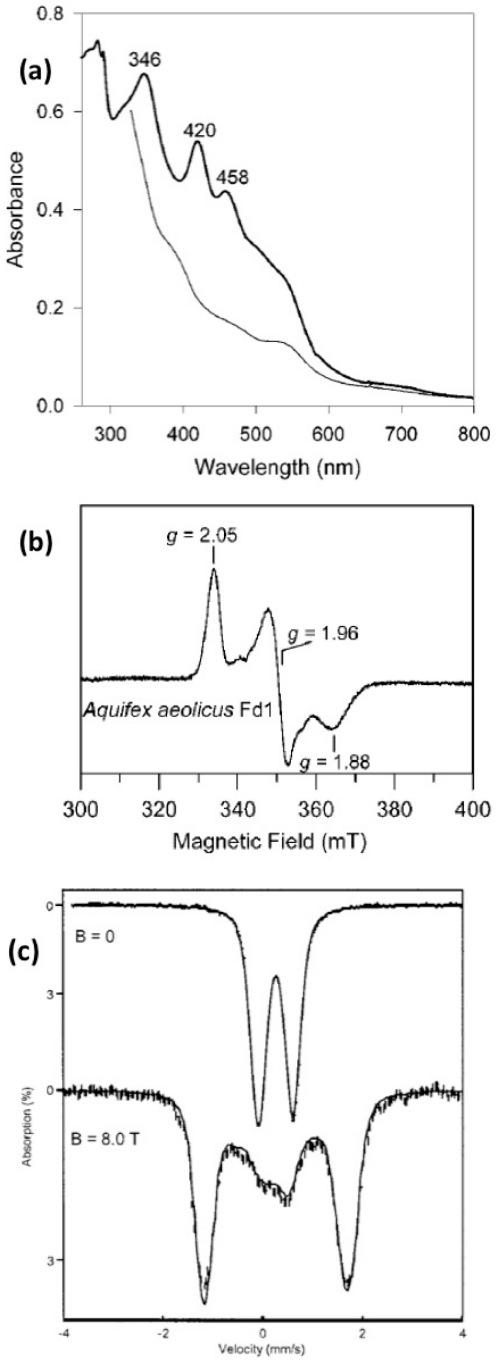

Figure 23. Representative spectra of 2Fe-2S ferredoxins:[728] a) UV-vis spectra of reduced (thin line) and oxidized form (thick line) of ferredoxin from *A. aeolicus*; b) X-band EPR of $[2Fe\text{-}2S]^{+}$ of ferredoxin from *A. aeolicus* at 20 K ; c) Mössbauer of $[2Fe\text{-}2S]^{2+}$ state of ferredoxin from *A. aeolicus* at 4.2 K in zero field (upper) and 8.0 T applied field parallel to the observed γ radiation. Reprinted with permission from ref [728]. Copyright 2002, American Chemical Society.

3.4.3.3. [3Fe-4S] and [4Fe-4S] clusters

3.4.3.3.1. Structural aspects

These clusters are mainly bacterial and usually consist of either one or two 3/4Fe-4S clusters. 4Fe-4S clusters are known to be the first clusters formed in the early earth environment, and function as a ubiquitous electron transfer members in most anaerobic bacteria. The cluster takes the form of a distorted cube, with iron and sulfur atoms positioned alternatively in apices. Three inorganic sulfurs and one thiol from a cysteine in the protein coordinate each iron. The cysteine ligands are arranged in a C-X_2-C-X_2-C motif, the so-called classic 4Fe-4S motif. The cluster resides in a common ferredoxin motif (βαββαβ) with four stranded β-sheets, two linking helices, and cluster binding loops. This fold is the most ancient ferredoxin fold and very versatile, with lots of insertions and deletions observed in different proteins of the family.[92,539]

The 2[4Fe-4S] or eight iron clusters are hypothesized to emerge from a gene duplication of ancestral 4Fe-4S cluster.[91] A Clostridial 2[4Fe-4S] protein was the first ferredoxin discovered. Due to high iron content, a large portion of the protein consists of inorganic material in these proteins. The positions of cysteine in all 4Fe-4S or 2[4Fe-4S] proteins are very similar. The proteins with two clusters can be divided into 5 subcategories based on their sequence and evolutionary relationship including: clostridial type, chromatium type from green and purple bacteria, Azotobacter [3Fe-4S][4Fe-4S] type, archaebacteria type, and single [4Fe-4S].[729] The essence of this characterization is sequence homology of 27 ferredoxins and their deviation from basal architecture, which is a two-subunit structure resulted from gene duplication with a three linker connector and a X_7-CysI-X_2-CysII-X_2-CysIII-X_8-CysIV motif in each subunit (Figure 24).[674]

Clostridial type ferredoxins follow the basal architecture and have a conserved motif of C-X_2-C-Gly-X-C-X_3-C-Pro. This motif usually contains no other cysteine except

in the case of a small number of proteins, including PaFd, which contains a ninth cysteine in its 22 position. The proteins consist of two homologous halves that arrange in a pseudo two-fold symmetry with three of the cysteine ligands come from one half and the fourth cysteine being provided by the second half, adjacent to a proline. In 2[4Fe-4S] clusters, the 4Fe-4S clusters are surrounded by two antiparallel β-strands and two α-helices. In the final arrangement of the protein, two sets of antiparallel β-sheets with two strands lie beneath the clusters and two short helices are positioned on the top of the cluster. An array of water molecules facilitates H-bonding between two halves of the protein. In clostridial ferredoxins, there is a conserved Pro after the last coordinating Cys. Although mutations of this Pro show that it is not necessary for the cluster arrangement, it provides an optimal environment for the next cluster by both providing hydrophobicity and supporting a specific turn mode for binding.[91,674,730]

In contrast, chromatium-type ferredoxins in most cases contain a ninth cysteine in position 2-8, between the second and third cysteines in clostridial core. They also have a C-terminal extension relative to clostridial sequences. Further classifications within this class are possible based on the position of their ninth cysteine and the length and arrangement of their extension including photosynthetic Fds, chromatium-type, and dimeric 2[4Fe-4S]. Chromatium-type ferredoxins have their ninth cysteine close to cluster I. In addition, they have an extended loop and a short α-helix next to the cluster II. The presence of this loop results in a positive torsion angle between Fe-S-C_α-C_β, compared to the negative angle in clostridial type ferredoxins. Moreover, the backbone orientation around this loop is changed so that this cluster I has one less NH…S H-bond.[731] Lack of this H-bond results in a slightly shorter Fe-S bond. These clusters are unstable at room temperature, pHs below 6.5, and in presence of oxygen.[674]

The Azotobacter-type ferredoxins have two residues inserted after CysII in their subunit 1 and the CysII is mutated to Ala. Their subunit 2 is intact, apart from a 48 to 49 residue extension of the C-terminus. While this extension is similar within members of the group, it differs substantially from other groups.[729]

The archaebacteria-type ferredoxins have a conserved central domain in each subunit, but further modifications are observed in regions before or after this, such as an extension of the N-terminus, or and insertion before the linker. The CysII in this class is

mutated to an Asp, resulting in a 3Fe-4S cluster that can become a 4Fe-4S cluster under certain conditions.[729]

The final group has both domains, but the conserved motif in subunit II is disrupted due to replacement of two to four of the cysteines to other non-ligating residues. Members of this group cannot be grouped further due to differences in their sequence and structure.[729]

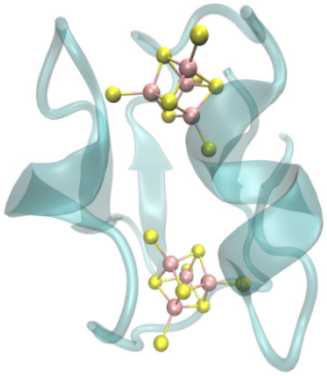

Clostridium type
PDB:1CLF

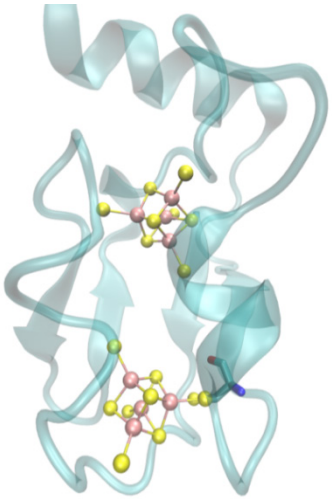

Chromatium type
PDB:1BLU

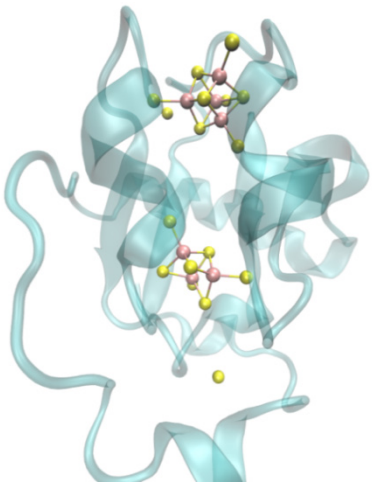

Azotobacter type
PDB:2FD2

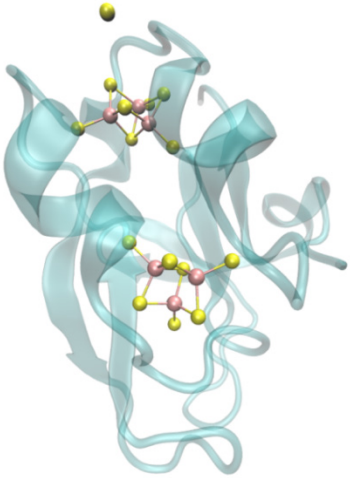

Archaea type
PDB:1XER

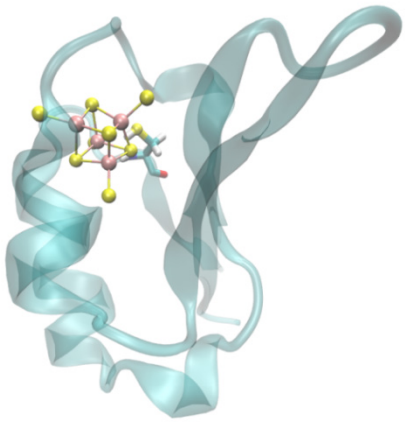

Group 5
PDB:1DFD

Figure 24. Structure of 5 classes of two-subunit ferredoxins.

Chemical modification studies showed that neither of the N- nor C-terminal Fe-S binding motif can form a stable cluster in 2[4Fe-4S] proteins, but their combination will result in formation of stable cluster.[674] Using a protein maquette of 4Fe-4S ferredoxins and step-by-step replacement and truncation of amino acids, several minimal essential features have been derived for formation of a 4Fe-4S cluster, including the spacing between Cys residues, the importance of non-coordinating amino acids in assembling and stabilizing the cluster, preferable use of Cys ligands, requirement of only 3 Cys ligands for formation of a single cluster, and the requirement of only a consensus core motif of CIACGAC.[732]

The [3Fe-4S] cluster can be thought of as a cubane 4Fe-4S cluster missing one of the irons. This class is found exclusively in bacteria, mainly anaerobic bacteria, and is involved in anaerobic metabolism. 3Fe-4S clusters can emerge from oxidative damage of 4Fe-4S clusters, as in the case of aconitase, treatment of 4Fe clusters with potassium ferricyanide, or can be found as intrinsic constituents of natural proteins, such as mitochondrial complex II and nitrate reductase. In all cases, the true reason for the presence of such clusters is not yet completely understood. It has been shown that 3Fe-4S and 4Fe-4S clusters can be interconverted under certain physiological conditions and the exchange between 3Fe to 4Fe can be used as a regulatory mechanism. 3Fe-4S clusters share the same C-X_2-C-X_2-C motif with the middle cysteine replaced by aspartate in most cases.[733] It has been shown that replacement of the Asp with Cys can change the cluster into a complete 4Fe-4S type.[734,735] Addition of two extra amino acids between the second and third cysteine can also change a [4Fe-4S] cluster into a [3Fe-4S] cluster.

Another common motif for 7Fe clusters, with some of them being thermo- and air-stable, is C-X_7-C. The presence of seven irons in [3Fe-4S][4Fe-4S] clusters has been confirmed by a combination of techniques such as EPR, Mössbauer, and x-ray crystallography. There are examples of Asp residues and hydroxyl groups from solvent as ligands. As with 2[4Fe-4S] clusters, [3Fe-4S][4Fe-4S] clusters are capable of two-electron transfer. The 3Fe-4S can be found in two states: $[3Fe\text{-}4S]^{1+}$ and $[3Fe\text{-}4S]^{0}$, with

overall spins of 1/2 and 2 respectively. H-bonds play an important role in stabilizing the reduced state. The number of these bonds is related to the extent of solvent accessibility of iron, but there are on average 6 such interactions that direct protons to the site. Two different loop motifs are present in 7Fe proteins, the long motif (C-X2-C-X_2-X_2-C or C-X_2-X_2-C-X_2-C) which is more flexible, and the short motif (C-X_2-C-X_2-C) in which CII is no longer neutral.[736] The N-terminal structure of 7Fe proteins is similar to 8Fe proteins, consisting of a central part with 4 stranded β-sheets that have the Fe-S cluster in the middle. Two short α helices connect the loops in β sheets. The structure has a partial two-fold symmetry that is disrupted at the N-terminus by differences in Cys ligands to the 3Fe cluster. There are two non-ligand Cys residues next to each cluster. Although the clusters are positioned close to the surface, the presence of hydrophobic and aromatic residues protects them from solvent. The 3Fe-4S cluster is very similar to the 4Fe-4S cluster, with Fe-Fe distances lower than S-S distances, and very similar Fe-S distances. However, the protein matrix distorts the 3Fe cluster while 4Fe cluster is more symmetric.[737]

Conserved hydrophobic residues are shown to be important for stability of the protein and not electron transfer.[738] The thermostable ferredoxins have been shown to have extra salt bridges that link residues in their N-terminus to those in C-terminus.[739]

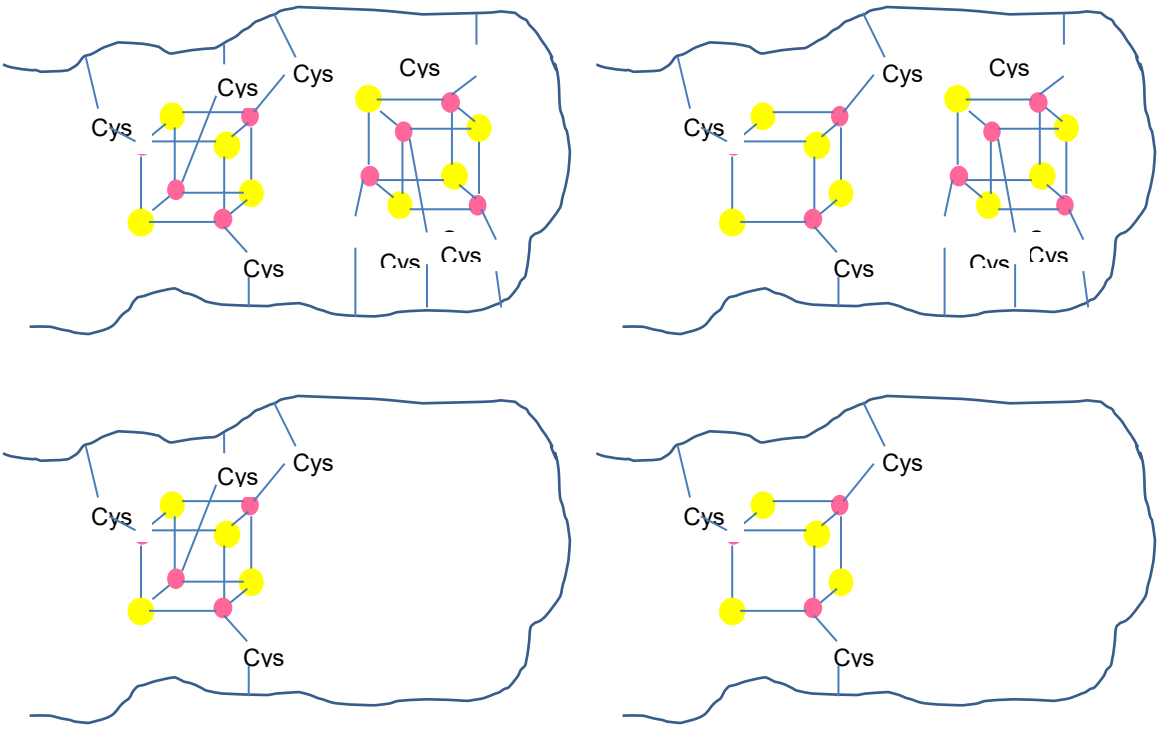

Figure 25. Consensus sequences in ferredoxins. Copyright University Science Books, Mill Valley, CA, all rights reserved. Used with permission from ref [740].

3.4.3.3.2. Function

4Fe-4S clusters are important in hydrogen evolution in anaerobic bacteria, in which the reduced form of ferredoxin transfers electrons to H^+ as the final acceptor. In *Clostridia,* reduction of ferredoxin is coupled to pyruvate oxidation. The hydrogenase complex further oxidizes the reduced ferredoxin. Ferredoxins have been shown to be important in reactions that couple oxidation of substrate with reduction of $NAD(P)^+$, FMN, FAD, riboflavin, sulfite, and N_2. They can bridge excitation of chlorophyll by light to reduction of NAD. Conversion of formate to CO_2 is often ferredoxin coupled.[674]

The role of 3Fe clusters is less well known. It has been reported that they can act in sulfite reduction. A role as iron storage has also been proposed. 3Fe-4S clusters have been observed in the monooxygenase system of *Sterptomyces griseolus*.[741]

2[4Fe-4S] clusters are mainly found in anaerobic bacteria and *Clostridial* species. However, there are multiple reports of their occurrence in other organisms such as

Micrococcus lactolyticus, *Peptostreptococcus esldenii*, *Metanobacillus omelianski*, certain photosynthetic bacteria such as *Chromatium vinosum*, *Chlorobium limicola*, and *Rb. Capsulatus*, and several extremophiles.[674]

There are several ways to test the activity of 3/4Fe class ferredoxins. Clostridial-type Fds are usually assayed using their ability to reduce NADP either in a NADP-ferredoxin reductase system or in phosphoroclastic system. Coupling H_2 oxidation to the reduction of an organic dye is another assay used to monitor the concentration and activity of ferredoxins.[674]

3.4.3.3.3. Important structural elements

3/4Fe-4S clusters are, like other ferredoxins, very low reduction potential proteins. The reduction potential of 4Fe clusters usually ranges from -400 to -650.[540] The common reduction potential for 3Fe clusters ranges from -150 to -450.[540] Several methods have been used to monitor the reduction potential of the clusters such as potentiometric CD titration, direct CV, and spectroscopic potentiometry.[737,742] In the case of 7/8Fe proteins, the reduction potential of the two sites can be similar (isopotential) or differ by values as high as 192 mV.[743] The same factors that control the reduction potential of clusters affect the reduction potential of each cluster within a multiple cluster protein. Usually the greater the difference between the reduction potentials of two clusters, the lower the electron transfer rate between the two. Mutational analyses of conserved residues that are thought to be important in the intramolecular electron transfer showed no significant decrease, but less stability. It was postulated that the geometry and relative orientation of the two clusters is the factor that is truly important in determining this rate.[737,744]

A major part of reduction potential analyses of these types of ferredoxins deal with roots of differences between them and HiPIPs. These types of studies are discussed in detail in HiPIP section.

Peptide models of 4Fe proteins showed that the reduction potential of the center is dependent on the number of Cys in the oligomer and will shift to more positive values with increasing cysteines. These studies also showed the importance of NH…S in

determining the reduction potential of 4Fe ferredoxins and their difference with HiPIPs.[717]

The reduction potential of the 3Fe cluster is pH dependent. The pH dependence is related to proton transfer via the conserved Asp next to the cluster.[737,745] Mutation of this Asp to Asn lowers the proton transfer and gates oxidation. Other studies show a less significant role for the conserved Asp, suggesting protonation of cluster itself as the main causative of pH-dependent behavior.[746] Also, it has been shown that in a protein film electrochemical set up, a hyper-reduced $[3Fe\text{-}4S]^{2-}$ can be formed.[747]

The presence of a fifth Cys residue close to the cluster can lead to formation of a SH…S H-bond and tune the activity by lowering the reduction potential. This effect is important in fine-tuning the reduction potential of proteins with two clusters. Moreover, there are around 15 partial positive charges in ferredoxins that result in an overall positive environment of the cluster, which is suggested to be a reason for the lower reduction potential of these ferredoxins compared to their higher reduction potential counterparts, HiPIPs.[674]

Introduction of a His near the cluster of a 7Fe protein causes a 100-200 mV increase in the reduction potential. The reduction potential of this variant was pH dependent. At pH values where the His was protonated, this large increase in reduction potential was attributed to placement of a positive charge next to the cluster. A dipole moment directed toward the cluster was proposed as the main cause of increased reduction potential when the His was neutral.[277]

Mutations of conserved Pro in CpFd resulted in slight but significant changes in reduction potentials of the two clusters. NMR studies of these mutants showed that signals from B-proton to cysteine sulfur were changed by these mutations.[730] Mutational analysis of conserved positive charges in the CpFd show negligible changes in redox properties.[748] Replacement of AvFdI amino acids with their counterparts in PaFd showed no change except for small changes in the case of a Phe → Ile mutation, casting doubt on the role of single amino acids in the reduction potential differences.[749] A Cys→ Ala mutation resulted in 100 mV lower reduction potential of the cluster, mainly due to changes in coordination geometry.[750]

Resonance Raman studies on the cluster showed a very similar environment of the cluster in different proteins and suggested a role for protein dynamics in differences observed in reduction potentials. These studies also suggest a role for the Fe-S-C_α-C_β torsional angle in fine-tuning the reduction potential of the site.[618,744,751]

Solvent accessibility and cluster solvation also play important roles in determining the reduction potential of these clusters. More buried clusters have higher reduction potentials.[92,749,752]

Protein Dipole Langevine Dipoles (PDLD) was used to analyze the important features for reduction potential. Based on these calculations the number and orientation of amide dipoles, and not necessarily their involvement in H-bonding, is the most important factor in defining the reduction potential. Addition of more amide dipoles by site directed mutagenesis indeed resulted in more positive reduction potential in cases where the backbone conformation didn't change drastically.[737] Another study claimed that not the absolute number of H-bonds, but the net dipole moment on the cluster is the determining factor in reduction potential of the cluster.[752]

It should be noted that factors important in determining reduction potentials of 3/4Fe clusters remain elusive. It seems that different factors have different degrees of importance in different proteins. While surface charges seem not to be important in CpFd, their mutation showed significant effects on reduction potential in other proteins. Studies on CvFd showed that the two clusters have different reduction potentials with one being extremely low, ~-600 mV. Although it seems that the cluster with classical geometry should be the one with normal reduction potential, thorough mutational and electrochemical studies on this protein proved it to be the other way.[753]

3.4.3.3.4. Spectroscopic features

Proteins with more than one cluster are usually brown in color, with a broad absorption in the 380-400 nm region. Usually an R(390)/Z(280) of more than 0.7 is observed for these proteins.[674] CD and MCD analyses showed that the 3Fe cluster of 7Fe proteins is protonated at acidic pH.[539,746]

4Fe clusters go from a $2Fe^{3+}$-$2Fe^{2+}$ EPR silent state (S = 0) to a Fe^{3+}-$3Fe^{2+}$ (S = 1/2) state with EPR signal of around 1.96, while 3Fe proteins have an EPR signal with a

feature at 2.01, going from $[3Fe\text{-}4S]^{1+}$ to $[3Fe\text{-}4S]^{0}$. Although the EPR signal is similar between this class of ferredoxins and 2Fe-2S ferredoxins, the relaxation time of 2Fe-2S clusters differs from that of 4Fe-4S type, with a common trend of [2Fe–2S] < [3Fe–4S]< $[4Fe–4S]^{3+}$ < ferredoxin-type $[4Fe–4S]^{1+}$. Therefore, the temperature dependence of EPR signal can be used as a guide to the cluster type. However, are should be taken in analysis of the signals, because spin-spin interactions between clusters can lead to enhanced relaxation time.[754]

3Fe-4S clusters have a Mössbauer spectrum with one quadruple doublet at d = 0.27 mm/s, showing three equivalent Fe^{3+} sites in oxidized state. The reduced form shows two doublets with a 1:2 ratio in intensity. The minor doublet at d = 0.32 mm/s is assigned to Fe^{3+} while the major doublet with d = 0.46 mm/s is attributed to a delocalized mixed valence $Fe^{2.5+}$ state.[529,754] The Mössbauer features of $[4Fe\text{-}4S]^{2+}$ have been discussed in detail in section dealing with spectroscopic features of HiPIP proteins.

NMR is one of the tools that have been extensively used to analyze 3/4Fe clusters. Higher number of total hyperfine shifted resonances in NMR can indicate the presence of more than one cluster in a given protein. 9 or 12 contact shifts are usually observed for [3Fe-4S] or [4Fe-4S] clusters, respectively. 4Fe-4S clusters are identified by the presence of peaks with anti-Curie temperature dependence, while Curie-type behavior is indicative of [3Fe-4S] cluster. Typical 7Fe ferredoxins show 5 downfield peaks, two with Curie temperature-dependent behavior. There are, however, 7Fe proteins with quiet different NMR spectra and more downfield peaks. These 7Fe proteins usually have a short symmetric motif. A peak at 30.0 ppm is characteristic of mononuclear 3Fe clusters.[736] In NMR studies of 3Fe clusters, it has been shown that the contact shifts of His close to the conserved Asp are pH dependent and correlate with the pK_a of the Asp residue. Also, the effects of disulfide bonds in the shifts were studied. NMR of 4Fe clusters showed very similar shifts for all Cys in the oxidized form.[755] Upon reduction, a similar pattern is observed for all 4Fe proteins with two Cys showing Curie-like behavior ($Fe^{2.5+}$) and two showing anti-Curie behavior (Fe^{2+}). This also suggests that there are two isoforms with $Fe^{2.5+}$ pair being on Cys I/III or Cys II/IV pair. The former is more preferred and this preference is stronger when a disulfide bond

is present, as shown by NMR studies.[754] The effects of other ligating residues were also analyzed in terms of NMR contact shift. NMR was also used to analyze self-exchange rate and hence reorganization energy in ferredoxins.[756] NMR studies provided structures of several ferredoxins such as [4Fe-4S] ferredoxin from *Thermotoga maritime* [757].

The resonance Raman spectra of 4Fe-4S ferredoxins can be explained without considering coupling between Fe-S and d(S-C-C) modes. For these proteins at least seven $\nu(Fe\text{-}S_\beta)$ bands and three $\nu(Fe\text{-}S_t)$ bands are observable with a band at 340 cm^{-1} being the most prominent due to total symmetry of the cubane structure. RR also used to study Se complexes of ferredoxins as well as presence of [3Fe-3S] clusters. RR studies revealed the solvent accessibility of H-bonds to cluster, the distorted D_{2d} symmetry of the cluster, and torsion angles of $Fe\text{-}S\text{-}C_\alpha\text{-}C_\beta$.[618,758] NRVS was also used to study the dynamics and the oxidized and reduced states of the 4Fe-4S cluster.[759]

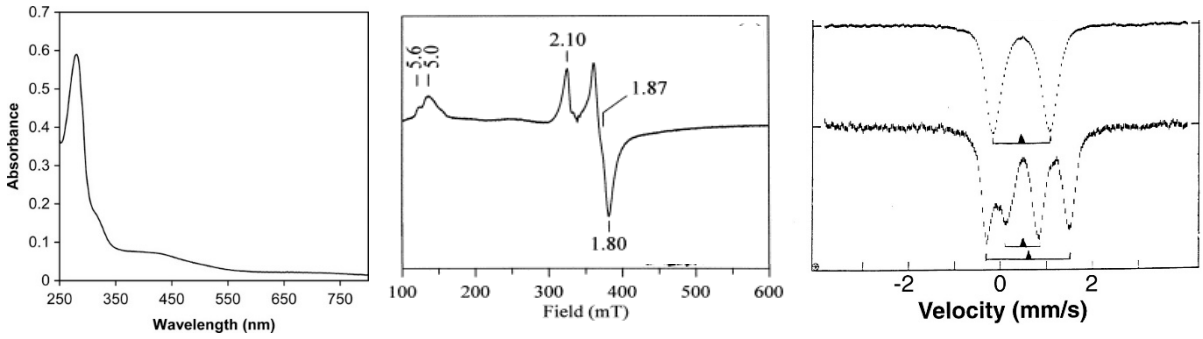

Figure 26. Representative spectra of 4Fe-4S proteins: a) UV-vis of oxidized form. Reprinted with permission from ref [760]. Copyright 2005, Springer-Verlag. b) EPR of $[4Fe\text{-}4S]^{1+}$ state. Reprinted from ref [761]. Copyright 1999, with permission from Elsevier; c) Mössbauer of $[Fe_4S_4]^{2+}$ cluster of *E. coli* FNR protein, T = 4.2 K (top) and $[Fe_4S_4]^{1+}$ cluster of *E. coli* sulfite reductase, T = 110 K (bottom). From ref [529]. Reprinted with permission from AAAS.

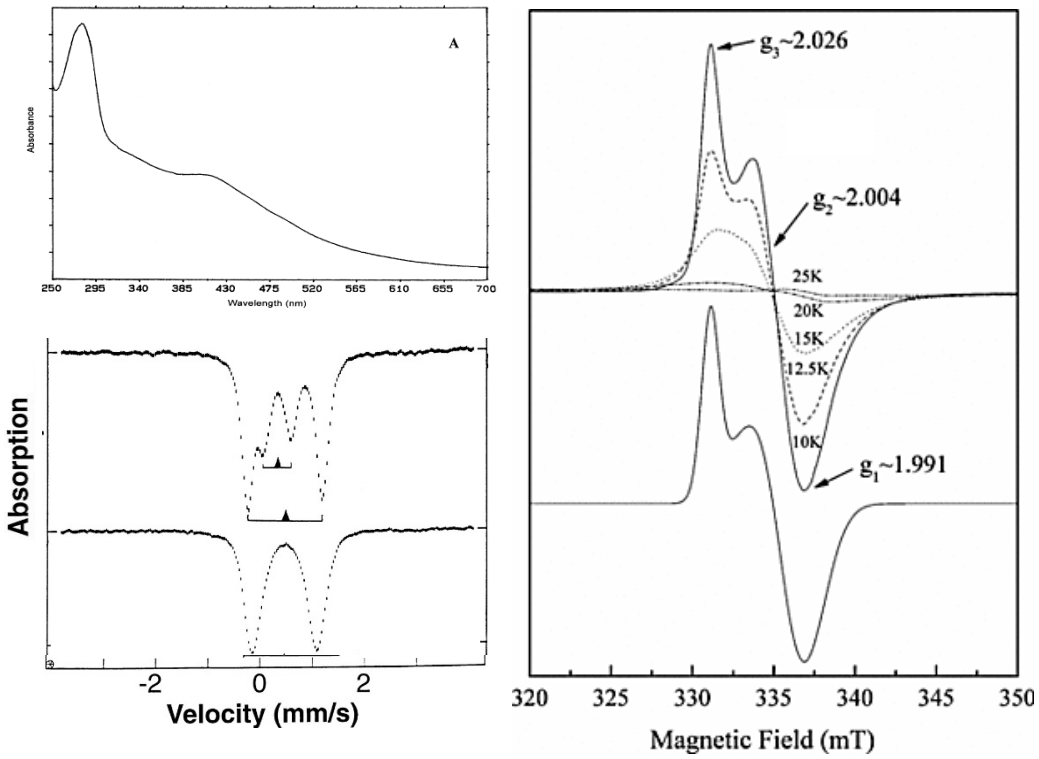

Figure 27. Representative spectra of 3Fe-4S cluster: a) UV-vis of oxidized form; b) Temperature dependent EPR of $[3Fe\text{-}4S]^{1+}$ Reprinted from ref [762]. Copyright 2002, with permission from Elsevier. c) Mössbauer of $[3Fe\text{-}4S]^{1+}$ (top) and $[3Fe\text{-}4S]^{0}$ (bottom). From ref [529]. Reprinted with permission from AAAS.

3.4.3.4. Ferredoxin like proteins

A class of so-called plant ferredoxin-like proteins (PLFP) has been discovered in the past few years. These proteins are known to play a role in several cellular processes. The first PFLP was discovered in sweet pepper. The protein consists of three domains: N-terminal signal peptide, 2Fe-2S domain, and a casein kinase II phosphorylation (CK2P) site at the C-terminus. Phosphorylation of this domain is postulated to be important in resistance to pathogens in *Arabidopsis thaliana*[763], and PLFPs are evolved in plant defense mechanism pathways.

4Fe-4S ferredoxin-like proteins are also common, and are found in some bacteria with modified C-X_2-C-X_2-C-X_3-C motif at the N-terminus or C-X_2-C-X_8-C-X_3-C-X_5-C at C-terminus. The ferredoxin-like protein in *Rhizobium meliloti* is shown to be important in nitrogen fixation. The protein is located in an operon with nif genes. Mutational analyses and molecular modeling showed the importance of extra amino acids in positioning the loop in a way that it could incorporate the cluster efficiently.[764,765]

A PLFP has been discovered in *Erwinia carotovora* that is regulated by quorum sensing. This ferredoxin has similarity to plant ferredoxins with no significant similarity to bacterial ferredoxins.[766,767] PFLP genes in *Helicobacter pylori* and its corresponding ferredoxin reductase have been shown to be important in imparting metronidazole resistance to the bacteria.[768] PFLPs are known to be important in enhancing plant resistant to bacterial pathogens. Transgenic expression of PFLP from sweet pepper in calla lily resulted in more resistance to soft rot bacterial diseases.[769] The same transformation in rice plants enhanced their resistance to *Xanthomonas oryzae* pv. *Oryzae*.[767]

3.4.5. Rieske centers

3.4.5.1. Introduction/history

Rieske proteins are 2Fe-2S iron-sulfur proteins that are distinguished by their unique His_2-Cys_2 ligation motif. The first example of these proteins was discovered by Rieske in 1964 by observation of an EPR signal with g = 1.90 in cytochrome bc_1 complex (complex III of mitochondrial electron transport chain[770]). Similar EPR signals were later observed in b_6f complex of photosynthetic chain, the membrane of bacteria with a hydroquinone-oxidizing electron transfer chain, and soluble bacterial dioxygenases. The coordination environment was first established by ENDOR and ESEEM magnetic spectroscopy and further proved by crystal structure. There have been multiple reports of presence of several isoforms of Rieske proteins in the genome of prokaryotes. Presence of these isoforms most likely aids the organism to adapt better with environmental changes.[771]

3.4.5.2. Structural aspects

3.4.5.2.1. Primary structure/amino acid sequence

The first Rieske protein to be sequenced was the Rieske protein from bc_1 complex of *Neurospora crassa*.[772] Subsequently other gene sequences of multiple Rieske proteins from a wide range of organisms have been obtained. Sequence alignment and analysis revealed a C-X-H-X_{15-47}-C-X-X-H motif as the conserved motif for 2Fe-2S ligands.[773] Based on these sequence analysis, the proteins can be divided into Rieske and Rieske-type sub-categories.

Rieske proteins can be found in *bc* complexes such as bc_1 complex of mitochondria and bacteria, b_6f complex of chloroplast, and corresponding subunits in menaquinone-oxidizing bacteria. Three residues other than Fe-S ligands are also conserved in this class of Rieske proteins, two of which are cysteine residues that form a disulfide bond important in stability of the protein,[774] and a Gly in a conserved C-X-H-X-G-C-X_{12-44}-C-X-C-H motif. Mutational analysis of this class confirmed the presence of two histidines and four cysteines essential for cluster formation.[775,776] Rieske proteins that are not part of *bc* complex also belong to this class. Some of these proteins are within complexes that are not well identified and some belong to organisms that are devoid of *bc* complex, such as TRP from *Thermus aquaticus*, and SoxF and SoxL from *Sulfolobus acidocaldarius*.[777]

Rieske-type proteins are typically part of water-soluble dioxygenases. This class of proteins can be further divided into four separate groups. *Bacterial Rieske-type ferredoxins* are water-soluble electron transfer proteins with a 2Fe-2S cluster that show no similarity to common ferredoxins and share a conserved C-X-H-X_{16-17}-C-X-X-H motif. They have diverse sequences but their three dimensional structures are very similar to other Rieske proteins. *Bacterial Rieske-type oxygenases* have a Rieske center and a mononuclear non-heme iron in their active site. In addition to four Rieske ligands, four other residues are conserved in these proteins including two glycine residues, one tryptophan and one arginine. Naphthalene dioxygenase (NDO) is the archetype of this class. *Eukaryotic homologues of bacterial Rieske-type oxygenases* also have a ligand set for Rieske coordination and a site for mononuclear non-heme iron. Choline monooxygenase and CMP-N-acetylneuraminic acid hydroxylase are examples of this

class. Lastly, there are proteins that have a *putative Rieske binding site*, with a common motif of C-Pro-H-X_{16}-C-Pro-X-H but the presence of Rieske cluster has not been confirmed in them yet.[773]

3.4.5.2.2. Three-dimensional structure/crystallographic analysis

The first structure for a Rieske protein was reported in 1984.[778] Since then crystal structures of several Rieske proteins from different categories have been solved. All Rieske proteins share the so-called “Rieske fold”. This fold consists of three antiparallel β-sheets that form a double β-sandwich (Figure 28). Sheet 1 consists of three conserved strands, 1, 10, and 9. Strands 2, 3, and 4 form sheet 2 and strands 5-8 are in sheet 3. Sheet 2 is longer and interacts with both sheets 1 and 3. The interactions between sheet 2 and 1 are mostly of hydrophobic nature. Most conserved residues are found in the loop regions connecting the β-strands, especially loops β1-β2, β2-β3, and β8-β9 (so called “Pro loop”).[91,773]

The cluster-binding subdomain is mainly located in sheet 3 and two of its adjacent loops (β4-β5 and β6-β7). Each loop provides one of the cysteine and histidine ligands, so the pattern is 2+2, in contrast to the 3+1 pattern observed in most ferredoxins. In mitochondrial and chloroplast Rieske proteins, there is a disulfide bridge that connects the loops in Rieske proteins. This disulfide bond is of prominent importance in maintaining structural integrity in these proteins because their loops are exposed to solvent. Rieske-type proteins do not have this conserved disulfide bridge. It has been argued that this difference is due to the fact that buried Rieske complexes are stable without the need to disulfide bond.[773]

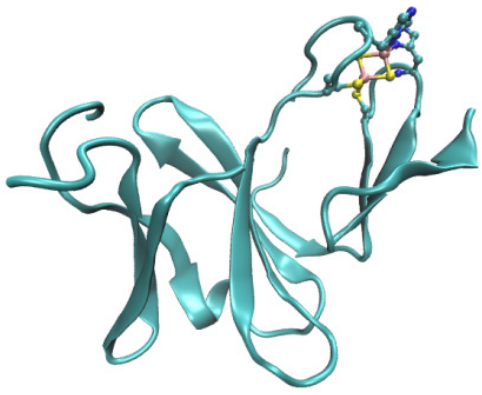

Figure 28 Minimal Rieske fold with 3 beta sheets and loops coordinating 2Fe-2S cluster with two His ligands and two Cys ligands (from PDB: 1NDO)

Rieske proteins from bc_1 or b_6f complexes have an additional "Pro loop" with highly conserved sequence of Gly-Pro-Ala-Gly that covers the cluster and has been shown to be critical for the stability.[779] In most cases the Fe^{2+} iron is the one that is more surface exposed and it is this iron atom that has two exposed His ligands. In buried Rieske complexes such as NDO, the histidines are not solvent exposed and usually form H-bonds with acidic side chains in the active site.[780] The geometry of the Fe-S cluster is the same between all Rieske proteins, forming a distorted tetrahedral conformation. In contrast to Cys ligands which impart a tetrahedral geometry, His ligands accommodate a geometry that is closer to octahedral.[773]

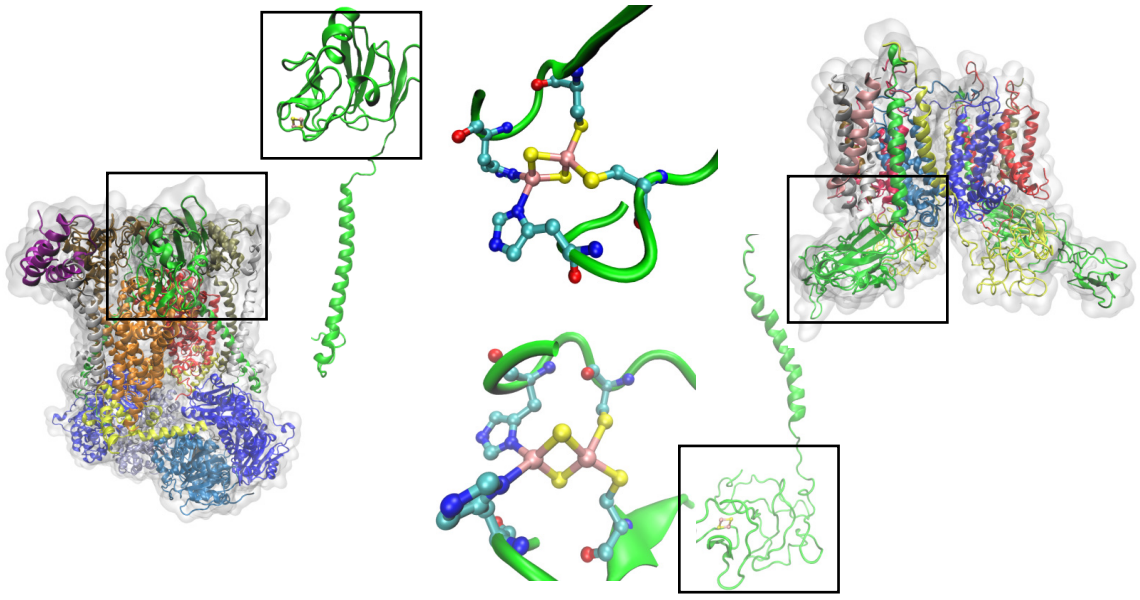

Figure 29. Structure of bc1 complex from chicken (PDB: 3H1J), its Rieske protein, and Rieske center (on left); and structure of b_6f complex from M. luminous (PDB: 1VF5), its Rieske protein and Rieske center.

Multiple H-bonds constrain and stabilize the cysteine ligands, which are conserved between most bc_1 and b_6f Rieske proteins. They are three bonds with sulfur

S-1, two with sulfur S-2, two with S_y of cysteine in loop 1, and 1 with S_y of loop 2. Usually there are H-bonds between sulfurs of coordinating cysteines and main chain nitrogen of residue i+2. These H-bonds are known to stabilize type-I turns. Two of these H-bonds are OH…S type. One from a conserved Ser to the bridging S-1, and one from a conserved Tyr to the Cys in loop 1. Rieske proteins from menaquinol-oxidizing organisms lack this Ser…Cys H-bond. Rieske-type proteins lack three of these conserved H-bonds due to lack of the conserved Ser and Tyr. Multiple site directed mutagenesis studies confirmed the importance of these two H-bonds in maintaining high reduction potential of Rieske proteins.[773,781]

Despite high degrees of structural similarity between different Rieske and Rieske-type proteins, each category has its unique features. It seems that although the cluster binding site and the minimal “Rieske fold” are highly conserved among all classes of Rieske and Rieske-type proteins, there are multiple insertions between elements of this minimal fold, mainly in loop regions. These significant differences make sequence alignments of Rieske proteins controversial, compared to their rRAN alignments.[782] Rieske-type ferredoxins have the closest structure to the minimal fold. Rieske proteins from b_6f complex usually have a C-terminal extension that is known to be important in stabilizing the open conformation required for the activity. The same role was proposed for helix-loop insertion in mitochondrial Rieske proteins. Chloroplast Rieske proteins also show a distortion in the β sheets, forming a β-barrel rather than a β-sandwich. Novel disulfide bonds have been reported at the C-terminus of a thermophilic Rieske protein from *Acidianus ambivalence,* that is reported to be important in higher stability of the protein.[783] A disulfide bond and extended C-terminal region have been observed in archaeal Rieske proteins.[784] Some acidophilic proteins have extended β strands in their cluster-binding domain. The peptide bond orientation differs in the “Pro loop” of bc_1 and b_6f complexes in regards to *cis* or *trans* configuration.[773] Some Rieske proteins have a very long loop in place of the “Pro loop” that is important for interacting with redox partners.[785] Although the pattern of H-bonding and salt bridges is similar, it is not identical, and the residues that are involved are not conserved.[773] Another difference between Rieske proteins lies in their surface charge distribution. These differences are required for interactions with different redox partners.

Different charge distribution also reflects the variation of pH in which the proteins work, as exemplified by a net negative charge on the surface of acidophilic proteins.[786]

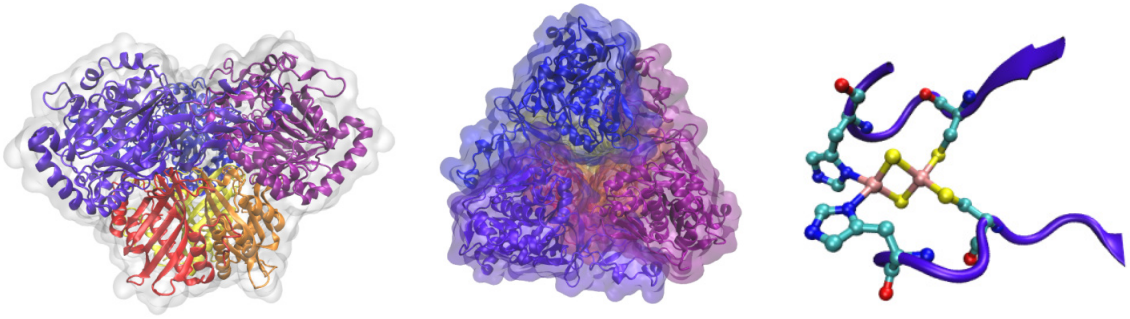

Figure 30. Structure of Naphtalene 1,2 Dioxygenase (PDB: 1NDO), the archetype of Rieske-type proteins from two different views and a close up of the active site Rieske center.

The “Rieske fold” and the geometry of the cluster are unique to Rieske and Rieske-type proteins and differ significantly from the other class of 2Fe-2S iron-sulfur proteins, ferredoxins. The most similar geometries are those of rubredoxins and the Zinc-ribbon domain, suggesting that the “Rieske fold” may have arisen from a mononuclear ancestral fold.[91]

3.4.5.3. Function

3.4.5.3.1. *Rieske clusters: cytochrome bc complexes*

Mitochondrial bc_1 complexes and chloroplast b_6f complexes are multi-subunit proteins with four redox centers organized in three subunits: two heme *b* centers in a transmembrane domain of cytochrome *b*, cytochrome $c_{1/f}$, and the Rieske iron-sulfur protein. All of them oxidize hydroquinone (ubihydroquinone/plastohydroquinone) and transfer electrons to either cytochrome *c* or plastocyanin, generating a proton gradient across the membrane through the Q-cycle. For proper function of this cycle, the hydroquinone oxidation reaction is strictly coupled. The Rieske protein is responsible for hydroquinone oxidation and acts as the first electron acceptor. Electron transfer is accomplished by direct interaction between the exposed His ligand and the quinone substrate.[787] Since the function of Fe-S cluster in these protein complexes is tied to hemes, a more detailed explanation will be presented in section 5.

3.4.5.3.2. Rieske-type clusters: dioxygenases

Rieske-type clusters are part of aromatic-ring hydroxylating dioxygenase enzymes that catalyze the conversion of aromatic compounds to cis-arene diols, a key step in aerobic degradation of aromatic compounds.[788] Dioxygenases contain a reductase, a terminal oxygenase and often a [2Fe-2S] ferredoxin. The reductase part can be of two types: ferredoxin-NADP or glutathione. The oxygenase part contains a Rieske center and a mononuclear non-heme iron center. The Rieske center transfers an electron from ferredoxin or reductase to the iron center. Although these two centers are in different domains that are far apart in a single subunit (45 Å), the quaternary structure with three-fold symmetry will bring them to a close distance within 12 Å. In most cases the His ligand of the Rieske center and one of the His ligands of iron are bridged by an Asp residue, ensuring the rapid electron transfer between the two centers (Figure 31). The removal of this conserved Asp abolishes the activity without changing the metalation.[789-791] In case of 2-oxoquinoline monooxygenase the Asp changes its position after reduction of Rieske center to H-bond with a His ligand that was protonated upon reduction. This repositioning will cause a conformational change that results in generating a five-coordinated iron geometry which is more active.[792] It has also been suggested that the H-bonds provided by this Asp can help Rieske center and catalytic center to sense the redox state and ligand state of each other. Mutational studies have been implemented to discover sites that are important in specific interactions between these Rieske centers and their redox partners.[793]

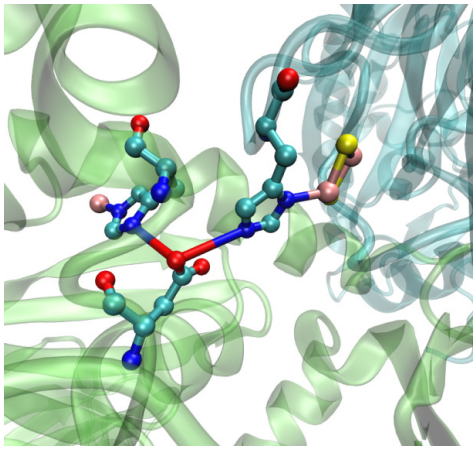

Figure 31. The interface between two monomers of NDO. Asp 205 from polypeptide chain on the left bridges two His that are ligands to Fe-S cluster and catalytic non-heme iron center (PDB: 1NDO).

3.4.5.4. Important structural elements

As with any other electron transfer center, the reduction potential of Rieske centers is one of the most important factors in determining its electron transfer rate and conveying its activity.[794] Any changes in reduction potential of Rieske and Rieske-type proteins have been shown to affect their activity and the kinetics of the electron transfer between these centers and their redox partners. Reduction potentials of Rieske centers vary a wide range of -100 to 490, which is significantly higher than average reduction potentials of ferredoxins. In general any factor that selectively stabilizes either the reduced or oxidized state of a Rieske center will influence its reduction potential. The difference between overall charge of the cluster (0/-1 in case of Rieske vs. -2/-3 in case of ferredoxins) and electronegativity of the ligands (histidine vs. cysteine) is the main reason for the higher reduction potential of Rieske proteins. Different H-bonds to bridging or terminal sulfurs, and solvent exposure of the clusters, are the main determinants of different reduction potential within the Rieske family. The reduction potential range differs depending on the type of Rieske complex: 265-310 mV in bc_1 complex and around 320 mV in b_6f complex. The reduction potentials of menahydroquinone-oxidizing complexes are 150 mV lower than that of ubihydroquinone bc_1 complex (the same difference that is observed between the two types of quinones[773]). This lower reduction potential has been attributed to lack of a H-bond donated from a conserved Ser, which is absent in the former class of Rieske proteins. Different methods of reduction potential measurement have been applied to Rieske proteins, such as chemical redox titration monitored by EPR[795] or CD[796], and direct cyclic voltammetry,[797-799] that enables measurement of thermodynamic parameters.[780] CV experiments also showed for the first time the second reduction step to a $2Fe^{2+}$ state at very low reduction potentials (~-840 mV).[797]

Computational studies showed that the cluster distortions caused by the protein environment play a prominent role in tuning the reduction potential of the center.

Accordingly, using resolved active site structures will result in calculations that agree much better with experimental values than idealized structures.[800]

An interesting feature of Rieske proteins is their pH dependent reduction potential, which decreases upon increasing pH and is attributed to deprotonation of a group in contact with the Rieske complex[801]. This phenomenon can be observed in the oxidized state where the pK_a values of one of the His ligands are near physiological pH (two pK_a values of 7.8 and 9.6 vs. one pK_a of around 12.5 in the reduced state[802]). This pH dependence can be important in interactions and binding of Rieske proteins to their redox partners. Moreover, this redox dependent ionization might be very important for their physiological function, as these proteins are part of proton coupled electron transfer systems. The biomimetic models of Rieske clusters prove the dependence of reduction potential of the center on the protonation state of its His ligands.[803] Shifts in the UV-Vis absorption peaks and CD features upon pH titration are consistent with the two protonation states of the oxidized form.[804] Several studies have shown that multiple inhibitors can bind to the His ligand and affect the reduction potential of the site.[787,805,806]

In a related study, diethyl pyrocarbonate (DEPC) was used to react with and trap deprotonated His. Addition of this ligand caused reduction of the cluster as well as an increase in overall reduction potential, a phenomenon that was observed in the case of inhibitors such as Stigmatellin, immobilizing it in the b conformation. Moreover, if the protein was reduced first, no addition would be observed, due to lack of available deprotonated His,[804,807] Analysis of some pH-independent low reduction potential Rieske proteins suggests that the coupling between the cluster oxidation state and the His protonation state also has a role in determining reduction potential of the cluster.[808]

The reduction potentials of Rieske-type clusters are lower than those of Rieske clusters, with values around -150 to -100 mV.[780] One reason for this difference is lack of three out of eight conserved H-bonds of Rieske proteins in Rieske-type proteins (Figure 32).[781] Another reason is that the cluster is more buried in Rieske-type proteins, which is also why the reduction potentials of these proteins are not pH-dependent.[809] There are examples of Rieske-type proteins that have many H-bond residues, but different loop orientations cause disruption of the H-bonding network, resulting in proteins with reduction potentials around 150 mV.[810] A Rieske-type ferredoxin has been found with a

reduction potential around 170 mV. The higher reduction potential in this Rieske-type protein has been attributed to presence of amino acid substitutions in positions around the metal center.[795]

The most important residues involved in H-bonding network in Rieske proteins are a conserved serine and a conserved tyrosine. It has been suggested that this H-bond network stabilizes the reduced state by charge delocalization, thereby increasing the reduction potential.[811] Electrostatic environment of the protein is another feature that can influence the reduction potential, meaning that the presence of charged residues on their own can increase the reduction potential of the center. In one study, removal of negatively charged residues in the vicinity of the Rieske center in Rieske ferredoxin from biphenyl dioxygenase of *Burkholderia* sp. resulted in a pK_a of the His ligands similar to that of mitochondrial Rieske proteins.[812]

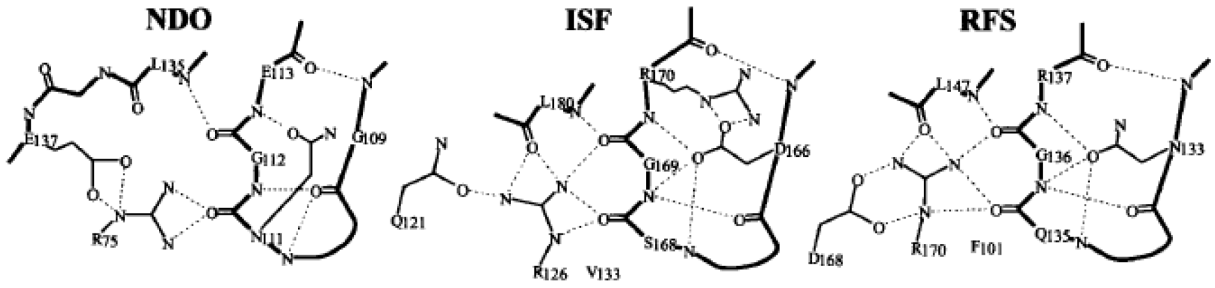

Figure 32 Differences in H-bond pattern between Rieske fragment of naphthalene dioxygenase, NDO (PDB: 2NDO); water soluble Rieske fragment of bc_1 complex, ISF (PDB: 1RIE); and Rieske fragment from b_6f complex, RFS (PDB: 1RFS). Reprinted from ref [773]. Copyright 1999, with permission from Elsevier.

Mutational analyses have been extensively used to reveal features that are important in tuning the reduction potential. Mutation of Gly143Asp, Pro146Leu, and Pro159Leu in “Pro loop” resulted in a shift of about 50-100 mV toward more negative reduction potentials, mostly due to distortion in Fe-S environment and changes in H-bond network around it.[774,779] The cluster content was decreased to 32-70% in these mutants.

Several site directed mutations were made with the goal of understanding the role of H-bonds from conserved Ser and Tyr in different organisms.[813,814] Mutations of Ser to Ala and Tyr to Phe both decreased the reduction potential.[781,815] When both

mutations were made, the effects on reduction potential were observed to be additive. It was shown that these mutations do not influence stability of the cluster or its interaction with quinone. However, the activity was decreased, demonstrating the importance of reduction potential in hydroquinone oxidation activity. These mutations also increased the pK_a values of His ligands.[815] Different effects were observed when these two residues were mutated into other amino acids. Mutations of Tyr to non-phenolic amino acids targeted the Rieske protein to cytosolic proteolytic cleavage machinery. A Ser to Cys mutation resulted in expression of proteins that could no longer incorporate a Rieske cluster, and in cases where it could, a slight increase in reduction potential was observed. A Ser to Thr mutation resulted in a protein with moderate changes in midpoint potential.[814]

Mutations of a conserved Thr that packs tightly against the “Pro loop” resulted in a lower reduction potential and a significant decrease in the activity.[816] Mutations of a conserved Leu residue that is supposed to protect the cluster from solvent were analyzed as well. Leu136Gly/Asp/Arg/His mutants were analyzed, and showed low activity and altered reduction potential. Replacement of Leu with a neutral residue such as Ala caused a similar change in both reduction potential and pK_a values of His ligands, suggesting a causative effect of change in water accessibility. Mutation to a negative residue such as Asp has marginal effects on reduction potential, probably due to movement of Asp side chain from His and its solvation. However, placing a positive charge here resulted in a significant increase in reduction potential.[817]

Several mutations in a flexible linker distant from the cluster-binding site have been shown to increase the reduction potential.[816] Mutations in a hinge region were shown to increase the E_m of the Rieske center of *Rodobacter capsulatus*. These mutations effect the reduction potential in two ways: by altering the interaction mode with quinone which is known to affect reduction potential, and by altering the positioning of head-group of the Rieske protein, which can impart changes in both reduction potential and EPR signal shape.[818] Mutations in the residues involved in disulfide bridge formation also showed decreased reduction potential values. This lower reduction potential is mainly due to removal of polarizable Cys groups, and disturbance of the loop conformation and pattern of H-bonds.[817,819] Analyses of a protein with a reduced

disulfide also showed a small decrease in reduction potential that was attributed mainly to changes in the H-bonding pattern and enthalpic effects.[820]

Similar mutational studies of conserved residues close to the cluster-binding domain of Rieske-type proteins have also been performed, showing different effects depending on the mutation type. Interestingly, replacement of an acidic glutamate close to the cluster with a neutral residue resulted in a decrease in reduction potential.[821] Mutations of a conserved Asp residue in Rieske oxygenase resulted in a lower reduction potential mainly due to deprotonation of a His ligand caused by loss of H-bond from Asp.[822]

Another important factor in determining reduction potential is the condition in which the protein performs its function. Studies on extremophilic organisms revealed that Rieske centers from acidophilic organisms have more positive midpoint potentials than neutral centers whereas potentials of acidophilic Rieske centers are significantly lower than the expected value. Interestingly, the pK_a of the His ligand also shifted correspondingly in these extremophilic organisms.[786,823]

It should be noted that there are exceptions to these general statements. There are high reduction potential Rieske proteins, such as Sulredoxin, which lacks the hydroxyl group responsible for redox modulation and shows a different pH dependent redox response than other high reduction potential Rieske proteins.[824]

Table 6. Reduction potential of different Rieske and Rieske type proteins [a]

Protein	Organism	E_m (mV)	Ref.
Rieske Proteins			
bc_1 complex	Pigeon heart	285	[825]
bc_1 complex	Beef heart	290	[806]
bc_1 complex	Beef heart	304	[826]
bc_1 complex	Beef heart	312	[798]
bc_1 complex	Beef heart	306	[827]
bc_1 complex	Beef heart	315	[828]
bc_1 complex	Yeast	262	[779]
bc_1 complex	Yeast	286	[829]
bc_1 complex	Yeast	285	[781]
bc_1 complex	*P. denitrificans*	298	[815]
bc_1 complex	*P. denitrificans*	280	[830]
bc_1 complex	*R. capsulatus*	310	[831]
bc_1 complex	*R. capsulatus*	321	[832]
bc_1 complex	*R. capsulatus*	294	[832]

bc_1 complex	*R.sphaeroides*	285	[831]
bc_1 complex	*R.sphaeroides*	300	[796]
bc_1 complex	*R.sphaeroides*	300	[796]
bc_1 complex	*C. viosum*	285	[833]
b_6f complex	Spinach	320	[834]
b_6f complex	Spinach	375	[835]
b_6f complex	Spinach	320	[835]
bc_1 complex	*Nostoc*	321	[836]
bc complex	*Chlorobium limicola*	160	[837]
bc complex	*B. alcalophilus*	150	[838]
bc complex	*H. chlorum*	120	[839]
bc complex	*Bacillus* PS3	165	[837]
bc complex	*B. firmus*	105	[840]
Rieske protein	*T. thermophilus*	140	[841]
SoxFII	*S.acidocaldarius*	375	[842]
Rieske-type proteins			
Fd_{BED}	*Ps. putida*	-155	[843]
Fd_{BED}	*Ps. putida*	-156	[844]
Fd_{BED}	*Ps. putida*	-155	[809]
Benzene-dioxygenase	*Ps. putida*	-112	[843]
2-halobenzoate 1,2-dioxygenase	*B. cepacia*	-125	[845]

2-oxo 1,2-dihydoquinoline 8-monooxygenase	*B. cepacia*	-100	[846]

[a] Reprinted from ref [773]. Copyright 1999, with permission from Elsevier.

3.4.5.5. Spectroscopic features of Rieske and Rieske type proteins

As with other Fe-S proteins, Rieske proteins have a broad absorption spectra resulting from overlapping bands from $S \rightarrow Fe^{3+}$ charge transfer. CD and MCD spectroscopy techniques were used to deconvolute some of these spectra. In their oxidized form, Rieske proteins have absorptions at 325 and 458 nm and a shoulder around 560-580 nm. Upon reduction, the position of bands shifts to 380-383, 425-432, and 505-550 nm and the intensity of bands will drop by 50%. The CD spectrum of Rieske proteins has features that are unique among Fe-S proteins, showing two positive bands between 310-350 nm, a negative band at 375-380 nm, and a set of positive bands between 400-500 nm in oxidized form. In the reduced form, CD shows a positive band at 314 nm, a negative band at 384-390 nm, and a negative band at 500 nm and a band at 760 nm. These bands are attributed to allow d-d transitions of Fe^{2+} from lowest lying d orbital into t_{2g} sets. The strong negative band at 500 nm in the reduced state is an indicator of the redox state even in the presence of other cofactors such as heme. This band has been assigned to the $d_{z2} \rightarrow d_{xz}$ transition,[809] although MO calculations cast doubts on this assignment. The CD of oxidized Rieske proteins is pH dependent in near UV and visible regions due to the presence of some deprotonation events.[804] Rieske proteins show temperature-dependent MCD spectra with multiple positive and negative bands in reduced state, but the intense negative band at 300-350 nm and positive band at 275 nm, which is observed in rubredoxins and 2Fe-2S ferredoxins, is not visible in them due to a blue shift of the bands to higher energies because of nitrogen ligation.[773]

Mössbauer studies of Rieske proteins show a temperature independent four line spectrum resulting from two quadruple doublets of the same intensity. The spectrum of the reduced form is very similar to that of ferredoxins with a more positively shifted d (0.68 mm/s at 200 K), which is due to less electron donating nature of histidine

ligands.[778,847] While the Fe^{3+} state shows quite isotropic features, the Fe^{2+} state has an anisotropic A tensor. The EFG tensor is symmetric around x for Fe^{2+}, with the largest component being positive.[529]

Resonance Raman studies of Rieske proteins excited at different wavelength showed very similar features to ferredoxins in both reduced and oxidized states, with some shifts in the bands and additional vibrations due to the presence of histidine ligands.[848] The higher number of bands in 250-450 cm^{-1} region is an indicator of lower symmetry of the Rieske proteins in comparison to all cysteinate 2Fe-2S ferredoxins (C_{2v} vs. D_{2h} or C_{2h} symmetry). Rieske proteins feature a weak peak at 266-270 cm^{-1} that is assigned to the Fe(III)-N(His) stretching mode, which is thought to have some Fe-Fe mixing parameter. The peak is shifted 8 cm^{-1} up in more basic pH, consistent with deprotonation of His. The peaks at 260-261 cm^{-1} are assigned to Fe-His bending modes and are also very sensitive to ^{15}N substitution. A peak at 357-360 cm^{-1} corresponds mainly to the Fe(III)-St stretching (B_{2t} mode).[848] This peak is very similar to that of ferredoxins, only upshifted due to either a different H-bond pattern or dihedral angles between Fe-S_γ-C_α-C_β, which is a sign of similar the Fe^{3+} environment in two classes of protein. This peak can be observed at 319-328 cm^{-1} after reduction.[725] RR pH-dependent studies at 250-450 regions show that there are no RR detectable changes at pK_a of first His ligands and changes are only observed above the pKa of second His ligand. These changes arise, however, from additional factors such as protonation of some amide backbones and not solely in regions related to Fe-N_{imid} vibrational frequency. Lack of changes at physiological pH can ensure rapid proton-coupled electron transfer.[849] No significant change was observed for Rieske-type proteins. Most RR features are due to the Fe-S stretch. The kinematic coupling observed by RR and rigidity of H-bond network around the cluster help minimize reorganization energy and hence facilitate electron transfer.[850] RR studies were also performed to analyze the role of the H-bonding network in Rieske proteins. It has been shown that presence or removal of the S…Tyr H-bond shows significant changes in RR bands at 320-400 cm^{-1}, whereas removal of the S…Ser H-bond doesn't show a detectable RR change.[824]

XAS analysis showed very similar geometry of clusters in Rieske proteins and ferredoxins, and also indicated the contraction of site upon oxidation. Early XAS

analyses were hampered by the fact that presence of His ligands was not known. XAS studies of Rieske oxygenases showed a small but significant change in bond length of Fe-S upon reduction. A larger increase in Fe-N_{imid} bond distance (0.1 A) was observed through reduction, which can facilitate electron transfer between the Rieske center and its redox partner. The edge feature has a shift toward lower energies upon reduction.[851]

EPR spectroscopy is one of the first techniques used to identify Fe-S proteins. g values of Rieske proteins are significantly lower than those of ferredoxins (1.9-1.91 vs. 1.945-1.975) due to the presence of nitrogen ligands. This EPR signal is mainly due to Fe^{2+} and its His ligands and environment.[773] The general theory explaining the EPR signals of Rieske proteins are similar to ferredoxins, starting from a ground state that has mixing between d_{z2} and d_{x2-y2}. However, EPR signals vary significantly among different groups of Rieske proteins with g_z = 2.008-2.042, g_y = 1.888-1.92, and g_x = 1.72-1.834. The rhombicity changes between 51% in z axis, and 100% to 59% in x axis.[773] In Rieske proteins all g values correlate with rhombicity, indicating that EPR properties are influenced mainly by protein environment. Changes in EPR signal upon binding to quinone or inhibitors will change the shape of the EPR signal and g values. These effects can also be correlated to rhombicity parameters.[773] An EPR study of a Rieske protein at pH 14 showed increased g values with broadened features. The appearance of these new features can be assigned to a decrease in energy difference between reductions of the Fe with two His ligands and the one with two Cys ligands due to deprotonation of both His ligands.[852]

ENDOR and ESEEM studies support the presence of two nitrogen ligands in both Rieske and Rieske type proteins.[853] Studies with ^{15}N labeled protein further support this geometry.[845,854-858] X-band ^{14}N-HYSCORE of reduced Rieske and Rieske type proteins is dominated by two histidine N_d ligands with hyperfine couplings of ~4-5 MHz. A combination of site-specific $^{14/15}N$ labeling together with orientation-selective HYSCORE studies was used to gain more insight in nature of H-bonding network around the cluster and through bond electrostatic effects.[814] ESEEM studies coupled with isotope exchange with H_2O were used to understand the proton environment around Rieske proteins from *Rb. sphaeroides*.[859] The magnetic and structural features of Cys and His ligand protons and the protons involved in the H-bonding network were

analyzed.[859] ^{1}H ENDOR analysis of Rieske from bovine mitochondrial *bc*$_1$ complex showed three peaks from orientation behavior; two from B protons of Cys ligands and one from the B proton of His141 ligand. The direction of g_{max} lies in the FeS plane with largest proton coupling along g_{int}.[860]

NMR studies have been applied to different Rieske and Rieske-type proteins.[861,862] Cysteines coordinated to Fe^{3+} show four strongly downshifted signals between 50-110 ppm. Temperature-dependent studies of H_B protons of the cysteines show that they follow Curie law. The $H_{\varepsilon 1}$ of one of the histidine ligands shows sharp resonance at 25 ppm, showing a weak Curie temperature dependent behavior. There are still complications in assigning all the resonances in NMR spectra due to unique features of Rieske NMR. NMR studies were used to monitor the H-bonding patterns[863] and solvent accessibility.[864] NMR studies on Rieske from *T. thermophilus* revealed slight conformational changes that are dependent on both oxidation state and ligand binding. ^{1}H, ^{15}N, and ^{13}C NMR analyses showed that two of observable prolyl backbones change from a *trans* to *cis* mode upon reduction.[865]

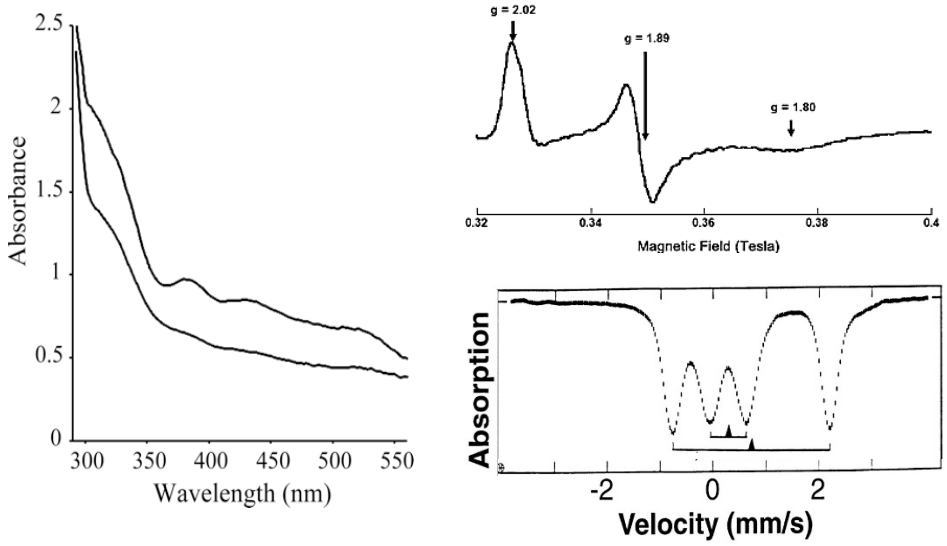

Figure 33. Representative spectra of Rieske centers: a) UV-vis of reduced and oxidized form. Reprinted from ref [866] with permission. Copyright (2004) National Academy of Sciences, U.S.A.; b) EPR of reduced form. Reprinted from ref [867] with permission. Copyright (2007) National Academy of Science, U.S.A.; c) Mössbauer of $[Fe_2S_2]^{1+}$ cluster of the Rieske protein from *Pseudomonas mendocina*, at temperature T = 200 K. From ref [529]. Reprinted with permission from AAAS.

3.4.6. HiPIP proteins

3.4.6.1. Introduction/history

High potential iron-sulfur proteins (HiPIPs) are a well-defined superfamily of Fe-S proteins found mainly in photosynthetic anaerobic bacteria although proteins from aerobic bacteria have also been reported. HiPIPs were expressed in both aerobic and anaerobic conditions.[868] HiPIPs contain a [4Fe-4S] cluster as with ferredoxins. However, higher reduction potential of HiPIPs results in one less electron in both the reduced and oxidized states of these proteins compared to ferredoxins, meaning a $[4Fe\text{-}4S]^{2+/3+}$ state.[869]

3.4.6.2. Structural aspects

HiPIPs are usually small proteins (6-11 kD). The [4Fe-4S] cluster is embedded within a characteristic fold of HiPIP proteins. HiPIP proteins are highly charged, either acidic or basic depending on the organism from which they have been purified. Despite low sequence homology, the structures of all HiPIP proteins share similar features, especially in loop regions. HiPIPs were the first iron-sulfur proteins for which a crystal structure in both oxidized and reduced form was obtained. Small size of the protein requires that the [4Fe-4S] cluster occupies a large portion of the total volume of protein. Their structures mainly consist of loops with 2 small α-helices and 5 β-strands. The cluster is positioned in the C-terminal domain of the protein (Figure 34). A conserved Tyr in most HiPIPs is located in a small helix in N-terminal packs against the cluster and interacts with one of the inorganic sulfurs, S3. Two of the Cys ligands are in two β-strands in a twisted β-sheet, and two hairpins provide the other two. Three of the four cysteines form H-bonds with backbone amides of residues i+2. Aromatic side chains from a C-terminal loop together with the conserved Tyr from N-terminal form a hydrophobic pocket that further shields the cluster from solvent. HiPIP proteins share the consensus motif of $C\text{-}X_2$ -C-$X_{8\text{-}16}$-C-$X_{10\text{-}13}$-G-W/Y-C to coordinate the [4Fe-4S] cluster. Several loops around the protein make a hydrophobic pocket for the protein to accommodate the cluster. In some cases conserved water ligands have been shown to be important for stabilizing the structure.[870]

The [4Fe-4S] cluster, as with ferredoxins, has a cubane structure in which each iron is coordinated with three inorganic sulfurs and one thiolate from cysteine. All the irons have tetrahedral geometry. Fe-Fe distances are significantly shorter than S-S distances (2.72 vs. 3.58), resulting in lower accessibility to the iron atoms. The spin coupling between pairs of irons leads to Jahn-Teller distortion and a D_{2d} state rather than a tetrahedral point group symmetry. There is also a conserved Gly close to the conserved Tyr in most HPIP proteins, which is believed to have a mainly steric function.[871] It has been shown that iron binds very tightly to these clusters, and removal of sulfur does not lead to loss of iron.[872,873]

Mutational analysis of conserved aromatic residues in HiPIP proteins confirmed a protective role for these residues against hydrolytic degradation by decreasing solvent accessibility.[715] Removal of this protection resulted in degradation of the cluster through a [3Fe-4S] intermediate as evidenced by HMQC NMR.[715] Some HiPIP proteins form higher quaternary structures; HiPIP from *Thiobacillus ferrooxidans*, for example, was isolated in a tetrameric state.[874] There are several aromatic residues in close proximity to the Fe-S cluster in HiPIP proteins. These residues have been hypothesized to play a role in electron transfer, reduction potential determination, and cluster stability. Several mutational studies suggest that these residues play a major supportive role against the degradation.[875-877]

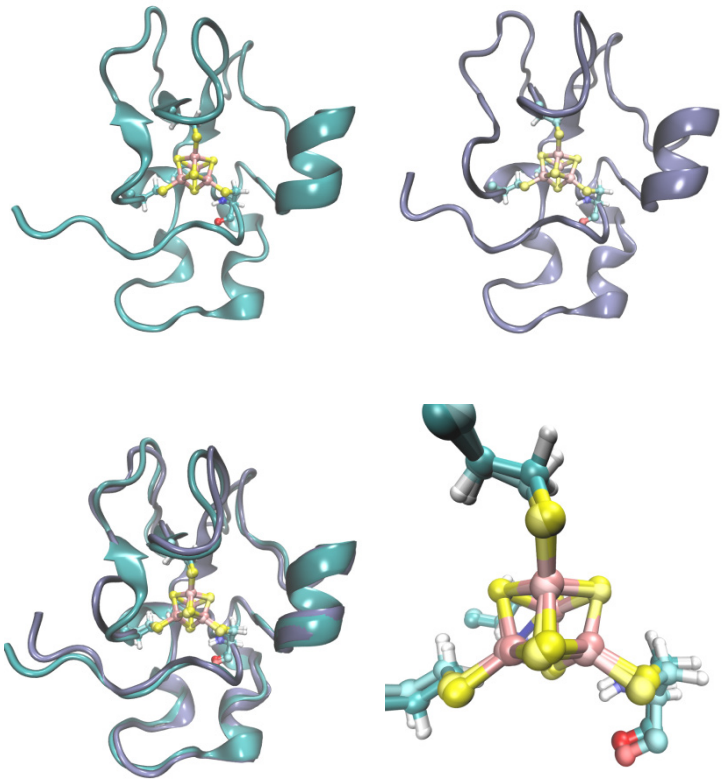

Figure 34. Structure of reduced (PDB: 1HRR) and oxidized (1NER) HiPIP from C. vinosum (Top left and Top right, respectively). The overlay of structures and zoom-in of Fe-S cluster is shown at the bottom. As shown, only slight structural changes occurred upon reduction.

3.4.6.3. Function

The HiPIP proteins appear to be unique to the bacterial kingdom and higher organisms replaced them by other more sophisticated electron transfer proteins. Despite thorough characterization of these proteins, their function is not yet fully understood. HiPIP proteins act as soluble periplasmic electron carriers in photosynthetic bacteria between the photosynthetic reaction center (RC) and the cytochrome bc_1 complex. Other functions have been reported, such as an iron-oxidizing enzyme in *Acidithiobacillus ferrooxidans*,[878] an electron donor to cytochrome *cd*-type nitrate reductase in *Paracoccus species,*[879] or a role in thiosulfate oxidation.[880] Relative distribution of HiPIP proteins and their redox behavior suggest an overlapping role of these proteins with cytochrome c_2 as a final electron acceptor in the photocycle.[872]

However, other studies have shown a distinct role for HiPIPs from Cytochrome *c*.[881] HiPIPs are also found in the membrane of some thermophilic organisms.[879] HiPIPs are mainly found in organisms with a photosynthetic reaction center having a tetraheme cytochrome (THC) subunit. Multiple studies have shown that HiPIPs could be the preferred electron carrier in purple sulfur bacteria. Crystal structure analysis, molecular docking studies, and computational modeling have suggested that the hydrophobic patch of HiPIPs can interact with a hydrophobic patch in THC so that it plays a role as a redox partner to this protein.[873,882,883]

3.4.6.4. Important structural elements

HiPIP proteins have three ferric ions and one ferrous ion that occur as a pair of two Fe^{3+} and a pair of two $Fe^{2.5+}$ ions. In the reduced state, the cluster will have two ferric and two ferrous ions, mainly existing as a set of mixed valence $Fe^{2.5+}$.[543,884] The reduction potentials of HiPIP proteins are extremely positive, occupying a range of 100 to 500 mV. Several methods have been applied to measure the reduction potential of HiPIPs including redox titration monitoring by EPR[879], chemical redox titration,[876] and direct electrochemistry[715]. Some studies have suggested further delineation of HiPIP proteins into two categories: the first with narrow reduction potential range of around 330, and a second with a broader range that depends on protein charges. However, only a few studies currently support this classification.[872,885]

Two classes of factors should be considered while studying reduction potential of HiPIPs. The first class includes factors that differentiate the reduction potentials of HiPIPs from ferredoxins. The main explanation for the difference in reduction potential between HiPIPs and ferredoxins has been well established now as the different redox states employed by the two proteins. While ferredoxins go through a $[4Fe\text{-}4S]^{1+/2+}$ transition, HiPIPs have a $[4Fe\text{-}4S]^{2+/3+}$ state. This oxidation state has an intrinsically higher reduction potential.[719] It has been reported, however, that HiPIP can form a super-reduced state of $[4Fe\text{-}4S]^{1+}$ if unfolded in 80% Me_2SO or by pulse radiolysis. The reduction potential of this $[4Fe\text{-}4S]^{2+/1+}$ state was calculated to be 400-600 mV lower than the same pair in ferredoxins. [886] There are studies in support of the importance of overall structural and backbone conformation in determining the overall potential range

of the protein.[887] Also, these studies demonstrated the role of protein environment in electron transfer not only by manipulating the driving force and reduction potential but also through changing the activation energy via environmental reorganization.[887] Resonance Raman, x-ray crystal structure analysis, computational analysis, and spin echo studies have all revealed an important role for solvent accessibility toward the higher reduction potential of HiPIPs vs. ferredoxins.[719] Moreover, crystal structure analyses of HiPIP proteins have revealed conserved NH_{amide}…S H-bonds to coordinating sulfurs.[872,873] These H-bonds stabilize the reduced form of the protein by decreasing the electron density on sulfurs, thereby increasing the reduction potential. This effect was demonstrated by replacing the backbone amide with chemically synthesized hydroxyl acid containing peptides=.[888] Ferredoxins have more of these amide H-bonds, resulting in the alternate oxidation state of the [4Fe-4S] cluster (Table 6).[93,617,618,719,887] When elongated or compressed, the [4Fe-4S] cubanes have different spin topologies; however, sulfur K-edge XAS, 2D NMR, and DFT calculations have shown that the structure is very similar in both ferredoxins and HiPIPs, resulting in a localized oxidation-reduction in both types of protein[889] and making cluster spin topology an unlikely source of redox state differentiation.

Specific interactions between hydrophobic residues are also considered a source of variation in reduction potential between HiPIPs and ferredoxins. While in HiPIP proteins aromatic…S interactions are through face of the protein, leading to interactions between the highest occupied orbital of the cluster and the lowest unoccupied Tyr orbital; ferredoxins have an edge interaction with the highest occupied Tyr orbital interacting with the lowest unoccupied cluster orbital.[872] Some studies have suggested that the main role of the conserved Tyr is to stabilize the cluster through these aromatic and H-bond interactions and not to have any profound effect on reduction potential;[877] however, because the Tyr in different proteins tends to take a different alignment, this hypothesis cannot be generalized to all HiPIPs.[540]

The second class of factors of important influence to the reduction potential of HiPIPs includes interactions that fine-tune the reduction potential. This class has not yet been fully elucidated; however, solvation and net charges on the protein are postulated to play a role in this class of proteins.[220,885,890,891] No correlation was found between the

orientation of aromatic residues in the protein and its reduction potential.[892] Thorough studies of different factors including net surface charge of the protein, partial charges of uncharged residues, polarizability of protein atoms, and solvent dipoles have been studied in a number of HiPIP proteins, and the only factor determined to correlate with reduction potential was the net charge on the protein surface (Table 7).[873,890]

The roles of different parameters involved in determining reduction potential of HiPIP proteins have been explored through mutational studies. In one such study, mutation of Cys77 ligand of *Chromatium vinosum* to Ser resulted in a 25 mV decrease in reduction potential.[893] NMR studies found negligible conformational changes in this mutant, suggesting that Ser-bound Fe is less reducible than Cys-ligated iron.[894] The role of the conserved Phe66 in the same protein was likewise investigated, finding that mutation to polar residues had minimal effects (<25 mV) on reduction potential.[799,876] Mutations in buried polar groups have indicated a role for these groups in reduction potential as well. Mutation of Ser79Pro in *C. vinosum* HiPIP resulted in a 104 mV loss in reduction potential. It has been suggested that the different electrostatic properties of the amide group between Ser and Phe and hence the ability to H-bond is the main reason for the observed effect.[895] Mutations of conserved hydrophobic residues around the Fe-S cluster (making the site more solvent accessible) resulted in minimal changes in midpoint potential as well as entropy and enthalpy of reduction.[875] Mutation of a conserved Phe to Lys showed similar marginal changes in reduction potential. However, a 15-fold decrease in the self exchange rate was observed upon addition of positive charge to the protein surface. Same protective roles have also been reported by mutation of conserved Tyr19 from *C. vinosum*.[873]

CD analysis of different HiPIP proteins has shown that pH-dependence of reduction potential in HiPIP proteins is very dependent on the proximity of a His residue to the cluster. In *T. reseopersicina*, which has His49, strong pH dependence was observed, while in *C. vinosum* and Rp. *Gelatinosa*, which have His42, show smaller pH dependence. In cases with no His, the reduction potential was independent of pH.[896] Recently, computational studies have been used to locate residues that cause the pH-dependence of a *C. vinosum* HiPIP and identified His42 as a candidate, which is consistent with previous observations.[897]

Studies have shown a more prominent role for enthalpy in determining the reduction potential of HiPIP proteins, noting a favorable change in bonding upon reduction. These proteins also show a negative entropy change. Increased loss of both entropy and enthalpy results from increasing temperature, mainly due to elongation and breakage of H-bonds in the oxidized state.[873] Covalency of the Fe-S bond and geometry of ligands in the structure have been shown to play a role in different redox states and reduction potential between HiPIPs and ferredoxins.[898] DFT and PES studies have further shown that this difference in covalency is mainly due to different arrangements of the ligands of the cluster.[899] Ligand K-edge XAS studies have also shown large differences in Fe-S covalency between HiPIPs and ferredoxins. The primary transition of the K-edge is from 1s → 4p; however, the covalent mixing from ligand 3p into unoccupied metal 3d orbitals results in an additional observable 1s → 3p transition. XAS studies demonstrated that the redox active molecular orbital (RAMO) in HiPIPs is the HOMO of the $[4Fe\text{-}4S]^{2+}$ resting state and has 50% sulfur ligand character. This results in a better super-exchange rate from cluster to surface, which is necessary for the buried cluster in HiPIPs to transfer electrons.[900] Another XAS study found that the difference in charge donation is due to different H-bonds to sulfur ligands between HiPIPs and ferredoxins. A more recent XAS study suggested hydration of the clusters as the main reason for the difference. This study showed that removal of water from ferredoxins results in higher covalency. In a similar way, exposure of HiPIP cluster by unfolding decreases the covalency.[901]

Table 7. Effect of net charge on the reduction potential of some HiPIP proteins[a]

Protein	E_m (mV)	Net charge	Ref.
Chromatium purpuratum	390	-	902
Chromatium tepidum	323	-4	903
Thiocapsa roseopersicina	346 or 325	-6	904
			905
			906
			907

Chromatium warmingii Bart	355	-4	908
Chromatium uinosum	356	-5	909
Chromatium gracile	350	-7	906 910
Thiocapsa pfennigii	350	-9	911
Ectothiorhodospira halophile	120 (iso I)	-12	896 912 913
Ectothiorhodospira uacuolata	260 (iso I), 150 (iso II)	-5 iso I, -8 iso II	914 896
Ectothiorhodospira shaposhnikouii	270 (isoI), 155 (iso II)	-6 sio I, -8 iso II	914
Rhodoferar fermentans	351	-	915 882 916
Rhodopila globiformis	450	-3	917 896
Rhodospirillum salinarum	265 (iso I)	-5 iso I, -1 isoII	914 918
Rhodopseudomonas marina	345	5	918
Rhodocyclus tenuis	300	2	914 917 919
Rhodocyclus gelatinosus	332	3	896 920 884
Paracoccus halodenitricans	282	-13	921
Thiobacillus ferrooxidans	380	1	878 878 917 874

[a] Reprinted from ref [873]. Copyright 1998, with permission from Elsevier.

Table 8. redox potenial of some HiPIP proteins and some ferredoxins with their H-bond NH…S[a]

Protein	E_m (mV)	H-bond contact	Ref.
Ectothiorhodospira halophila I HiPIP	120	5	922
Ectothiorhodspira vacuolata I1 HiPIP	150	5	892
Chromatium vinosum HiPIP	360	5	923
Rhodocyclus tenuis HiPIP	303	5	919
Bacillus thermoproteolyticus Fd'	-280	8	924

Peptococcus aerogenes Fdf	430	-	8	[923]
Azotobacter vinelandii Fd Ib	650	-	8	[925]

[a] Reprinted from ref [873]. Copyright 1998, with permission from Elsevier.

3.4.6.5. Spectroscopic features

HiPIP proteins have a brownish-green color with a prominent band at 388 nm, with R/z ratio or ~0.5, which is bleached after oxidation. The oxidized form has a very broad band with shoulders at 450, 735, and 350 nm. Both forms have 280 nm absorptions that are much higher than what is expected from aromatic contents, indicating that the cluster has some absorption in that region as well. CD (visible as well as far/near UV) has been used to probe the effect of protein environment in the properties of HiPIP proteins. It has been shown that visible CD spectra of reduced HiPIP proteins are very similar, implying strong homology in their cluster environment. Most of the spectra show a positive feature at 450 nm and two distinct negative features at 350 and 390 nm regions, with some of them showing a positive ellipticity at 330 nm. A group of HiPIP proteins show completely different features, having two positive bands between 350 and 440 nm and a negative feature at around 460 nm. CD studies indicate that the maximum band observable in absorption spectroscopy consists of several transitions, mainly an S → Fe charge transition. Visible CD of oxidized HiPIPs is usually featureless with broad maxima at 350, 400, and 450 nm. Near UV CD spectra is very dependent on the position of aromatic residues in the protein. Far UV CD spectra showed ~12-20% α-helical content in protein structure and slight changes upon oxidation and reduction.[926]

HiPIP proteins were the first class of paramagnetic proteins for which a thorough solution NMR was able to determine structure in both the reduced and oxidized forms.[927] ^{1}H NMR studies confirmed the mixed valence state in HiPIPs[884] and provided additional structural insights for these proteins.[928,929] NMR was also used to find Fe-S-C_a-C_B dihedral angles based on hyperfine shifts of B protons and A carbons.[930] Differences in electronic features of iron pairs in oxidized and reduced forms cause a significant hyperfine shift of ^{1}H and ^{13}C of cysteine ligands of the cluster. Similar shifts of B carbons in the reduced state confirm the notion that they all have similar electronic

features. Most HiPIPs show at least two isomeric electronic states apparent by room temperature NMR studies. The best explanation for this phenomenon is that the mixed valence pair can switch from iron II-III pair to iron III-IV pair. The reduction potential of irons in the cluster usually follows this trend: Fe(III) > Fe(IV)~=Fe(II)>Fe(I), so only two states are observable in the oxidized state of HiPIP proteins, which explains the presence of two electronic isomers observed in NMR and EPR.[884] NMR of the oxidized pair shows two downfield signals arising from the mixed valence pair and two upfield signals (or extrapolated upfield, which is two downfield signals with anti-Curie temperature dependence) assigned to the ferric pair with inverted electron polarization.[895,931] ^{1}H 2D EXSY NMR studies have analyzed self-exchange rates for HiPIP from *C. vinosum* and its aromatic mutants. An exchange rate of 2.3 x 104 $M^{-1}S^{-1}$ was observed for the native protein at 298 K, with rates within two folds for the mutants. This study ruled out the role of aromatic residues in electron transfer.[876] B-protons from cysteine ligands of the cluster experience large contact shifts. Eight signals from +110 to -40 can be assigned to eight protons from four B-CH_2 Cys ligands. The assignment of protons that are involved in amide-S H-bond is more difficult due to their broad features that overlap with other protons.[929,932] NMR experiments have also been used to assess water accessibility of the cluster and its mutants through analyzing the H_2O/D_2O exchange rates. ^{1}H-^{13}C HECTOR NMR was used to show that the oxidized cluster has an overall shorter relaxation time than the reduced state.[933]

EPR of HiPIP proteins shows a nearly axial signal with *g* values at 2.13 and 2.03 that result from an S = 1/2 ground state in the oxidized from.[934] In contrast to ferredoxins, HiPIPs are EPR silent in their reduced state. Some HiPIP proteins show heterogeneous signals, probably due to sample preparation or dimerization of the cluster.[799] ENDOR studies confirmed the presence of two pairs of irons in the oxidized from of protein.[935,936] EPR of most HiPIPs has shown at least two populations. Four species can be observed by EPR of HiPIPs with g_l = 2.15-2.13, 2.13-2.11, 2.06-2.08, and maybe 2.09-2.11; with the first two often being the most dominant species.[760] Assignment of these two species can be performed by correlating the EPR data with room temperature ^{1}H NMR.[760]

Zero field Mössbauer studies of HiPIP proteins at temperatures above 100 K show a broad quadruple splitting, indicative of fast electronic relaxation, with d = 0.29-

0.33 mm/s with splitting values of 0.74-0.80 mm/s. At lower temperature (4.2 K) the spectra show two non-equivalent iron pairs, one of which increases splitting with increased applied field whereas the other decreases splitting. The subsets are assigned to a ferric pair (d = 0.27, with -0.87 splitting), and a ferric-ferrous pair (d = 0.37 mm/s with splitting values of -0.94 mm/s)[895]. Mössbauer of reduced HiPIP shows non-distinguishable iron atoms in reduced HiPIP proteins. Mössbauer studies of mutated Cys→Ser HiPIP have shown loss of covalent iron features due to replacement of S with O and a different spectrum of the Ser bound iron in the reduced form, suggesting the importance of Cys residues to maintain the mixed valence state of the cluster.[937] Mössbauer analyses of partially unfolded HiPIP have found a slight increase in Fe-S bond distances without significant changes in the core cluster, indicating that the cluster is not denatured in early steps of unfolding.[529,938]

EXAFS analysis of the structure of the core cluster of HiPIP proteins and Fe-S distances has found a small temperature dependence. Analyses of Cys → Ser mutants result in slight changes to the core structure and the Fe-S distances of intact cysteines, while the Fe-O bond is shortened, suggesting that the entire cluster is shifted toward the Ser ligand.[937] Ligand K-edge XAS studies have also elucidated some of the differences between HiPIPs and ferredoxins.[900]

3.4.7. Complex Fe-S centers

3.4.7.1. Hydrogenases

3.4.7.1.1. [NiFe] hydrogenase cluster

[NiFe] hydrogenases catalyze interconversion of H_2 and H^+ in microorganisms and ultimately provide electrons for ATP synthesis. [NiFe] hydrogenases from different sources have a conserved large domain of ~60 kDa, containing the binuclear Ni-Fe active site and a small Fe-S cluster domain for electron transfer. [NiFe] hydrogenases from *D. gigas* contains two [4Fe-4S] and one [3Fe-4S] cluster, supported by EPR, Mossbauer,[939] and crystallographic studies.[940,941] The reduction potentials of the clusters are -70 mV for $[3Fe\text{-}4S]^{+,0}$, and -290 and -340 mV for the two flanking $[4Fe\text{-}4S]^{2+,+}$. The fully oxidized state of the two clusters ($[4Fe\text{-}4S]^{2+}$) gives an isomer shift of 0.35 mm/s and quadruple splitting of 1.10 mm/s. Upon reduction, the two clusters are

separated. Cluster I gives an isomer shift of 0.525 mm/s and quadruple splitting of 1.15 mm/s, and cluster II gives 0.47 mm/s and 1.35 mm/s, respectively. The parameters of $[3Fe\text{-}4S]^{1+}$ are δ = 0.47 mm/s and ΔE_Q = 1.67 mm/s, and those of $[3Fe\text{-}4S]^{0}$ are δ = 0.39 mm/s and ΔE_Q = 0.38 mm/s. The three Fe-S clusters are arranged linearly in the 3-D structure, with one [4Fe-4S] proximal to the Ni-Fe-S catalytic center, the other [4Fe-4S] at the surface, and the [3Fe-4S] cluster sits in the middle of them (

Figure 35),[940,941] indicating the existence of an electron transfer pathway.

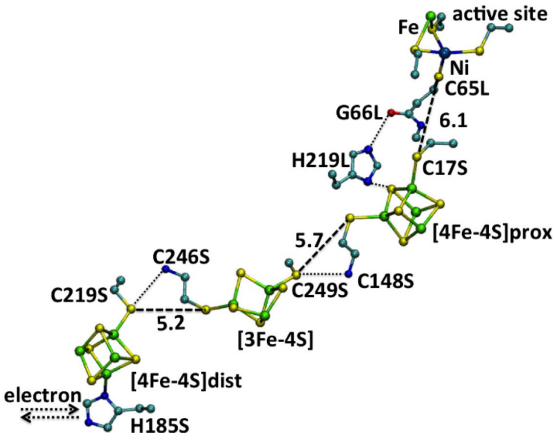

Figure 35. Proposed electron transfer pathway in *D. gigas* [NiFe]-hydrogenase. Selected distances are given in angstroms. PDB code: 1FRV. Color code: Fe, green; Ni, grey blue; C, cyan; S, yellow, O, red; N, blue. Reprinted by permission from Macmillan Publishers Ltd: Nature (ref [940]), copyright 1995.

[NiSeFe] hydrogenase, a subclass of [NiFe] hydrogenases, contains three [4Fe-4S] clusters.[942,943] The crystal structure reveals that a cysteine residue near the middle cluster, as opposed to proline usually observed in [NiFe] hydrogenases, serves as an extra ligand and results in a [4Fe-4S] cluster instead of [3Fe-4S].

[NiFe] hydrogenase from *D. fructosovorans* is structurally similar to that from *D. gigas*.[944] Based on observations made with respect to [NiSeFe] hydrogenases, a P238C mutation has been made. The $[3Fe\text{-}4S]^{+,0}$ was successfully converted to $[4Fe\text{-}4S]^{2+,+}$, and resulted in a 300 mV decrease of reduction potential with little influence on activity, indicating that $[3Fe\text{-}4S]^{+,+}$ is not essential in the electron transfer pathway of [NiFe] hydrogenase.

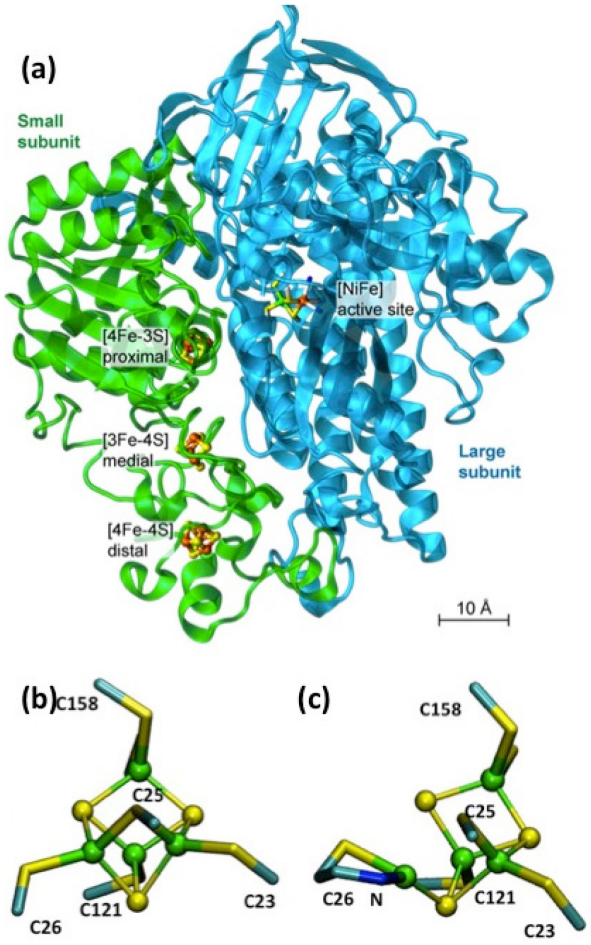

Figure 36 (a) Crystal structure of O_2-tolerant membrane bound hydrogenase from *Ralstonia eutropha*, PDB code: 3RGW. Reprinted with permission from ref [945]. Copyright 2013, American Chemical Society. (b) Reduced [4Fe-3S] cluster from MBH. PDB code: 3AYX. (c) Oxidized [4Fe-3S] cluster from MBH. PDB code: 3AYZ. Color code: Color code: Fe, green; C, cyan; S, yellow; N, blue. Reprinted with permission from ref [946]. Copyright 2012, Wiley-VCH.

Recently, a new kind of [NiFe] hydrogenase has been discovered. Unlike the usually air-sensitive members of the family, [NiFe] hydrogenases from the bacterium *Ralstonia eutropha*, *Ralstonia metallidurans*, *Hydrogenovibrio marinus*, and *Aquifex aeolicus* could tolerate O_2 to a limited extent.[947] The oxygen tolerance arises from neither modification of the [Ni-Fe] active site, nor limited access to O_2. Crystal structures of the proteins have revealed a novel Fe-S cluster proximal to the Ni-Fe center (Figure 36a).[948,949] Instead of the normal proximal [4Fe-4S] cluster coordinated by four cysteines from the protein, this cluster is a plastic [4Fe-3S] cluster bound by six cysteines with a flexible glutamic acid residue nearby. Upon oxidation, the backbone amide of the

coordinating Cys26 is deprotonated by the nearby glutamic carboxylate and replaces the bridging Cys25 (Figure 36b,c), analogous to the P cluster in nitrogenases. The negative charge of amide will help to stabilize the oxidized state. As a result, the [4Fe-3S] cluster could transfer two electrons in a window of 200 mV, and remain stable in three oxidation states.[950] DFT calculations have revealed that the supernumerary coordination frame provided by the six cysteines and the flexible coordination sphere of the Cys26-bound Fe lead to plasticity of the unique proximal [4Fe-3S] cluster and, consequently, low reorganization energy in reduced state.[945] Hence, the proximal cluster could not only transfer electrons efficiently from the active site during H_2 oxidation, but also rapidly supply two electrons to the active sites upon O_2 binding, which in combination with one electron from the middle [3Fe-4S] cluster, would efficiently reduce O_2 to H_2O and prevent formation of an inactive [Ni^{3+}- $^{-}$OOH-Fe^{2+}], the so called Ni-A state, and over-oxidation by O_2.[951-953]

3.4.7.1.2. [FeFe]-hydrogenase

[FeFe]-hydrogenases share a conserved catalytic subunit-binding metal cluster, called the H-cluster, as the catalytic site and have various Fe-S subunits harboring different Fe-S clusters for electron transfer to and from the H-cluster. The Fe-S domains are usually located at the N-terminus of the catalytic domain and contain [4Fe-4S] or [2Fe-2S] binding motifs similar to ferredoxins.[954-956] For example, [FeFe]-hydrogenase from *Desulfovibrio desulfuricans* ATCC 7757 possesses two [4Fe-4S] clusters for electron transfer,[957] and that the protein from *C. pasteurianum* contains one [2Fe-2S] and three [4Fe-4S] clusters.[958] The Fe-S clusters in *C. pasteurianum* [FeFe]-hydrogenase are separated by 8 - 11 Å, indicating potential electron transfer pathways through covalent bonds or an H-bonding network (Figure 37). FS4C and FS2 near the protein surface possibly function as the initial electron acceptors of external electron donors and transfer electrons to FS4B at the junction position. FS4A is 10 Å from cluster FS4B and 9 Å from the H-cluster and could mediate sequential electron transfer to and from the catalytic site.

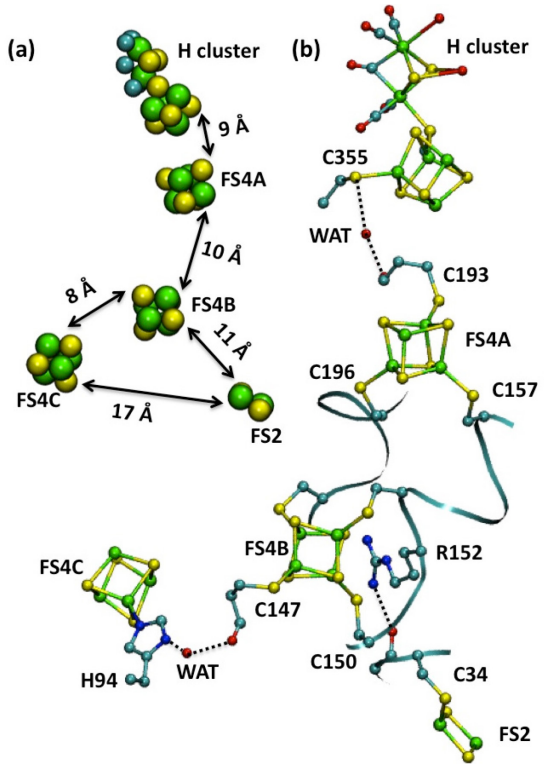

Figure 37 (a) Location of Fe-S clusters in [FeFe] hydrogenase. PDB code: 1FEH. (b) Proposed electron transfer pathways for [FeFe] hydrogenase. From ref [958]. Reprinted with permission from AAAS.

3.4.7.2 Molybdonum-Containing enzymes[273]

3.4.7.2.1 [4Fe-4S] Cluster and P-Cluster in Nitrogenase

Four types of nitrogenases have been discovered: two containing Mo and Fe, one containing V and Fe, and one containing only Fe in the catalytic site in a large domain with molecular weight of 220 to 250 kDa. Among them, FeMo Nitrogenase has been the most extensively studied (Figure 38a). Besides the active site, all nitrogenases contain an iron protein as α_2 dimers with molecular weight of 60 to 70 kDa. It contains a single [4Fe-4S] cluster between the two monomers, which is coordinated by one conserved cysteine from each monomer and is exposed to water.[959] The cluster transfers electrons efficiently via a MgATP hydrolysis reaction at the larger domain containing catalytic site, along with other functions including involvement in biosynthesis and insertion of FeMoCo into FeMo nitrogenase and regulation of biosynthesis in other nitrogenases.[960]

Three oxidation states +2, +1, and 0 have been observed for the [4Fe-4S] cluster, indicating that the cluster could transfer 1 or 2 electrons to the catalytic domain. The reduction potential to achieve an all-ferrous $[4Fe\text{-}4S]^0$ is -460 mV, and it is the first example of this oxidation state for [4Fe-4S] clusters, both in proteins and model complexes.[961-963] EXAFS studies show that changes of Fe-S and Fe-Fe distances are less than 0.02 Å from $[4Fe\text{-}4S]^{2+}$ to $[4Fe\text{-}4S]^{1+}$.[964] The cluster also can self oxidize from +1 to +2 state in the presence of dithionite.[960]

The Fe protein can bind 2 equivalents of MgATP or MgADP, each in a Walker A binding motif on one monomer. The Walker A binding site is 15-20 Å away from the [4Fe-4S] cluster with a series of salt bridges and H-bonds in between. However, reduction potential of the [4Fe-4S] cluster decreases ~ 100 mV upon binding of either nucleotide, possibly arising from protein conformational changes induced by binding and hydrolysis reactions.[965-970] The reduction potential change is proposed to be the driving force for electron transfer.[968] UV-Vis, resonance Raman and EPR spectroscopic studies indicate that the [4Fe-4S] cluster could reversibly cycle between a regular [4Fe-4S] cluster in the reduced state and two [2Fe-2S] clusters in oxidized state.[971]

The FeMo domain contains the FeMoco cluster and a P cluster. The FeMoCo center is the catalytic center, and will not be discussed here. The P cluster is situated at the interface of the α and β subunits of the FeMo domain. It is an [8Fe-7S] cluster, with a hexacoordinate sulfur at the center. The structure of the P cluster changes with oxidation state. The dithionite reduced P cluster (PN) is bound by six cysteines from the protein, four of which coordinate a single iron, and the remaining two function as bridging ligands (Figure 38b).[972] After two-electron oxidation of PN, a form called Pox is obtained. In the Pox cluster, the coordination between the center hexacoordinate sulfur and two irons associated with β subunit are replaced by amide N of Cys88 of α subunit and side chain hydroxyl of Ser188 of β subunit (Figure 38c), similar to the changes of oxygen tolerant [NiFe] hydrogenases mentioned above (see Figure 36). The changes are proposed to relate to the proton-coupled-electron-transfer (PCET) process in nitrogenases.[972-974]

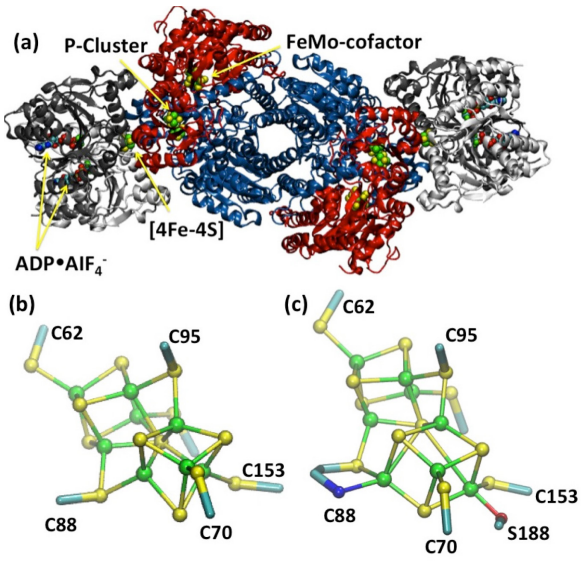

Figure 38. (a) The overall structure of nitrogenase. Cofactors are shown as spheres and denoted. PDB code: 1N2C. Reprinted by permission from Nature (ref [965]), copyright 1997Macmillan Publishers Ltd. (b) reduced P cluster from nitrogenase. PDB code: 3U7Q. (c) oxidized P cluster from nitrogenase. PDB code: 2MIN. Reprinted with permission from ref [946]. Copyright 2012, Wiley-VCH.

3.4.7.2.2. Aldehyde Oxidoreductases

Aldehyde oxidoreductase belongs to the molybdo-flavoenzymes, along with xanthine oxidase. It is a homodimer and usually requires Fe-S clusters, a molybdopterin or tungstopterin site and sometimes a FAD cofactor for substrate oxidation. Aldehyde Oxidoreductase (AOR) from *D. gigas* is composed of four domains, including two small N-terminus domains binding two types of [2Fe-2S] clusters and two large domains containing the molybdopterin cofactors.[975,976] The first Fe-S domain (residue 1-76) is similar to spinach ferredoxins, and the [2Fe-2S] cluster is coordinated by Cys40, 45 47 and 60. The second Fe-S domain (residues 84-156) is a four-helix bundle, and the [2Fe-2S] cluster is coordinated by Cys100, 103, 137, and 139. The molybdopterin is 15 Å from the surface and 14.9 Å from the Fe-S cluster of the second domain. Recently, the crystal structure of aldehyde oxidase of mouse liver has been reported. The overall fold is very similar to that of *D. gigas,* but the one of mammalian protein has an additional FAD domain.[977]

EPR studies revealed two types of [2Fe-2S] clusters, named Fe-SI and Fe-SII.[978-981] Fe-SI is observable at 77 K with *g* values of 2.021, 1.938, and 1.919, while Fe-SII is only observable below 40 K with *g* values of 2.057, 1.970, and 1.900. The reduction potential of Fe-SI and II are -260 mV and -280 mV, respectively.

In the presence of the substrate benzaldehyde, partial reduction of the Fe-S clusters has been detected in Mössbauer studies, indicating participation of the Fe-S clusters in the catalytic reaction, and fast electron transfer from the molybdopterin center.[982]

3.4.7.3. Ni-containing CO dehydrogenase and hybrid cluster protein

3.4.7.3.1. Ni-containing CO dehydrogenase

CO dehydrogenases (CODHs) catalyze oxidation of CO to CO_2 along with dehydrogenation of water and release of protons and electrons. It is important in oxygen-based respiratory process in hydrogenogenic bacteria. There are two types of CODHs. One is Mo based CODHs with a mono Mo cofactor coordinated by dithiolene sulfurs of a pterin ligand found in aerobic organisms, which is beyond the scope of this review but which has been reviewed extensively in other papers.[983,984] The other is Ni containing CODHs with a Ni-Fe-S cluster as well as multiple Fe-S clusters found in anaerobic organisms,[985-987] and will be discussed briefly below.

Ni CODHs are β_2 homodimers.[988,989] Each monomer contains a Ni-Fe-S cluster (cluster C) as the catalytic site and a [4Fe-4S] cluster (cluster B). In addition, another [4Fe-4S] cluster (cluster D) is situated at the interface of the two monomers and coordinated by residues from both monomers (Figure 39a). Cluster B and D transfer electrons between cluster C and external redox regents. It also complexes with acetyl-CoA synthases to form $\alpha_2\beta_2$ bifunctional enzymes acetyl-CoA synthases/carbon monoxide dehydrogenase (ACS/CODHs).[990] Two additional [4Fe-4S] clusters E and F have been found in an extra subunit of ACS/CODH complex.[991] The crystal structure of Ni CODH from *C. hydrogenoformans* reveals that cluster C is a [Ni-4Fe-5S] cluster (Figure 39b). The geometries of irons are approximately tetrahedral, and that of Ni is close to square planar. It is associated with the protein through four cysteines and one histidine.[988] On the other hand, the structures of *R. rubrum* Ni CODHs[989] and *M.*

thermoacetica ACS/CODH complex[991] show cluster C as [Ni-4Fe-4S], coordinated similarly by five cysteines and one histidine from the protein (Figure 39c). The Ni is also coordinated by an external nonprotein ligand.

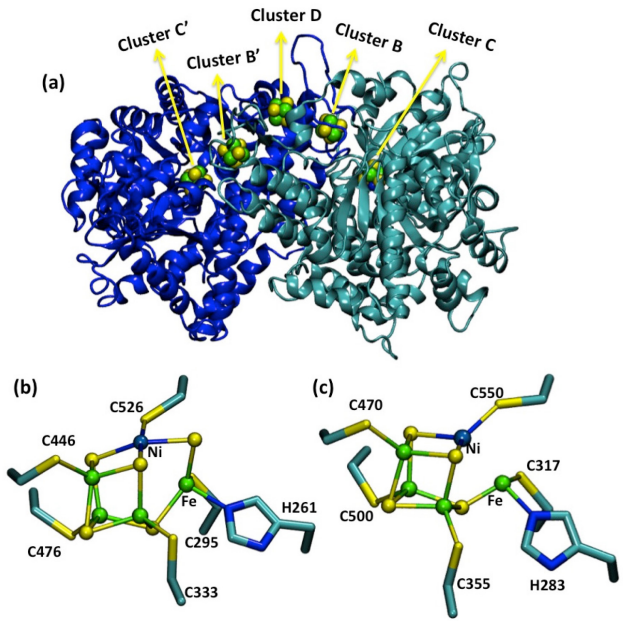

Figure 39. (a) Crystal structure of R. rubrum Ni CODH. Clusters are shown as spheres. PDB code: 1JQK. (b) [4Fe-5S-Ni] cluster C of C. hydrogenoformans Ni CODH. PDB code: 1SU8. (c) [4Fe-4S-Ni] cluster C of M. thermoacetica Ni CODH. PDB code: 1MJG. Reprinted from ref [990]. Copyright 2011, with permission from Elsevier.

3.4.7.3.2. Hybrid Cluster Proteins

Hybrid cluster proteins (HCP) are a type of Fe-S proteins with unknown functions. However, they been detected in more than 15 bacteria and archaea. There are three categories of HCP. The first is found in anaerobic bacteria such as *Desulfovibrio vulgaris*, *Desulfovibrio desulfuricans*, or methanogen archeon *Methanococcus jannaschii*, with coordinating cysteines arranged in the sequence of C-X_2-C-X_{7-8}-C-X_5-C. The second is found in facultative anaerobic Gram-negative bacteria like *E. coli*, *Morganella morganii*, or *Thiobacillus ferroxidans*, with the sequence of C-X_2-C-X_{11}-C-X_6-C. The third is found in (hyper)thermophilic bacteria or archaea including *Methabobacterium thermoautotrophicum*, *Pyrococcus abyssi*, or *Thermotoga maritima*,

with the same sequence arrangement as the first category but with smaller size due to residue deletion down-stream of N-terminal cysteine region.

HCP from *D. vulgaris* contains three domains (Figure 40a).[992,993] A [4Fe-4S] cluster is bound to domain 1 by Cys3, Cys6, Cys15 and Cys21 from the N-terminal region, similar to the cubane cluster in ferredoxins except that no cysteine is from C-terminal region. This C-X_2-C-X_8-C-X_5-C motif is conserved in all HCPs, and HCPs from both categories one and three contain a [4Fe-4S] cluster linked by this motif. HCP from category two, on the other hand, might instead have two [2Fe-2S] clusters at this position.[994]

HCP also contains a unique hybrid cluster which is [4Fe-2S-3O], which was isolated in the oxidized form from *D. vulgaris* HCP (Figure 40c),[995] and [4Fe-3S] with a water molecule between Glu494 and His244 in the reduced form (Figure 40d).[996] In the former state, the cluster is linked to the protein by Cys12, Cys434, Cys459, thiocys406, His244, Glu268, and Glu494; and in the latter case thiocys406 is reduced to cysteine. The EPR signal of HCP is similar to prismane model complex $(Et_4N)_3[Fe_6S_6(SC_6H_4\text{-}p\text{-}Me)_6]^{3+}$.[997] Therefore, the four oxidation states of the hybrid cluster are named analogously to those of the prismane complex as ‘3+’, ‘4+’, ‘5+’ and ‘6+’, respectively. The midpoint reduction potentials of the *D. vulgaris* HCP hybrid cluster range from -200 to +300 mV at pH 7.5.[998]

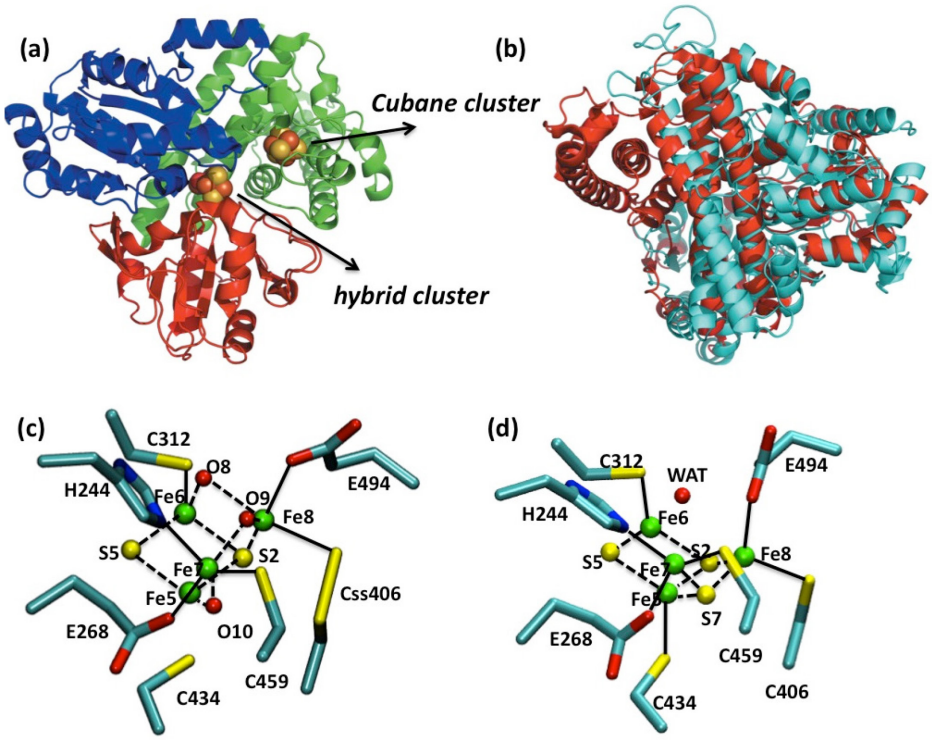

Figure 40. The hybrid clusters in HCP. (a) The overall structure of as isolated D. vulgaris HCP. Metal clusters are shown in spheres. PDB code: 1W9M. (b) Superposition of D. vulgaris HCP (cyan) and NiCODH (red, PDB code: 1SU7). (c) The hybrid cluster in as-isolated oxidized form of D. vulgaris HCP prepared anaerobically. PDB code: 1W9M. (d) The hybrid cluster in reduced form of D. vulgaris HCP. PDB code: 1OA1. Residue backbones are omitted for clarity. Bonds inside the cluster are shown as dotted lines, and bonds between residues and the cluster are shown as solid lines. Color code: Fe, green; C, cyan; S, yellow, O, red; N, blue. Reproduced from ref [995] with permission of the international Union of Crystallography. Copyright 2008.

It is noteworthy that HCPs demonstrate a high degree of similarity to Ni CODHs.[992,993,999] Not only do they share similar overall folding, but they also exhibit similar cluster positions and structures inside the monomer (Figure 40b). The closest distance between the [4Fe-4S] cluster and hybrid cluster is 10.9 Å, with Tyr493, Thr71, Asn72, and Glu494 in between. In addition, two tryptophan residues, Trp292 and Trp293, are located between the hybrid cluster and the protein surface. The arrangements indicate possible electron transfer pathways, yet no involvement in such processes has been detected so far. The protein can be reduced by NAD(P)H

oxidoreductase,[994] but there is no genomic evidence for the existence of a similar redox partner in the sources from which HCP has been detected or isolated.

3.4.7.4. Siroheme Fe-S proteins

Siroheme is an iron containing reduced tetrahydroporphyrin of the isobacteriochlorin class (Figure 41a). Siroheme proteins are a type of iron sulfur protein containing a siroheme conjugated to a [4Fe-4S] cluster through a thiolate bridge.[1000] Siroheme is the catalytic center, and the [4Fe-4S] cluster serves as an electron trapping and storage site. Siroheme proteins includes sulfite reductases and nitrite reductases, and they important in assimilation and dissimilation of sulfite and nitrite.[1001,1002]

3.4.7.4.1. Nitrite reductase

Nitrite reductase (NiR) catalyzes the six-electron reduction of nitrite to ammonium. It exists in both eukaryotes and prokaryotes. There are two types of NiR categorized by physiological electron donor: ferredoxin-dependent NiR in photosynthetic organisms and NAD(P)H dependent NiR in most heterotrophic organisms.[276,1003-1005] Ferredoxin dependent NiR contains a siroheme and a [4Fe-4S] cluster, while NAD(P)H dependent NAR contains an additional FAD cofactor bound at an extended N-terminal region.[276]

Spinach nitrite reductase is a type of ferredoxin dependent NiR isolated from higher plants. It is composed of 594 amino acids divided into three α/β domains. The siroheme cofactor is situated at the interface of the three domains and bridged to the [4Fe-4S] cluster via Cys486 (Figure 41b). The [4Fe-4S] cluster is also coordinated by Cys441, 447, and 482. The midpoint reduction potentials are -290 mV for the siroheme and -365 mV for the [4Fe-4S] cluster. Although the two cofactors are magnetically coupled with a distance of 4.2 Å, they are independent in redox titration processes.[1006,1007] Spinach NiR can form a 1:1 complex with ferredoxin with electrostatic interactions between acidic residues from Nir and basic residues from ferredoxin. The interprotein electron transfer chain has been established as from photo-excited Photosystem I via the [2Fe-2S] cluster of ferredoxin to the [4Fe-4S] cluster of NiR followed by intraprotein transfer to the siroheme.[1006-1008]

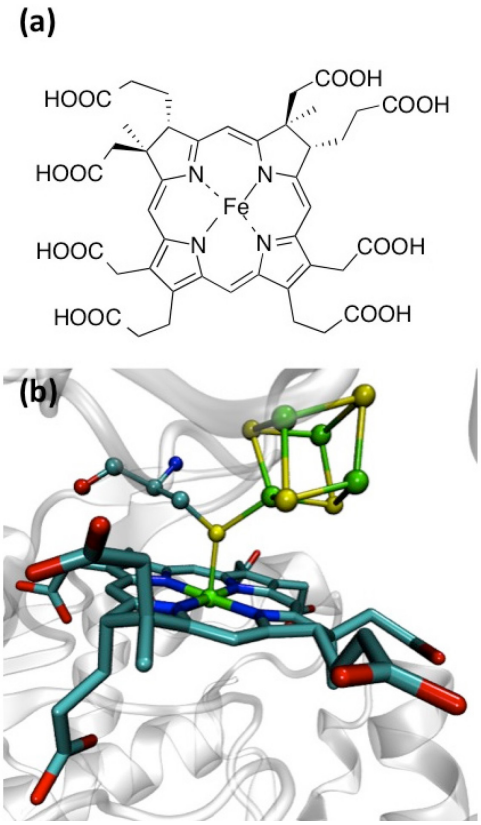

Figure 41. (a) Structure of siroheme. (b) The siroheme and [4Fe-4S] cluster of spinach nitrite reductase. PDB code: 2AKJ. Color code: Fe, green; C, cyan; S, yellow, O, red; N, blue.

3.4.7.4.2. Sulfite reductase

Sulfite reductase catalyzes the six-electron reduction of sulfite to sulfide in biological systems and can be categorized as assimilatory sulfite reductase (aSiR) or dissimilatory sulfite reductase (dSiR). aSiR reduces sulfite directly to sulfide, while dSiR provides a mixture of sulfide, trithionate, and thiosulfate in *in vitro* experiments.[1009]

The aSiRs are found in archaebacteria, bacteria, fungi, and plants.[1010,1011] Assimilatory ferredoxin dependent sulfite reductases from plant chloroplasts and cyanobacteria are soluble monomeric proteins with molecular weights of ~65 kDa. They contain a siroheme linked to a [4Fe-4S] cluster structurally similar to those in nitrite reductase, and they undergo reduction by ferredoxin from photo-reduced Photosystem I as well.[1002] They can also catalyze the reduction of nitrite to ammonium, the reaction catalyzed by NiR, but with a higher K_M for nitrite than sulfite, further demonstrating the

significant similarity of the two types of enzymes.[1002,1012,1013] For maize sulfite reductase, the midpoint potentials of siroheme and [4Fe-4S] cluster have been determined to be -285±5 mV and -400±5 mV respectively at pH 7.5 in Tris buffer by redox titrations. Although the E^o of [4Fe-4S] is more negative than that of spinach nitrite reductase (E^o = -375+10 mV at pH 7.5 in Tris buffer), reduction by ferredoxin (E^o=-430 mV) is still a thermodynamically favorable process. In the presence of cyanide, the E^o of siroheme shifts positively to -155±5 mV, while that of [4Fe-4S] shifts negatively to -455±10 mV, possibly due to decreased affinity of the enzyme for cyanide upon reduction of the [4Fe-4S] cluster. Similar trends are observed in spinach nitrite reductase as well.[1014] The aSiR from *E. coli* is a 780 kDa hemeoflavoprotein with $\alpha_8\beta_4$ arrangement. The α subunit, known as sulfite reductase flavoprotein, contains FAD and FMN, while the β unit, named sulfite reductase hemoprotein, harbors the associated [4Fe-4S] cluster and siroheme. The electron transfer pathway is in the sequence of FAD-FMN-[4Fe-4S]-siroheme with NADPH as the initial donor and sulfite as the terminal acceptor.[1015]

Dissimilatory sulfite reductases (dSiRs) exist in sulphate reducing microorganisms.[1010,1011] dSiR is composed of two types of subunits, DsrA and DsrB, generally in heterotetrametric $\alpha_2\beta_2$ arrangement with similar overall folds for all dSiRs from different sources.[1016,1017] Some dSiRs form a complex with two additional subunits of DsrC and result in a $\alpha_2\beta_2\gamma_2$ arrangement. dSiR contains eight [4Fe-4S] clusters together with four sirohemes or two sirohemes and two sirohydrochlorins (the metal-free form of siroheme) (Figure 42a,b), and only two of the four sites are catalytically active. In *D. gigas desulfoviridin*, a subcategory of dSiR, a [3Fe-4S] cluster is associated with the siroheme instead of [4Fe-4S] in one active form, Dsr-II (Figure 42c). The relative position of siroheme and [4Fe-4S] cluster is similar to that in aSiRs, and both the [4Fe-4S] cluster proximal to and remote from the siroheme are coordinated by four cysteines from the protein.[1018-1020]

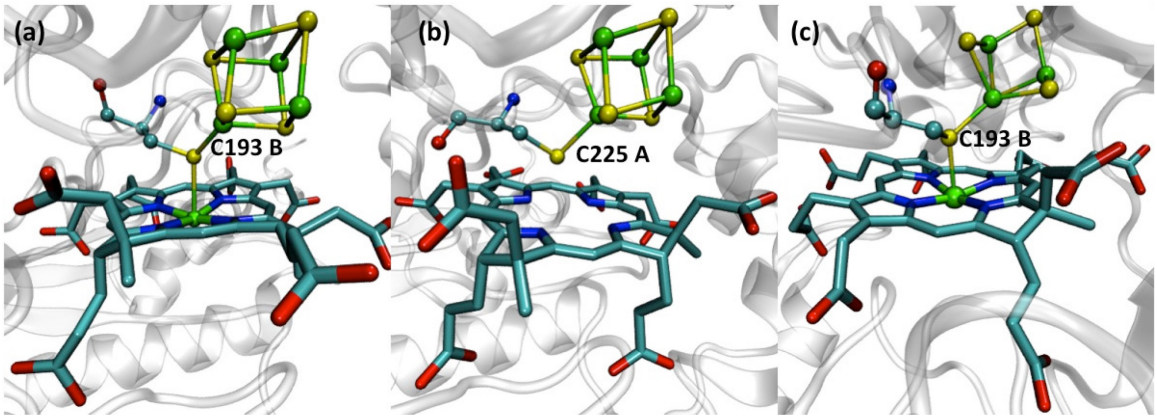

Figure 42. (a) the siroheme group and [4Fe-4S] cluster of DsrI. PDB code: 3OR1. (b), the sirohydrochlorin group and [4Fe-4S] cluster of DsrII. PDB code: 3OR2. (c) The siroheme group and [3Fe-4S] cluster of DsrII. PDB code: 3OR2. Color code: Fe, green; C, cyan; S, yellow, O, red; N, blue.

3.4.7.5 Respiratory complex chain

Mitochondrial respiratory system is the main energy producer in eukaryotic cells.[1021,1022] It consists of five membrane complexes, including Complex I,[1023] Complex II (succinate dehydrogenase),[1024,1025] Complex III (cytochrome bc_1 complex),[1026-1029] Complex IV (cytochrome *c* oxidase complex),[1030,1031] and Complex V (ATPase).[1032] The first four complexes are located on the inner membrane and function by transferring electrons from electron donors, NADH and succinate, to the final electron acceptor, oxygen, and meanwhile pump protons across the membrane. This proton gradient is utilized by ATPase to generate ATP.

3.4.7.5.1. Respiratory Complex I

Respiratory complex I (CI), also known as NADH:ubiquinone oxidoreductase or NADH dehydrogenase, is involved in one of the electron transfer pathways of the respiratory chain. It is composed of the following steps: (1) NADH donates electrons through CI to reduce ubiquinone to ubiquinol; (2) Ubiquinol transfers electrons through Complex III to cytochrome *c*; (3) Cytochrome *c* is oxidized by Complex IV and transfers electrons to O_2 to produce water. In this process, each electron transferred is associated with five protons pumped from the matrix to the inner membrane space.

Although CI is the most complicated complex in the mitochondrial respiratory chain, important breakthroughs have been achieved, and multiple structures have been reported recently.[1023,1033-1036] Mammalian CI (~980 kDa) is composed of up to 45 different subunits including 7 subunits in hydrophilic parts harboring one FMN (flavin mononucleotide) and eight Fe-S clusters, 7 subunits in transmembrane parts, and ~30 accessory subunits.[1022,1037] Bacterial NADH dehydrogenase (~550 kDa) only contains 13 to 16 subunits, which is sufficient for complete CI function as well.[1023,1038-1040] The crystal structure of the hydrophilic part of Complex I from *T. thermophilus*[1023] reveals for the first time the main electron transfer pathway of the protein as shown in Figure 43: electrons from NADH are transferred through FMN to N3, followed by N1b, N4, N5, N6a, and N6b sequentially, and finally through N2 to ubiquinone coupled with proton translocation.[1022]

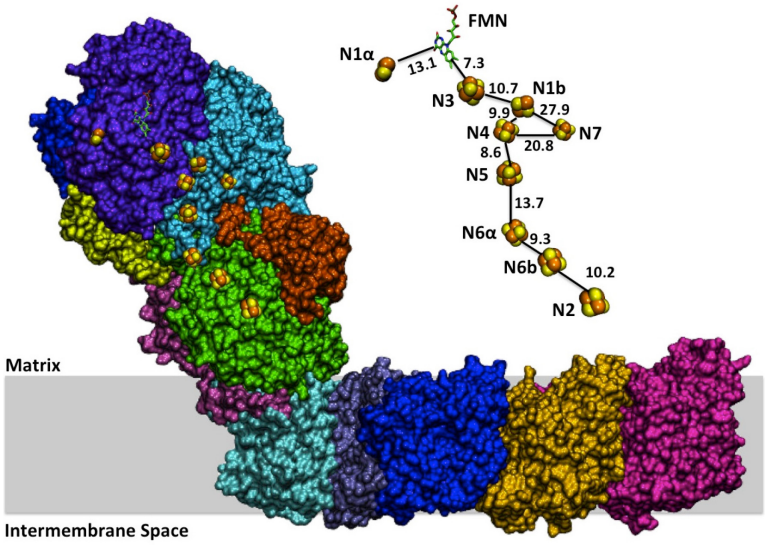

Figure 43. Crystal structure of mitochondrial respiratory Complex I from *T. thermophilus*. PDB code: 4HEA. Cofactors involved in electron transfer pathway are shown on the right side with distances directions denoted. Reprinted with permission from ref [1022]. Copyright 2013 Elsevier.

3.4.7.5.2. Respiratory Complex II (Succinate dehydrogenase) and fumarate reducatse

Complex II in respiratory chain (CII), also known as succinate dehydrogenase or succinate:quinone reductase, is a membrane bound protein involved in the citric acid

cycle and the second electron transfer pathway in the mitochondrial respiratory chain. In mitochondrial respiratory chain, electrons are transferred from succinate to ubiquinone through Complex II, then to cytochrome *c* through Complex III, and finally to O_2 through complex IV. This process is less efficient than the process associated with Complex I, and each electron transferred will pump only three protons across the membrane.

CII catalyzes oxidation of succinate to fumarate by a hydrophilic catalytic domain composed of a large flavoprotein (65~79 kDa, Fp) with a covalently bound FAD cofactor (flavin adenine dinucleotide) and iron-sulfur protein (25~37 kDa, Ip) containing [2Fe-2S] (center S1), [4Fe-4S] (center S2) and [3Fe-4S] (center S3).[1024,1025,1041] The catalytic domain is anchored to the membrane by one or two hydrophobic domains (CybL, CybS) harboring usually *b* type cytochromes (Figure 44). The [2Fe-2S] center is coordinated by four cysteines close to the N-terminus, and the [4Fe-4S] and [3Fe-4S] clusters are coordinated near the C-terminus by two cysteine-containing sequences: C-X_2-C-X_2-C-X_3-P and C-X_2-X-X_2-C-X_3-C-P(X = Ile, Val, Leu or Ala), similar to 7Fe ferredoxins. The [4Fe-4S] cluster usually has low reduction potential and functions as the energy barrier of the electron transfer process to direct the electron flow and, consequently, the reaction pathway.[1042] The [3Fe-4S] cluster is involved in a direct electron transfer process from the initial electron donor quinones.[1043-1045] The midpoint reduction potential of the $[3Fe\text{-}4S]^{+,0}$ cluster is in the range of +60 to +90 mV, and the potential of the initial electron donor ubiquinone is +65 mV.[1046] SDH from *S. acidocaldarius* harbors a [4Fe-4S] instead of [3Fe-4S] for cluster S2 and displays poor reactivity towards caldariella quinone. [1047]

It is noteworthy that heme *b* (E^o = +35 mV) in the hydrophobic domain of SDH is not involved in the electron transfer pathway mentioned above. It is proposed that heme *b* in SDH of *E. coli* functions as an electron-sink and reduces ROS species to protect FAD and Fe-S clusters.[1025] However, the reduction potential of heme *b* in SDH of porcine is -185 mV,[1048] much lower than that of *E. coli.* Therefore, the electron sink mechanism is less effective in this case and needs further investigation.

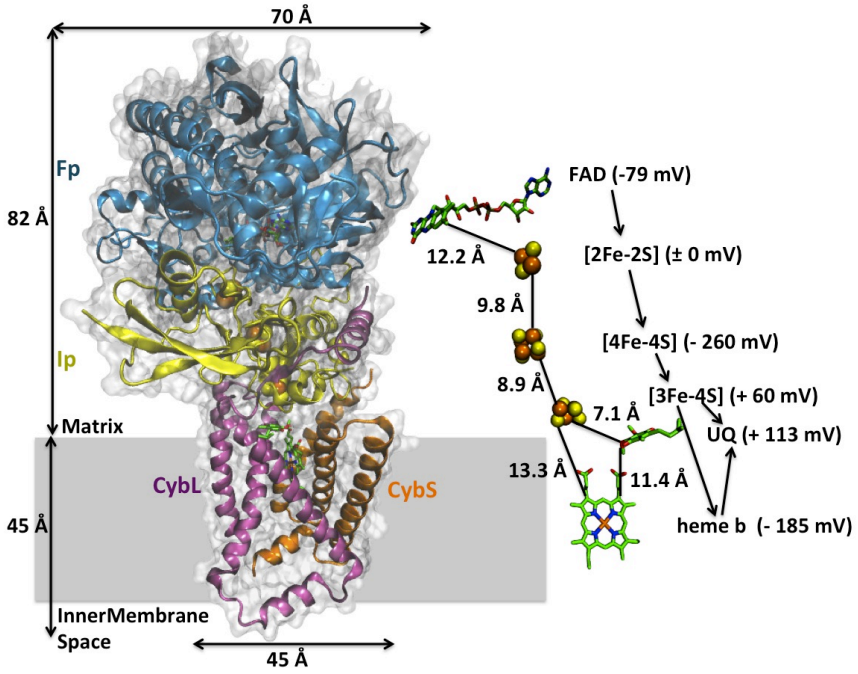

Figure 44. Crystal structure of Mitochondrial Respiratory Complex II. FAD binding protein (Fp) is shown in blue; iron-sulfur protein (Ip) is shown in cream; hydrophobic domains are shown in pink and orange; the putative membrane is shown in grey shade. PDB code: 1ZOY. Cofactors involved in electron transfer pathway are shown on the right side, with distances, reduction potential, and directions denoted. Reprinted from ref [1024]. Copyright 2005, with permission from Elsevier.

Fumarate reductase is a member of the succinate-ubiquinone oxidoreductase superfamily as well. It catalyzes the reduction of fumarate to succinate, the reverse reaction of SDH. It is very similar to SDH in subunit composition and cofactors.[1049,1050] Its three iron-sulfur clusters are linked to the protein by cysteine residues in *E. coli*, which are conserved in other fumarate reductases too. The midpoint reduction potential is between -70 to -20 mV, and that of the initial electron donor menaquinol is -74 mV.[1046]

3.5. Engineered Fe-S proteins

3.5.1. Artificial rubredoxins

A rubredoxin-like [$FeCys_4$] center has been constructed into thioredoxin by computational design. The first coordination sphere is composed of two cysteines, Cys32 and Cys35, which form a disulfide bond in wild type thioredoxin, as well as two cysteines introduced by mutation, Trp28Cys and Ile75Cys. The resulting mono-iron center resembles Rd in UV-Vis and EPR spectra, and the mimic protein is able to undergo three cycles of air oxidation and β-mercaptoethanol reduction.[1051]

The redox process of rubredoxin is not fully reversible due to the instability of the reduced form. Nanda et al. have constructed a minimal rubredoxin mimic RM1 based on computational design for more restraint tertiary structure derived from *Pf*Rd. RM1 is a domain-swapped dimer fused with a highly stable hairpin motif tryptophan zipper and displays spectroscopic properties very similar to native Rds. Moreover, it shows a reduction potential of 55 mV vs. NHE and maintains redox activity for up to 16 cycles under aerobic conditions.[1051]

3.5.2. Artificial 4Fe-4S clusters

There have been numerous studies focusing on making model compounds of ferredoxins[1052-1054] and using those models to elucidate features of natural Fe-S clusters using several methods.[803,1055-1057] In addition to organic models of ferredoxins that are discussed in a review in this journal, protein and peptide models of ferredoxins have also been made. These models have been discussed in details in another review in this thematic issue and we will discuss them here only briefly.

Almost all of these mimics are modeled after [4Fe-4S] clusters, usually made by simply placing the conserved motif within a scaffold. Work from Dutton and Gibney have been focused on unraveling the minimal structures required for binding of Fe-S clusters.[732,1052,1058,1059]

A 16-amino acid peptide has been modeled to incorporate a low potential (ferredoxin) [4Fe-4S] cluster. Interestingly, the substitution of Cys ligands by Ala in this model did not have a significant effect on the cluster. This peptide, however, was not

able to assemble a [4Fe-4S] cluster in aqueous solvent, indicating that intervening sequences are important in cluster binding. More detailed sequence alignments resulted in design of peptides with better cluster binding features that mimic F_A and F_B of photosystem I.[705] Other peptide models have also been made to analyze reduction potential properties of different Fe-S clusters including [4Fe-4S] clusters, 2Fe clusters, and rubredoxins.[717]

Four-helix bundle models of [4Fe-4S] clusters are among the most common systems to build and study these clusters. Both a single [4Fe-4S] cluster and a [4Fe-4S] cluster together with a heme cofactor have been designed in such 4-helix bundles.[1061,1062] Recently a “metal first” approach has been taken to introduce a [4Fe-4S] cluster into a non-natural a-helical coiled coil structure. The design then went through further optimization and addition of secondary sphere interactions to stabilize the reduced form and prevent aggregation. Such designs that are independent of structural motifs can be used as a platform for the future design of multi-clusters to be used as bio-wires.[1063]

3.6. Cluster interconversion

Although Fe-S clusters are mostly classified based on the number of iron atoms in the site, it is worth noting that this number by no means is restrictive and there are several cases in which changing of one cluster to another type have been observed, so called “cluster interconversion”. These cluster interconversions can happen through three types of processes: natural changes in the environment of the cluster, chemical treatments of the cluster, or amino acid replacement.

One of the most common types of cluster interconversion is the [4Fe-4S] change into [2Fe-2S]. This kind of conversion has been observed in hydrogenases and nitrogenases. While CD and MCD analysis show that MgATP/ADP binding to [4Fe-4S] cluster of Fe hydrogenase does not result in conversion to a [2Fe-2S] cluster,[1064] decomposition of the [4Fe-4S] cluster of nitrogenase upon α,α’-dipyridyl treatment resulted in formation of a [2Fe-2S] cluster in the presence of MgATP.[1065,1066] [4Fe-4S] to [2Fe-2S] conversion has been observed in enzymes such as ribonucleotide

reductase[1067] and pyruvate formate activating enzyme[1068] as well, usually upon oxidation in air or chemical treatment.

A very well studied case of the role of [4Fe-4S] to [2Fe-2S] cluster conversion in regulating cellular responses is the case of fumarate nitrate reduction transcription factor (FNR). It has been shown that this protein undergoes the conversion upon O_2 stress. The excess oxygen will oxidize S ligands and generate disulfide cysteines. The formation of a disulfide-Cys ligated [2Fe-2S] cluster will result in a monomerization of FNR dimer, hence unbinding from DNA.[1069,1070] The conversion is composed of two steps: first, the [4Fe-4S] cluster undergoes a one electron oxidation to form a $[3Fe\text{-}4S]^{1+}$ intermediate after releasing an Fe^{2+}. Second, the $[3Fe\text{-}4S]^{1+}$ converts to a [2Fe-2S] cluster and releases an Fe^{3+} and two sulfide ions.[1071,1072] Mutating Ser24 into Phe and shielding Cys23 could inhibit Step one.[1073] Chelators of both Fe^{2+} and Fe^{3+} could accelerate step two significantly.[1074]

Another very common interconversion is 4Fe to 3Fe interconversion. [4Fe-4S] clusters are very sensitive, and oxidation in air can remove one of the irons, resulting in a 3Fe cluster.[1075] The most well studied case of this interconversion is the enzyme aconitase. Aconitase has a [4Fe-4S] cluster in its active form, which is very sensitive to air. Aerobic purification of the protein causes formation of an inactive enzyme with a 3Fe cluster. Addition of extra Fe, however, can reverse the conversion and reactivate the enzyme.[1076] Exposure of the 3Fe aconitase to high pH (>9.0) will result in the formation of a purple specie that has been attributed to a linear [3Fe-4S] cluster. This purple protein can be activated again through reduction in the presence of Fe.[1077]

While more often clusters of higher iron number collapse into clusters with fewer iron atoms, the reverse case has also been observed. In biotin synthase, there are two [2Fe-2S] clusters that can convert to a [4Fe-4S] cluster after reduction. UV-Vis and EPR studies reveal that the conversion process occurs through dissociation of Fe from the protein followed by slow re-association.[1078] Ferredoxin II of *Desulfivibrio gigas* has a [3Fe-3S] cluster that can convert into a [4Fe-4S] cluster through incubation with excess Fe, presumably through a non-Cys ligand.[1079] $[3Fe\text{-}4S]^{+}$ and $[2Fe\text{-}2S]^{2+}$ clusters in isolated Pyruvate formate-lyase can both be converted to [4Fe-4S] clusters with mixed valences of +1 and +2 upon dithionite reduction.[1080]

Interconversion between 4Fe and 3Fe clusters has been investigated through mutational studies. Removal of Cys ligands in 4Fe clusters results in the formation of 3Fe clusters. Replacement of the conserved Asp in 3Fe clusters with a ligating residue such as His or Cys causes formation of 4Fe clusters.[735,944,1081,1082] In [NiFe] hydrogenase, mutating a conserved Pro residue into Cys near the [3Fe-4S] cluster has successfully converted it to a [4Fe-4S] cluster accompanied by a 300 mV decrease in reduction potential[944] while in F_{420}-reducing hydrogenase of *Methanococcus voltae* [4Fe-4S] to [3Fe-4S] conversion has been achieved by replacing a Cys residue, producing a ~400 mV increase in reduction potential.[1081]

The presence of other metal ions in place of the 4th iron in a 3Fe cluster is sometimes also called interconversion. There are multiple reports of the formation of such hybrid clusters with Zn, Tl, and other metal ions.[1083,1084]

3.7. Features controlling redox chemistry of Fe-S proteins

The Fe-S proteins cover a wide range of reduction potentials, mostly in the lower or negative end of the range. Several parameters are known to be important in the ability of Fe-S proteins to accommodate such a wide range of reduction potentials. Unique electronic structures of iron in different clusters and different protein environments are among the most important factors. The ability of each iron to go through 2+ to 3+ oxidation states will allow multiple states for the core cluster, each of which having a different reduction potential range. This factor is more evident in case of HiPIP vs. ferredoxins. Solvent accessibility, H-bonding pattern around the cluster, net charge of the protein, partial charges around the cluster, and the identity of the ligands are among the other features that contribute to fine-tuning the reduction potential. Detailed examples of the role of each feature are discussed in the section 3.4.3.3, “important structural elements.” Below is a summary of these features and their effects in different Fe-S proteins.

3.7.1. Roles of geometry and redox state of the cluster

As with other redox active metal centers, the primary coordination sphere of a metal ion plays an important role in its redox properties. The iron center(s) has the

same distorted tetrahedral structure in almost all Fe-S proteins; however, it has been shown that slight changes in this structure will result in changes in reduction potentials. Differences in torsional angle of Fe-S-C_α-C_β,[618,731,1085] and distortion of cuboidal structure in some [3Fe-4S] clusters[1086] are examples of this distortion. Different geometries can lead to slight differences in electronic structures that will affect the redox properties of the protein.

Another important feature that influences the reduction potential is the number of redox centers in the cluster and the redox state of the cluster. While rubredoxin has only one iron that simply switches between Fe^{2+} and Fe^{3+} states, the same transition differs significantly in a [4Fe-4S] cluster in an environment with 3 more irons and a mixed valence state (e.g., $2Fe^{3+}$-$2Fe^{2.5+}$ and $Fe^{2.5+}$). Even the same cluster can undergo different redox transitions, as has been observed in the case of HiPIP and ferredoxins.[719]

3.7.2. Role of ligands

While sulfurs are the most dominant ligands in Fe-S proteins, it has been shown that other ligands can replace sulfurs in some cases and that these ligands play a prominent role in fine-tuning the reduction potential of the proteins.[541] Generally speaking, ligands that are less electron donating than sulfur will increase the reduction potentials by selectively destabilizing the oxidized state. A well-established example of this principle is the increased reduction potential of [2Fe-2S] clusters in Rieske proteins compared to ferredoxins due to replacement of two of the Cys ligands with His residues. Mutational studies on Cys ligands, mostly replacement with Ser, have shown an increased reduction potential compared to WT ligand.[721,750,893,1087]

3.7.3. Role of cellular environment

As mentioned in this review, some Fe-S proteins such as vertebrate ferredoxins and certain [3Fe-4S] cluster and Rieske proteins show pH dependent redox behavior. This behavior can be due to the presence of a His residue near the active site or among the ligands.[712,742,746,801] Therefore, proteins present at different pH in different cellular compartments should demonstrate different reduction potentials. Another effect of the

environment is indirect through evolution: as shown in the case of ferredoxins, organisms subjected to extreme environments will result in changes in overall charges of proteins and hence affect reduction potentials.[823] Peptide models of different Fe-S clusters have demonstrated the impact of solvent composition in electron transfer features of the cluster. [717]

3.7.4. Role of protein environment

Several studies have shown the importance of protein environment in fine-tuning the reduction potential of metal centers. Protein environment is one of the, if not the, most important factors determining reduction potential in Fe-S proteins because the general geometry and primary coordination of iron is very similar in this family of proteins. Protein environment conveys its effect via several routes:

3.7.4.1. Solvent accessibility/cluster burial

Solvent accessibility has been shown to be a very important factor in reduction potential for different metal centers including Cu centers, hemes, and Fe-S clusters. As a general rule of thumb, the more buried a cluster, the higher or more positive the reduction potential will be. This is mainly due to the electrostatic destabilization of more charges in clusters. Being more buried is proposed to be one of the most important reasons behind the difference between the reduction potential of the [4Fe-4S] cluster in HiPIP vs. ferredoxin proteins.[618,749,752] Hydration of the cluster can influence the covalency of Fe-S bonds, hence affecting the reduction potential.[901]

Cluster burial can be accomplished through physical positioning of the cluster by covering it with more secondary structure elements, or partially via more hydrophobic residues around the cluster. As explained before, there are exceptions to this trend and there are clusters that are significantly more solvent exposed, but no reduction potential change is observed for them.[875] It should be noted that cluster burial is dependent on the size of the protein, the location of the cluster, and the extent of solvent interaction, so it is difficult to make a fair comparison of the effect of cluster burial among a variety of proteins. [92]

3.7.4.2. Secondary coordination sphere:

While primary coordination sphere ligands are, with no doubt, very important in the reduction potential of Fe-S centers, the role of secondary coordination sphere interactions cannot be ignored. A mounting number of studies support the essential role of these interactions in fine-tuning reduction potential.[1088] In the case of Fe-S proteins, secondary coordination interactions are the major cause of differences in reduction potential within a class of proteins.[617,618] The number of backbone to amide H-bonds has been shown to be important in redox differences between HiPIPs and ferredoxins.[617,618] As described in each section, a conserved H-bonding pattern is observed in each sub-class of ferredoxins, and this pattern differs from one sub-class to another.[718,719] Removal of some conserved H-bonds from this pattern is shown to be one of the main causes of different reduction potential between different types of ferredoxins.[718,719] Removal of conserved H-bonds in several cases resulted in a decrease in reduction potential.[773,780] It is important to mention that although H-bonds are important, they are not the sole cause of differences in reduction potentials. Moreover, their analyses are complicated in some cases due to ambiguity in their assignment and variation in their number based on environmental condition.[92]

3.7.4.3. Electrostatics and local charges:

Local charges can selectively stabilize either the reduced or oxidized form of the cluster and influence the reduction potential. Many studies of Fe-S proteins showed that although these proteins usually have conserved charged residues (like positive charges in ferredoxins), these charges are mainly important for interaction with the redox partner, and usually their mutations do not cause significant changes in reduction potential.[749] In cases when these residues are very close to the cluster, unpredictable effects have been observed.[611] However, the total charge of the cluster has been suggested to be an important factor influencing the higher reduction potential of Rieske proteins compared to ferredoxins.[773] Mutational analysis on Rubredoxins and Thioredoxin-like ferredoxins confirmed an important role for the charges around the cluster in the reduction potential of the protein. There is convincing evidence for the role of backbone amides and partial positive charges in the reduction potential of Fe-S centers.[887] It has been proposed that

the electrostatic environment caused by these backbone amides and resulting dipole can influence the reduction potential of different clusters, such as HiPIP and ferredoxins. Net protein charge and the dipole induced from backbone amides have been shown to be important in determining the reduction potential of HiPIPs.[715,752,890]

While all these features are important, it should be noted that none of them is the sole determinant of reduction potential in Fe-S proteins, and it has been found that different features act as the major contributors to differences in reduction potential between different classes of Fe-S proteins. Even among members of a class, the same factor might not play the same role.

3.7.5. Computational analysis of reduction potentials of Fe-S proteins

To further understand factors influencing reduction potentials, computational methods have been developed for calculating the reduction potential of Fe-S proteins based on their structures.[591,887] One of these methods uses Gunner's multiconformational continuum electrostatics method and has been calibrated using proteins with known structure and reduction potential.[780] In another method a combined quantum-chemical and electrostatic calculation was used to generate predictions for reduction potentials. Poisson-Boltzman electrostatic methods in combination with QM/MM studies have also been used to analyze reduction potentials of Fe-S proteins.[93] Protein Dipoles Langeive dipole (PDLP) method was applied to HiPIPs to analyze the effects of solvent accessibility in reduction potentials of these proteins.[92,719] B3LYP density functional methods have been used in combination with broken symmetry to analyze factors that are important in tuning reduction potential of Rieske proteins.[800] Broken symmetry in combination with hybrid density functional theory has also been used to characterize Rieske proteins.[1089]

4. Copper redox centers

4.1. Introduction to copper redox centers

Copper is the second most abundant transition metal in biological systems, next to iron.[1090] Copper-containing proteins catalyze various reactions, in addition to being

electron transfer centers. In this section, we focus on copper proteins that merely function as electron transfer mediators, which include blue or type 1 (T1) copper and Cu_A centers. A number of reviews on these two centers have appeared in literature.[94-104]

Early endeavors to understand the structure and function of copper redox centers were successful despite the fact that no modern structural biology and computational method was available at the time. This success was in part due to strong colors and interesting magnetic properties displayed by these redox centers that allow various spectroscopic studies. The blue copper proteins were such named because they display an intense blue color, due to a strong absorption around 600 nm first noticed in the 1960s.[1091,1092] It was found that this T1 copper protein also displayed unusual EPR spectrum with narrow hyperfine splittings, which suggests the T1 copper proteins have a different ground state than that of the normal copper complexes.[1093] The electronic structure of the blue copper center was further elucidated with low temperature absorption, CD, MCD, single crystal EPR, XAS, and computational studies[96,99,1094,1095] which together showed that the 600 nm band is associated with S→Cu charge transfer transition and that the highly covalent nature of the Cu-S bond is responsible for the narrow hyperfine splitting in the EPR spectra. The crystal structure of poplar plastocyanin later confirmed that T1 copper proteins contain a copper site with an unusual geometry.[1096]

Although the existence of copper in cytochrome *c* oxidases (C*c*Os) has been known since the 1930s, the nature of their Cu_A centers was not established until much later due to the presence of heme cofactors that complicated interpretation of the spectroscopic results.[1097] EPR and chemical analysis studies have revealed that two copper-binding sites exist in C*c*Os.[1098-1100] MCD studies by Thomson and coworkers showed features at 475, 525, and 830 nm corresponding to a Cu_A center.[1101,1102] Kinetic measurement of reoxidation of reduced C*c*O, performed by a flow-flash technique, indicated that the Cu_A is the electron transfer center in C*c*O. [1103,1104] From 1987-1993, Buse and coworkers performed chemical analysis of C*c*O with inductively coupled plasma atomic emission spectroscopy, leading to the conclusion that three copper atoms exist in one protein along with two hemes.[1105,1106] Later, resonance Raman,[1107]

EXAFS,[1108] and finally crystal structures[1030,1109] revealed an unusual dinuclear copper structure of Cu_A, which will be discussed in detail in section 4.5.

4.2. Classification of copper proteins

As a diverse family of proteins, copper proteins could be divided into several types according to ligand sets, spectroscopic features, and functions (Table 9).[1110,1111] Mononuclear type 1 (T1) copper centers and dinuclear Cu_A centers are the two types which act only as electron transfer mediators. T1 copper centers and Cu_A centers share several common features. First, both centers contain Cu-thiolate bond(s), which are highly covalent and display rich spectroscopic signatures.[99,1095,1112-1115] Second, both centers are located in a cupredoxin fold.[94,100,103] Lastly, they are highly optimized for electron transfer, showing low reorganization energies and high electron transfer rate constants. These two types of copper proteins are collectively called cupredoxins, analogous to ferredoxin for Fe-S based electron transfer centers.[1116] Other types of copper proteins may also involve electron transfer as part of their enzymatic reactions, including peptidylglycine α-hydroxylating monooxygenase and dopamine β-monooxygenase,[1117] but will not be discussed here.

Table 9 Different types of copper proteins[a]

	Mononuclear		**Dinuclear**		**Tetranuclear**
Type	**Type 1**	**Type 2**	**Type 3**	**Cu_A**	**Cu_Z**
UV-vis Spectrum	Strong absorption ~ 600 nm and (in some proteins) 450 nm	Weak absorption ~ 700 nm	300-400 nm	Strong absorption ~ 480 and 530 nm	Strong absorption ~ 640 nm
EPR spectrum	4-line ($A_{\|\|}$ < 80 x 10^{-4}	4-line ($A_{\|\|}$ ~ (130-180) x	non-detectable	7-line ($A_{\|\|}$ ~ 30-40 x	2x4-line ($A_{\|\|}$ ~ 61x 10^{-4} cm^{-1} & $A_{\|\|}$ ~ 24 x

	cm^{-1})	10^{-4} cm^{-1})		10^{-4} cm^{-1})	10^{-4} cm^{-1})
Common ligands	His, Cys, (Met)	His, Asp, (Tyr)	His, (Tyr)	His, Cys, (Met)	His, S^{2-}
Active site geometry	Trigonal pyramidal or Distorted tetrahedral	Distorted tetragonal	Tetragonal	Trigonal planar	m_4-S^{2-} tetracopper cluster
Examples	Azurin Plastocyanin Stellacyanin Nitrite reductase Laccase	Superoxide dismutase Galactose oxidase Amine oxidase Nitrite reductase Laccase	Hemocyanin Tyrosinase Catechol oxidase Laccase	Cyt *c* oxidase N_2O reductase Menaquinol NO- reductase	N_2O reductase

[a]Reprinted with permission from ref[98]. Copyright 2004 Elsevier.

4.3. Native type 1 copper proteins

Exclusively serving as electron transfer centers, T1 copper proteins are distinct from other copper proteins because of their unique geometry and ligand sets. The copper ion is normally coordinated to two histidines and one cysteine in a trigonal plane with the axial position often occupied by a methionine at a relatively longer distance. It contains a highly covalent copper-thiolate bond that imparts intense blue colors to the T1 centers due to absorption at ~600nm and narrow four line hyperfine splitting in the EPR spectra.[99,1118]

The T1 copper centers reside in either single- or multi-domain proteins.[1119] The former includes the most common T1 copper proteins, such as plastocyanin, azurin, and amicyanin while the latter includes stellacyanin, uclacyanin, and dicyanin. The T1 copper centers are also found in multi-copper centers involving other types of copper centers, such as in nitrite reductases, laccases, and ascorbate oxidases. We will

discuss the T1 copper centers in single and multidomain proteins in this section, while the T1 copper centers in multicopper proteins will be discussed in section 4.3.4.

The T1 copper proteins are found in archaea, bacteria and plants. In addition to the cupredoxin fold, genes containing the T1 copper proteins may contain other components (Figure 47). All T1 copper proteins have an N-terminal signal peptide or transit peptide. With the signal peptide, the T1 copper proteins from bacteria or archaea are directed into periplasmic space. Their counterparts in plants, on the other hand, are transported to the extracellular milieu and anchored to the cell surface through an additional C-terminal hydrophobic sequence.[1119] Plastocyanin is guided to the chloroplast in plant cells by a transit peptide sequence that is cleaved in the mature protein.[1120]

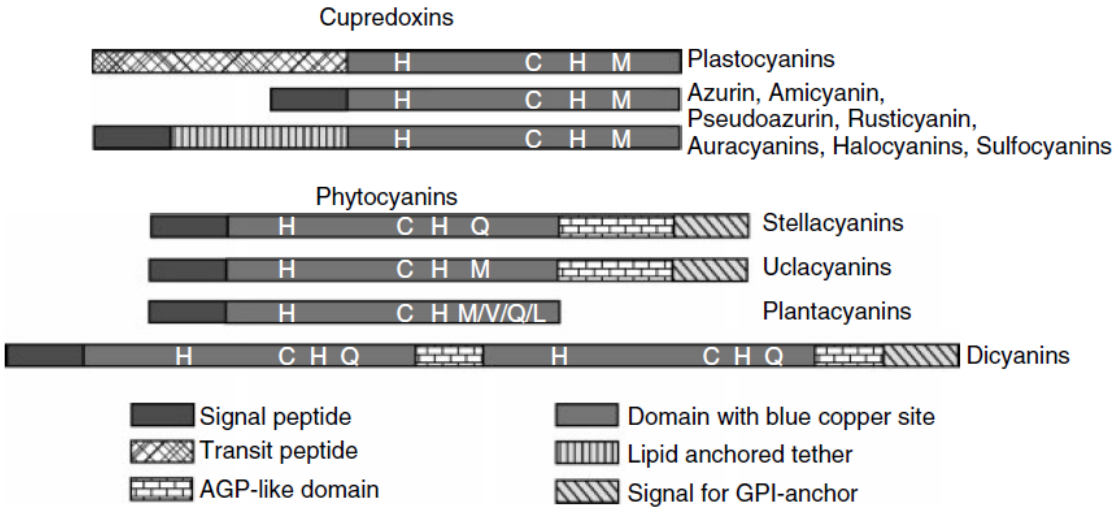

Figure 45. Domain arrangement of Type 1 copper protein. Reprinted with permission from ref [1119]. Copyright 2006 Wiley-VCH.

Table 10. Properties of T1 copper proteins

Name	Organism isolated from	First reported	PDB code for first structure	Ligand set	$E_{m\ (mV)}$	Redox partner
Single domain						

Azurin	Bacteria	1962[1121]	1AZU	1Cys,2His, 1Met, 1Carbonyl oxygen	310[1122]	-
Amicyanin	Mehtylotrophic bacteria	1981[1123]	1MDA	1Cys, 2His, 1Met	260[1124]	methylamine dehydrogenase, cytochrome c551
Plastocyanin	Plant/algae/cyanobacteria	1960[1125]	1PLC	1Cys, 2His, 1Met	370[1126]	cytochrome *f*, P700+
Pseudoazurin	Denitrifying bacteria and methylotrophs	1973[1127]	1PAZ	1Cys, 2His, 1Met	280[1128]	nitrite reductase
Rusticyanin	Acidophilic bacteria	1975[1129]	1RCY	1Cys, 2His, 1Met	670[1130]	cytochrome c, cytochrome c4
Auracyanin	Photosynthetic bacteria	1992[1131]	1QHQ	1Cys, 2His, 1Met	240[1131]	-
Plantacyanin	Plants	1974[1132]	2CBP	1Cys, 2His, 1Met	310[1133]	-
Halocyanin	Haloalkaliphilic archaea Natronobacterium pharaonis	1993[1134]	-	1Cys, 2His, 1Met	183[1134]	-
Sulfocyanin	Acidophilic archaea Sulfolobus acidocaldarius	2001[1135]	-	1Cys, 2His, 1Met	300[1135]	-
Nitrosocyanin	Autotrophic bacteria	2001[1136]	1IBY	1Cys, 2His, 1Glu, 1H2O	85[1137]	-
Multidomain protein with T1 center						
Stellacyanin	Plants	1967[1138]	1JER	1Cys, 2His, 1Gln	190[1133]	-
Uclacyanin	Plants	1998[1139]	-	1Cys, 2His, 1Met	320[1139]	-
Dicyani	Plants	2000	-	1Cys, 2His,	-	-

n		[1140]		1Gln		
Multidomain protein with T1 center and other copper center						
Laccase	fungi	-	1A65	1Cys, 2His, (1Leu/Phe)	465-778[1141-1143]	-
	Plants	-		1Cys, 2His, 1Met	434[1144,1145]	-
Ascorbate oxidase	Plants	-	1AOZ	1Cys, 2His, 1Met	350[1146]	-
Ceruloplasmin	animals	1948[1147]	1KCW	1Cys, 2His, (1Leu)	>1000[1148](redox inactive)	-
Ceruloplasmin				1Cys, 2His, 1Met	448[1149](redox active)	-
Hephaestin	Mammals	1999[150]	-			
Fet3p	yeast	1994[151]	1ZPU	1Cys, 2His	427[1152]	-
Nitrite reductase	Plants, bacteria	-	1NIA	1Cys,2His, 1Met, 1Carbonyl oxygen	260[1153]	-

4.3.1. Structures of the type 1 copper proteins

The first crystal structure of the T1 copper protein plastocyanin from poplar leaves (*Populus nigra* var. *italica*) was reported in 1978.[1096] Since then, crystal structures of eight T1 copper proteins have been reported, as listed in Table 10. Despite the fact that sequence identity between the T1 copper proteins is less than 20%,[1154] the overall structure of different T1 copper proteins is highly conserved. The fold of T1 copper proteins is called a cupredoxin fold, which consists of eight β strands arranged

into a Greek key β barrel as shown in Figure 46 and Figure 47.[94] There are also 1-2 α helices in different locations outside the core fold of the protein. This fold is present not only in T1 copper proteins and the Cu_A domain[1155] but also in other copper proteins, such as Cu-Zn SOD,[94,1156] and in proteins without metal cofactors, such as immunoglobins.[94,1157]

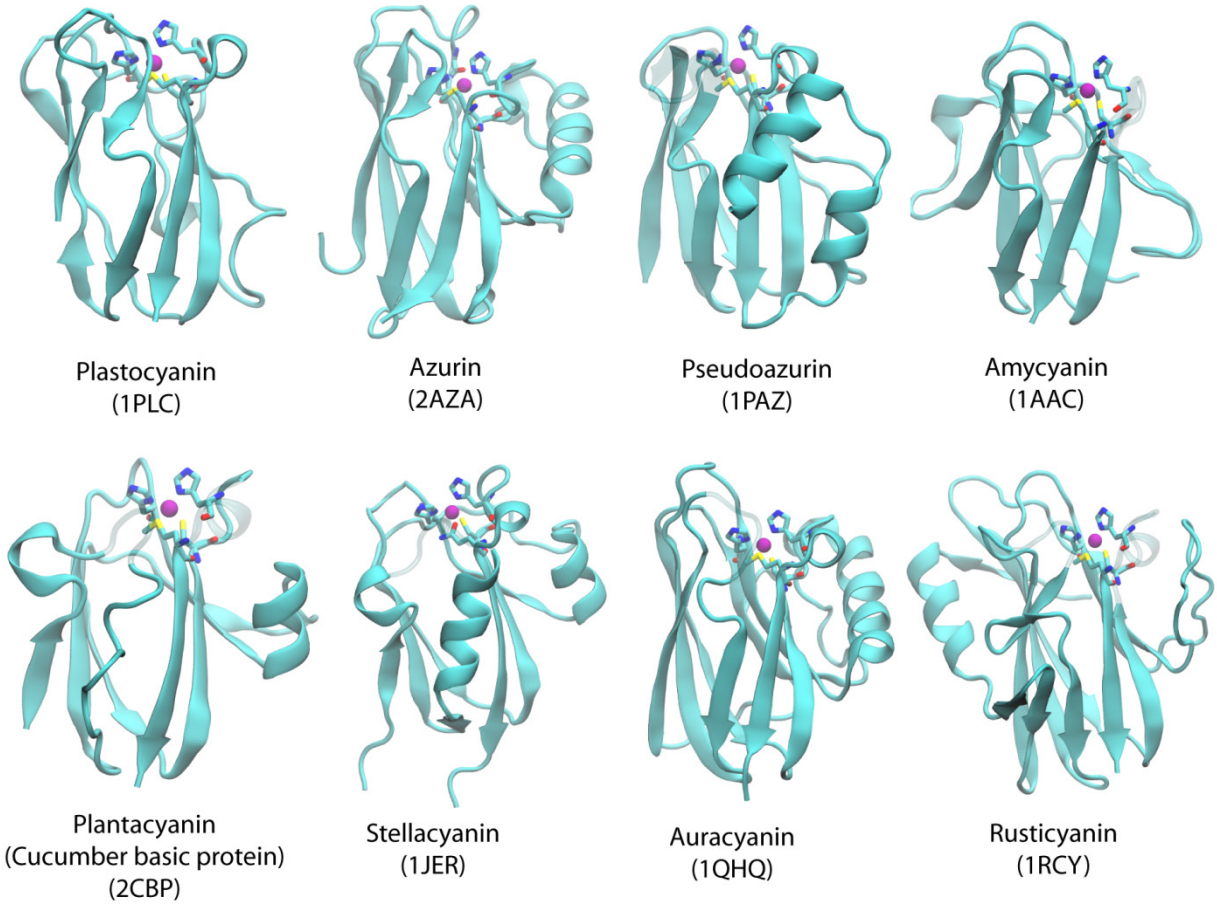

Figure 46. Crystal structures of the T1 copper proteins. Secondary structure (α helix and β sheet) is shown in carton format, copper is shown as a purple ball, and ligands are shown in licorice format. The name of the protein and its PDB ID are below each structure.

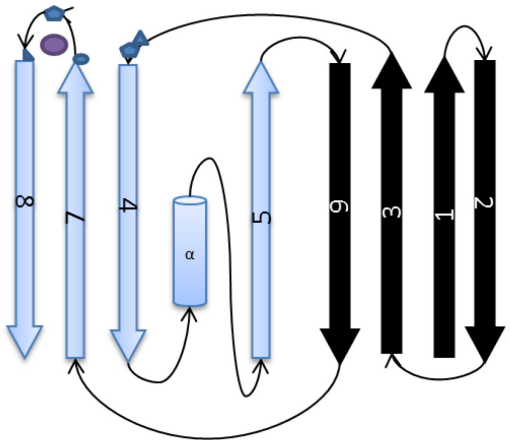

Figure 47. Topology diagram showing the scheme of secondary structure of azurin. β strands are shown as arrows and the α helix as a cylinder. Copper ligands between β strands 3 and 4 and between β strands 7 and 8 are shown as blue polygons while copper is shown as a purple circle.

The T1 copper center resides at the N-terminal end of the cupredoxin fold. As shown in Figure 47, one of His ligands is the first residue of the 4th β strand and is referred to as N-terminal His. Carbonyl oxygen, the fifth ligand of azurin, is located in the loop between the 3rd and 4th β strands. Other ligands, including Cys, the second His on the trigonal plane, and the axial ligand are located in or adjacent to the loop between the 7th and 8th β strands, close to C-terminus of the protein. Cys is the last residue of the 7th β strand while the His is in the middle of the loop and is referred as the C-terminal His. Met is the first residue of the 8th β strand. The three ligands are arranged in Cys-X_n-His-X_m-Met fashion where n and m could vary between 2 and 4 in different T1 copper proteins. This variation in length and amino acid composition is important for the function of T1 copper proteins. In section 4.4.5 we discuss the implications of the variations based on loop-directed mutagenesis.

While X-ray crystallography could give a fairly good description of the overall structure, EXAFS is more accurate in determining metal-ligand distance in a way that it is sensitive to the metal's oxidation state.[1158] The short Cu-S distance was first revealed by EXAFS.[99,1159] By comparing data from oxidized and reduced plastocyanin and azurin, it was found that an average increase of ~0.06 Å and ~0.08 Å for Cu-N(His) and Cu-

S(Cys) happens upon reduction.[99] These small changes upon reduction are consistent with data from crystallography and indicate small reorganization energies for redox processes.

4.3.1.1. Copper ligands

Even though the amino acid sequences and overall structures vary among different T1 copper proteins, the ligand composition, ligand-metal distance, and geometry of the T1 copper centers are almost identical.[94,95,99] As the most conserved structural feature, T1 copper centers invariably contains two His and one Cys as equatorial copper ligands. In T1 copper proteins, His coordinates with copper through N^{δ}, in contrast to N^{ε} used by T2 and other copper proteins. The Cu-His bond length is about 2.0 Å in T1 copper proteins, which is normal for such types of bonds. On the other hand, the Cu-Cys bond lengths range from 2.07 to 2.26 Å, which is short compared to normal copper complexes and other copper proteins (Table 11). The short Cu-S distance is key to the unique spectroscopic properties of T1 copper and is maintained through extensive hydrogen bonding within the protein scaffold, as will be discussed later in this section. 2N/1S from His and Cys form a pseudotrigonal plane, with average bond angles in Cu(II) protein being 101°, 117°, and 134° with RMS deviations of 2.5°, 4.1°, and 2.8°, calculated from crystal structures with 2.0 Å or higher resolution.[1119] The Cu–Sγ–Cβ–Cα and Sγ–Cβ–Cα–N dihedral angles are also consistently close to 180°, making Cu–Sγ bond coplanar with the Cys side chain and backbone.

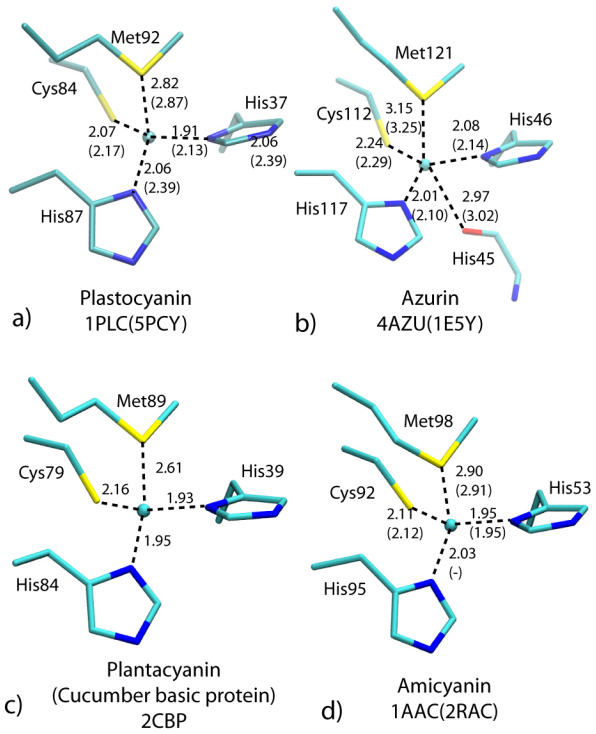

Figure 48. T1 copper center in plastocyanin, azurin, plantacyanin and amicyanin Reprinted with permission from ref [1119]. Copyright 2006 Wiley-VCH.

The axial ligand in T1 copper center is less conserved. A Met is present at 2.6-3.2 Å in this axial position in most proteins, while a Gln is found in stellacyanin and dicyanin. In the T1 center of fungal laccase and ceruloplasmin, a non-coordinating ligand such as Phe or Leu takes this axial position. In azurin, there is an additional backbone carbonyl oxygen at the opposite end of axial position to Met, making the T1 copper site in a trigonal bipyrimidal geometry.

Table 11 Distances between Cu or other substituted metal and ligands in T1 copper proteins.[a]

P. aeruginosa azurin	pH	Cu-Nδ(His46)[b]	Cu-S(Cys112)[b]	Cu-Nδ(His117)[b]	Cu-S(Met121)[b]	Cu–O(Gly45)[b]	Resolution (Å)	PDB ID	Ref
Cu(II)	5.5	2.08(6)	2.24(5)	2.01(7)	3.15(7)	2.97(10)	1.9	4AZU	1160
Cu(I)	5.5	2.14(9)	2.29(2)	2.10(9)	3.25(7)	3.02(8)	2.0	1E5Y	
Cu(II)	9.	2.06(6)	2.26(4)	2.03(4)	3.12(7)	2.94(11)	1.9	5AZ	11

	0							U	[60]
Cu(I)	9.0	2.20(11)	2.30(23)	2.21(12)	3.16(9)	3.11(11)	2.0	1E5Z	
T. ferrooxidans rusticyanin		Cu-Nδ(His85)	Cu-S(Cys138)	Cu-Nδ(His143)	Cu-S(Met148)	-			
Cu(II)	4.6	2.04	2.26	1.89	2.88	-	1.9	1RCY	[11][61]
Cu(I)	4.6	2.22	2.25	1.96	2.75	-	2.0	1A3Z	
P. nigra plastocyanin		Cu-Nδ(His37)	Cu-S(Cys84)	Cu-Nδ(His87)	Cu-S(Met92)	-			
Cu(II)	6.0	1.91	2.07	2.06	2.82	-	1.33	1PLC	[11][62]
Cu(I)	7.0	2.13	2.17	2.39	2.87	-	1.80	5PCY	[11][63]
P. denitrificans amicyanin		Cu-Nδ(His53)	Cu-S(Cys92)	Cu-Nδ(His95)	Cu-S(Met98)	-			
Cu(II)	6.0	1.95	2.11	2.03	2.90	-	1.31	1AAC	[11][64]
Cu(I)	7.7	1.95	2.12	unbound	2.91	-	1.30	2RAC	[11][65]
C. sativus cucumber basic protein		Cu-Nδ(His39)	Cu-S(Cys79)	Cu-Nδ(His84)	Cu-S(Met89)	-			
Cu(II)	6.0	1.93	2.16	1.95	2.61	-	1.80	2CBP	[11][66]
C. sativus stellacyanin		Cu-Nδ(His46)	Cu-S(Cys89)	Cu-Nδ(His94)	-	-			
Cu(II)	7.0	1.96	2.18	2.04	-	2.21	1.60	1JER	[11][67]

[a] Adapted from table 1 of ref [104].

[b] Average of distances for four molecules in the asymmetric unit. Errors are one standard deviation.

4.3.1.2. Secondary coordination sphere

While the above ligands exert significant influence on the properties of T1 copper centers, the protein scaffold should not be viewed as a passive entity to hold the copper site. To the contrary, it can play important roles. First, it can shield the copper site from water, raising the reduction potential and lowering the reorganization energy for electron transfer. More importantly, the extensive H-bond network surrounding it can fine-tune the properties of the T1 copper site.[94]

As shown in Figure 49, Cys112 in azurin forms two hydrogen bonds with adjacent backbone amide groups at ~3.5 Å. Together with S-Cu and S-Cβ covalent bonds, they form a tetrahedral geometry around Sγ of Cys (Figure 49A). Plastocyanin, pseudoazurin, and amicyanin have only one hydrogen bond around Cys as a Pro in the site eliminates the other amide bond. Additionally, cucumber basic protein has a very weak hydrogen bond at 3.7-3.8 Å. Hydrogen bonds increase electron density of S on Cys, which is crucial for the highly covalent nature of the Cu-S bond.

In azurin, N-terminal His coordinates with Cu through N^{δ}, whereas N^{ε} is hydrogen bonded to carbonyl oxygen. The same His is hydrogen bonded with the Gln49 side chain in amicyanin, the side chain of Asn80 in rusticyanin, and a water molecule in phytocyanins. C-terminal His is in a hydrophobic patch of the T1 copper proteins packed with other residues. N^{ε} of C-terminal His is hydrogen bonded to a water molecule. The axial Met/Gln usually packs against aromatic side chains such as Phe15 in azurin (Figure 49). As the fifth ligand in azurin, carbonyl oxygen is held in place by the secondary structure of the loop and packs with Phe114.

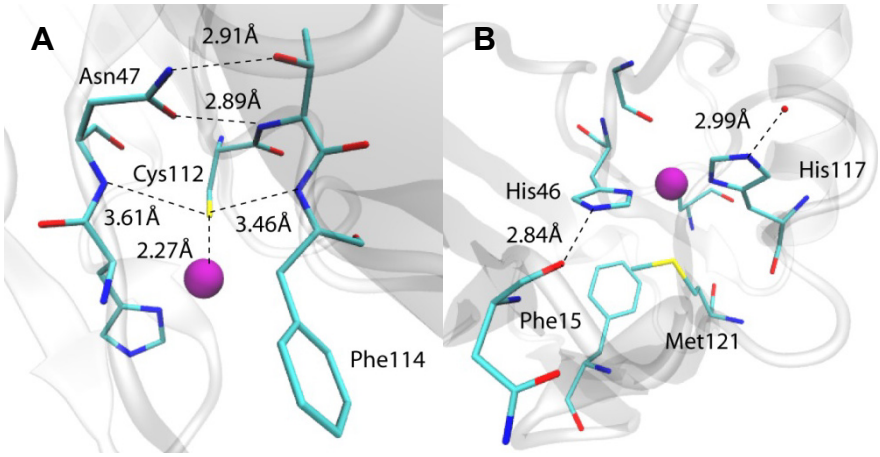

Figure 49. H-bonding around Cys112 (A) and other ligands (B) of azurin. PDB ID: 4AZU

There are more hydrogen bonding interactions beyond the copper center. Asn close to N-terminal His in the first ligand loop is hydrogen bonded to residues from the other ligand loop. This interaction, acting like a zipper, further holds the copper site together.

Extensive hydrogen bonding around the copper site in T1 copper proteins has important functional implications, as we will address in section 4.4.2.

4.3.1.3 Comparison of structures at different states

As suggested by the "rack mechanism"[1168,1169] or entatic state,[1170] active site structure is predetermined by protein scaffold. Thus, there should be little change in the structures of T1 copper proteins at different oxidation states, with different metals, or even in the absence of metal ions or other cofactors.

As shown in Table 11, compared to the same protein with Cu(II), the protein with Cu(I) has metal to ligand bond elongated by 0.1 Å or less. Similar results were obtained by EXAFS, which provides a more accurate estimation of bond length.[99] The small change in bond length is crucial for low reorganization energy of T1 copper site and, thus, fast electron transfer for its function. However, bond lengths in X-ray crystal structures should be interpreted with caution, as it has been shown that Cu(II) ions in protein undergo photoreduction during X-ray exposure.[1171,1172] It will be useful to conduct single-crystal microspectrophotometry concurrent with X-ray diffraction to make sure that the oxidized protein is not reduced during diffraction.[1173] On the other hand, the oxidation state of Cu ion can be easily monitored at the edge and XANES regions of

its X-ray absorption spectrum. Bond lengths derived from carefully designed and conducted EXAFS should reflect the actual bond lengths at the corresponding oxidation states.

Besides structures with copper at oxidized or reduced states, crystal structures of apo and metal substituted T1 copper proteins also shed light on how proteins interact with copper. Structures of apo-forms of azurin,[1174,1175] plastocyanin,[1176] pseudoazurin,[1177] and amicyanin[1178] show little difference (0.1-0.3 Å) from the copper-bound form, confirming the hypothesis.

Metal substitution is useful in spectroscopic studies, such as electronic absorption[1118,1179] and NMR.[1180] Due to the different sizes and ligand affinities of different metals, bond length and overall geometry are changed upon substitution, but only to a small extent due to confinement of protein scaffold.[1181-1183]

4.3.2. Spectroscopy and electronic structure

Intense (~5000 $M^{-1}cm^{-1}$) electronic absorption at ~600nm is the hallmark of T1 copper proteins. Solomon and coworkers attribute the origin of ~600nm absorption to S(Cys)pπ→Cu_x^2-$_y^2$ ligand to metal charge transfer transition (LMCT).[1094,1184,1185] Another feature at ~400nm is not seen in plastocyanin or azurin but is more pronounced in perturbed T1 copper site like cucumber basic protein. This is attributed to S(Cys)pπ→Cu_x^2-$_y^2$ LMCT. Geometry of the copper site is believed to be important for the ratio between these two peaks at ~600 and ~400 nm.[1095,1186] A series of weak absorption peaks from 650 nm to 1050 nm are attributed to a d→d transition or ligand field transition.[1184]

EPR provides a sensitive way to determine copper site geometry. T1 copper protein exhibit a distinctive small hyperfine splitting (< 100×10^{-4} cm^{-1}) on EPR spectrum, as opposed to that of T2 copper and other complexes (> 150×10^{-4} cm^{-1}).[1119] Through S K-edge XAS, Solomon and coworkers showed that the small hyperfine splitting is due to high covalency between Cu and S, which delocalizes unpaired electrons onto S, thus decreasing electron density on Cu.[1187]

Other spectroscopic techniques, such as resonance Raman spectroscopy and Cu L-edge and S K-edge X-ray absorption spectroscopy, have also been important to

decipher the electronic structures of T1 copper proteins. They are beyond the scope of this review, but there are excellent reviews elsewhere[1095,1119] and in this issue.

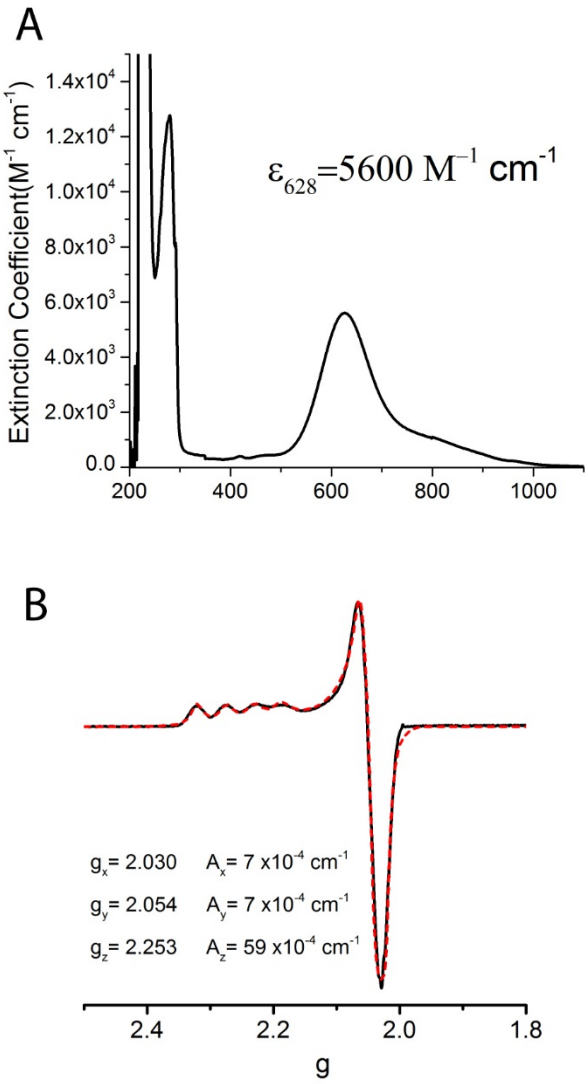

Figure 50. Electronic absorption (A) and EPR (B) spectra of Azurin.

4.3.3. Redox chemistry of type 1 copper protein

As a class of proteins dedicated to electron transfer, T1 copper proteins display various features for facile redox chemistry.

4.3.3.1. Redox partner

T1 copper proteins shuttle electrons between donor and acceptor proteins as redox partners. So far five T1 copper proteins with known physiological redox partners have been identified: plastocyanin, amicyanin, rusticyanin, pseudoazurin, and azurin. As a redox center in chloroplasts in plants, plastocyanin accepts electrons from cytochrome *f* of membrane-bound cytochrome b_6f complex and transfers them to $P700^+$ from photosystem I. [256,1188-1192] Amicyanin accepts electrons from methylamine dehydrogenase and transfers them to cytochrome *c* oxidase via a *c*-type cytochrome. [279,1193-1200] Rusticyanin is suggested to shuttle electrons between cytochrome *c* and cytochrome c_4.[1201 1202] Pseudoazurin reduces nitrite reductase, but its electron donor is not yet known.[1203-1207] Azurin is likely to interact with aromatic amine dehydrogenase *in vivo*, as suggested by co-expression, kinetics of reduction, and crystal structure.[1208-1210]

Interaction between a T1 copper protein and its redox partner is generally weak and transient. NMR and crystallographic studies have revealed a structural basis for this interaction. Interactions between plastocyanin from various origins and cyt *f* have been extensively studied by NMR spectroscopy (Figure 51). Chemical-shift analysis and rigid-body structure calculations have demonstrated that the hydrophobic patch around His87, the C-terminal His ligand to copper, mediate an interaction between plastocyanin and cyt *f*.[1211,1212] Besides that, two acidic patches around Tyr83 have been shown to interact with positively charged residues of cyt *f*.[1213] Mutation of Tyr83 to Phe or Leu drastically decreases electron transfer rate, indicating Tyr83 binds to cyt *f* and is involved in electron transfer.[1214] Absence of acidic patches also demolishes electron transfer activity at low ionic strength, showing they are involved in the interaction with cyt *f*.[1215,1216] However, interaction between acidic patches and cyt *f* is not very specific as small changes in acidic patches have a minimal effect on the interaction between two proteins.[1216,1217]

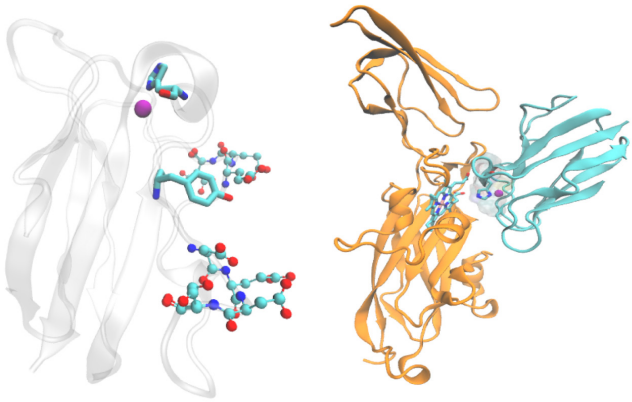

Figure 51. Structure of plastocyanin (left) and complex of plastocyanin and cyt *f* (right). Left: copper ion is represented as a purple ball; His87 and Tyr 83 are represented in licorice format while residues in two acidic patches are represented as ball and stick models. Right: plastocyanin is colored cyan while cyt *f* is orange. Copper ion and His87 from plastocyanin and heme from cyt *f* are also shown.

Another demonstration of the interaction between the T1 copper proteins and their redox partners comes from X-ray crystallography. The structures of amicyanin-methylamine dehydrogenase complex and methylamine dehydrogenase-amicyanin-cytochrome c_{551} ternary complex have been determined.[279,1196] These structures further confirmed that the hydrophobic patch surrounding His95 (the C-terminal His ligand equivalent to His87 in plastocyanin and His117 in azurin) interacts with a hydrophobic patch on methylamine dehydrogenase. An electron transfer pathway from Trp57 and Trp108 in methylamine dehydrogenase to His95 in amicyanin and eventually to copper has been proposed from these structures.

Recently, crystal structure of azurin and aromatic amine dehydrogenase complex from *Alcaligenes faecalis* has been solved.[1208] In this structure, only one azurin molecule is present with four molecules of aromatic amine dehydrogenase in a heterodimeric form. B-factor of azurin is high except those residues in the interface. This is consistent with the transient nature of the interaction between the T1 copper proteins and their redox partners. The interaction is very similar to the interaction between amicyanin-methylamine dehydrogenase.

T1 copper proteins show promiscuity in reacting with proteins other than their physiological redox partners,[64,1218] including small inorganic complexes such as $[Fe(CN)_6]^{3-}$ and $[Co(phen)_3]^{3+}$,[31,44,1219] small molecules such as flavins and ascorbate, and the proteins themselves through electron self-exchange reactions.[100] Gray and coworkers have used Ru derivatives of T1 copper proteins as a model to study long range electron transfer in biological systems.[24 31,44]

4.3.3.2. Electron transfer rate

T1 copper proteins are involved in long range electron transfer *in vivo* and *in vitro*. For a more detailed review of long range electron transfer, please refer to a review in the same issue by Gray *et al*. The process can be described by the semi-classical Marcus equation (Equation 1).

$$k_{ET} = \left(\frac{\pi}{\hbar^2 \lambda k_B T}\right)^{\frac{1}{2}} (H_{AB})^2 \exp\left[\frac{-(\Delta E^{\circ} + \lambda)^2}{4\lambda k_B T}\right] \quad (1)$$

Equation 1 Marcus theory

In this equation, ΔE° is the difference in reduction potential between the donor and acceptor sites (a.k.a., the driving force), H_{AB} is the donor–acceptor electron coupling or electron matrix coupling element, and λ is the reorganization energy required for electron transfer. Under the same driving force, the rate is maximized when H_{AB} is large and λ is small. In long-range electron transfer, there is no direct coupling between the donor and the acceptor. The coupling is mediated by intervening atoms via super-exchange mechanism. H_{AB} is determined by the distance between donor and acceptor and the covalency of the metal-ligand bond.[1220-1222]

Electron transfer rates between T1 copper proteins and their redox partners have been measured by kinetic UV-vis spectroscopy or cyclic voltammetry.[1223-1226] The k_{ET} between plastocyanin and cyt *f* has been determined to be 2.8-62 s^{-1} [1227-1229]while the constant between plastocyanin and $P700^+$ has been determined to be 38-58 s^{-1}.[1191,1192,1230,1231] Davidson and coworkers have used kinetic UV-vis spectroscopy to measure k_{ET} between amicyanin and methylamine dehydrogenase, which was determined to be ~10 s^{-1}.[1232,1233] Suzuki and coworkers have determined the k_{ET} between pseudoazurin and nitrite reductase to be (0.8-7)×10^5 M^{-1} s^{-1} by kinetic UV-vis spectroscopy or cyclic voltammetry.[1204,1224,1234-1236]

As several studies have pointed out, the rate constant measurement for inter-protein electron transfer processes is complicated by other processes, such as multiple binding sites of the two proteins, transient formation of conformational intermediates, and protonation/deprotonation processes.[1225,1237] There are two methods to measure electron transfer rate in T1 copper proteins without involvement of a redox partner: pulse radiolysis and NMR. Pulse radiolysis[1238] uses a short pulse (typically 0.1–1 μs) of high energy (2–10 MeV) electrons to excite and decompose solvent molecules. A typical reaction generates CO_2^- radical:

$$e^-(aq) + N_2O + H_2O \rightarrow N_2 + OH + OH^-$$

$$HCO_2^- + OH/H \rightarrow H_2O/H_2 + CO_2^-$$

Radicals generated in solvent molecules trigger downstream reactions. In azurin, CO_2^- can either reduce Cu(II) or the disulfide bond between Cys3 and Cys26 in a nearly diffusion controlled rate. Molecules with a reduced disulfide bond ($RSSR^-$) can further reduce Cu(II) in the same protein via intramolecular electron transfer.[101]

$$RSSR - Az(Cu^{II}) + CO_2^- \rightarrow RSSR - Az(Cu^{I}) + CO_2$$

$$RSSR - Az(Cu^{II}) + CO_2^- \rightarrow RSSR^- - Az(Cu^{II}) + CO_2$$

$$RSSR^- - Az(Cu^{II}) \rightarrow RSSR - Az(Cu^{I})$$

By monitoring absorbance changes at 410nm ($RSSR^-$) and 625nm (Cu^{II}), a fast reduction process corresponding to reduction of Cu^{II} or RSSR by CO_2^- and a slower process of intramolecular ET between RSSR and Cu^{II} can be resolved. ET rate and driving force (ΔG°) can be calculated from kinetics of intramolecular electron transfer. By running experiments at different temperatures, activation enthalpy and activation entropy of the electron transfer process can be calculated.

Using this method, Farver and Pecht determined intramolecular ET of WT azurin to be 44±7 s^{-1} at pH7.0 and 25°C with driving force ΔG°=-68.9 kJ mol^{-1}. Activation enthalpy and activation entropy were calculated to be 47.5±4.0 kJ mol^{-1} and -56.5±7.0 J K^{-1} mol^{-1}.[1239] ET rates for azurin of different origins and mutations have measured and reviewed by Farver and Pecht.[101]

Electron self-exchange is an intrinsic property of all redox systems.[1240] Exchange of electrons happens to two molecules of the same complex at different oxidation states. Only one redox couple is involved, and there is no driving force for this reaction. Measuring electron self-exchange rate constants by NMR provides a more universal way to measure ET transfer activity as it is carried out in T1 copper centers[1241-1249] (reviewed in[100]) as well as in other redox centers.[1250-1252] Electron self-exchange rate constants (k_{SES}) of T1 copper proteins range from 10^3 to 10^6 $M^{-1}s^{-1}$ at moderate to low ionic strength. The electron self-exchange is thought to happen through a hydrophobic patch as the rate constant is affected by the presence of an acidic patch[1248] or basic residues[1253] close to the hydrophobic patch.

4.3.3.3. Reduction potential

T1 copper proteins have reduction potentials ranging from 183 mV to 800 mV (see Table 10). Compared to aqueous Cu(I)/Cu(II) couple–which has a reduction potential of ~150mV–copper complexes, and other copper proteins, T1 copper proteins have unusually high reduction potentials. Their potentials also span a wide range (> 600mV), nearly half the range of biologically relevant potentials (

Figure 1). Within the T1 copper proteins, groups of proteins are apparent when sorted based on the midpoint reduction potential (E_m). Nitrite reductases,[1153] stellacyanins,[1133] amicyanins[1124] and pseudoazurins[1128] natively have substantially lower (~100 mV) E_m values as compared to azurin.[98] Azurin and umecyanins have moderate E_m values natively around 200-300 mV vs. the normal hydrogen electrode (NHE). On the other end of the scale, rusticyanins have E_m values ~400 mV higher than azurin. Understanding the origin of variance and tuning reduction potential are also of great importance. By comparing native protein with different axial ligands (Table 12), it is revealed that proteins with Gln as an axial ligand generally have lower reduction potential (190-320mV), proteins with Met axial ligands have higher potentials (183-670mV), and proteins with a non-coordinating ligand in multicopper proteins have the highest potentials (354-800mV). This trend is further confirmed by mutagenesis studies that are discussed in section 4.4.1.

Variation within proteins with the same axial ligand indicates that there are more factors affecting the reduction potentials of T1 copper center. These factors have been uncovered by mutagenesis and engineering of copper protein, and are discussed in section 4.4.

Table 12. Dependence of E_0 on the Axial Ligand in Blue Cu Proteins[a]

Axial ligand and E^0 (mV)	Phe/Leu/Thr	Met	Gln	ref
fungal laccase	770	680		1254-1256
Azurin	412	310	285	1122,1257
cuc. Stellacyanin	500	420	260	1139
nitrite reductase	354	247		1258
rusticyanin	800	667	563	1259
mavicyanin		400	213	1260
amicyanin		250	165	1261

[a] Reprinted with permission from ref [99]. Copyright 2004 American Chemical Society.

4.3.4. T1 copper center in multicopper proteins

The T1 copper center not only exists in single domain proteins, but also in multi-domain proteins with multiple copper cofactors. These proteins include multicopper oxidases and nitrite reductases (Table 9). The former contains a T1 copper (blue copper), a type II copper (non-blue copper, abbreviated as T2), and a pair of type III coppers (Figure 53).[1262-1266] The latter contains T1 and T2 copper center and is evolutionarily related to the multicopper oxidases.[1265-1267] As shown in Figure 52, multicopper oxidases and nitrite reductases are closely related and are composed of 2, 3, or 6 domains.[1265] In multicopper oxidases, T1 copper center resides in cupredoxin-like domain while T2/T3 copper centers are located in between domains.

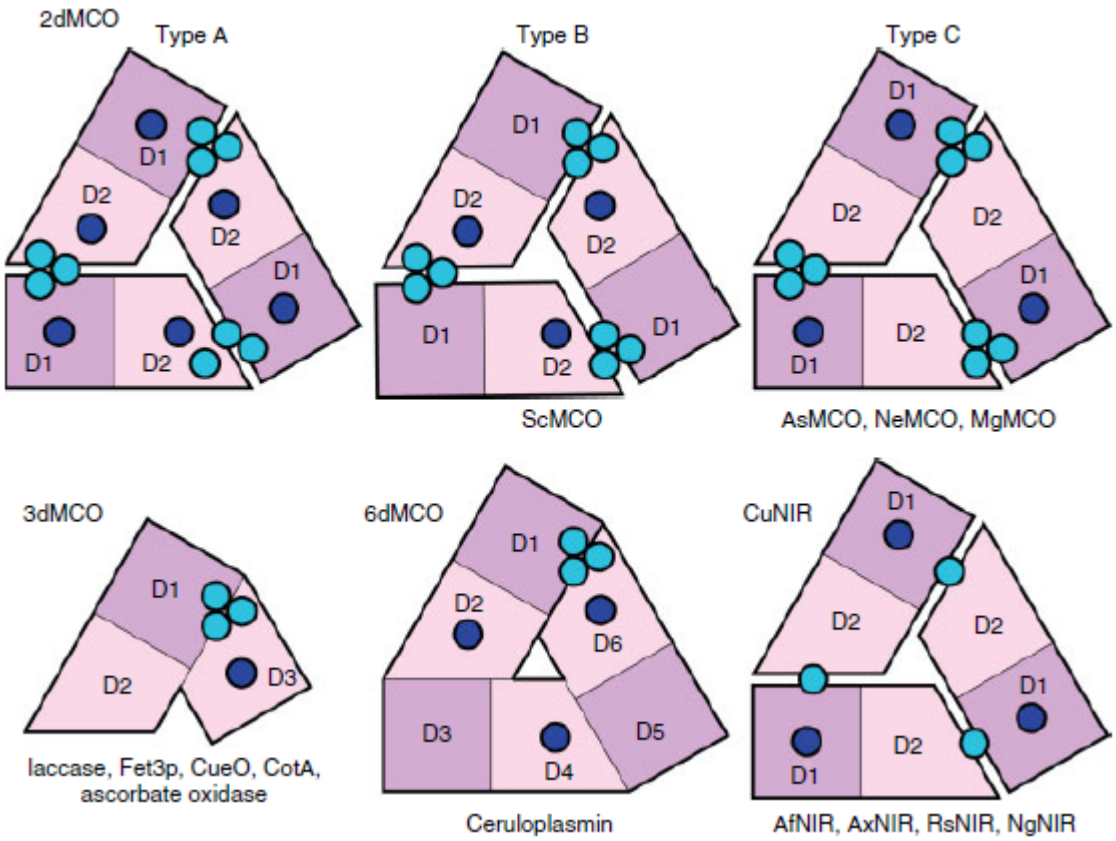

Figure 52. Domain organization and copper center distribution in multicopper oxidases. Reprinted with permission from ref [1265]. Copyright 2011 Wiley-VCH.

T1 copper centers in multi copper oxidases (MCOs) are very similar to single domain T1 copper proteins. Copper ion is coordinated by 1 Cys and 2 His at its equatorial positions. In plant laccases, ascorbate oxidases, and nitrite reductases, axial Met coordinates with copper and forms a trigonal pyramidal geometry. In fungal laccase, ceruloplasmin, and Fet3p, the axial ligand is a non-coordinating Leu or Phe, leaving equatorial ligands and copper in a more trigonal geometry.[1262,1265,1266] One noticeable feature for T1 copper centers in MCOs is their high reduction potential compared with single domain T1 copper proteins. Ceruloplasmin has the highest reduction potential[1148] (>1000mV) reported in T1 centers while TvLac has the second highest reduction potential[1141-1143] (778mV). The high reduction potential is partially attributed to more hydrophobic axial ligand while other factors such as hydrogen bond may contribute too.[1268]

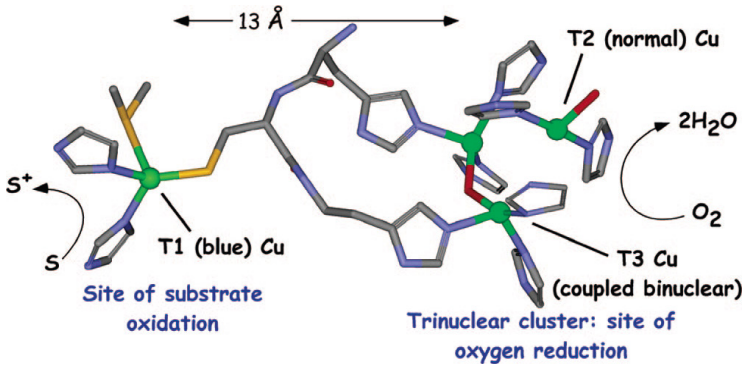

Figure 53. Active site of the multicopper oxidases. Cu sites are shown in green spheres. Figure generated from the crystal structure of ascorbate oxidase (PDB accession number 1AOZ). Reprinted with permission from ref [1264]. Copyright 2007 American Chemical Society.

4.3.5. A novel red copper protein—nitrosocyanin

Recently, a mononuclear red copper protein, nitrosocyanin from *N. europaea*, an ammonia oxidizing bacterium, was isolated and structurally characterized.[1137,1269-1271] The crystal structure shows that the copper ion is coordinated by 2 His, 1 S(Cys), a side chain O (Glu), and has an additional fifth water ligand in the oxidized form but not in the reduced form. Nitrosocyanin shows a strong absorption band at 390 nm (ε = 7000 $M^{-1}cm^{-1}$), a large hyperfine splitting value (147×10^{-4} cm^{-1}) on EPR spectrum, and a very low reduction potential of 85 mV compared to the T1 copper proteins, which are in the range of 150-800 mV.[1137,1271] With an exogenous water ligand, reorganization energy of this protein is calculated to be 2.2 eV, significantly higher than T1 copper proteins.[1271] Similar to T1 copper proteins, nitrosocyanin has copper-thiolate coordination and strong UV-vis absorbance. However, the water ligand in nitrosocyanin has not been seen in T1 copper proteins before. Its copper site geometry and absorption at ~400nm are also different from T1 copper. Its EPR spectrum, reorganization energy, and reduction potential more closely resemble T2 copper proteins. Solomon and coworkers attribute these properties to relative orientation of the CuNNS and the CuSCβ planes, which in turn is due to “coupled distortion” between axial ligand and the whole copper center.[1095,1186,1271]

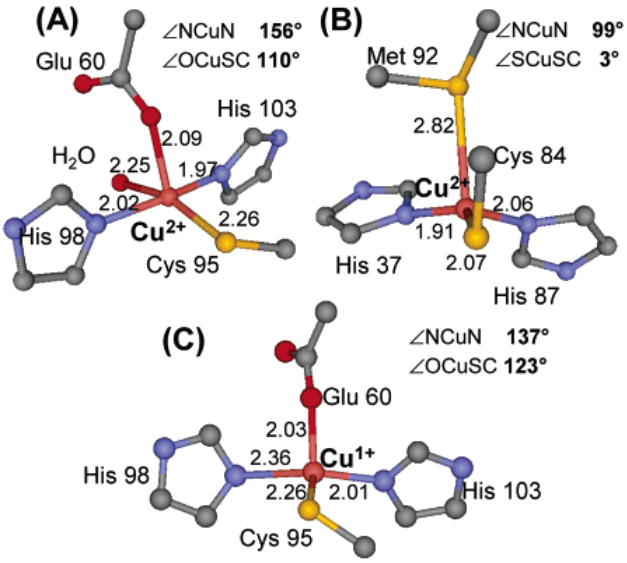

Figure 54. Crystal structures of (A) the oxidized red copper site in nitrosocyanin, (B) the oxidized T1 copper site in plastocyanin, and (C) the reduced red copper site in nitrosocyanin. . Reprinted with permission from ref [1271]. Copyright 2005 American Chemical Society.

The biological role of this protein, however, has not yet been identified. It has been proposed that it might be involved in electron transfer or serve some as-yet unknown catalytic function due to the presence of the open coordination site.[1269,1270]

4.4. Features of type 1 copper proteins revealed by mutagenesis

Although the study of native proteins provides information about structure, spectroscopy, and function of T1 copper proteins, it is hard to draw any conclusion only by comparing copper centers from different scaffolds with low sequence homology. With the advent of modern molecular biology, powerful tools such as mutagenesis are available to general research groups, enabling the amino acid sequence to be modified at will. Methods of unnatural amino acid mutagenesis have further expanded the toolbox for bioinorganic chemists. [1272-1274] With these methods, not only amino acid residues directly coordinating to copper, but also residues beyond the first coordination sphere have been mutated. Mutagenesis reveals how different components of protein contribute to structure, spectroscopy, and function, especially in reduction potential tuning.

4.4.1. Axial Met affects reduction potential and spectroscopic features

The T1 copper center has highly conserved equatorial ligands, 2His and 1Cys. The axial position for T1 copper center shows more variation, as Met/Gln/non-coordinating residues can all be found in native protein. Mutagenesis of the axial ligand has been carried out in azurin,[1122,1275-1278] nitrite reductase,[1235,1258,1279] amicyanin,[1261] rusticyanin,[1259] pseudoazurin,[1234] laccase,[1256] and stellacyanin.[1139,1280,1281] Mutation of the axial ligand in different T1 copper proteins generally results in a protein that retains copper binding ability but with a different reduction potential or altered spectroscopic properties. An early work replaced Met121 in azurin with all other 19 amino acids without altering the T1 character of copper center.[1276] While changing the axial ligand to hydrophobic ligands such as Ala, Val, Leu, or Ile increases reduction potential by 40-160mV,[1122] substitution with Glu or Gln decreases reduction potential by 100-260mV.[1122,1257] As the axial ligand is changed from Gln to Met to more hydrophobic residues, reduction potential of the protein increases. It has also been suggested from theoretical studies that the axial ligand is involved in tuning potential.[1282,1283] To test the role of the axial ligand in tuning reduction potential of T1 copper protein, Lu and coworkers incorporated Met analogues with different hydrophobicity at the axial position in azurin.[1284,1285] The reduction potential varied from 222 to 449 mV at pH 4.0 correlated to the hydrophobicity of the axial ligand. Likewise, Dennison and coworker mutated axial Met of cucumber basic protein to Gln and Val. As the axial ligand was changed from Gln to Met to Val, the electron self-exchange rate increased by one order of magnitude, and the reduction potential increased by ~350 mV.[1286] These studies have firmly established a correlation between hydrophobicity and reduction potential, and they have underscored the role of the axial ligand in reduction potential tuning.

Within T1 copper proteins, there are two classes of proteins with slightly different spectroscopic features. Typical T1 copper proteins, such as plastocyanin and azurin have absorption at ~600nm and axial EPR signal, whereas “perturbed” T1 copper protein or green copper proteins have an additional ~400 nm absorption peak in their UV-vis spectra, as well as rhombic EPR signals. At the same time, the “perturbed” T1 copper proteins have longer Cu-S(Cys) distances and shorter Cu-axial ligand

distances.[1283] A more extreme case comes from the newly discovered nitrosocyanin, which has a cysteine ligand and dominant ~400nm absorption in its UV-vis spectrum, giving it a red color.[1137,1271] Although the strong absorption and 1Cys/2His/1Glu ligand set resembles T1 copper proteins, nitrosocyanin has large hyperfine splittings ($A_{||}$ ~ $150\times10^{-4}cm^{-1}$) in its EPR spectrum and a low reduction potential (85mV), which falls into the range of T2 copper proteins.[1136,1137,1271] Solomon and coworkers proposed "coupled distortion" theory based on a suite of spectroscopic studies in combination with theoretical calculations to explain the variance in electronic absorption and concomitant color change from blue to green to red in native proteins. This theory states that shorter Cu-axial ligand distances result in distortion of the T1 copper geometry toward tetragonal, which elongates the Cu-S(Cys) distance.[1283] This distortion renders the pσ(Cys)-Cu CT more favorable than pπ(Cys)-Cu CT, which manifests as an increase in the ~400nm absorption over the ~600nm absorption in the UV-vis spectrum. Mutational studies on axial ligand of various T1 copper proteins have validated the "coupled distortion theory." By changing a weak Met to His[1277,1287,1288] or Glu,[1289-1291] the blue copper protein azurin can be converted to a green copper protein. By mutating Met to a weaker ligand such as Thr, the natively green copper protein, nitrite reductase, has been converted to a blue copper protein.[1292] Recently, Lu and coworkers mutated axial Met to Cys, a strong ligand, then to the unnatural amino acid homocysteine (Hcy), a strong ligand with a longer side chain. The resulting Met121Cys azurin has an additional ~450 nm absorption while in Met121Hcy ~410 nm dominates over the ~625 nm peak. Together with EPR evidence, it was suggested that within the same scaffold, blue copper protein azurin was converted a green copper protein, then to a red copper protein.[1293] Interestingly, the engineered red copper protein, Met121Hcy azurin, has a low reduction potential (113 mV) similar to that of nitrosocyanin (85 mV).

4.4.2. His are on electron transfer pathway and important to maintain spectroscopic features

Although equatorial His is highly conserved in T1 copper proteins, its mutation does not impair the copper binding ability of the protein. Canters and coworkers mutated two His into Gly separately, and the resulting protein still had T1

characters.[1294,1295] As His to Gly mutation creates extra space around copper, exogenous ligands such as halides, azides, and imidazoles could diffuse into His46Gly and His117Gly azurins and coordinate with copper. Depending on the type of external ligand, the mutants will be either T1 or T2 copper proteins.[1294-1296] His117Gly and His46Gly mutations also change solvent exposure of the copper site. Without added external ligands, His117Gly azurin has a reduction potential of 670 mV, much higher than that of WT azurin (310 mV). The high reduction potential is due to loss of a water ligand during reduction. Addition of external ligands will lower reduction potential.[1297] The open coordination site of His117Gly makes it possible to study ET using imidazole-modified complexes.[1298,1299] The mutants generally exhibit a lower electron transfer rate. As the properties of imidazoles present affect ET rate, it is implicated that His is also important in WT protein.[1300]

4.4.3. Cys is indispensable for type 1 copper protein

As the Cu-S(Cys) bond defines the properties of type I copper sites,[99] mutation of Cys to other natural amino acids will dramatically alter the copper site. Substitution of any other amino acid for Cys will result in loss of the intense LMCT charge transfer bands, arising from the interaction of the Cys-S with copper. As an isostructural analogue of Cys, Selenocysteine (SeC) can replace Cys without major structural perturbation. This strategy has been employed by Lu and coworkers as a spectroscopic probe for T1 copper centers.[1301-1303] The protein Cys112SeC azurin showed a reduction potential similar to WT azurin (328 mV vs. 316mV at pH4) and a red shifted LMCT band at 677 nm.[1301] So far, only Cys112Asp mutation in azurin has been characterized. Mutation of Cys to Asp makes azurin a T2 copper protein, as evidenced by large hyperfine splitting ($A_{||}$ ~ $152\times10^{-4}cm^{-1}$) in the EPR spectrum and slow electron transfer.[1304-1307] Addition of another mutation at the axial position, Met121Leu(Phe/Ile), results in a novel type zero copper center, which has the small parallel hyperfine splittings and rapid electron transfer characteristic of T1 copper centers but which no longer fits the classification of T1 copper due to the loss of the copper-thiolate interaction.[1308-1311] Moreover, there is only a slight increase of reorganization energy (0.9-1.1 eV) compared with WT azurin, much less than T2 copper proteins. ET rate of

type zero protein is 100-fold higher than Cys112Asp mutant, a typical T2 protein.[1308,1309,1311]

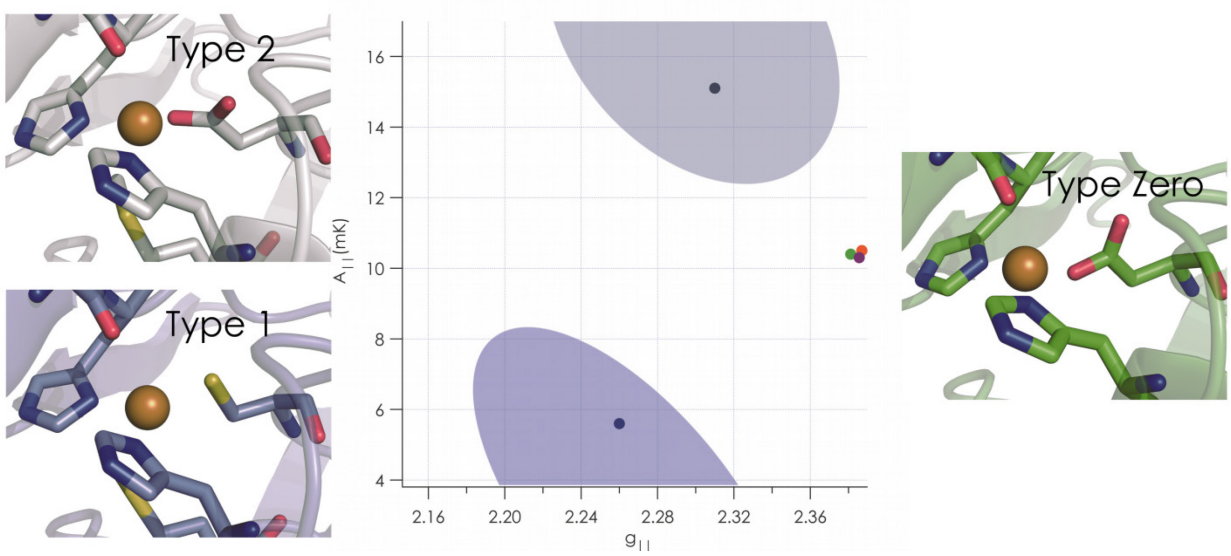

Figure 55. Active sites of type 2, type 1, and the newly constructed type 0 copper. In the center, a plot showing (in the shaded ovals) the typical values of two electron paramagnetic resonance spectroscopy parameters, $A_{\parallel}$ and $g_{\parallel}$, for type 1 (lower) and type 2 (upper) copper sites, and the values of type 0 copper (green, red, black points, right center), showing that type 0 copper does not fall into the typical ranges for these other kinds of sites. Reprinted by permission from Macmillan Publishers Ltd: Nature Chemistry ref [1308], copyright 2009.

4.4.4. Hydrogen bonds in secondary coordination sphere fine tune reduction potential

Copper ligands exert great influence on the spectroscopic features and reduction potentials of T1 copper proteins. However, copper ligands cannot fully account for variation in the reduction potentials of T1 copper proteins. Mutation of copper ligands usually results in loss of T1 characteristics or reduction of electron transfer activity. For the limited mutations that maintain T1 characteristics and electron transfer activity, the reduction potential is tuned over a 227 mV range by introducing Met analogues at the axial position, which is far less than the 600 mV range in native proteins.[1285] As discussed in section 4.3.3, the hydrogen bonding network beyond T1 copper center

plays an important role in maintaining structure and function of T1 copper centers. Mutagenesis directed to hydrogen bonds has revealed important information about how reduction potential and other properties are tuned in T1 copper proteins.

Rusticyanin has a higher potential relative to other T1 copper proteins. By sequence comparison, it is identified that there is a Ser in rusticyanin at the position corresponding to Asn that “zips” two ligand loops together. Asn has been proposed to raise the E_m by strengthening the hydrogen bonding interactions between two ligand-containing loops. Mutating Ser86 in rusticyanin to Asn established such a hydrogen bond and lowered the Em by 77 mV.[1312] On the other hand, changing Asn in azurin to Ser eliminates one hydrogen bond between two loops (Figure 56) and results in a protein with 131 mV higher reduction potential.[1293]

By comparing certain cupredoxins that natively have lower E_m than the rest of the family, it is observed that they have a conserved Pro residue two residues after the copper-ligating Cys.[114,1313] The backbone amide in the equivalent residue in azurin hydrogen bonds to the thiolate of Cys112.[1160] Placing a Pro in this position converts this secondary amide to a tertiary amide, which is incapable of donating a hydrogen bond. The Phe114Pro mutant has a lower reduction potential.[114] It is proposed that deleting the hydrogen bond to the thiolate gives Cys112 more conformational freedom, and it allows for the electron density that was previously tied up in a hydrogen bond to contribute to the Cu-S_{Cys} interaction.[114]

Another examination of cupredoxin crystal structures reveals the presence of backbone carbonyl oxygen from Gly45 near the copper ion in azurin, which is missing in other cupredoxins such as rusticyanin.[97,98,1314] This ionic interaction in azurin is proposed to result in higher electron density near the copper, preferentially stabilizing the Cu(II) form of the protein and, therefore, lowering the E_m.[98,481,1315] Such a mutation, Phe114Asn, was made in azurin and showed 129 mV higher reduction potential compared to wild type.[1088]

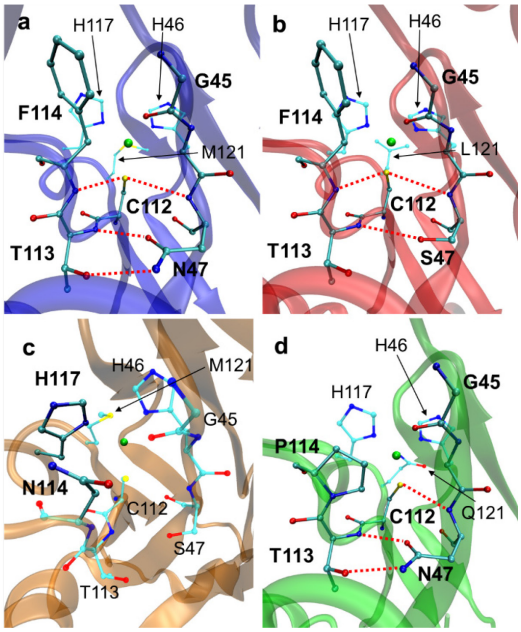

Figure 56. X-ray structures of Az and selected variants. a) Native azurin (PDB 4AZU). b) N47S/M121L azurin (PDB ID: 3JT2). c) N47S/F114N azurin (PDB ID: 3JTB). d) F114P/ M121Q azurin (PDB ID: 3IN0). Copper is shown in green, carbon in cyan, nitrogen in blue, oxygen in red, and sulfur in yellow. Hydrogen-bonding interactions are shown by dashed red lines. Reprinted from ref [1088].

With all of these individual factors in mind, Lu and coworkers combined mutations on both the copper ligands and on residues in the secondary coordination sphere. These mutations showed an additive effect on reduction potential in azurin. With different combinations, reduction potential was tuned from 90 to 640mV, which is beyond the range of native T1 copper proteins (Figure 57).[1088]

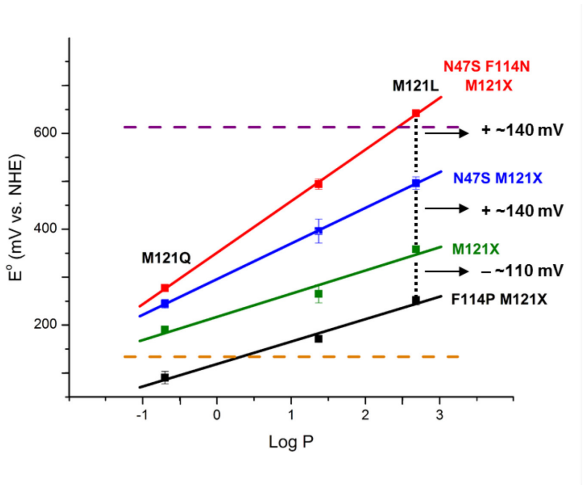

Figure 57. Plot of the reduction potentials for a number of Az mutants versus a measure of the hydrophobicity (LogP), revealing the linear trend with respect to the axial position (residue 121). Reprinted from ref [1088].

Unlike mutations on copper ligands, mutations of residues in the secondary coordination sphere are less likely to change T1 characters according to UV-vis, EPR,[1293] and resonance Raman[1316] spectroscopy. DFT studies were able to separate the effects of covalent interaction and non-local electrostatic components, each has a different effect on hydrogen bonds and dipole moment: both the covalent and nonlocal electrostatic contributions can be significant and additive for active H-bonds while they can be additive or oppose one another for dipoles (Figure 58).

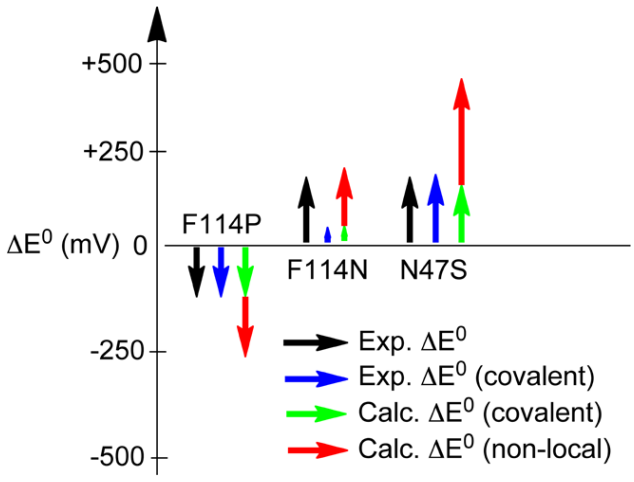

Figure 58. Illustration of the experimentally derived covalent and nonlocal electrostatic contributions to E^0 for the variants of Az relative to WT Az and their comparison to calculations. Reprinted with permission from ref [1316]. Copyright 2012 American Chemical Society.

Lower reorganization energies in the ET process generally increase ET rate constants and efficiency. However, rational design of ET centers to lower the reorganization energy has so far not been demonstrated. Such a task is particularly challenging for ET proteins like the blue copper protein azurin that have already been shown to possess very low reorganization energies in comparison to the majority of other proteins. A study of intramolecular ET by pulse radiolytically produced disulfide radicals to Cu(II) in the above rationally designed azurin mutants showed that the reorganization energy of ET is smaller than that of WT azurin, increasing the intramolecular ET rate constants almost 10-fold.[1317] More interestingly, analysis of structural parameters of these mutants suggested that this lowering in reorganization energy is correlated with increased flexibility of the copper center.

4.4.5. Ligand loop affects redox properties of T1 copper proteins

Besides directly mutating ligands, loop directed mutagenesis enables manipulation of ligands by changing protein structure in a broader scale. T1 copper proteins and Cu_A domains in heme-copper oxidases share the same cupredoxin fold, with 3 ligands of T1 copper and 4 ligands of Cu_A in the "ligand loop" (Figure 59). By careful design, it is possible to transplant the ligand loop of one protein into another, enabling interconversion between T1 copper and Cu_A and between different T1 copper proteins. (Section 4.5.3)

An early example of loop directed mutagenesis comes from interconversion between different copper centers, as two research groups independently installed ligand loop from Cu_A domain of cytochrome *c* oxidases on amicyanin and azurin, converting a T1 copper protein to a Cu_A protein,[1318,1319] discussed in detail in section 4.5. Recently, Berry and coworkers transplanted the ligand loop of nitrosocyanin, a newly discovered red cooper protein, to azurin.[1320] The resulting protein, NCAz, has similar UV-vis and EPR features as nitrosocyanin despite having His instead of Glu as the fourth ligand.

Although the T1 copper proteins have a conserved ligand set (section 4.3.1.1), the ligand loops from different proteins show variation in length and sequence (Figure 59). Loop directed mutagenesis has been carried out between different T1 copper proteins. Ligand loops from azurin, pseudoazurin, plastocyanin, rusticyanin, and nitrite reductase were introduced into the amicyanin scaffold to replace the short loop of amicyanin to create loop elongation mutants.[1321-1324] Later, the ligand loop from amicyanin, which is the shortest among T1 copper proteins, was introduced into azurin, pseudoazurin, and plastocyanin scaffolds to create loop contraction mutants.[1325,1326] The ligand loop from plastocyanin was introduced into the azurin scaffold as well.[1327] All of the loop-directed mutants maintain T1 copper spectroscopic characteristics, indicating they have a similar structure in a Cu(II) state. On the other hand, loop length has been shown to affect pK_a of C-terminal His and Cu(I)-N(His) distance.[1326,1327] It has been observed that introducing the short loop of amicyanin into pseudoazurin and plastocyanin increases the pK_a of C-terminal His, probably due to an entropically favored Cu(I)-N(His) interaction with a longer , more flexible loop.[1324-1326]

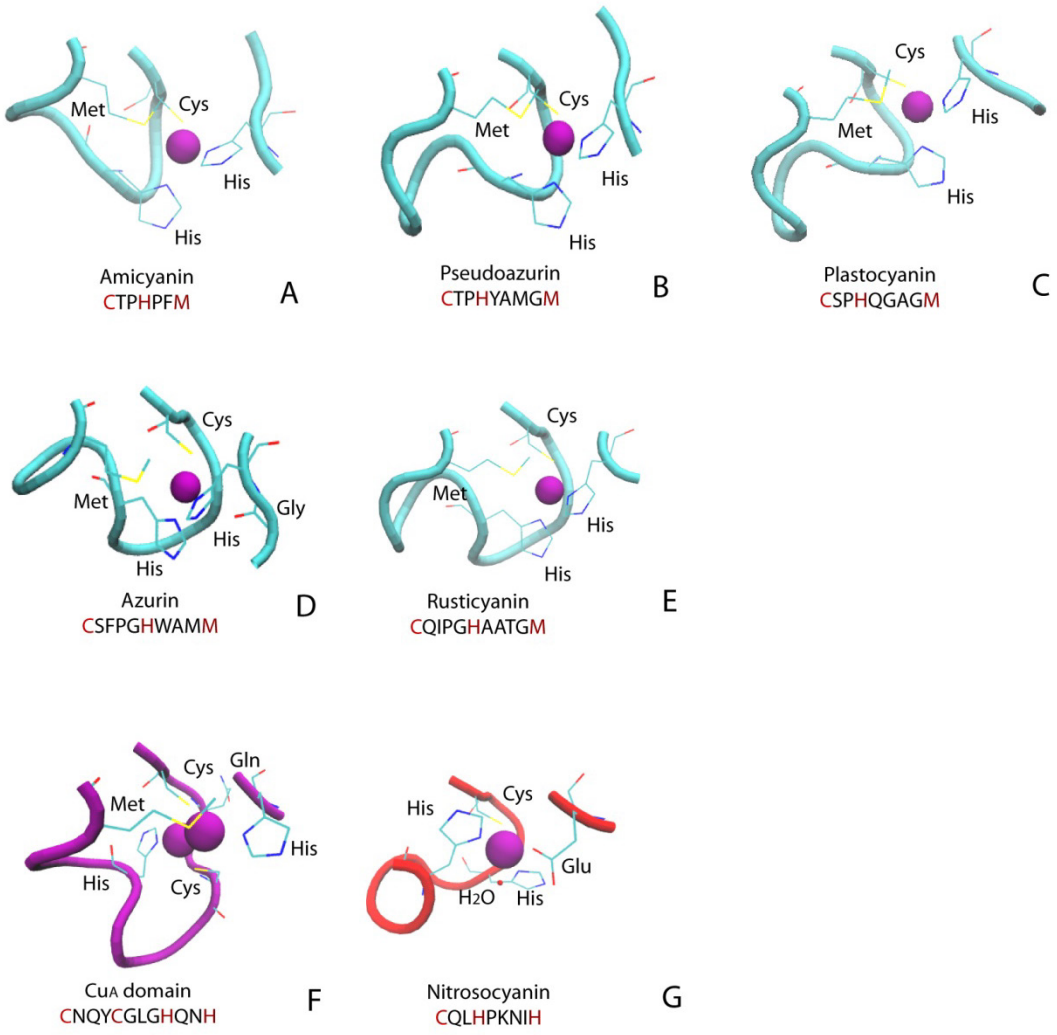

Figure 59. Ligand and loop structure in different T1 copper proteins, Cu_A from *T. thermophilus* heme-copper oxidase and red copper protein nitrosocyanin. A: amicyanin, PDB: 1AAC; B: pseudoazurin, PDB:1PAZ; C: plastocyanin, PDB: 1PLC; D: azurin, PDB: 2AZA; E: rusticyanin, PDB: 1RCY; F: Cu_A from *T. thermophilus* heme-copper oxidase, PDB: 1CUA; G: nitrosocyanin, PDB:1IBY.

As expected, reduction potentials of loop-directed mutants are between reduction potentials of donors of the loops and scaffolds. Amicyanin has the second lowest reduction potential in T1 copper proteins (see Table 10). Introducing the amicyanin loop into other copper protein scaffolds decreases their reduction potentials by 30-60mV.[1326] On the other hand, introducing loops of other T1 copper proteins to it increase the reduction potential of amicyanin.[1322-1324]

The electron transfer activity of loop directed mutants has been measured by electron self-exchange rate constant (k_{SES}). Loop elongation mutants generally have 10 fold lower k_{SES} while loop contraction has less influence on k_{SES}.[1322,1323,1326] Generally, T1 copper proteins can accommodate changes in loops and assume the same active site structure, consistent with “rack-induced bonding” or entatic state.[95,1168,1170]

4.5. Cu_A Centers

4.5.1. Overview of the Cu_A centers

Cu_A is a binuclear copper center bridged by two cysteine ligands to form a Cu_2S_2 “diamond-core” structure, which has only been found naturally in cytochrome *c* oxidases (C*c*Os),[1030,1109,1328] nitrous oxide reductases (N_2ORs),[1329,1330], the oxidase from *Sulfolobus acidocaldarius* (SoxH),[1331] and a Nitric Oxide Reductase (qCu_ANOR)[1332,1333] to date. Interestingly, all of these proteins are terminal electron acceptors of electron transfer processes, e.g. C*c*O is the terminal electron acceptor in aerobic respiration and N_2OR is the terminal electron acceptor in anaerobic respiration. One of the most important features in Cu_A sites is that the two copper ions form a direct metal-metal bond. Therefore, the unpaired electron is delocalized between two copper ions and the resting state of the Cu_A center is a Cu(+1.5)-Cu(+1.5) rather than Cu(+2)-Cu(+1). Cu_A is the first example of a metal-metal bond in biology, which makes it very unique compared to other metalloproteins. In addition to the bridging Cys ligands, the copper ions are coordinated by a His from equatorial position to form a trigonal NS_2 coordination. There is a weak distal axial ligand on each copper ion. The axial ligands are a methionine at one copper and a backbone carbonyl at the other. Considering only each copper ion, Cu_A center is very similar to the T1 blue copper protein, which has an overall distorted tetrahedral geometry. In this way, the Cu_A center can be treated of as two T1 copper centers joined together and form a Cu-Cu bond in between, indicating the evolutionary relationship between these two centers. Indeed, such a relationship has been proposed on the basis of three-dimensional structures comparison and

construction of phylogenetic trees, indicating that T1 copper and Cu_A proteins share a common ancestor and developed in part by divergent evolution.[1334,1335]

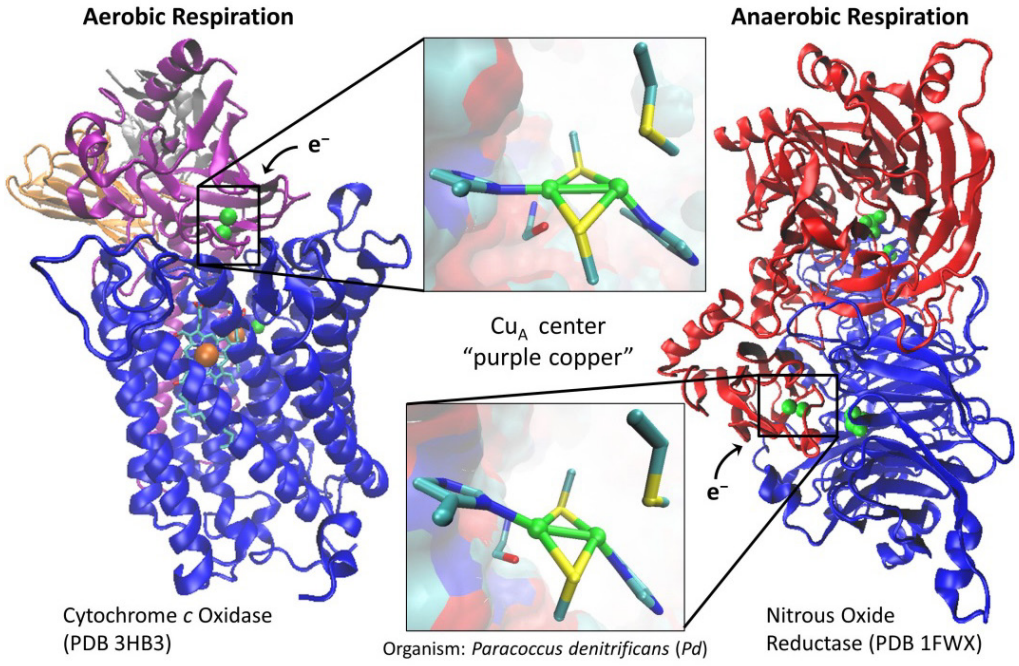

Figure 60. The crystal structure of cytochrome *c* oxidase (PDB: 3HB3) and nitrous oxide reductase (PDB: 1FWX). The CuA sites are highlighted (copper is in green, sulfur is in yellow, nitrogen is in blue and carbon is in cyan).

The UV-vis absorption spectrum of Cu_A shows two intense absorbance at ~480 nm and 530 nm which arises from S(Cys) → Cu charge transfer bands in the visible region and also a broad band at ~ 760-800 nm which arises from Cu(+1.5)-Cu(+1.5) intervalence charge transfer.[860,1113-1115] The reduced Cu(I)-Cu(I) form is colorless because of the d^{10} electronic configuration at each copper center. The more oxidized Cu(II)-Cu(II) state has not been observed to date.[1336,1337] Attempts to oxidize the Cu_A site normally give an irreversible anodic current at around 1 V, probably due to oxidation of the bridging dithiolate to disulfide.[1337,1338] Therefore, Cu_A site acts as one-electron transfer center.[72]

Table 13 Summary of spectroscopic parameters of Cu_A sites in different proteins.

Cu_A site containing proteins	Organism	λ_{max} (nm) (extinction coefficient) ($M^{-1}cm^{-1}$)	Reduction potential vs. NHE (mV)	ERP parameters (g_x, g_y, g_z)	Cu-Cu distance (Å)	Reference
subunit II of cytochrome *c* oxidase	*Paracoccus denitrificans*	363 (1200), 480 (3000), 530, 808 (1600) (pH7)	240	g_x,g_y = 2.03, g_z = 2.18, A_z = 3.5 mT	2.6	742,1109, 1339,1340
subunit II of cytochrome ba_3	*Thermus thermophilus*	363(1300), 480(3100), 530(3200), 790(1900)	250(pH8.1), 240(pH8) 297(pH4.6)	g_x = 1.99, g_y = 2.00, g_z = 2.17 A_z = 3.1 mT	2.43	1337,1341-1344
subunit II of caa_3-type cytochrome *c* oxidase	*Bacillus subtilis*	365, 480, 530, 775-800		g_x,g_y = 1.99 ~ 2.03, g_z = 2.178, A_z = 3.82 mT	2.44	1344,1345
Nitrous oxide reductase	*Paracoccus dentrificans*	480, 540(1700), 800				1330
Nitrous oxide reductase	*Pseudomonas stutzeri*	480, 540		g_x,g_y = 2.03, g_z = 2.18, A_z = 3.83 mT	2.44	1346
Nitrous oxide reductase	*Achromobacter cycloclastes*	350, 481(5200), 534(5300), 780 (2900)		g_x, g_y = 2.045		1347
Biosynthetic model in CyoA protein	*Escherichia coli*	360, 538(2000),		g_x = 2.03, g_y = 2.03, g_z = 2.18, A_z = 6.8, 5.3 mT	2.48	1114,1348,1349
Biosynthetic model in amicyanin		360, 483, 532, 790		$g_{x,y}$ = 1.99 – 2.02, g_z = 2.18, A_z = 3.24 mT		1318

Biosynthetic model in azurin		360(550), 485(3730), 530(3370), 770(1640)		g_x,g_y = 2.06, g_z = 2.17, A_z = 5.5 mT	2.39	[1319,1350]
Nitrous oxide reductase	*Pseudomonas nautica 617*	480, 540, 800	260	$g_{x,y}$ = 2.021, g_z= 2.178, A_z = 7mT		[1351]
Subunit II of SoxM	*Sulfolobus acidocaldrius*	361(2300), 478(3200), 538(3700), 789(2400)	237	$g_{x,y}$ = 2.01, g_z = 2.20		[1331]
Subunit II of cytochrome *c* oxidase	*Synechocystis PCC 6803*	359(1580), 482(2820), 535(3080), 785(1840)	216(pH7)			[1352]

The Cu-Cu bond in Cu_A sites has been subject of extensive debate.[1353] Later, the structure of Cu_A site was confirmed by different spectroscopic methods. Blackburn et al. reported the extended X-ray absorption fine structure (EXAFS) studies of Cu_A-binding domain of *Bacillus subtilis (B. subtilis)* C*c*O which showed a strong Cu-Cu interaction of ~2.5 Å together with a short 2.2 Å Cu-S interaction.[1108] The Cu-Cu bond distance is nearly identical to the similar EXAFS studies of native C*c*O from bovine-heart mitochondria which is 2.46 Å.[1354] The dinuclear nature and the unusually short Cu-Cu distance of ~2.55 Å were confirmed by x-ray crystal structures of C*c*O from *P. denitrificans* and bovine-heart mitochondria, reported by two independent groups,[1030,1109] as well as an engineered Cu_A center in CyoA.[1349] Similar structures were also observed in the crystal structure of N_2OR from *Pseudomonas nautical*.[1329,1330] The most intense bands at 339 cm^{-1}, 260 cm^{-1} and 138 cm^{-1} observed in resonance Raman (RR) spectroscopy of *P. denitrificans* C*c*O Cu_A domain were assigned to symmetric stretches involving primarily the Cu-S (Cys), Cu-N(His) and Cu-Cu bonds, respectively.[1107]

The Cu-Cu bond in the Cu_A site causes a valence delocalization between the two copper ions and produces a 7-line hyperfine splitting pattern in the EPR spectra. This unique EPR pattern can be explained by the delocalized unpaired electron coupled with

two nuclear spin I = 3/2 copper ions equivalently.[1112,1355,1356] Compared to T1 blue copper proteins, Cu_A centers show even smaller $A_{//}$ based on EPR simulations,[1114,1339,1342,1345,1346,1357] reflecting greater covalent interaction and unpaired electron delocalization between the copper ions and the bridging Cys residues.

4.5.2. Truncated water-soluble Cu_A center containing domains from native proteins

Historically, studying the biochemical role and probing unique structure of Cu_A centers has not been easy due to the Cu_A site only appearing in some native enzymes such as C*c*O and N_2OR, which contain other metal centers that make the spectroscopic characterization of Cu_A sites extremely complicated. For instance, C*c*O is a membrane protein containing two heme groups (heme *a,* and heme a_3), two copper centers (Cu_A and Cu_B) as well as a zinc and a magnesium ion. These cofactors significantly complicate the spectroscopic studies of the Cu_A site. To overcome these inherent difficulties in studying native Cu_A centers, two strategies are developed: producing truncates of native Cu_A enzymes[742,1331,1339,1341,1342,1345,1352,1358-1361] and designing Cu_A centers into small, soluble proteins.[1318,1362,1363]

In the first strategy, the sequence of the Cu_A-subunit from C*c*O or SoxH was isolated and recombinantly expressed without the membrane-spanning helices that normally anchor this domain to the membrane. This way, a water-soluble protein containing only a Cu_A site was obtained. Such truncates have been constructed for C*c*O from *B. subtilis*,[1345] *P. dentrificans*,[742,1339,1358,1361] *P. versutus*,[1360] *Synechocystis PCC 6803,*[1352] and *T. thermophilus* [1341,1342,1359,1361] and for SoxH from *S. acidocaldarius*.[1331] The UV-vis, EPR and EXAFS spectroscopic characterizations as well as the reduction potentials measured for these soluble truncates are consistent with each other (Table 13).[742,1339,1358,1361] To date, only the truncated from *T. thermophilus* has been successfully crystallized.[1359]

4.5.3. Engineered Cu_A centers in Greek-key β-barrel protein scaffolds

The second strategy to study Cu_A sites is designing this site into other proteins and was first accomplished in a quinol oxidase.[1362] The authors first aligned subunit II of cytochrome *c* and quinol oxidases and found that the C-terminal of both proteins

contained a subdomain, which was in Greek-key β-barrel scaffold. This alignment suggested that both proteins contain a basic structural motif characteristic of cupredoxins. The CyoA lacked the putative ligands for the formation of the Cu_A in C*c*O. The Cu_A ligand set was thus introduced by extensive mutagenesis of the isolated cupredoxin domain. This engineered CyoA bound copper and showed two strong peaks at 358 nm and 536 nm, a shoulder at 475 nm and a broad peak between 750 and 780 nm, as well as an EPR pattern similar to the pattern observed in native Cu_A from C*c*O. Later, the crystal structure of CyoA was reported with 2.3 Å resolution.[1349] The distance between the two coppers is 2.5 Å. Shortly after the release of the purple CyoA study, two other research groups independently developed designed Cu_A centers in T1 copper proteins.[1318,1319] Dennison et al. replaced the C-terminal loop of the blue copper protein amicyanin, which contained three of the four active ligands, with a Cu_A binding loop. After copper binding, a purple protein was produced with UV-vis absorbance at 360, 483, 532 nm and a broad absorption at approximately 790 nm, almost identical to that of the native Cu_A domain of C*c*O from *B. subtilis*. The EPR spectrum of the Cu_A amicyanin contained signals from two Cu(II) species. One is a distinctive type II copper site and the other is characteristic of a Cu_A center.[1364]

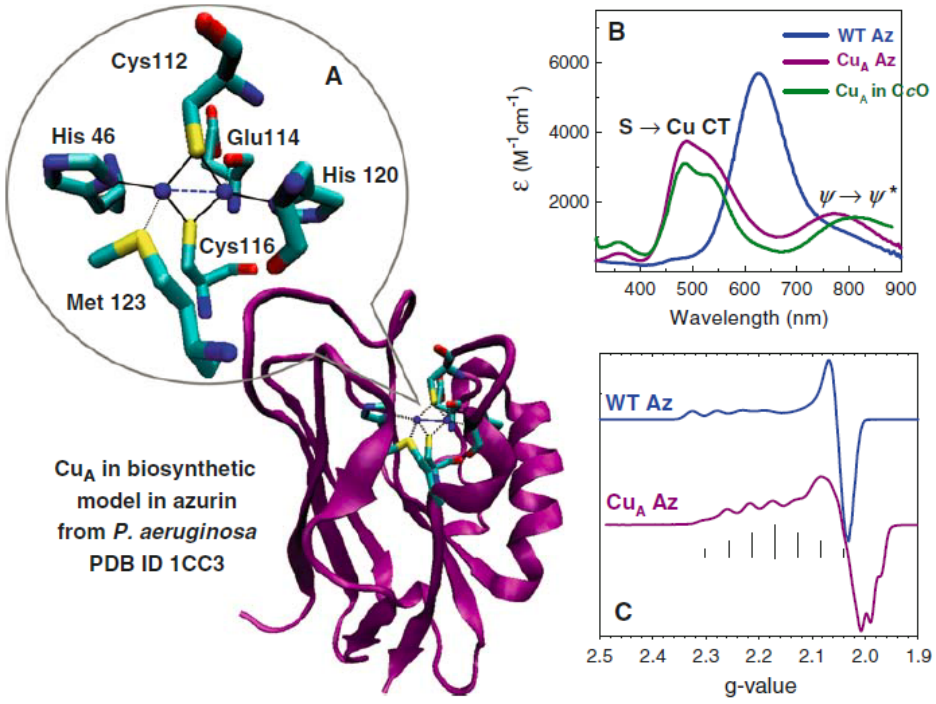

Figure 61. (A) Crystal structure of biosynthetic model of Cu_A site in azurin (PDB: 1CC3). (B) The comparison of UV-vis spectra between soluble Cu_A domain in cytochrome *c* oxidase (green line), wild type azurin (blue line) and biosynthetic CuA model in azurin (purple line). (C) The comparison of x-band CW EPR between wild type azurin (blue line) and biosynthetic CuA model in azurin (purple line), 4-line splitting vs. 7-line splitting. Reprinted with permission from ref [1365]. Copyright 2010 Springer-Verlag.

Hay et al. constructed a purple copper protein from a recombinant blue copper protein, *P. aeruginosa* azurin, by replacing the loop containing the three ligands to the blue copper center with the corresponding loop of the Cu_A site in C*c*O from *P. dentrificans*.[1319] The UV-vis and EPR spectra of this protein (Cu_AAz) were remarkably similar to those of native Cu_A sites in C*c*O from *P. dentrificans*. The UV-vis absorption spectrum of Cu_AAz features two S(Cys)→Cu CT bands at 485 (ε ~3700 $M^{-1}cm^{-1}$) and 530 nm (ε ~ 3400 $M^{-1}cm^{-1}$)[1113,1350], compared to 480-485 nm and 530-540 nm for native Cu_A centers.[98] Cu_AAz also featured a broad band centered at 760-800 nm (ε ~ 2000 $M^{-1}cm^{-1}$), typical of the Cu-Cu $\psi \rightarrow \psi^*$ transition, suggesting that Cu_AAz had reproduced the Cu-Cu bond. Additionally, the EPR spectrum of Cu_AAz displayed a 7-line hyperfine splitting pattern, demonstrating that this biosynthetic model duplicated the mixed-valence ground state of native Cu_A centers.[1319,1350] EXAFS, CD, MCD, and resonance

Raman analyses of the Cu_A in azurin also suggested a high level of electronic and structural identity with Cu_A centers from C*c*O.[1113,1319,1350,1364,1366] X-ray crystal structure of Cu_AAz showed a very similar arrangement of ligands about the copper ions, and a Cu-Cu distance that was even slightly shorter than the native Cu_A center in C*c*O, confirming the presence of a Cu-Cu bond.[1367] Cu_AAz's small size and relative ease of expression and purification make this biosynthetic model highly amenable to mutagenesis studies.

4.5.4. Mutations to axial Met ligand

The weaker axial methionine ligand has been investigated by mutagenesis in C*c*O from *P. denitrificans* and *Rb. sphaeroides*. The Met227Ile in C*c*O from *P. denitrificans* resulted in a protein with unchanged stoichiometry of metals. However, the two copper ions in Cu_A site were no longer equivalent and converted from delocalized Cu(+1.5)-Cu(+1.5) to localized Cu(+1)-Cu(+2) system based on EPR and near-IR studies.[1368] The electron transfer from cytochrome *c* to Cu_A was not affected, but the rate of electron transfer to heme a was significantly diminished in the mutant protein compared with the wild type protein due to altered reduction potential of the Cu_A site. It was concluded that the weak axial Met was not essential for copper binding but it was important for maintaining the mixed-valence electronic structure of the Cu_A site. The Met263Leu in C*c*O from *Rb. sphaeroides* also showed the binding of two copper ions and proton pumping activity. Multifrequency EPR studies showed that the two copper ions in Cu_A site were still electronically coupled. While all the other metals remained unchanged based on UV-vis, EPR and FTIR spectroscopy but the mutant only maintained 10% of the activity[1369] shown by the native enzyme The kinetic analysis of electron transfer showed that Met263Leu decreased the electron transfer rate from heme *c* to Cu_A to 16,000 s^{-1}, compared to 40,000 s^{-1} in wild type. The rate constant for the reverse reaction was increased to 66,000 s^{-1}, compared to 17,000 s^{-1} in wild type. This was attributed to an increased reduction potential of 120 mV relative to the native enzyme.[1370]

The perturbation of weak axial methionine ligand was also tested in soluble Cu_A containing subunit of cytochrome ba_3 from *T. thermophilus*.[1357] The mutants, Met160Gln

and Met160Glu, affected the g_z region of EPR spectra where the Cu hyperfine became more resolved and larger in both mutants. Notably, the A_z values of both mutants were increased from 3.1 mT to 4.2 mT, larger than most of the characterized native Cu_A sites. The UV-vis spectra showed enhanced intensity and a blue shift relative the wild type. The EPR and UV-vis data suggested that the strength of axial ligand increased from wild type to Met160Gln to Met160Glu. The effect of both mutations were further studied by pulsed EPR/ENDOR spectroscopy.[1371] The results from this study showed an increase of $A_{//}$, larger hyperfine coupling, reduction in the isotropic hyperfine interaction and the axial g-tensor. All these effects were associated with an increase in the Cu-Cu distance and changes in the geometry of Cu_2S_2 core structure. The mutant Met160Gln was also studied by paramagnetic ^{1}H NMR spectra.[1372] The fast nuclear relaxation in this mutant suggested that a low-lying excited state had shifted to higher energies compared to that of the wild type protein.

Blackburn et al. reported a selenomethionine-substituted *T. thermophilus* cytochrome ba_3 and characterized it with Cu K-edge EXAFS.[1373] Interestingly, the optical and EPR spectra of selenomethionine-substituted Cu_A site were essentially identical to the native Cu_A site as well as the reduction potential. These data suggested that whatever role the S(Met) atom played in electronic structure of Cu_A site was also carried out by the Se(Met) atom.

The axial Met in Cu_AAz was mutated to Asp, Glu and Leu, spanning the entire range of the hydrophobicity series among the natural amino acids. The reduction potentials measured for these axial Met variants showed very little change from original Cu_AAz, spanning only ~20 mV, despite some visible perturbation to the UV–vis and EPR spectra of these mutants. The significantly smaller axial tuning effect in Cu_AAz may reflect the resilience of the diamond core of Cu_A. The stability of the interactions making up the diamond core—the bridging Cys thiolates and copper–copper bond—may lead to greater resistance to perturbations arising from the axial position.[1374] However, recently a different set of axial Met mutants was generated in the truncated water soluble Cu_A domain from *T. thermophilus*.[1375] By introducing Gln, His, Ser, Tyr and Leu at axial Met position, the resulting changes to reduction potentials were ~ 200 mV. The difference

between the truncated Cu_A domain and Cu_AAz was attributed to the difference in Cu-S(Met) bond lengths in these two systems: 2.47 Å in truncated Cu_A domain vs. 3.07 Å in Cu_AAz. Another explanation is that Cu_AAz contains the shortest Cu-Cu bond length (~ 2.4 Å), which enhances the diamond core structure towards ligand changes.

It is interesting to note that the reduction potentials of native Cu_A site from soluble fragment of subunit II of *T. thermophilus* ba_3 at different pH values showed no significant changes.[1376] However, the engineered Cu_A site in azurin exhibited strong pH dependence of redox properties. This difference might be caused by protonation and dissociation of one histidine ligand in engineered Cu_A center, whereas in native protein the redox properties are more strictly regulated.

4.5.5. Mutations of the equatorial His ligand

The equatorial His ligand strongly binds to the copper ion with bond length ~ 2.0 Å. In principle, the mutation at His position would result in a significant perturbation of the Cu_A site. This assumption has been proven to be true in the native system. The His260Asn mutant in cytochrome *c* oxidase from *R. sphaeroides* only exhibited 1% of the wild type activity.[1369] The 850nm band was shifted and the extinction coefficient was diminished to around 1230 $M^{-1}cm^{-1}$, compared with 1900 $M^{-1}cm^{-1}$ in wild type. No apparent hyperfine splitting pattern was observed in the EPR spectrum. The kinetic analysis of electron rates showed that the rate constant for electron transfer from Cu_A to heme c was decreased to 11,000 s^{-1}, compared to 40,000 s^{-1} in wild type. The electron transfer rate from Cu_A to heme c was decreased to 45 s^{-1}, compared with 90,000 s^{-1} in wild type. An increase of 90 mV in reduction potential was also observed.[1370]

However, dramatic differences were observed in biosynthetic model of Cu_A in azurin. The mutation of His120 to Ala yielded a UV-vis spectrum similar to that of original Cu_AAz, including the Cu-Cu $\psi \rightarrow \psi^*$ band at ~760 nm.[1377,1378] The EPR spectrum of His120Ala only showed a 4-line hyperfine splitting pattern, suggesting that the active site had undergone a transformation to trapped valence although Q-band ENDOR study of His120Ala Cu_AAz showed evidence for the Cu_A site still being delocalized.[1379] Xie et al. applied a series of spectroscopic techniques, including EPR, UV-vis, MCD, rR and XAS to both Cu_AAz and His120Ala Cu_AAz, and correlated the

results with DFT calculations.[1380] The surprising conclusion of this work was that a minute, 1% mixing of the 4s orbital of one copper ion into the ground-state spin wave function caused the collapse to a 4-line hyperfine splitting pattern in the EPR spectrum of His120Ala, not a change from valence delocalized to trapped valence. The rR and MCD spectra both demonstrated that the valence delocalization of the Cu_A center was still intact, although slightly perturbed, despite the loss of His120 as a ligand. The authors attributed the ability of Cu_A in azurin to remain valence delocalized, even with the loss of such a strong ligand, to the large electronic coupling matrix element, which arises from the strong and direct Cu-Cu bond. Thus, the diamond core of Cu_A plays an immense role in the robust nature of this center.

4.5.6. Mutations of the bridging Cys ligands

Mutagenic studies of the Cu_A binding ligands in native C*c*O from *P. denitrificans* and N_2OR from *P. stutzeri* have demonstrated that the cysteine ligands play an important role in the functions of the enzymes and the spectroscopic features of Cu_A. Mutating one of the two bridging cysteines to serine, Cys216Ser, in C*c*O from *P. denitrificans* resulted in a type 1 blue copper site with 4-line EPR hyperfine splitting rather than the 7-line EPR signal in Cu_A site and only retained below 1% of wild-type activity. The Cys216Ser mutant no longer exhibited the near-IR absorption in the optical spectrum, also indicating the loss of the Cu-Cu bond. Mutation of the second cysteine, Cys220Ser, resulted in 5–10% activity of the wild type. The higher activity in Cys220Ser is suggested to be due to intact binuclear copper site based on metal:protein ratio and copper:iron ratio.[1381] The Cys618Asp mutant in N_2OR resulted in almost complete loss of activity and the copper was bound only weakly and was hardly detectable after gel filtration column. In contrast to Cys618Asp mutant, the Cys622Asp mutant retained some copper-binding ability and activity; although, the characteristic multiline feature of the mixed-valence Cu_A was no longer resolved in EPR.[1382]

Similar to the studies in the native system, the bridging Cys ligands were also individually mutated to Ser in the biosynthetic model of Cu_A in azurin.[1383] Although the resulting mutants still bound to the copper ions, the features of Cu-Cu bond were completely lost in that the Cys112Ser mutant resulted in two type 2 copper sites and

Cys116Ser resulted in a type 1 copper site. To consider the loss of symmetry in a single Cys to Ser mutant, a double Cys to Ser construct was made.[1384] At high pH, the double mutant indeed bound two coppers, but the EPR spectrum showed that the two copper ions were in two distinct type 2 copper sites rather than a mixed valence site with 7-line hyperfine splitting.

4.5.7. Tuning the Cu_A site through non-covalent interactions

The hydrogen bonding and hydrophobic interactions around the active site of copper proteins can significantly tune the electron transfer process.[1088] Two mutations, Asn47Ser and Glu114Pro were made in Cu_AAz.[1385] Both the Asn47Ser and Phe114Pro mutations alter hydrogen bonding interactions near the Cys112 ligated to copper ion, but Phe114Pro decreases the reduction potential by deleting the hydrogen bond between Cys112 and backbone NH group,[114] while Asn47Ser increases the reduction potential by affecting the rigidity of the copper binding site and most likely the direct hydrogen bonds between the protein backbone and Cys112.[1088]

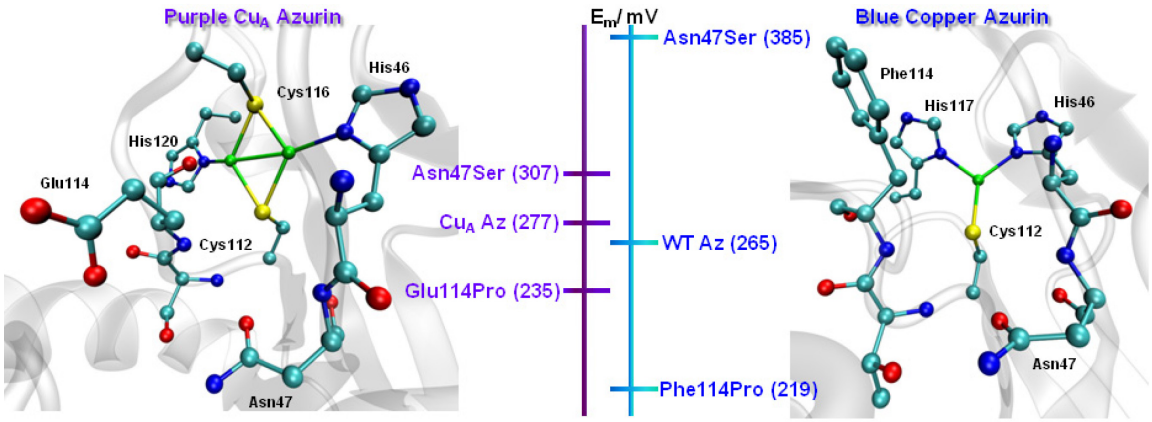

Figure 62 Tuning the reduction potential at blue copper azurin and Cu_A azurin by redesigning the second coordination sphere. The effects of these mutants are in the same direction but the magnitude is smaller in Cu_A site due to the electron delocalization between to two copper ions. Adapted from ref [1385] with permission of The Royal Society of Chemistry.

4.5.8. Electron transfer properties of the Cu_A centers

The Cu_A site is the point of entry of the electron from cytochrome *c*. In C*c*O, Cu_A receives electrons from cytochrome *c* and transfers them to cytochrome *a*. However, in N_2OR, Cu_A is believed to transfer electrons between cytochrome *c* and the catalytic site where nitrous oxide is reduced. The characterization of the electron transfer between cytochrome *c* and cytochrome *c* oxidase has been a difficult problem. Stopped-flow has been used to study the kinetics but does not have sufficient time resolution to monitor such a rapid electron transfer process.

The electron transfers between bovine cytochrome *c* oxidase and horse cytochrome *c* labeled with (dicarboxybipyridine)bis(bipyridine)ruthenium(II) were studied by laser flash photolysis.[1386] The electron was transferred from Lys25 ruthenium-labeled cytochrome *c* to the Cu_A site with a rate constant of 11,000 s^{-1}. The Cu_A site then transferred an electron to cytochrome *a* with a rate constant of 23,000 s^{-1}. Lys 7, 39, 55 and 60 ruthenium-labeled derivatives showed nearly the same kinetics.

The intramolecular electron transfer between the Cu_A site and heme a in bovine cytochrome *c* oxidase was measured by pulse radiolysis.[1387] The rate constant of electron transfer from Cu_A site to heme *a* was 13,000 s^{-1} and for the reverse process was 3,700 s^{-1}. From this study a low activation barrier was observed, indicating small reorganization energy during the electron transfer process. The method was also applied to study the electron transfer between the Cu_A site and heme a in cytochrome *c* oxidase from *P. denitrificans*.[1340] The electron transfer rates were found to be 20,400 s^{-1} and 10,030s^{-1} for forward and reverse reactions respectively.

The type 1 blue copper sites and Cu_A sites are commonly used as electron transfer centers found in many biological systems. However, direct comparison between the electron transfer rates of these two centers is hard to achieve due to different protein scaffolds and redox partners. The engineered Cu_A site in azurin provides a great opportunity to eliminate the protein structure contribution to the electron transfer process since the electron transfer rates are measured in the same azurin scaffold.[1388] The authors first radiolytically reduced the disulfide bond within azurin scaffold and then measured the long-rage electron transfer rate from the reduced disulfide bond to the

oxidized Cu_A center. The rate constant of this intramolecular electron transfer process in Cu_A Az is ~650 s^{-1}. Although Cu_AAz has smaller driving force (0.69 eV for Cu_AAz vs. 0.76 eV for blue copper azurin), the electron transfer rate of Cu_AAz is almost 3-fold faster than for the same process in the wild type single blue copper azurin (~250 s^{-1}). The calculated reorganization energy of the Cu_A center is only ~ 0.4 eV, which is 50% of that found for the blue copper azurin. The low reorganization energy of Cu_A was also observed in the truncated soluble Cu_A domain of C*c*O from *T. thermophilus*.[1337] Farver et al. studied the electron transfer rates and reorganization energies of mixed valence Cu_AAz site and trapped valence His120Ala Cu_AAz.[1389] They found that changing from mixed valence to trapped valence state increased the reorganization energy by 0.18 eV, but lowering the pH from 8.0 to 4.0 resulted a ~ 0.4 eV decrease in reorganization energy, suggesting that the mixed valence state only played a secondary role in controlling the electron transfer property.

4.5.9. pH-dependent effects

As an electron entry site for cytochrome *c* oxidase, the Cu_A center receives electrons from cytochrome *c* and transfers the electrons to the heme a site. The electrons are finally transferred to the heme a_3-Cu_B site where dioxygen reduction takes place. The reduction results in a proton gradient, which in turns drives the synthesis of ATP. For cytochrome *c* oxidase to function well, a regulator is needed for initiating and shutting down the whole electron transfer process and dioxygen reduction reaction. A pH-dependent study on engineered Cu_AAz suggested that the Cu_A site may play such a role.[1390] The Cu_AAz displayed a 7-line EPR hyperfine with mixed valence state. When lowering pH from 7.0 to 4.0, the absorption at 760 nm shifted to 810 nm, at the same time, a 4-line EPR hyperfine was observed. The pH-dependence was reversible, and the mixed valence state was restored when increasing the pH back to 7.0. A dramatically increased reduction potential was also observed, from 160 mV to 340 mV, when increasing pH from 7.0 to 4.0. It was identified that the protonation of C-terminal His120 caused such a pH-dependence transition, as the His120Ala mutant completely abolished this observation. A feedback mechanism was proposed to explain how the Cu_A site regulated the function of cytochrome *c* oxidase. The pumped proton may result

in protonation of the C-terminal His and then cause trapped valence of the Cu_A site. The increased reduction potential in the trapped valence state will stop the whole electron transfer process and proton pumping (Figure 63). This hypothesis is further supported by electron transfer studies in the His260Asn mutant in cytochrome *c* oxidase from *Rh. sphaeroides* which showed that protonation of the C-terminal histidine resulted in a change in the valence state and increasing the reduction potential by 90 mV.[1370] The electron transfer rate from the Cu_A site to heme a decreased by over four orders of magnitude. The His260 in cytochrome *c* oxidase corresponds to His120 in Cu_AAz.

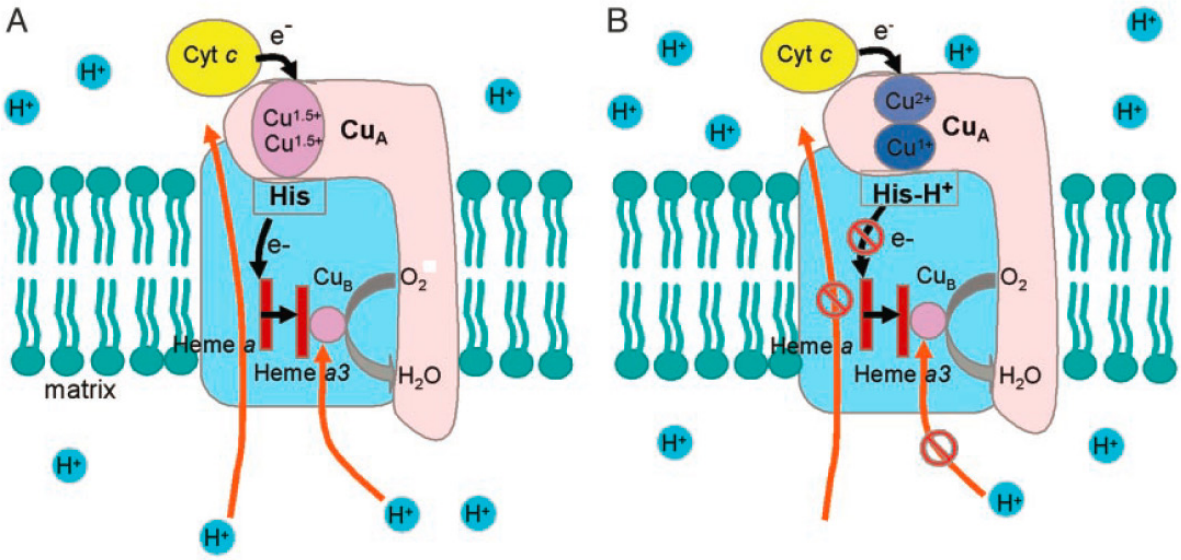

Figure 63. Schematic model of different states of Cu_A center in cytochrome *c* oxidase. (A) Mixed valence form at neutral pH and (B) trapped valence form at low pH. Subunit I is in light blue, and subunit II is in pink. Black arrows represent the flow of electrons, and orange arrows represent the flow of protons. Reprinted from ref [1390] with permission. Copyright (2004) National Academy of Sciences, U.S.A.

4.5.10. Copper incorporation into the Cu_A centers

The question of how copper ions are delivered into the Cu_A sites *in vivo* is still poorly understood. In the cytoplasm, copper levels are rigorously regulated and free copper levels are extremely low and estimated to be at the attomolar level.[1391-1397] Although it has been proposed that a metallochaperone called Sco is responsible for

metalation of the Cu_A site, delivering the copper ions to Cu_A site in C*c*O by Sco proteins has not been demonstrated.[1398]

Besides the delivery of copper ions by Sco proteins, another possibility is unmediated metalation. The C*c*Os from eukaryotes are located in mitochondrial membranes.[1399] In Gram-negative bacteria, Cu_A in C*c*O is exposed to the periplasmic space. However, in Gram-positive bacteria, Cu_A in C*c*O is exposed to the extracellular space.[1109,1393,1400,1401] N_2OR is a soluble protein also located in the periplasmic space.[1402] In periplasmic and extracellular spaces, copper levels are not regulated as rigorously as inside the cell, and free copper ion concentration could be much higher. In fact, unmediated Cu_A metalation has been considered as a possibility for Cu_A metalation in N_2OR.[1403-1405] From this view, the studies of free copper ion incorporation into Cu_A sites *in vitro* may provide important insights into this process, although it does not perfectly reflect the process *in vivo*.

In an early study of Cu_AAz, the metalation of the apo-Cu_AAz by adding ten-fold excess of $CuSO_4$ was observed by stopped-flow UV–vis spectroscopy.[1406] A single intermediate with intense absorbance at 385 nm was observed which is the characteristic of the Cys-S→Cu CT bands of tetragonal type 2 copper centers.[98,1095] This type 2 copper intermediate formed with k_{obs} = 1.2×10^3 s^{-1} and subsequently decayed with k_{obs} = 3.1 s^{-1}, meanwhile the absorptions correspond to Cu_A site increased. An isosbestic point between the ~385 nm band and the ~485 nm band of Cu_A site was observed; indicating T2 copper intermediate was converted to Cu_A. Because only Cu(II) ion was added during metalation, a reducing agent must be supplied by the system itself to form a Cu(+1.5)-Cu(+1.5) site, indicating that the free thiols in apo-Cu_AAz were providing electrons by forming disulfide bonds.[1407-1409]. Adding ascorbate or Cu(I) salt increased the yield of Cu_A centers.

A similar study was investigated in N_2OR from *P. denitrificans*.[1410] Different from the previous study, two intermediates were observed upon adding Cu(II) salt. These two intermediates formed within a similar timescale and also decayed at the same time with simultaneous formation of Cu_A sites. Two isosbestic points were present between the absorption bands of both intermediates and the Cu_AAz absorption bands, strongly

suggesting conversion of these intermediates to Cu_A. One of these two intermediates has spectral features typical of T2 copper centers with thiolate ligation, and another shows the characteristics of a T1 copper center. These observations suggested that the purple Cu_A site contained the essential elements of T1 and T2 copper centers and provided experimental evidence *in vitro* for a previously proposed evolutionary link between the cupredoxin proteins.[1334,1335]

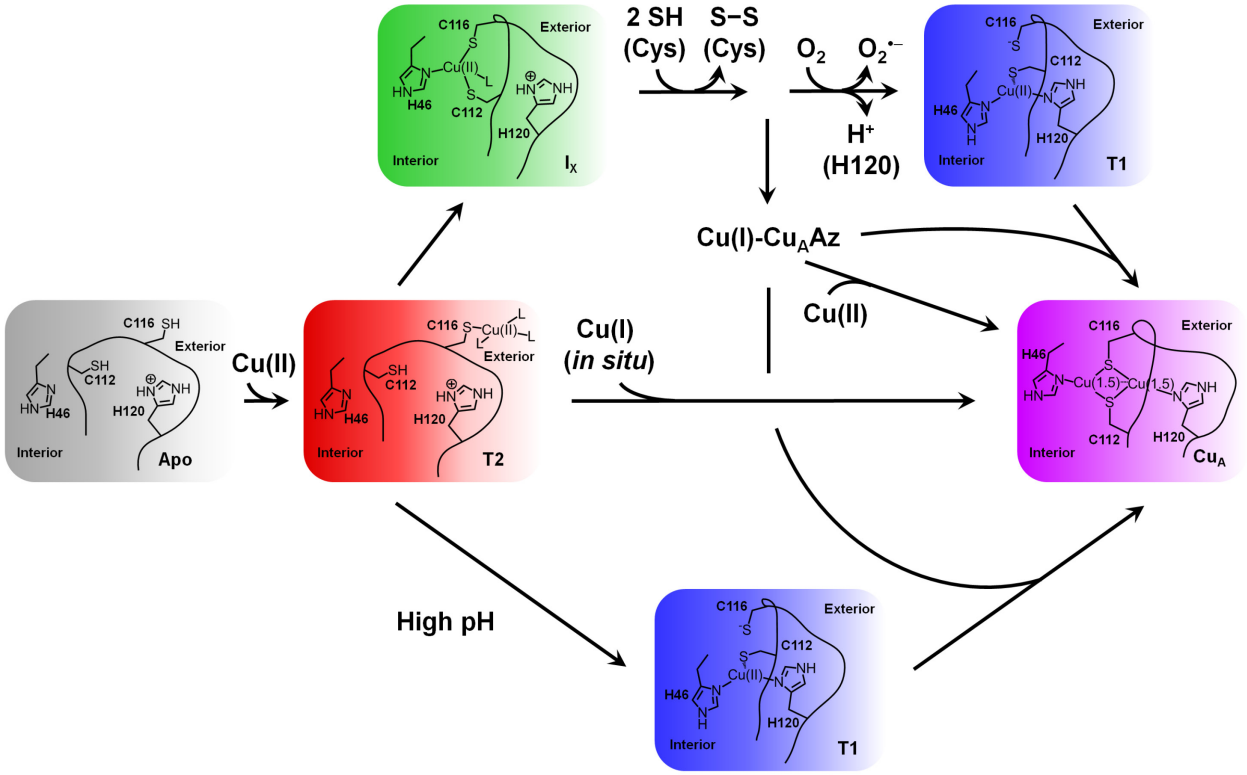

Figure 64. Proposed mechanism of copper incorporation into the biosynthetic Cu_A model in azurin. Reprinted from ref [103] with permission from American Chemical Society.

Guided by the observation of both T1 copper and T2 copper intermediates in the metalation of Cu_A site in N_2OR, the metalation of Cu_AAz was revisited by varying both copper concentration and pH.[1411] When the Cu_AAz concentration was greater than the $CuSO_4$ concentration, both T2 copper and T1 copper intermediates were observed, similar to the results obtained for N_2OR. Global fitting of the UV–vis absorption kinetic data and time-dependent EPR together with previously studied mutants of Cu_AAz provided valuable information about the mechanism of copper incorporation where a

new intermediate I_x was observed. When Cys112 was mutated to Ser, a T2 copper site formed, with similar UV–vis and EPR spectra to the T2 copper intermediate. From this study it was inferred that the T2 copper intermediate is a capture complex with Cys116, which is also supported by the greater solution accessibility of this residue, compared to Cys112. Conversely, when Cys116 was changed to Ser, a T1 copper center formed, with nearly identical UV–vis and EPR spectra to the T1 copper intermediate.[1383]

4.5.11. Synthetic models of the Cu_A centers

Another approach to study the Cu_A center is to synthesize small-molecule mimics of Cu_A.[1412] This has been proven to be a difficult task because of the formation of disulfide bonds between free thiols mediated by copper ions.[1338] Also, the most important feature in Cu_A site, the diamond core structure that Cu-Cu bond bridging by thiolates, is hard to achieve. Besides the first coordination sphere, the second coordination sphere has also proven to be important in tuning the properties of the Cu_A site, which is even harder to mimic in small-molecule compounds.[1385] However, model compounds have met with varying degrees of success and possess some but not all of the features of Cu_A.[369,1413-1428]

Houser et al. reported a fully delocalized mixed-valence dicopper complex with bis(thiolate) bridging which was the first closet small-molecule Cu_A mimic. The crystal structure of this model complex showed that the Cu_2S_2 core is planar with an average Cu-Cu distance of 2.92 Å. However, it is still longer than the Cu-Cu distance (2.46 Å by EXAFS[1354] and 2.55 by x-ray crystal structures[1030,1109]) in native Cu_A centers.[1416] The EPR spectrum recorded at 4.2 K clearly showed the 7-line hyperfine splitting indicating the fully delocalized electronic structure.

More recently, Gennari et al. reported a new bis(μ-thiolato) dicopper complex that mimicked most of the important spectroscopic features of the Cu_A site.[1429] Notably, unlike Tolman's complex which could not be reduced to Cu(+1)-Cu(+1) state, this dicopper complex is the first Cu_A model with Cu_2S_2 core that can be reversibly oxidized or reduced between Cu(+1.5)-Cu(+1.5) and Cu(+1)-Cu(+1). However, the short Cu(+1)-Cu(+1) distance (2.64 Å) and long Cu(+1.5)-Cu(+1.5) distance (2.93 Å) significantly increased the reorganization energy of electron transfer which was much higher

compared to the reorganization energy observed in water-soluble Cu_A domain of *Thermus thermophilus* cytochrome ba_3.[1337]

4.6. Features controlling redox chemistry of the cupredoxins

4.6.1. Role of ligands

As the immediate residues that coordinate to the copper centers, the ligands exert huge influence on the redox properties of cupredoxins. The strong Cu-thiolate bond(s) play the dominant role in defining T1Cu and Cu_A centers in both their electronic structures and ET functions. Except for a few unnatural amino acids, mutation of Cys will change T1 copper character. The same happens in Cu_A center that mutation of Cys to Ser will result in either T1 or T2 center.

The His residues are important for shielding the copper center from the solvent and for directing electron transfer. C-terminal His is on a hydrophobic patch of T1 copper proteins. The hydrophobic patch directly interacts with redox partners of T1 copper proteins. Mutation of either His to Gly creates an open binding site, where external ligands could coordinate with copper and influence properties of T1 copper proteins. Due to the open binding site, the His to Gly mutant exhibited high reorganization energy and low electron transfer rate.

The Axial Met is less conserved in T1 copper proteins. Besides Met, native T1 copper proteins could have the more hydrophilic Gln or the more hydrophobic, non-coordinating Leu/Phe at the axial position. There is a general trend that proteins with Gln as their axial ligand have the lowest reduction potentials, proteins with Met have intermediate reduction potentials, while proteins with Leu/Phe have the highest potentials. The reduction potential tuning role of the axial ligand has been further confirmed by mutagenesis studies. The correlation between hydrophobicity of the axial ligand and reduction potential has been established by incorporation of a series of Met analogues. The role of the highly conserved axial methionine ligand was replaced by glutamate, aspartate, and leucine in the engineered Cu_AAz.[1374] In contrast to the same substitutions in the structurally related blue copper azurin, much smaller changes (~ 20 mV) in reduction potential were observed, indicating that the diamond core structure of

the Cu_A is much more resistant to variation in axial ligand interactions than the distorted tetrahedral structure of the blue copper protein.

4.6.2. Role of protein environment

The first coordination sphere directly affects spectroscopic properties and electron transfer of T1 copper protein. Beyond the first coordination sphere, the protein scaffold holds copper ligands together and forces trigonal geometry regardless of the oxidation state of copper, as suggested by the “rack mechanism”[1168] or the entatic state.[1170] Furthermore, the environment around the primary coordination sphere can fine-tune the electronic structure and redox properties of the copper centers by non-covalent interactions such as a hydrogen bonding network to the copper ligands.[94,1119,1430] Through manipulating hydrogen bonding networks in the secondary coordination sphere, Marshall et al. managed to tune the reduction potential of azurin over the natural range while maintaining T1 character in the copper center.[1088] The same mutations that affected the non-covalent interactions in azurin were introduced to tune the reduction potentials of engineered Cu_AAz.[1385] The effects of these mutations were in the same direction but with smaller magnitude in the Cu_A site due to dissipation of the effects by two copper ions rather than the single copper ion in blue copper proteins.

All these findings are important in understanding the different roles of the two cupredoxins. Since blue copper proteins are used in a wide range of electron transfer processes, the reduction potentials of the blue copper proteins need to be tuned to fit a wide range. Such a tuning is mainly achieved by changing the axial ligands and hydrogen-bonding network in the secondary coordination sphere.[95,1088] However, the Cu_A sites are only found in terminal electron acceptors with very small potential differences between redox partners where a wide range of reduction potentials is not preferred. The diamond core structure of Cu_A sites decreases the reorganization energies and enables fast electron transfer processes.

4.6.3 Blue type 1 copper sites vs. purple Cu_A sites

The type 1 blue copper sites are widely found as electron transfer centers common in many biological systems. However, the Cu_A sites are only found in cytochrome *c* oxidases (C*c*Os), nitrous oxide reductases (N_2ORs), and the oxidase from *Sulfolobus acidocaldarius* (SoxH). Several key questions that have been raised regarding these sites are concerned with how such a mixed valence binuclear copper site was selected, what is the advantage of such a site compared to type 1 blue copper sites, and why the Cu_A sites are only found in terminal electron acceptors. To answer these questions, a direct comparison of the electron transfer rates of these two centers is required. The engineered Cu_A site in azurin provides a great opportunity to eliminate the protein structure contribution to the electron transfer process since the electron transfer rates are measured in the same azurin scaffold.[1388] Cu_A azurin demonstrated that Cu_A is a more efficient electron transfer site even with a smaller driving force between the reduced disulfide and Cu_A site than between the reduced disulfide and blue copper site. The calculated reorganization energy of Cu_A site is only half that of the blue copper site which is due to the rigid structure of diamond core in Cu_A site. Both C*c*Os and N_2ORs are large enzymes that contain multiple electron transfer sites. As the electrons transfer along the chain, the difference in reduction potentials as the driving force must fall within a narrow range of values. In this case, the electron transfer sites with lower reorganization energy would be preferred such that the driving force might be small.

5. Enzymes Employing a Combination of Different Types of Electron Transfer Cofactors

5.1. Enzymes Using Both Heme and Cu as Electron Transfer Sites

5.1.1. Cytochrome *c* and Cu_A as Redox Partners to Cytochrome c Oxidases (C*c*Os).

Cytochrome *c* oxidase (C*c*O) is a terminal protein complex in the respiratory electron transport chain located in the bacterial or mitochondrial membranes. This large

protein complex receives four electrons from four molecules of cyt *c,* one each, that are used to efficiently reduce molecular oxygen to water with the help of four protons from the aqueous phase without producing any reactive oxygen species. In addition, it translocates four protons across the membrane, which establishes an electrochemical potential gradient used for ATP synthesis.

Out of many different types of C*c*Os from various different organisms the families involved in aerobic respiration that generally use cyt *c* as their biological electron donors are *caa*$_3$*, aa*$_3$*, cbb*$_3$*, ba*$_3$*, co, bb*$_3$*, cao,* and *bd* oxidases.[1431] Cyts *caa*$_3$ *and cbb*$_3$ oxidases contain a distinct cyt *c* domain integrated into the cyt *c* oxidase enzyme complex. Cyt *aa*$_3$ oxidase is the mitochondrial counterpart of cyt *caa*$_3$ except that it does not contain the cyt *c* domain at the C-terminal end of the subunit II (Cox2) of the enzyme complex. Subunit II also contains the binuclear Cu_A center. Cyt *cbb*$_3$ oxidases do not contain the Cu_A center, but they contain both a monocytochrome *c* subunit (FixO or CcoO) and a di-cytochrome *c* subunit (FixP or CcoP).[79,1432] Many facultative anaerobes use *bo* and *bo*$_3$ oxidases which use quinol as the substrate instead of cyts *c*. Depending on the organism, the cyts *c* are associated to the enzyme complex either by covalent or non-covalent interactions.[1433] For example, in the bacterium PS_3, cyt *c* binds covalently to the protein complex at the C-terminal end of subunit II.[1434-1438] In *P. denitrificans*, the cyt *c* subunit is tightly bound to the oxidase subunit by covalent interactions and can be removed by treatment of high concentration of detergent. In eukaryotes, cyts *c* bind to the cyt *c* oxidase loosely which can be removed at high salt concentrations. Mammalian cyts *c* oxidases have been shown to bind one molecule of cyt *c* at a high affinity site, which serves as the electron entry point.[1439-1441] There is evidence of the presence of a second low affinity site, but the role of such secondary interactions between cyt *c* and the oxidase is not well known. It has been shown that Cyts *c* use a series of several (6-7) positively charged lysines near the heme edge which form complimentary electrostatic interactions with negatively charged carboxylates on the high affinity site of subunit II of the oxidase. Such electrostatic interactions are important for placing the substrate in the correct orientation to bind to the oxidase complex.[1442,1443]

Available data suggest that electrons are transferred from reduced cyt *c,* one at a time, to the oxidized Cu_A.[1444,1445] Then internal electron transfer takes place from the

reduced Cu_A to the LS heme *a,* and to the binuclear active site consisting of HS heme a_3 and Cu_B where the dioxygen reduction takes place (Figure 65). The reaction requires the transfer of four electrons from four molecules of cyt *c* and four protons. It has been measured that the electron transfer rate constant from Cu_A to heme a is 20,400 s^{-1} and the rate of reverse process, from heme a to Cu_A, is 10,030 s^{-1} in *P. denitrificans* cytochrome c oxidase by pulse radiolysis.[1340] Similar study is also applied to cytochrome ba_3 from *T. thermophilus* and the first order rate constants are 11200 s^{-1} and 770 s^{-1} respectively.[1340] Electron transfer from cyt *c* to Cu_A and Cu_A to heme *a* is fast,[1445,1446] while the intermolecular electron transfer from the heme *a* to the heme a_3/Cu_B site is slow and has been proven to be the rate limiting step of the reaction.[1447,1448] It has also been shown that the presence of Cu_A is not required for the oxidase activity as the deletion of the Cu_A gene from beef heart cyt *c* oxidase slows down the electron transfer rate, but still maintains some oxidase activity.[1449,1450]

Binding of cyt *c* to the oxidase causes conformational changes in the both the protein partners.[1451,1452] The major changes are observed upon reduction of the Cu_A and heme *a* centers. It has been proposed that the reduction of these two redox centers causes a conformational change of the binuclear active site from closed to open state that facilitates the intramolecular electron transfer that couples the subsequent redox reaction and proton translocation.[1453-1456] Nuclear resonance vibrational spectroscopy (NRVS) on cyt c_{552} from *Hydrogenobacter thermophilus* have indicated that the presence of strong vibrational dynamic coupling between the heme and the conserved -Cys-Xxx-Xxx-Cys-His- motif of the polypeptide chain.[1457] Such vibrational coupling has been proposed to lower the energy barrier for electron transfer by either transferring the vibration energy released upon protein-protein complex formation or by modulating heme vibrations.

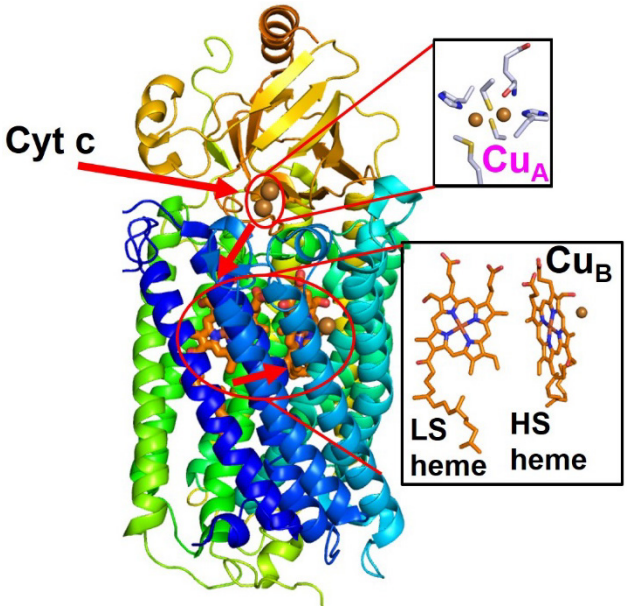

Figure 65. Cyt c oxidase from P. denitrificans (PDB ID 3HB3). Electron transfer pathway is shown as arrows.

A recent NMR study has shown that the hydrophobic residues near the heme of cyt *c* form hydrophobic interactions with cyt *c* oxidase, and are major contributor to the complex formation, while the charged residues near the hydrophobic core dictate the alignment and orientation of cyt *c* with the enzyme to ensure efficient electron transfer.[1458] The affinity of oxidized cyt *c* for complex formation with C*c*O is significantly lower, suggesting that electron transfer is gated by the dissociation of oxidized cyt *c* from C*c*O. The rate of dissociation of oxidized cyt *c* is dictated by the affinity of oxidized cyt *c* for C*c*O that provides facile electron transfer.

5.1.2. Cu_A and Heme b as Redox Partners to Nitric Oxide Reductases (NORs)

Although the NORs Gram-negative bacteria use cyt *c* as the biological electron donor to the heme *c*, one NOR (qCu_ANOR) purified from the Gram-positive bacterium *Bacillus azotoformans* shows the presence of a quinol binding site and uses the binuclear Cu_A site as electron acceptor instead of heme *c*.[1332,1333] This family of NOR uses melaquinol as the physiological electron donor to the Cu_A site instead of cyt *c*. Electrons are passed

from melaquinol to the CuA site which are then transferred to the LS heme *b* and onto the binuclear active site consisting of a HS heme b_3 and a non-heme Fe_B site.

5.1.3. Cytochrome c and Cu_A as Redox Partners to Nitrous Oxide Reductases (N_2ORs)

Nitrous oxide reductase (N_2ORs) is the last enzyme in the denitrification pathway which reduces nitric oxide to dinitrogen.[1329,1330,1459] N_2ORs are homodimeric periplasmic enzymes containing the binuclear electron transfer site Cu_A which receives electrons from cyt *c*, and a tetranuclear catalytic site Cu_Z. A unique N_2OR has been reported from *Wolinella succinogenes* which has a C-terminal cytochrome *c* domain that is suggested to be the biological electron donor to the Cu_A center.[1460]

5.2. Enzymes Using Both Heme and Iron-Sulfur Clusters as Electron Transfer Sites

5.2.1. As Redox Partner to the Cytochrome bc_1 Complex.

The coenzyme Q-cytochrome *c* oxidoreductase also called the cytochrome bc_1 complex or complex III is the third complex in the electron transport chain playing a crucial role in oxidative phosphorylation or ATP generation. The bc_1 complex is a multi-subunit trans-membrane protein complex located at the mitochondrial and bacterial inner membrane that catalyze the oxidation of ubihydroquinone and the reduction of cyt *c*[1461] coupled to the proton translocation from the matrix to the cytosol. The catalytic core of the bc_1 complex consists of three respiratory subunits: 1) subunit cyt *b* that contains two *b*-type hemes, b_L and b_H, 2) subunit cyt *c,* containing a heme c_1, and 3) iron-sulfur protein subunit containing a Rieske-type 2Fe-2S cluster (Figure 66). While in some α proteobacteria like *Paracoccus*, *Rhodospirillum rubrum*, and *Rb. capsulatus*, this enzymatic core containing the three subunits is catalytically active, several additional (7-8) subunits are present in the mitochondrial cytochromes bc_1 complexes.[86,1462]

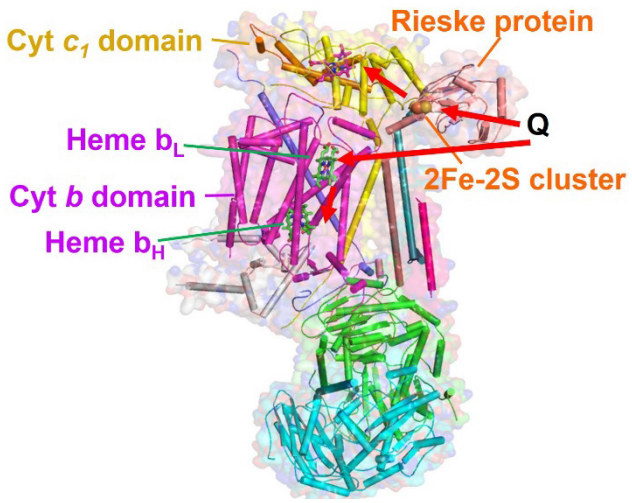

Figure 66. Bovine cytochrome bc_1 complex (PDB ID 1BE3). Different electron transfer domains and their cofactors are shown. b_L = low potential heme, b_H = high potential heme. Q = ubiquinol. Electron transfer pathways in both the enzymes are shown as arrows.

Structures of the bc_1 complex from various resources such as yeast, chicken,[1029] rabbit,[1029] and cow[1026,1029,1463] show that the cyt *b* subunit consist of eight transmembrane helices designated as A-H. The hemes b_L and b_H, are contained in a four-helix bundle formed by helices A-D and are separated by a distance of 8.2 Å. The axial ligands for both hemes are all His and are located in helices B and D. His83, His182 are bound to heme b_L while His97, and His196 are axial ligands for heme b_H. The cyt *c* subunit containing cyt c_1 is anchored to the membrane by a cytoplasmic domain and belong to the Ambler's type I cyt *c* based on the protein fold and the presence of the signature sequence -Cys-Xxx-Xxx-Cys-His-. Electron transfer has been proposed to occur through the exposed "front" face of the corner of the pyrrole II ring.[1029] One of the His residues that act as a ligand to the 2Fe-2S cluster is 4.0 Å from an oxygen atom of the heme propionate-6 and 8.2 Å from the C3D atom of the heme edge of cyt c_1. Such proximity of the heme group and the Rieske-type cluster has been proposed to facilitate electron transfer. Using this distance of 8.2 Å, a rough estimation of the electron transfer rate from the iron–sulfur protein to cyt c_1 has been calculated to be 4.8–80x 10^6 s^{-1}.

Based on the relative orientations of the prosthetic groups as discussed above, an electron transfer pathway has been proposed where in round I an electron is

transferred from a bound ubiquinol to the Rieske-type cluster into the cyt c_1 via its heme propionate-6 and out of cyt c_1 via its pyrrole II heme edge to the cyt *c* (not the same as cyt c_1).[78,1029] At the same time the low potential heme (b_L) pulls off an electron from the ubiquinol and transfers it to the high potential heme (b_H) which is ultimately picked up by an oxidized ubiquinone. The same cycle is repeated in round II.

Mitochondrial cyt *c* or bacterial cyt c_2 connect the bc_1 complex with photosynthetic reaction center or cyt *c* oxidase.[80,1464] The mode of interaction between cyt *c* (or c_2) with its redox partners has been proposed to involve docking of cyt *c* with its solvent exposed heme edge (called the "front" side). There are multiple dynamic hydrogen-bonding and salt bridge interactions between the cyt *c* and cyt c_1 of the bc_1 complex.[1465] The "front" side is composed of a ring of positively charged Lys residues near the exposed heme edge. The opposite side, called the "back" side is composed of several negatively charged residues. This charge separation creates a dipole moment in both bacterial cyts c_2 and mitochondrial cyt *c*.[1466,1467] The positively charged "front" side forms complimentary interactions with the negatively charged surface of its partner, which orients the electron donor in proper alignment for facile electron transfer. EPR experiments with cyt c_2 from *Rb. capsulatus* have demonstrated that the dipolar nature of cyt c_2 influences its orientations, which facilitate electron, transfer to its partner under physiological conditions.[1468-1470]

Rieske protein can accommodate three conformations in the complex: c1 position in which the His ligand is H-bonded to propionate of heme in cyt c and fast electron transfer (60000 S^{-1}) [1471] between the two will occur. [1026] At this state the cluster is far from quinone binding site. B position allows interaction between cluster and quinone. This position was stabilized by interaction of H161 with inhibitor stigmatellin that mimics H-bond pattern of semiquinone. [223,1029] And an intermediate state in which Rieske protein cannot interact with either of cytochrome or quinone. [865]

The cycle starts from an intermediate state. Upon binding of reduced hydroquinone, the Rieske protein will move to state b and an electron will be transferred to hydroquinone generating a semiquinone, which binds tightly to Rieske protein. This tight interaction will get loose by transfer of second electron from semiquinone to heme

b_L and generation of quinone. The thermodynamically disfavored reduction of heme b_L by semiquinone is coupled to favorable oxidation of hydroquinone by Rieske center. As a result reduction potential of Rieske center is of significant importance in rate of reduction of heme b_L. Reduction of Rieske and heme b_L happens within a half-life of 250 μs as evident by freeze quench EPR. Semiquinone intermediate has a very high affinity to Rieske protein. This tight binding will increase the reduction potential of Rieske center by 250 mV. This binding mode and increased reduction potential will assure that Rieske center will not reduce cyt *c* before heme b_L is reduced and quinone is formed. The reduced Rieske will then move to its c_1 state and transfer an electron to cyt *c*. After complete transfer of both electrons, the Rieske protein will go back to its intermediate state for the second cycle (Figure 67). [787,865] The binding of quinone and Rieske protein is redox-dependent. While the kinetic of electron transfer to cyt *c* is pH dependent due to pH dependence of reduction potential, it has been proposed that the rate limiting step in this reaction is mostly the state transition and not the electron transfer, considering the same rate observed in mutants with different reduction potentials. [1078]

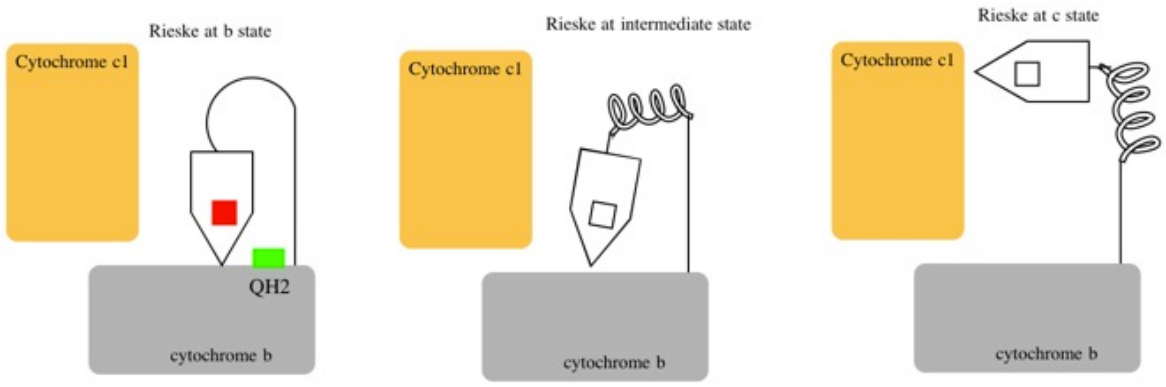

Figure 67. **Schematic cycle of Rieske positions in bc_1 complex.** Reprinted with permission from ref [865]. Copyright 2013 American Chemical Society.

Although the mechanism of proton transfer is not very well understood in this system, evidence suggested that the two protons are bound to the Rieske center, one to each His in reduced state. The oxidized state can have no, one, or two protons

depending on the pH. It has been shown that removal or mutation of Rieske cluster will result in a proton permeable *bc*$_1$ complex, suggesting a role as a proton-gate for Rieske protein. [1472] NMR was used to calculate pK_a of His ligands in *Thermus thermophilus* Rieske protein. In this study, a residue-selective labeling was used to unambiguously assign the NMR shifts. The results were consistent with other pH dependent studies of Rieske proteins, showing that one of the water exposed His ligands that is close to quinone, undergoes large redox dependent ionization changes. Their system also support proton coupled electron transfer in Rieske-quinone system. Analysis of driving forces using a Marcus-Bronsted method in mutants that had distorted H-bonding due to mutation of either conserved Ser or Tyr resulted in proposing a proton-first-then-electron mechanism in which the electron transfer follows the transfer of a proton between hydroquinone and imidazole ligand of Rieske cluster. [814]

5.2.2. As Redox Partner to Cytochrome *b*$_6$*f Complex*

Cyt *b*$_6$*f* (plastoquinol-plastocyanin or cyt *c*$_6$ oxidoreductase) is a protein complex belonging to a 'Rieske-cytochrome *b'* family of energy transducing protein complexes found in the thylakoid membrane in the chloroplasts of green algae, cyanobacteria, and plants, and catalyze electron transfer from plastoquinol to plastocyanin or cyt *c*$_6$ (PSII to PSI) coupled with the proton translocation across the membrane for ATP generation.[282,1473-1476] It is located in between the Photosystem II (PSII) and Photosystem I (PSI) reaction centers in oxygenic photosynthesis (Figure 68). The *b*$_6$*f*

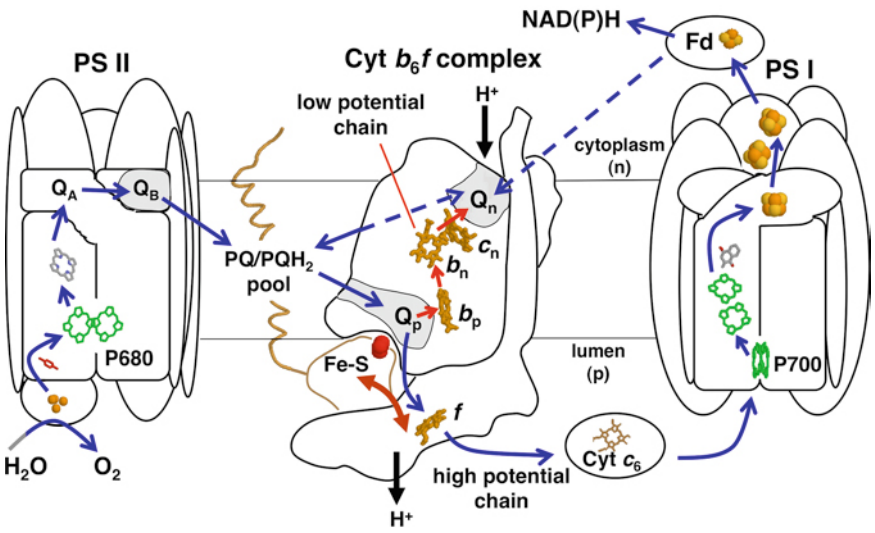

Figure 68. Cyt b_6f complex in photosynthetic electron transport chain. P680 = reaction center chlorophylls of PS II; QA, QB = quinones of PS II; PQ/PQH2 pool = plastoquinone/plastoquinol pool; Fe–S = Rieske cluster; f = cyt *f* of the high potential chains (blue arrows); Qp, Qn = plastoquinol-oxidation and plastoquinone-reduction sites; bp, bn, cn = hemes of the low-potential chain (red arrows); Fd = ferredoxin; P700 = reaction center chlorophylls of PS I. The domain movement of the Rieske protein is shown by two-sided arrow. The direction of proton translocation across the membrane is shown by proton arrows. The electronegative (cytoplasmic) (n) and electropositive (luminal) (p) sides of the membrane are labeled and electron transfer pathways are shown by arrows. A possible direct electron transfer path from PS I to the cyt b_6f complex is shown as the dashed line from Fd to the Qn-site. Reprinted with kind permission from Springer Science+Business Media (ref[1477]).

complex is analogous to the bc_1 complex of the mitochondrial electron transport chain. The b_6f complex comprises of seven subunits: a cyt b_6 with a low potential (b_p) and a high potential (b_n) heme, a cyt *f*, a Rieske iron sulfur protein, subunit IV, and three low-molecular-weight (~4 kDa) transmembrane subunits.[1473] There are a total of seven prosthetic groups that are found in the b6f complex: cyt *f*, hemes b_n, b_p, Rieske Fe2-S2 cluster, chlorophyll *a*, β-carotene, and a *c*-type heme designated as c_n or c_x or c_i. This heme, located close to the quinone-reductase site near the electronegative side of the membrane is linked to the protein via a single thioether linkage and lacks any axial ligands and has been shown to be critical for function of the b_6f complex.[225,1478-1481] The cyt b_6 subunit contains two bis-His ligated hemes, a high potential heme (–45 mV) on the luminal side and a low potential heme (–150 mV) on the stromal side of the thylakoid membrane. EPR and Mössbauer data reveal that both hemes are 6cLS and

have the His planes that are perpendicular. Cyt b_6 and subunit IV of b_6f complex are structurally similar to cyt *c* of the bc_1 complex,[184] while there is no structural similarity between cyt *f* and cyt c_1 even though they are functionally similar.[123,1029] Cyt b_6f complex takes part in linear electron flow between PSII and PSI where it links the plastoquinone pool of PSII to plastocyanin or cyt c_6 to PSI as well as in cyclic electron flow within PSI (Figure 68). The linear electron flow path involves oxidation of quinol to quinone from PSII to PSI coupled to the generation of ATP and reduced ferredoxin (Fd), which reduces $NADP^+$ to NADPH via an oxidoreductase FNR. Cyclic electron flow in PSI involves the electron flow via the b_6f back to the P700 reaction center of PSI. In both the cases two electrons are passed from plastoquinol at the quinol oxidation site (Q_P) near the lumenal, electropositive site of the membrane to the one-electron acceptor plastocyanin which are coupled to the "Q-cycle"[1482,1483] involving proton translocation across the membrane. One of the electrons from plastoquinol is transferred to PSI via the high potential chain while the second electron is passed onto the low potential, transmembrane chain on the electronegative side of the membrane where plastoquinone reduction takes place.

On the His ligation side of the heme, a chain of conserved five water molecules oriented in an L shape manner, have been identified from X-ray structure, which form hydrogen bonds with ten amino acid residues from the protein, seven of which are conserved.[1473,1484,1485] These water molecules have been proposed to act as "proton wires" in coupling of the electron transfer with proton transfer across the membrane.[1485,1486] The heme of cyt *f* is located in a hydrophobic environment and is protected from the solvent by Tyr1, Pro2, Ile3, and Phe4 (or Trp4 in cyanobacteria).[161] The side of chain of residue 4 is located close to the heme edge and oriented almost perpendicular to the heme plane (Figure 69).[1485] This edge-to-face interaction of the Trp4 and the heme has been proposed to be responsible for tuning the reduction potential of the heme by interaction with the porphyrin π molecular orbitals. Such edge-to-face interactions have been observed in cyt b_5 (Phe58, Phe35),[141,366] cyt b_{562} (Phe61),[382] and peptide-sandwich mesoheme model systems reported by Benson and co-workers (Trp or Phe).[423,1487] In these peptide mesoheme sandwich complexes the heme-Trp

interaction has been shown to be important to stabilize the α-helical scaffold as well as the ferric state of the heme iron.[1488] Such interactions also stabilize the ferric state of the heme iron in the cyanobacterium cyt *f*.

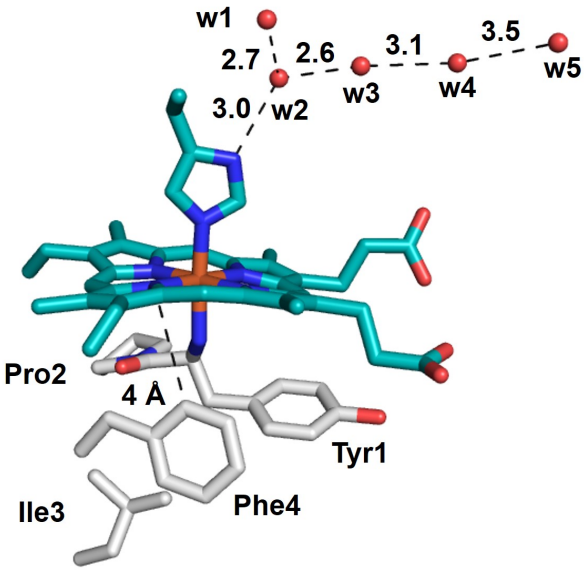

Figure 69. Environment around the heme of cyt *f* (PDB ID 1HCZ). Hydrophobic residues are shown as gray sticks. The 'edge-to-face' interaction at 4Å between Phe4 and the heme that is proposed to be important to tune the reduction potential of the heme iron is shown. The five conserved molecules that have been proposed to act as "proton wires" that couple electron transfer with proton transfer are shown as red spheres. Residue numbering of waters is arbitrary.

The chloroplast Rieske proteins work in the same way. It has been shown that the movement of these Rieske proteins will also function as a redox state sensor that can balance the light capacity of the two photosystems. This state transition can also act as a switch between cyclic and linear electron flow.[1489]

5.2.3. As Redox Centers in Formate Dehydrogenases

Formate dehydrogenases (Fdh) catalyze decomposition of formate to CO_2. It exists in both prokaryotes and eukaryotes. Fdhs are mainly NAD^+-dependent in aerobic organisms, and NAD^+-independent in anaerobic prokaryotes, donating electrons from formate to terminal electron acceptor other than O_2.[1490] Structural studies reveal that Fdhs contain one to three subunits with either W or Mo in the active site.[1491-1493]

Fdh-N from *E. coli* is among the most well studied Fdhs. It is important in the nitrate respiratory pathway under anaerobic conditions. It is a membrane bound trimer ($\alpha_3\beta_3\gamma_3$) with molecular weight of 510 kDa. It harbors a Mo-*bis*-MGD cofactor and a [4Fe-4S] cluster in the catalytic α subunit, four [4Fe-4S] clusters in β subunit, and two heme *b* groups in γ subunit (Figure 70).[1492] The β subunit transfers electrons between α and γ subunits, similar to other membrane-bound oxidoreductases that bind four [4Fe-4S] clusters, such as nitrate reductases, [NiFe]-hydrogenases, DMSO reductase and thiosulfate reductase.[1494]

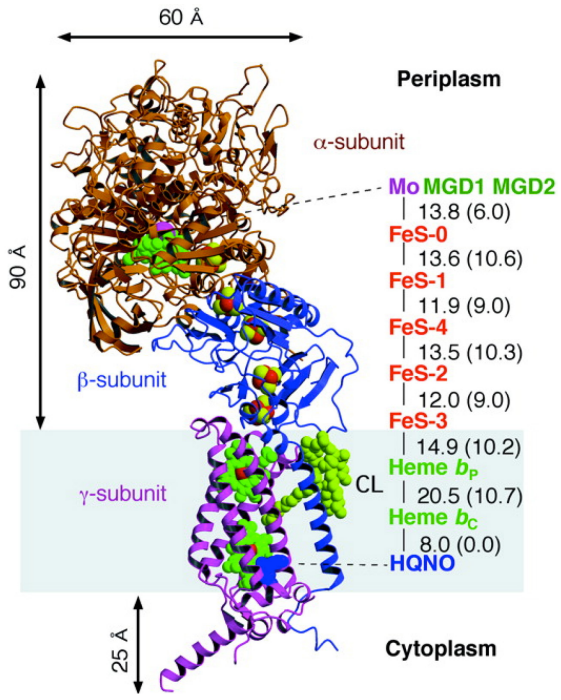

Figure 70. Overall structure of Fdh-N from E. coli. Cofactors are displayed as spheres and denoted accordingly on the right. Putative membrane is shown as gray shade. PDB code: 1KQF. From ref [1492]. Reprinted with permission from AAAS.

Fdh from *D. desulfuricans* is an αβγ protein with a molecular weight of ~150 kDa. It contains four different types of redox centers including four heme *c* centers, two [4Fe-4S] clusters, and a molybdopterin.[1495] EPR studies showed the existence of two types of Fe-S clusters after reduction, *i.e.* center I with g value of 2.050, 1.947 and 1.896, and

center II with g value of 2.071, 1.926 and 1.865. Midpoint reduction potentials of the two Fe-S clusters are -350 ± 5 mV for center I, and -335 ± 5 mV for center II.

Fdh from *D. gigas* is an αβ protein[1493] containing tungsten instead of molybdenum. It also possesses two [4Fe-4S] clusters similar to Fdh from *D. desulfuricans*.[981,1496]

5.2.4. As Redox Centers in Nitrate Reductase

Nitrate reductases (NARs) reduce nitrate to nitrile, a vital component in the nitrogen respiratory cycle. Most NARs isolated so far contains three subunits NarG (112-140 kDa), NarH (52-64 kDa), and NarI (19-25 kDa). NarG harbors a Mo-*bis*-MGD cofactor, and a [4Fe-4S] cluster, NarH contains one [3Fe-4S] cluster and three [4Fe-4S] clusters, and NarI immersed in membrane binds two *b* type hemes (Figure 71).[1497-1502] The overall folding and cofactor positions are strongly homologous to formate dehydrogenase (Fdh) from *E. coli*.[1503] The eight redox centers are separated by 12 to 15 Å from each other, and form an electron transfer pathway about 90 Å long. NAR from *Cupriavidus necator* does not contain the NarH domain, and harbors two *c* type heme in the small subunit.[1504]

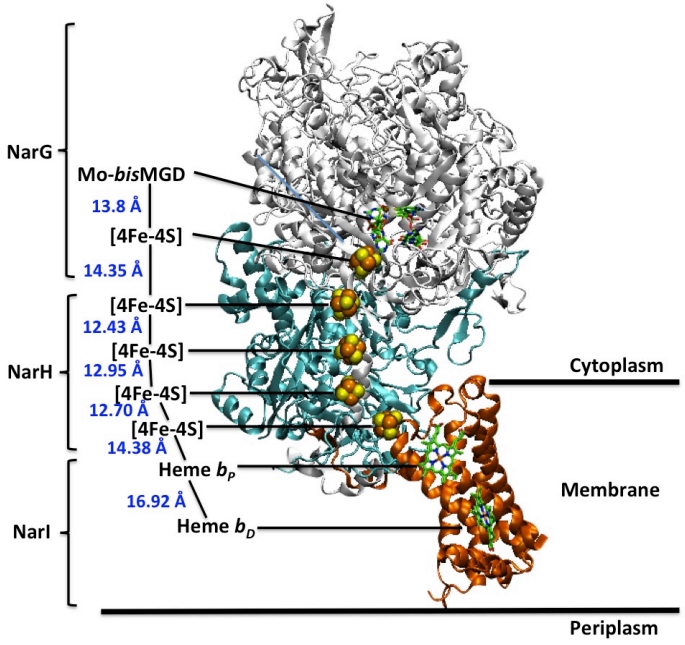

Figure 71. Overall three-dimensional structure of NarGHI from E. col K12. PDB code: 1Q16. Subunit and cofactor names are denoted. Reprinted with permission from ref [1505]. Copyright 2006 Elsevier.

6. Summary and Outlook

This review summarizes three important classes of redox centers involved in ET processes. Although each class spans a wide range of reduction potentials, none of them can cover the whole range needed for biological processes. Together, however, they can cover the whole range, with cytochromes in the middle, Fe-S centers toward the lower end while the cupredoxins toward the higher end (**Figure 1**). All three redox centers have structural features that make them unique and yet they also show many similarities that make them excellent choices for ET processes.

For cytochromes, because the redox active iron is fixed into a rigid porphyrin that accounts for four of the iron's six coordination sites, most of its electronic structure and redox properties remain similar between different cytochromes. In completing the primary coordination sphere of the iron, cytochromes typically use a combination of nitrogen and sulfur ligation from histidine or methionine side chains, respectively; terminal amine ligation has also been observed. In general, mutagenesis studies reveal that methionine ligation raises the reduction potential 100-200 mV, relative to histidine ligation, primarily due to the lower affinity of thioester to the higher oxidation state of the heme, and that the effect is generally additive.[192,386,461-463,465] Heme puckering or flexing has been demonstrated to tune the reduction potentials by up to 200 mV.[513] Changes in the heme type between b- and c- would be expected to change the electronic properties of the heme; however, the effect on reduction potential is small and varies depending on the systems studied.[446,448] It is clear, on the other hand, that the electron-withdrawing formyl group on heme *a* appears to be responsible for the increase the reduction potential by ~160 mV.[459,460]

For iron-sulfur proteins, the reduction potentials ranges are influenced to some extent by the number of irons because it affects the redox states and transitions. In case of clusters with the same number of irons, the higher the redox pair, the higher the reduction potentials (e.g., HiPIPs have $[4Fe\text{-}4S]^{2+/3+}$ pair while ferredoxins have [4Fe-

4S]$^{1+/2+}$ pair).[719] In addition, the cluster geometry such as torsional angles between Fe-S*γ*-C*α*-C*β*; Fe-Fe distance, covalency of Fe-S bonds also play important roles in some proteins.[618,901,1085,1506] Electron delocalization of the cluster and net charge of the cluster is also important. For example, it has been shown that the net charge of the protein is the main factor determining the reduction potential within HiPIPs. Electrostatic effects of the charged residues in the secondary coordination sphere can influence the solvent accessibility and consequently dielectric constant around the metal center. However, the effects are usually complicated, and difficult to rationalize by just Coulomb's law. For example, in rubredoxin from *C. pasteurianum*, replacement of neutral surface residue by positively charged Arg or negatively charged Asp has lead to increase of reduction potentials in both cases.[611,612] Finally, the direct ligands to iron and H-bonding interactions with the direct ligands make significant contributions to the reduction potential.[541] When the common Cys thiolate ligand was replaced with His imidazole ligand, naturally in the Rieske proteins, or with Ser by site-directed mutagenesis, the reduction potentials changed accordingly.[721,893,1087] The multiple NH…S H-bonding interactions in rubredoxin can contribute to a decrease of the reduction potential of the [FeCys$_4$] center to -100 to +50 mV, while E^o of corresponding model complexes without the H-bonding networks is around 1 V.[92,588-590] NH…S H-bonds have also been shown to be important in determining reduction potentials between different ferredoxins as well as ferredoxins vs. HiPIPs.[617,618,718,719]

For cupredoxins, the metal centers cannot be easily fixed by either porphyrin or thermodynamically stable iron-sulfur clusters, proteins play a more prominent role in enforcing the unique trigonal geometry and strong copper-thiolate bond in order to maintain a low reorganization energy for the ET function. In this class of proteins, both the geometry and the ligands, particularly the strictly conserved Cys, play a dominant role in controlling the redox properties. In T1 copper protein azurin, changing axial Met to a stronger cysteine or homocysteine induced geometry change and weakened Cu-S bond. These in turn resulted in > 100 mV decrease in reduction potential.[1293] Deleting the hydrogen bonding to Cys, realized through the Phe114Pro mutation in azurin,

affected the covalency of Cu-S bond and lowered the reduction potential of azurin.[114,1088,1316]

Despite the differences in the primary coordination spheres, all three redox centers employ non-covalent secondary coordination interactions in fine-tuning the redox properties. The first common feature is the control the degree of solvent exposure; the deeper the redox centers are buried into the hydrophobic center of the protein, the higher the reduction potential and the less in changes of reorganization energy due to influences by solvent. For example, redox center burial is considered to be one of the main factors for differences in reduction potentials between different HiPIPs and ferredoxins.[618,719,749,752] Furthermore, a computational study of heme proteins over an 800 mV range has attributed the greatest correlation with reduction potential to solvent exposure.[457]

The second common feature is the electrostatic interactions. For example, the net charge of protein is shown to be the only factor that correlates with reduction potentials of different HiPIPs.[715,752,890] Number of amide dipoles and not necessarily the H-bonding is shown to be important in reduction potential determination in ferredoxins.[718,719] In myoglobin, the Val68, which was in the van der Waals interaction with the heme group, was replaced by Glu, Asp, and Asn. A 200 mV decrease in reduction potential was observed for the Glu and Asp mutants compared to the wild type.[481] This study demonstrated that replacement of hydrophobic Val68 by charged and polar residues led to substantial changes in reduction potential of the heme iron. In a number of different cytochromes, electrostatic polar and charged groups near the heme were shown to vary the potential by 100 to 200 mV.[169,479,481,482] For instance, in cyts c_6 and c_{6A}, the glutamine at positions 52 and 51, respectively, were shown to raise the potential ~100 mV,[479] and in cyt c, the Tyr48Lys mutation raised the potential 117 mV;[480] all these effects can be attributed to charge compensation in the heme pocket. Similarly, replacing Met121 with Glu or Asp in T1 copper azurin resulted in 100 and 20 mV decreases in reduction potentials, respectively.[1278,1289] Beyond copper ligands, mutating Met44 in azurin to Lys destabilizes Cu^{II}, causing a 40 mV increase of reduction potential.[1507]

The final common feature is the presence of hydrogen-bonding network around the ligands to the metal center, especially those to the ligand that dominates the metal-ligand interactions. For examples, the $NH_{amide}…S_{cys}$ H-bonds are known to be important in different reduction potentials between rubredoxins, HiPIPs and ferredoxins.[617,618,718,719] They are also shown to play a role in different reduction potentials of different ferredoxins. Other than backbone amide H-bonds, H-bonds from side chains are also important. A good example of such is H-bonds from conserved Ser and Tyr in Rieske proteins and lack of thereof in Rieske-type proteins, hence differences in reduction potential.[781] In cytochromes, hydrogen bonding interactions with the axial ligands can tune the potential by up to 100 mV.[474,476,477,1508] For instance, increasing the imidazolate character of the axial His ligand in cyt c by strengthening H-bonding from the $H\text{-}N_{\varepsilon}$, increased the potential by nearly 100 mV,[474] and disrupting the hydrogen bond donation from Tyr67 to the axial Met resulted in a 56 mV decrease in potential.[476,1508] Similarly, the hydrogen bonding interactions to the Cys in cupredoxins is known be responsible for their reduction potential differences.[114]

A test of how much we understand these structural features responsible for the redox properties is to start with a native redox center and use the above knowledge to fine-tune the redox properties. A pioneering work in this area is the demonstration of a ~200 mV decrease in reduction potential of myoglobin when a buried ionizable amino acid (Glu) was introduced into the distal pocket of the protein and such a change has been attributed to electrostatic interactions.[481] Since then, not many examples have shown similar magnitude changes of reduction potentials by electrostatic interactions, perhaps due to compensation effect by ions in the buffer or other ionizable residues nearby. Instead, hydrophobicity and hydrogen bonding network has been shown to play increasing roles, and a combination of these effects has been shpwn to fine-tune the reduction potentials of T1 copper azurins by more than 700 mV, beyond its natural range.[1088] These features were further shown to be additive, making reduction potential tuning predictable. Such rational design also allowed the lowering of the reorganization energy of azurin, which is already known to be very low in comparison to other redox centers. With more such successful examples in other systems, we will be able to

achieve deeper understanding of ET reactivity in proteins and facilitate *de novo* design of ET centers for applications such as advanced energy conversions.

AUTHOR INFORMATION

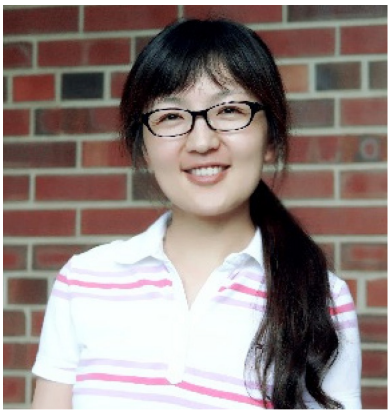

Corresponding Author

*E-mail yi-lu@illinois.edu; phone 217-333-2619; fax 217-244-3186.

‖ These authors contributed equally to this review

Notes

The authors declare no competing financial interest.

Biographies

Jing Liu was born in Inner Mongolia, China. She obtained her BA degree in chemistry from Nankai University (China) in 2003. Then she moved to Peking University (China), and worked under the guidance of Prof. Zhen Yang and Prof. Jiahua Chen, focusing on mechanistic and kinetic investigation of sulfur-contained ligands in palladium catalysis. During graduate studies, she also worked with Prof. Todd B. Marder in Durham University (UK) and Prof. Aiwen Lei in Wuhan University (China). She completed her Ph.D in 2008. Afterwards, she joined Prof. Yi Lu's group as a postdoctoral researcher in University of Illinois at Urbana Champaign. Her current research focuses on engineering artificial nonheme iron enzymes, and developing biocatalysts.

Saumen Chakraborty. Saumen Chakraborty did his B.Sc. in Chemistry (Hons.) from the University of Calcutta in 2004, and M.Sc. in Chemistry from Indian Institute of Technology, Madras in 2006. He came to the University of Michigan in 2006 for graduate research and joined Prof. Vincent Pecoraro's group working in the area of *de novo* metalloprotein design using three-stranded coiled coils and three-helix bundles with emphasis on

creation of novel metal coordination sites, understanding how to control and fine tune metal ion properties within a protein matrix, and determining ligand and metal exchange dynamics. After completing his Ph.D. in 2011 he joined Prof. Yi Lu's group at the University of Illinois at Urbana-Champaign as a postdoctoral researcher. His current research interests include biosynthetic metalloprotein design, preparation of protein-based structural and functional analogues of various enzymes, biochemical mechanisms, non-heme iron centers, and cobalt metalloproteins. He enjoys traveling and photography.

Parisa Hosseinzadeh was born in Neyshabour, Iran. She received her B.Sc degree in Biotechnology from University of Tehran in 2010. She is a PhD candidate in Biochemistry at University of Illinois at Urbana-Champaign. Her research in Dr. Yi Lu's lab focuses on rationally tuning protein features using secondary coordination sphere interactions and characterizing engineered proteins with several biochemical and bioinorganic techniques.

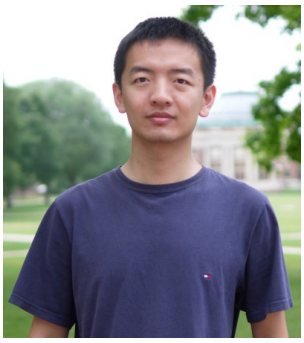

Yang Yu was born in Xinzhou, China. He received his B.S. in biology from Peking University in 2008. He is pursuing a PhD degree in biophysics and computational biology at University of Illinois at Urbana Champaign under the supervision of Dr. Yi Lu. His current research interests include using unnatural amino acids for metalloprotein engineering and x-ray absorption spectroscopy for metalloproteins.

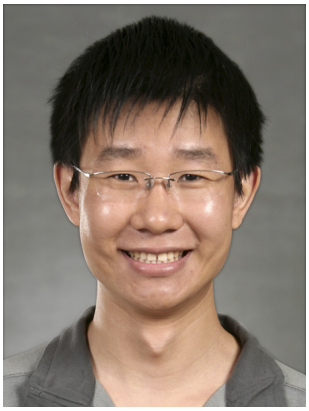

Shiliang Tian received his B.S. in Chemistry in 2005 from the School of Chemistry and Chemical Engineering, Nanjing University, China. He then joined Prof. Zhang-Jie Shi's lab at Peking University, working on the C-H activation using transition metals. After receiving the master degree in organic chemistry, he joined Prof. Yi Lu's lab at the University of Illinois at Urbana-Champaign in 2010. He is currently a Ph.D candidate, working on designing the metalloenzyme for biocatalysis, primarily focusing on copper proteins and non-heme iron proteins.

Igor Petrik was born in L'viv, Ukraine and grew up in Philadelphia, PA. From 2006 to 2009, he attended the University of the Sciences in Philadelphia, where he investigated the physicochemical properties of ionic liquids by NMR and MD techniques, under the mentorship of Prof. Guillermo Moyna. After graduating with a B.S. in Chemistry and a minor in Forensics, he began his PhD studies in Chemical Biology in the lab of Prof. Yi Lu at the University of Illinois at Urbana-Champaign. He is interested in rational design of metalloenzymes, and is focusing on understanding and improving activity of biosynthetic models of terminal oxidases.

Ambika Bhagi was born in Moradabad, India. She received her BSc from St. Stephen's College, Delhi in 2009, followed by a Masters degree in Chemistry from the Indian Institute of Technology, Delhi in 2011. She is currently a PhD candidate in Chemical Biology at the University of Illinois, Urbana-Champaign. Her research focuses on elucidating the role of the heme iron redox potential towards tuning oxygen reduction rates in terminal oxidases.

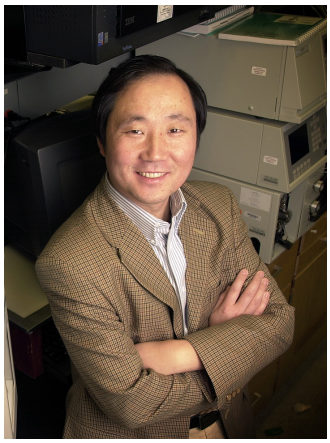

Yi Lu received his BS degree from Peking University in 1986, and a PhD degree from University of California at Los Angeles in 1992 under Professor Joan S. Valentine. After 2 years of postdoctoral research in Professor Harry B. Gray's group at the California Institute of Technology, Lu started his own independent career in the Department of Chemistry at the University of Illinois at Urbana Champaign in 1994. He is now a Jay and Ann Schenck Professor of Chemistry and a HHMI Professor in the Departments of Chemistry, Biochemistry, Bioengineering and Materials Science and Engineering. He is also a member of the Center for Biophysics and Computational Biology and Beckman Institute for Advanced Science and Technology. His research interests lie at the interface between chemistry and biology. His group is developing new chemical approaches to provide deeper insight into biological systems. At the same

time, they take advantage of recently developed biological tools to advance many areas in chemistry. Lu has received numerous research and teaching awards, including the Fellow of the American Association for the Advancement of Science (2007), Early Career Award, Society of Biological Inorganic Chemistry (2007), Howard Hughes Medical Institute Professor Award (2002), Camile Dreyfus Teacher-Scholar Award (1999), Alfred P. Sloan Research Fellowship (1998), Research Corporation Cottrell Scholars Award (1997), and the Beckman Young Investigators Award (1996).

ACKNOWLEDGMENTS

The research in the Lu group was supported by a grant from the National Science Foundation (CHE1058959) and the National Institute of Health (GM062211).

ABBREVIATIONS

ET:	Electron Transfer
Cyts:	Cytochromes
6cLS:	6-Coordinate Low Spin
HP Heme:	High Potential Heme
LP Heme:	Low Potential Heme
C*c*P:	Cytochrome *c* Peroxidase
NiR:	Nitrite Reductase
NR:	Nitrate Reductase
PQQ:	Pyrroloquinoline Quinone
PCMH:	P-Cresol Methylhydroxylase
PS:	Photosystem
RC:	Reaction Center
SHP:	Sphaeroides Heme Protein
HAO:	Hydroxylamine Oxidoreductase

PSM:	Peptide Sandwiched Mesoheme
TASP:	Template-Assisted Synthetic Protein
HiPIP:	High Potential Iron-sulfur Protein
DFT:	Density Functional Theory
CpRd:	Rubredoxin from mesophilic Clostridium pasteurianum
PoRd:	Rubredoxin from Pseudomonas oleovorans
RR:	Rubredoxin Reductase
ROS:	Reactive Oxygen Species
H-bond:	Hydrogen bond
LMCT:	Ligand to Metal Charge Transfer
FNR:	Ferredoxin:NADH Reductase
FTR:	Ferredoxin:Thioredoxin Reductase
Dfx:	Desulfoferredoxin
SOR:	Superoxide Reductase
Rr:	Rubrerythrin
FdI:	Ferredoxin I
Adx:	Adrenodoxin
SiR:	Sulfite Reductase
CpFd:	C. pasteurium Ferredoxin
CvFd:	C. vinosum Ferredoxin
PDLP:	Protein Dipole Langevine Dipoles
PLFP:	Plant Ferredoxin-like Proteins
NDO:	Naphthalene Dioxygenase
MO:	Molecular Orbitals
THC:	Tetraheme Cytochrome

PCET:	Proton-Coupled-Electron-Transfer
AOR:	Aldehyde Oxidoreductase
CODHs:	Carbon Monoxide Dehydrogenases
ACS/CODHs:	Acetyl-CoA Synthases/Carbon monoxide Dehydrogenase
HCP:	Hybrid Cluster Protein
CII:	Complex II in respiratory chain
T1 Cu:	Type 1 Cu
EPR:	Electron Paramagnetic Resonance
NMR:	Nuclear Magnetic Resonance
XAS:	X-ray Absorption Spectroscopy
EXAFS:	X-ray Absorption Fine Structure
rR	Resonance Raman Spectroscopy
MCO:	Multi Copper Oxidase
C*c*O:	Cytochrome *c* oxidase
N_2OR:	Nitrous Oxide Reductase
NOR:	Nitric Oxide Reductase

References

(1) Malkin, R.; Rabinowitz, J. C. *Annu. Rev. Biochem.* **1967**, *36*, 113.
(2) Adman, E. T. *Biochim. Biophys. Acta, Rev. Bioengerg.* **1979**, *549*, 107.
(3) Brunori, M.; Colosimo, A.; Silvestrini, M. C. *Pure Appl. Chem.* **1983**, *55*, 1049.
(4) Thomson, A. J. *Nachr. Chem., Tech. Lab.* **1984**, *32*, 326.
(5) Chiara, S., Maria; Brunori, M. *Life Chem. Rep.* **1987**, *5*, 155.
(6) Gil'manshin, R. I.; Lazarev, P. I. *Mater. Sci.* **1987**, *13*, 71.
(7) Armstrong, F. A.; Hill, H. A. O.; Walton, N. J. *Acc. Chem. Res.* **1988**, *21*, 407.
(8) Cusanovich, M. A.; Meyer, T. E. *Heme proteins*; Elsevier: Amsterdam, 1988; Vol. 7.
(9) McLendon, G. *Acc. Chem. Res.* **1988**, *21*, 160.
(10) Huber, R. *Prix Nobel* **1989**, 189.

(11) Meyer, T. E.; Cusanovich, M. A. *Biochim. Biophys. Acta, Bioenerg.* **1989**, *975*, 1.
(12) Gray, H. B.; Malmstroem, B. G. *Biochemistry* **1989**, *28*, 7499.
(13) Bowler, B. E.; Raphael, A. L.; Gray, H. B. *Prog. Inorg. Chem.* **1990**, *38*, 259.
(14) Malmstroem, B. G. *Biol. Met.* **1990**, *3*, 64.
(15) Blondin, G.; Girerd, J. J. *Chem. Rev.* **1990**, *90*, 1359.
(16) Gray, H. B. *Aldrichimica Acta* **1990**, *23*, 87.
(17) Lee, H.; DeFelippis, M. H.; Faraggi, M.; Klapper, M. H.; Pergamon: 1991, p 246.
(18) Glusker, J. P. *Adv. Protein Chem.* **1991**, *42*, 1.
(19) Mauk, A. G. *Struct. Bonding (Berlin, Ger.)* **1991**, *75*, 131.
(20) Isied, S. S. *Met. Ions Biol. Syst.* **1991**, *27*, 1.
(21) Kostic, N. M. *Met. Ions Biol. Syst.* **1991**, *27*, 129.
(22) Beratan, D. N.; Onuchic, J. N.; Winkler, J. R.; Gray, H. B. *Science* **1992**, *258*, 1740.
(23) Canters, G. W.; Van, d. K. M. *Curr. Opin. Struct. Biol.* **1992**, *2*, 859.
(24) Winkler, J. R.; Gray, H. B. *Chem. Rev.* **1992**, *92*, 369.
(25) Mathews, F. S.; White, S. *Curr. Opin. Struct. Biol.* **1993**, *3*, 902.
(26) Farid, R. S.; Moser, C. C.; Dutton, P. L. *Curr. Opin. Struct. Biol.* **1993**, *3*, 225.
(27) Friesner, R. A. *Structure (London, U. K.)* **1994**, *2*, 339.
(28) Dong, S.; Niu, J.; Cotton, T. M. *Methods Enzymol.* **1995**, *246*, 701.
(29) Chen, L.; Liu, M.-Y.; Le, G., Jean. *Biotechnol. Handb.* **1995**, *8*, 113.
(30) Chapman, S. K.; Mount, A. R. *Nat. Prod. Rep.* **1995**, *12*, 93.
(31) Gray, H. B.; Winkler, J. R. *Annu. Rev. Biochem.* **1996**, *65*, 537.
(32) Mathews, F. S.; Durley, R. C. E. In *Protein Electron Transfer*; Bendall, D. S., Ed.; BIOS Scientific Publishers Ltd.: Oxford, 1996, p 99.
(33) Bendall, D. S. *Protein electron transfer*; BIOS scientific publishers ltd.: Oxford, 1996.
(34) Hill, H. A. O.; Moore, C. B.; NabiRahni, D. M. A. *Bioelectrochem.: Princ. Pract.* **1997**, *5*, 183.
(35) Hayashi, T.; Ogoshi, H. *Chem. Soc. Rev.* **1997**, *26*, 355.
(36) Beratan, D. N.; Skourtis, S. S. *Curr. Opin. Chem. Biol.* **1998**, *2*, 235.
(37) Malmstrom, B. G.; Wittung-Stafshede, P. *Coord. Chem. Rev.* **1999**, *185-186*, 127.
(38) Kennedy, M. L.; Gibney, B. R. *Curr. Opin. Struct. Biol.* **2001**, *11*, 485.
(39) Ichiye, T.; Marcel Dekker, Inc.: 2001, p 393.
(40) Bellelli, A.; Brunori, M.; Brzezinski, P.; Wilson, M. T. *Methods* **2001**, *24*, 139.
(41) Davidson, V. L. *Biochemistry* **2002**, *41*, 14633.
(42) Gray, H. B.; Winkler, J. R. *Q. Rev. Biophys.* **2003**, *36*, 341.
(43) Winkler, J. R.; Gray, H. B.; Prytkova, T. R.; Kurnikov, I. V.; Beratan, D. N. In *Bioelectronics*; Willner, I., Katz, E., Eds.; Wiley-VCH: 2005, p 15.
(44) Gray, H. B.; Winkler, J. R. *Proc. Natl. Acad. Sci. U. S. A.* **2005**, *102*, 3534.
(45) Gunner, M. R.; Mao, J.; Song, Y.; Kim, J. *Biochim. Biophys. Acta, Bioenerg.* **2006**, *1757*, 942.
(46) Banci, L.; Bertini, I.; Luchinat, C.; Turano, P. In *Bioinorganic chemistry*; Bertini, I., Gray, H. B., Stiefel, E. I., Valentine, J. S., Eds.; University Science Books: Sausalito, 2007.
(47) Farver, O.; Pecht, I. *Prog. Inorg. Chem.* **2007**, *55*, 1.
(48) Bollinger, J. M., Jr. *Science* **2008**, *320*, 1730.
(49) Hammes-Schiffer, S.; Soudackov, A. V. *J. Phys. Chem. B* **2008**, *112*, 14108.
(50) Brittain, T. *Protein Pept. Lett.* **2008**, *15*, 556.
(51) Cordes, M.; Giese, B. *Chem. Soc. Rev.* **2009**, *38*, 892.
(52) Gray, H. B.; Winkler, J. R. *Chem. Phys. Lett.* **2009**, *483*, 1.

(53) Bashir, Q.; Scanu, S.; Ubbink, M. *FEBS Journal* **2011**, *278*, 1391.
(54) Choi, M.; Davidson, V. L. *Metallomics* **2011**, *3*, 140.
(55) de la Lande, A.; Babcock, N. S.; Rezac, J.; Levy, B.; Sanders, B. C.; Salahub, D. R. *Phys. Chem. Chem. Phys.* **2012**, *14*, 5902.
(56) Giese, B.; Eckhardt, S.; Lauz, M. In *Encyclopedia of Radicals in Chemistry, Biology and Materials*; John Wiley & Sons, Ltd: 2012.
(57) Marshall, N. M.; Miner, K. D.; Wilson, T. D.; Lu, Y. In *Coordination Chemistry in Protein Cages*; John Wiley & Sons, Inc.: 2013, p 111.
(58) Wherland, S.; Gray, H. B. In *Biological Aspects of Inorganic Chemistry*; Dolphin, D., Ed.; John Wiley: New York, 1977, p 289.
(59) Sutin, N.; Brunschwig, B. S. *Adv. Chem. Ser.* **1990**, *226*, 65.
(60) McLendon, G. *Met. Ions Biol. Syst.* **1991**, *27*, 183.
(61) McLendon, G.; Hake, R.; Zhang, Q.; Corin, A. *Mol. Cryst. Liq. Cryst.* **1991**, *194*, 225.
(62) Tollin, G.; Hazzard, J. T. *Arch. Biochem. Biophys.* **1991**, *287*, 1.
(63) Vervoort, J. *Curr. Opin. Struct. Biol.* **1991**, *1*, 889.
(64) McLendon, G.; Hake, R. *Chem. Rev.* **1992**, *92*, 481.
(65) Onuchic, J. N.; Beratan, D. N.; Winkler, J. R.; Gray, H. B. *Annu. Rev. Biophys. Biomol. Struct.* **1992**, *21*, 349.
(66) Wampler, J. E. *Methods Enzymol.* **1994**, *243*, 559.
(67) Moser, C. C.; Dutton, P. L. In *Protein Electron Transfer*; Bendall, D. S., Ed.; BIOS Scientific Publishers Ltd.: Oxford, 1996, p 1.
(68) Telford, J. R.; Wittung-Stafshede, P.; Gray, H. B.; Winkler, J. R. *Acc. Chem. Res.* **1998**, *31*, 755.
(69) Sharp, R. E.; Chapman, S. K. *Biochim. Biophys. Acta, Protein Struct. Mol. Enzymol.* **1999**, *1432*, 143.
(70) Sticht, H. *Recent Res. Dev. Biochem.* **1999**, *1*, 1.
(71) Supkowski, R. M.; Bolender, J. P.; Smith, W. D.; Reynolds, L. E. L.; Horrocks, W. D., Jr. *Coord. Chem. Rev.* **1999**, *185-186*, 307.
(72) Randall, D. W.; Gamelin, D. R.; LaCroix, L. B.; Solomon, E. I. *JBIC, J. Biol. Inorg. Chem.* **2000**, *5*, 16.
(73) Page, C. C.; Moser, C. C.; Dutton, P. L. *Curr. Opin. Chem. Biol.* **2003**, *7*, 551.
(74) Wheeler, R. A. *ACS Symp. Ser.* **2004**, *883*, 1.
(75) Noodleman, L.; Han, W.-G. *JBIC, J. Biol. Inorg. Chem.* **2006**, *11*, 674.
(76) Solomon, E. I.; Xie, X.; Dey, A. *Chem. Soc. Rev.* **2008**, *37*, 623.
(77) Prabhulkar, S.; Tian, H.; Wang, X.; Zhu, J.-J.; Li, C.-Z. *Antioxid. Redox Signaling* **2012**, *17*, 1796.
(78) Rodgers, K. R.; Lukat-Rodgers, G. S. In *Comprehensive Coordination Chemistry II*; McCleverty, J., Meyer, T. J., Eds.; Pergamon: Oxford, 2004; Vol. 8, p 17.
(79) Bertini, I.; Cavallaro, G.; Rosato, A. *Chem. Rev.* **2006**, *106*, 90.
(80) Moore, G. R.; Pettigrew, G. W. *Cytochromes c: Evolutionary, Structural and Physicochemical Aspects*; Springer-Verlag: Berlin, 1990.
(81) Reedy, C. J.; Gibney, B. R. *Chem. Rev.* **2004**, *104*, 617.
(82) Simonneaux, G.; Bondon, A. *Chem. Rev.* **2005**, *105*, 2627.
(83) Walker, F. A. *Chem. Rev.* **2004**, *104*, 589.
(84) Weiss, R.; Gold, A.; Terner, J. *Chem. Rev.* **2006**, *106*, 2550.
(85) Schultz, B. E.; Chan, S. I. *Annu. Rev. Biophys. Biomol. Struct.* **2001**, *30*, 23.

(86) Berry, E. A.; Guergova-Kuras, M.; Huang, L. S.; Crofts, A. R. *Annu. Rev. Biochem.* **2000**, *69*, 1005.
(87) Brayer, G. D.; Murphy, M. E. P.; Scott, R. A., Mauk, A. G., Eds.; University Science Books: Sausalito, CA, 1996, p 103.
(88) Meyer, T. E.; Scott, R. A., Mauk, A. G., Eds.; University Science Books: Sausalito, CA, 1996, p 33.
(89) Ambler, R. P. *From Cyclotrons to Cytochromes*; Academic Press: Weinheim, 1982.
(90) Meyer, T. E.; Kamen, M. D. *Adv. Protein Chem.* **1982**, *35*, 105.
(91) Meyer, J. *JBIC, J. Biol. Inorg. Chem.* **2008**, *13*, 157.
(92) Stephens, P. J.; Jollie, D. R.; Warshel, A. *Chem. Rev.* **1996**, *96*, 2491.
(93) Noodleman, L.; Pique, M. E.; Roberts, V. A.; John Wiley & Sons, Inc.: 2009; Vol. 2, p 458.
(94) Adman, E. T. *Adv. Protein Chem.* **1991**, *42*, 145.
(95) Gray, H. B.; Malmstrom, B. G.; Williams, R. J. *JBIC, J. Biol. Inorg. Chem.* **2000**, *5*, 551.
(96) Solomon, E. I.; Randall, D. W.; Glaser, T. *Coord. Chem. Rev.* **2000**, *200–202*, 595.
(97) Vila, A. J.; Fernandez, C. O. In *Handbook on Metalloproteins*; Bertini, I., Sigel, A., Sigel, H., Eds.; Marcel Dekker: New York, NY, 2001, p 813.
(98) Lu, Y. In *Biocoordination Chemistry*; Que, J. L., Tolman, W. B., Eds.; Elsevier: Oxford, UK, 2004; Vol. 8, p 91.
(99) Solomon, E. I.; Szilagyi, R. K.; DeBeer George, S.; Basumallick, L. *Chem. Rev.* **2004**, *104*, 419.
(100) Dennison, C. *Coord. Chem. Rev.* **2005**, *249*, 3025.
(101) Farver, O.; Pecht, I. In *Prog. Inorg. Chem.*; John Wiley & Sons, Inc.: 2008, p 1.
(102) Kolczak, U.; Dennison, C.; Messerschmidt, A.; Canters, G. W. In *Encyclopedia of Inorganic and Bioinorganic Chemistry*; John Wiley & Sons, Ltd: 2011.
(103) Wilson, T. D.; Yu, Y.; Lu, Y. *Coord. Chem. Rev.* **2012**, *257*, 260.
(104) Warren, J. J.; Lancaster, K. M.; Richards, J. H.; Gray, H. B. *J. Inorg. Biochem.* **2012**, *115*, 119.
(105) Noodleman, L.; Han, W.-G. *JBIC, J. Biol. Inorg. Chem.* **2006**, *11*, 674.
(106) Szilagyi, R. K.; Solomon, E. I. *Curr. Opin. Chem. Biol.* **2002**, *6*, 250.
(107) Solomon, E. I.; Hadt, R. G. *Coord. Chem. Rev.* **2011**, *255*, 774.
(108) Neese, F. *Coord. Chem. Rev.* **2009**, *253*, 526.
(109) Solomon, E. I.; Xie, X.; Dey, A. *Chem. Soc. Rev.* **2008**, *37*, 623.
(110) Yoon, J.; Solomon, E. I. *Biol. Magn. Reson.* **2009**, *28*, 471.
(111) Margoliash, E.; Schejter, A. *Trends Biochem. Sci.* **1984**, *9*, 364.
(112) Keilin, D. *Proc. R. Soc. London, Ser. B* **1925**, *98*, 312.
(113) Yaoi, H.; Tamiya, H. *Proc. Imp. Acad. Jpn.* **1928**, *4*, 436.
(114) Yanagisawa, S.; Banfield, M. J.; Dennison, C. *Biochemistry* **2006**, *45*, 8812.
(115) Jiang, X. J.; Wang, X. D. *Annu. Rev. Biochem.* **2004**, *73*, 87.
(116) Yamanaka, T. *The Biochemistry of Bacterial Cytochromes*; Japan Scientific Societies Press, SPRINGER-VERLAG, 1992.
(117) Vonjagow, G.; Sebald, W. *Annu. Rev. Biochem.* **1980**, *49*, 281.
(118) Kamen, M. D.; Horio, T. *Annu. Rev. Biochem.* **1970**, *39*, 673.
(119) Puustinen, A.; Wikstrom, M. *Proc. Natl. Acad. Sci. U. S. A.* **1991**, *88*, 6122.
(120) Frolow, F.; Kalb, A. J.; Yariv, J. *Nat. Struct. Biol.* **1994**, *1*, 453.
(121) LeBrun, N. E.; Thomson, A. J.; Moore, G. R. *Metal Sites in Proteins and Models* **1997**, *88*, 103.

(122) Iverson, T. M.; Arciero, D. M.; Hsu, B. T.; Logan, M. S. P.; Hooper, A. B.; Rees, D. C. *Nat. Struct. Biol.* **1998**, *5*, 1005.

(123) Martinez, S. E.; Huang, D.; Szczepaniak, A.; Cramer, W. A.; Smith, J. L. *Structure* **1994**, *2*, 95.

(124) Liu, X. S.; Kim, C. N.; Yang, J.; Jemmerson, R.; Wang, X. D. *Cell* **1996**, *86*, 147.

(125) Yang, J.; Liu, X. S.; Bhalla, K.; Kim, C. N.; Ibrado, A. M.; Cai, J. Y.; Peng, T. I.; Jones, D. P.; Wang, X. D. *Science* **1997**, *275*, 1129.

(126) Kluck, R. M.; BossyWetzel, E.; Green, D. R.; Newmeyer, D. D. *Science* **1997**, *275*, 1132.

(127) Mauk, A. G., 75, 132–157. *Struct. Bonding (Berlin)* **1991**, *75*, 132.

(128) Wilson, M. T.; Greenwood, C. *Cytochrome c: A Multidisciplinary Approach*; University Science Books: Sausalito, CA, 1996.

(129) Mauk, A. G.; Moore, G. R. *JBIC, J. Biol. Inorg. Chem.* **1997**, *2*, 119.

(130) McGee, W. A.; Rosell, F. I.; Liggins, J. R.; RodriguezGhidarpour, S.; Luo, Y. G.; Chen, J.; Brayer, G. D.; Mauk, A. G.; Nall, B. T. *Biochemistry* **1996**, *35*, 1995.

(131) Rafferty, S. P.; Guillemette, J. G.; Berghuis, A. M.; Smith, M.; Brayer, G. D.; Mauk, A. G. *Biochemistry* **1996**, *35*, 10784.

(132) Bjerrum, M. J.; Casimiro, D. R.; Chang, I. J.; Di Bilio, A. J.; Gray, H. B.; Hill, M. G.; Langen, R.; Mines, G. A.; Skov, L. K.; Winkler, J. R.; et al. *J. Bioenerg. Biomembr.* **1995**, *27*, 295.

(133) Therien, M. J.; Chang, J.; Raphael, A. L.; Bowler, B. E.; Gray, H. B. *Struct. Bonding (Berlin, Ger.)* **1991**, *75*, 109.

(134) Brzezinski, P.; Wilson, M. T. *Proc. Natl. Acad. Sci. U. S. A.* **1997**, *94*, 6176.

(135) Dopner, S.; Hildebrandt, P.; Rosell, F. I.; Mauk, A. G.; von Walter, M.; Buse, G.; Soulimane, T. *Eur. J. Biochem.* **1999**, *261*, 379.

(136) Hildebrandt, P.; Heimburg, T.; Marsh, D.; Powell, G. L. *Biochemistry* **1990**, *29*, 1661.

(137) Hildebrandt, P.; Vanhecke, F.; Heibel, G.; Mauk, A. G. *Biochemistry* **1993**, *32*, 14158.

(138) Weber, C.; Michel, B.; Bosshard, H. R. *Proc. Natl. Acad. Sci. U. S. A.* **1987**, *84*, 6687.

(139) Durham, B.; Fairris, J. L.; McLean, M.; Millett, F.; Scott, J. R.; Sligar, S. G.; Willie, A. *J. Bioenerg. Biomembr.* **1995**, *27*, 331.

(140) Mauk, A. G.; Mauk, M. R.; Moore, G. R.; Northrup, S. H. *J. Bioenerg. Biomembr.* **1995**, *27*, 311.

(141) Rodriguez-Maranon, M. J.; Qiu, F.; Stark, R. E.; White, S. P.; Zhang, X.; Foundling, S. I.; Rodriguez, V.; Schilling, C. L., 3rd; Bunce, R. A.; Rivera, M. *Biochemistry* **1996**, *35*, 16378.

(142) Ullmann, G. M.; Kostic, N. M. *J. Am. Chem. Soc.* **1995**, *117*, 4766.

(143) Crnogorac, M. M.; Ullmann, G. M.; Kostic, N. M. *J. Am. Chem. Soc.* **2001**, *123*, 10789.

(144) Pletneva, E. V.; Fulton, D. B.; Kohzuma, T.; Kostic, N. M. *J. Am. Chem. Soc.* **2000**, *122*, 1034.

(145) Zhou, J. S.; Kostic, N. M. *J. Am. Chem. Soc.* **1992**, *114*, 3562.

(146) Hoffman, B. M.; Natan, M. J.; Nocek, J. M.; Wallin, S. A. *Struct. Bonding (Berlin, Ger.)* **1991**, *75*, 85.

(147) Liang, N.; Mauk, A. G.; Pielak, G. J.; Johnson, J. A.; Smith, M.; Hoffman, B. M. *Science* **1988**, *240*, 311.

(148) McLendon, G. *Struct. Bonding (Berlin, Ger.)* **1991**, *75*, 159.

(149) Nocek, J. M.; Zhou, J. S.; DeForest, S.; Priyadarshy, S.; Beratan, D. N.; Onuchic, J. N.; Hoffman, B. M. *Chem. Rev.* **1996**, *96*, 2459.

(150) Ferguson, S. J.; Stevens, J. M.; Allen, J. W. A.; Robertson, I. B. *Biochim. Biophys. Acta, Bioenerg.* **2008**, *1777*, 980.

(151) Stevens, T. H.; Martin, C. T.; Wang, H.; Brudvig, G. W.; Scholes, C. P.; Chan, S. I. *J. Biol. Chem.* **1982**, *257*, 12106.
(152) Ambler, R. P. *Biochim. Biophys. Acta* **1991**, *1058*, 42.
(153) Arciero, D. M.; Hooper, A. B. *J. Biol. Chem.* **1994**, *269*, 11878.
(154) Shimizu, H.; Schuller, D. J.; Lanzilotta, W. N.; Sundaramoorthy, M.; Arciero, D. M.; Hooper, A. B.; Poulos, T. L. *Biochemistry* **2001**, *40*, 13483.
(155) Menin, L.; Schoepp, B.; Garcia, D.; Parot, P.; Vermeglio, A. *Biochemistry* **1997**, *36*, 12175.
(156) Bertrand, P.; Mbarki, O.; Asso, M.; Blanchard, L.; Guerlesquin, F.; Tegoni, M. *Biochemistry* **1995**, *34*, 11071.
(157) Gunner, M. R.; Honig, B. *Proc. Natl. Acad. Sci. U. S. A.* **1991**, *88*, 9151.
(158) Caffrey, M. S.; Cusanovich, M. A. *Biochim. Biophys. Acta, Bioenerg.* **1994**, *1187*, 277.
(159) Caffrey, M. S.; Daldal, F.; Holden, H. M.; Cusanovich, M. A. *Biochemistry* **1991**, *30*, 4119.
(160) Zhao, D. Z.; Hutton, H. M.; Meyer, T. E.; Walker, F. A.; MacKenzie, N. E.; Cusanovich, M. A. *Biochemistry* **2000**, *39*, 4053.
(161) Ponamarev, M. V.; Schlarb, B. G.; Howe, C. J.; Carrell, C. J.; Smith, J. L.; Bendall, D. S.; Cramer, W. A. *Biochemistry* **2000**, *39*, 5971.
(162) Grönberg, K. L.; Roldάn, M. D.; Prior, L.; Butland, G.; Cheesman, M. R.; Richardson, D. J.; Spiro, S.; Thomson, A. J.; Watmough, N. J. *Biochemistry* **1999**, *38*, 13780.
(163) Ellfolk, N.; Ronnberg, M.; Aasa, R.; Andreasson, L. E.; Vanngard, T. *Biochim. Biophys. Acta* **1983**, *743*, 23.
(164) Sawaya, M. R.; Krogmann, D. W.; Serag, A.; Ho, K. K.; Yeates, T. O.; Kerfeld, C. A. *Biochemistry* **2001**, *40*, 9215.
(165) Hickey, D. R.; Berghuis, A. M.; Lafond, G.; Jaeger, J. A.; Cardillo, T. S.; McLendon, D.; Das, G.; Sherman, F.; Brayer, G. D.; McLendon, G. *J. Biol. Chem.* **1991**, *266*, 11686.
(166) Döpner, S.; Hildebrandt, P.; Rosell, F. I.; Mauk, A. G. *J. Am. Chem. Soc.* **1998**, *120*, 11246.
(167) Rosell, F. I.; Ferrer, J. C.; Mauk, A. G. *J. Am. Chem. Soc.* **1998**, *120*, 11234.
(168) Cutler, R. L.; Davies, A. M.; Creighton, S.; Warshel, A.; Moore, G. R.; Smith, M.; Mauk, A. G. *Biochemistry* **1989**, *28*, 3188.
(169) Lett, C. M.; Berghuis, A. M.; Frey, H. E.; Lepock, J. R.; Guillemette, J. G. *J. Biol. Chem.* **1996**, *271*, 29088.
(170) Pearce, L. L.; Gartner, A. L.; Smith, M.; Mauk, A. G. *Biochemistry* **1989**, *28*, 3152.
(171) Rafferty, S. P.; Pearce, L. L.; Barker, P. D.; Guillemette, J. G.; Kay, C. M.; Smith, M.; Mauk, A. G. *Biochemistry* **1990**, *29*, 9365.
(172) Rosell, F. I.; Harris, T. R.; Hildebrand, D. P.; Dopner, S.; Hildebrandt, P.; Mauk, A. G. *Biochemistry* **2000**, *39*, 9047.
(173) Komarpanicucci, S.; Bixler, J.; Bakker, G.; Sherman, F.; McLendon, G. *J. Am. Chem. Soc.* **1992**, *114*, 5443.
(174) Raphael, A. L.; Gray, H. B. *J. Am. Chem. Soc.* **1991**, *113*, 1038.
(175) Springs, S. L.; Bass, S. E.; McLendon, G. L. *Biochemistry* **2000**, *39*, 6075.
(176) Barker, P. D.; Butler, J. L.; de Oliveira, P.; Hill, H. A. O.; Hunt, N. I. *Inorg. Chim. Acta.* **1996**, *252*, 71.
(177) Walker, F. A.; Emrick, D.; Rivera, J. E.; Hanquet, B. J.; Buttlaire, D. H. *J. Am. Chem. Soc.* **1988**, *110*, 6234.
(178) Fantuzzi, A.; Sadeghi, S.; Valetti, F.; Rossi, G. L.; Gilardi, G. *Biochemistry* **2002**, *41*, 8718.
(179) Funk, W. D.; Lo, T. P.; Mauk, M. R.; Brayer, G. D.; Macgillivray, R. T. A.; Mauk, A. G. *Biochemistry* **1990**, *29*, 5500.
(180) Rodgers, K. K.; Sligar, S. G. *J. Am. Chem. Soc.* **1991**, *113*, 9419.

(181) Xue, L. L.; Wang, Y. H.; Xie, Y.; Yao, P.; Wang, W. H.; Qian, W.; Huang, Z. X.; Wu, J.; Xia, Z. X. *Biochemistry* **1999**, *38*, 11961.

(182) Grein, F.; Venceslau, S. S.; Schneider, L.; Hildebrandt, P.; Todorovic, S.; Pereira, I. s. A.; Dahl, C. *Biochemistry* **2010**, *49*, 8290.

(183) Klarskov, K.; Van Driessche, G.; Backers, K.; Dumortier, C.; Meyer, T. E.; Tollin, G.; Cusanovich, M. A.; Van Beeumen, J. J. *Biochemistry* **1998**, *37*, 5995.

(184) Widger, W. R.; Cramer, W. A.; Herrmann, R. G.; Trebst, A. *Proc. Natl. Acad. Sci. U. S. A.* **1984**, *81*, 674.

(185) Guerrero, F.; Sedoud, A.; Kirilovsky, D.; Rutherford, A. W.; Ortega, J. M.; Roncel, M. *J. Biol. Chem.* **2011**, *286*, 5985.

(186) Siponen, M.; Adryanczyk, G.; Ginet, N.; Arnoux, P.; Pignol, D. *Biochem. Soc. Trans.* **2012**, *40*, 1319.

(187) Rivera, M.; Seetharaman, R.; Girdhar, D.; Wirtz, M.; Zhang, X.; Wang, X.; White, S. *Biochemistry* **1998**, *37*, 1485.

(188) Rodriguez, J. C.; Rivera, M. *Biochemistry* **1998**, *37*, 13082.

(189) Kay, C. J.; Barber, M. J.; Solomonson, L. P. *Biochemistry* **1988**, *27*, 6142.

(190) Spence, J. T.; Barber, M. J.; Solomonson, L. P. *Biochem. J* **1988**, *250*, 921.

(191) Kostanjevecki, V.; Leys, D.; Van Driessche, G.; Meyer, T. E.; Cusanovich, M. A.; Fischer, U.; Guisez, Y.; Van Beeumen, J. *J. Biol. Chem.* **1999**, *274*, 35614.

(192) Dolla, A.; Florens, L.; Bianco, P.; Haladjian, J.; Voordouw, G.; Forest, E.; Wall, J.; Guerlesquin, F.; Bruschi, M. *J. Biol. Chem.* **1994**, *269*, 6340.

(193) Musveteau, I.; Dolla, A.; Guerlesquin, F.; Payan, F.; Czjzek, M.; Haser, R.; Bianco, P.; Haladjian, J.; Rappgiles, B. J.; Wall, J. D.; Voordouw, G.; Bruschi, M. *J. Biol. Chem.* **1992**, *267*, 16851.

(194) Shibata, N.; Iba, S.; Misaki, S.; Meyer, T. E.; Bartsch, R. G.; Cusanovich, M. A.; Morimoto, Y.; Higuchi, Y.; Yasuoka, N. *J. Mol. Biol.* **1998**, *284*, 751.

(195) Tahirov, T. H.; Misaki, S.; Meyer, T. E.; Cusanovich, M. A.; Higuchi, Y.; Yasuoka, N. *J. Mol. Biol.* **1996**, *259*, 467.

(196) Fujii, S.; Yoshimura, T.; Kamada, H.; Yamaguchi, K.; Suzuki, S.; Shidara, S.; Takakuwa, S. *Biochim. Biophys. Acta, Protein Struct. Mol. Enzymol.* **1995**, *1251*, 161.

(197) Lamar, G. N.; Jackson, J. T.; Dugad, L. B.; Cusanovich, M. A.; Bartsch, R. G. *J. Biol. Chem.* **1990**, *265*, 16173.

(198) Tsan, P.; Caffrey, M.; Daku, M. L.; Cusanovich, M.; Marion, D.; Gans, P. *J. Am. Chem. Soc.* **2001**, *123*, 2231.

(199) Zahn, J. A.; Arciero, D. M.; Hooper, A. B.; DiSpirito, A. A. *Eur. J. Biochem.* **1996**, *240*, 684.

(200) Korszun, Z. R.; Bunker, G.; Khalid, S.; Scheidt, W. R.; Cusanovich, M. A.; Meyer, T. E. *Biochemistry* **1989**, *28*, 1513.

(201) Monkara, F.; Bingham, S. J.; Kadir, F. H. A.; McEwan, A. G.; Thomson, A. J.; Thurgood, A. G. P.; Moore, G. R. *Biochim. Biophys. Acta* **1992**, *1100*, 184.

(202) Yoshimura, T.; Suzuki, S.; Nakahara, A.; Iwasaki, H.; Masuko, M.; Matsubara, T. *Biochim. Biophys. Acta* **1985**, *831*, 267.

(203) Maltempo, M. M. *J. Chem. Phys.* **1974**, *61*, 2540.

(204) Ambler, R. P.; Bartsch, R. G.; Daniel, M.; Kamen, M. D.; McLellan, L.; Meyer, T. E.; Vanbeeumen, J. *Proc. Natl. Acad. Sci. U. S. A.* **1981**, *78*, 6854.

(205) Ambler, R. P.; Meyer, T. E.; Bartsch, R. G.; Cusanovich, M. A. *Arch. Biochem. Biophys.* **2001**, *388*, 25.

(206) Bartsch, R. G.; Ambler, R. P.; Meyer, T. E.; Cusanovich, M. A. *Arch. Biochem. Biophys.* **1989**, *271*, 433.

(207) Assfalg, M.; Banci, L.; Bertini, I.; Bruschi, M.; Giudici-Orticoni, M. T.; Turano, P. *Eur. J. Biochem.* **1999**, *266*, 634.

(208) Banci, L.; Bertini, I.; Bruschi, M.; Sompornpisut, P.; Turano, P. *Proc. Natl. Acad. Sci. U. S. A.* **1996**, *93*, 14396.

(209) Matias, P. M.; Coelho, R.; Pereira, I. A. C.; Coelho, A. V.; Thompson, A. W.; Sieker, L. C.; Le Gall, J.; Carrondo, M. A. *Struct. Fold. Des.* **1999**, *7*, 119.

(210) Pereira, I. A. C.; Pacheco, I.; Liu, M. Y.; Legall, J.; Xavier, A. V.; Teixeira, M. *Eur. J. Biochem.* **1997**, *248*, 323.

(211) Pettigrew, G. W.; Moore, G. R. *Cytochromes C: Biological Aspects*; Springer: Berlin, 1987.

(212) Ferguson, S. J. *Biochim. Biophys. Acta, Bioenerg.* **2012**, *1817*, 1754.

(213) Louro, R. O.; Catarino, T.; LeGall, J.; Xavier, A. V. *J. Biol. Inorg. Chem.* **1997**, *2*, 488.

(214) Paixão, V. B.; Vis, H.; Turner, D. L. *Biochemistry* **2010**, *49*, 9620.

(215) Haser, R.; Pierrot, M.; Frey, M.; Payan, F.; Astier, J. P.; Bruschi, M.; Legall, J. *Nature* **1979**, *282*, 806.

(216) Higuchi, Y.; Kusunoki, M.; Matsuura, Y.; Yasuoka, N.; Kakudo, M. *J. Mol. Biol.* **1984**, *172*, 109.

(217) Morais, J.; Palma, P. N.; Frazao, C.; Caldeira, J.; LeGall, J.; Moura, I.; Moura, J. J.; Carrondo, M. A. *Biochemistry* **1995**, *34*, 12830.

(218) Pierrot, M.; Haser, R.; Frey, M.; Payan, F.; Astier, J. P. *J. Biol. Chem.* **1982**, *257*, 4341.

(219) Sieker, L. C.; Jensen, L. H.; Legall, J. *FEBS Lett.* **1986**, *209*, 261.

(220) Banci, L.; Bertini, I.; Quacquarini, G.; Walter, O.; Diaz, A.; Hervas, M.; delaRosa, M. A. *JBIC, J. Biol. Inorg. Chem.* **1996**, *1*, 330.

(221) Roden, E. E.; Lovley, D. R. *Appl. Environ. Microbiol.* **1993**, *59*, 734.

(222) Fiechtner, M. D.; Kassner, R. J. *Biochim. Biophys. Acta* **1979**, *579*, 269.

(223) Lancaster, C. R. D.; Michel, H. *Structure* **1997**, *5*, 1339.

(224) Iverson, T. M.; Arciero, D. M.; Hooper, A. B.; Rees, D. C. *JBIC, J. Biol. Inorg. Chem.* **2001**, *6*, 390.

(225) Stroebel, D.; Choquet, Y.; Popot, J. L.; Picot, D. *Nature* **2003**, *426*, 413.

(226) Allen, J. W. A.; Ginger, M. L.; Ferguson, S. J. *Biochem. J.* **2004**, *383*, 537.

(227) Pettigrew, G. W.; Leaver, J. L.; Meyer, T. E.; Ryle, A. P. *Biochem. J.* **1975**, *147*, 291.

(228) Ginger, M. L.; Sam, K. A.; Allen, J. W. A. *Biochem. J.* **2012**, *448*, 253.

(229) Murphy, M. E.; Nall, B. T.; Brayer, G. D. *J. Mol. Biol.* **1992**, *227*, 160.

(230) Berghuis, A. M.; Brayer, G. D. *J. Mol. Biol.* **1992**, *223*, 959.

(231) Bushnell, G. W.; Louie, G. V.; Brayer, G. D. *J. Mol. Biol.* **1990**, *214*, 585.

(232) Louie, G. V.; Brayer, G. D. *J. Mol. Biol.* **1990**, *214*, 527.

(233) Ochi, H.; Hata, Y.; Tanaka, N.; Kakudo, M.; Sakurai, T.; Aihara, S.; Morita, Y. *J. Mol. Biol.* **1983**, *166*, 407.

(234) Takano, T.; Dickerson, R. E. *Proc. Natl. Acad. Sci. U. S. A. Biol. Sci.* **1980**, *77*, 6371.

(235) Takano, T.; Dickerson, R. E. *J. Mol. Biol.* **1981**, *153*, 79.

(236) Banci, L.; Bertini, I.; Rosato, A.; Varani, G. *JBIC, J. Biol. Inorg. Chem.* **1999**, *4*, 824.

(237) Qi, P. X.; Urbauer, J. L.; Fuentes, E. J.; Leopold, M. F.; Wand, A. J. *Nat. Struct. Biol.* **1994**, *1*, 378.

(238) Qi, P. X. R.; Beckman, R. A.; Wand, A. J. *Biochemistry* **1996**, *35*, 12275.

(239) Benning, M. M.; Wesenberg, G.; Caffrey, M. S.; Bartsch, R. G.; Meyer, T. E.; Cusanovich, M. A.; Rayment, I.; Holden, H. M. *J. Mol. Biol.* **1991**, *220*, 673.

(240) Cordier, F.; Caffrey, M.; Brutscher, B.; Cusanovich, M. A.; Marion, D.; Blackledge, M. *J. Mol. Biol.* **1998**, *281*, 341.

(241) Gooley, P. R.; Zhao, D.; Mackenzie, N. E. *J. Biomol. NMR* **1991**, *1*, 145.
(242) Zhao, D. Z.; Hutton, H. M.; Cusanovich, M. A.; Mackenzie, N. E. *Protein Sci.* **1996**, *5*, 1816.
(243) Banci, L.; Bertini, I.; De la Rosa, M. A.; Koulougliotis, D.; Navarro, J. A.; Walter, O. *Biochemistry* **1998**, *37*, 4831.
(244) Frazao, C.; Soares, C. M.; Carrondo, M. A.; Pohl, E.; Dauter, Z.; Wilson, K. S.; Hervas, M.; Navarro, J. A.; Delarosa, M. A.; Sheldrick, G. M. *Structure* **1995**, *3*, 1159.
(245) Harrenga, A.; Reincke, B.; Ruterjans, H.; Ludwig, B.; Michel, H. *J. Mol. Biol.* **2000**, *295*, 667.
(246) Rajendran, C.; Ermler, U.; Ludwig, B.; Michel, H. *Acta Crystallogr. D Biol. Crystallogr.* **2010**, *66*, 850.
(247) Reincke, B.; Thony-Meyer, L.; Dannehl, C.; Odenwald, A.; Aidim, M.; Witt, H.; Ruterjans, H.; Ludwig, B. *Biochim. Biophys. Acta, Bioenerg.* **1999**, *1411*, 114.
(248) Anthony, C. *Biochim. Biophys. Acta* **1992**, *1099*, 1.
(249) Read, J.; Gill, R.; Dales, S. L.; Cooper, J. B.; Wood, S. P.; Anthony, C. *Protein Sci.* **1999**, *8*, 1232.
(250) Than, M. E.; Hof, P.; Huber, R.; Bourenkov, G. P.; Bartunik, H. D.; Buse, G.; Soulimane, T. *J. Mol. Biol.* **1997**, *271*, 629.
(251) Atack, J. M.; Kelly, D. J. *Adv. Microb. Physiol.* **2007**, *52*, 73.
(252) Erman, J. E.; Vitello, L. B. *Biochim. Biophys. Acta* **2002**, *1597*, 193.
(253) Ronnberg, M.; Araiso, T.; Ellfolk, N.; Dunford, H. B. *J. Biol. Chem.* **1981**, *256*, 2471.
(254) De Smet, L.; Pettigrew, G. W.; Van Beeumen, J. J. *Eur. J. Biochem.* **2001**, *268*, 6559.
(255) Fulop, V.; Ridout, C. J.; Greenwood, C.; Hajdu, J. *Structure* **1995**, *3*, 1225.
(256) Crowley, P. B.; Ubbink, M. *Acc. Chem. Res.* **2003**, *36*, 723.
(257) Hart, S. E.; Schlarb-Ridley, B. G.; Delon, C.; Bendall, D. S.; Howe, C. J. *Biochemistry* **2003**, *42*, 4829.
(258) Koh, M.; Meyer, T. E.; De Smet, L.; Van Beeumen, J. J.; Cusanovich, M. A. *Arch. Biochem. Biophys.* **2003**, *410*, 230.
(259) Alves, T.; Besson, S.; Duarte, L. C.; Pettigrew, G. W.; Girio, F. M. F.; Devreese, B.; Vandenberghe, I.; Van Beeumen, J.; Fauque, G.; Moura, I. *Biochim. Biophys. Acta, Protein Struct. Mol. Enzymol.* **1999**, *1434*, 248.
(260) Pettigrew, G. W.; Goodhew, C. F.; Cooper, A.; Nutley, M.; Jumel, K.; Harding, S. E. *Biochemistry* **2003**, *42*, 2046.
(261) Pettigrew, G. W.; Prazeres, S.; Costa, C.; Palma, N.; Krippahl, L.; Moura, I.; Moura, J. J. *J. Biol. Chem.* **1999**, *274*, 11383.
(262) Berks, B. C.; Ferguson, S. J.; Moir, J. W.; Richardson, D. J. *Biochim. Biophys. Acta, Bioenerg.* **1995**, *1232*, 97.
(263) Ferguson, S. J. *Curr. Opin. Chem. Biol.* **1998**, *2*, 182.
(264) Philippot, L. *Biochim. Biophys. Acta, Gene Struct. Expression* **2002**, *1577*, 355.
(265) Cheesman, M. R.; Ferguson, S. J.; Moir, J. W.; Richardson, D. J.; Zumft, W. G.; Thomson, A. J. *Biochemistry* **1997**, *36*, 16267.
(266) Nurizzo, D.; Silvestrini, M.-C.; Mathieu, M.; Cutruzzolà, F.; Bourgeois, D.; Fülöp, V.; Hajdu, J.; Brunori, M.; Tegoni, M.; Cambillau, C. *Structure* **1997**, *5*, 1157.
(267) Dodd, F. E.; Van Beeumen, J.; Eady, R. R.; Hasnain, S. S. *J. Mol. Biol.* **1998**, *282*, 369.
(268) Murphy, M. E. P.; Turley, S.; Adman, E. T. *J. Biol. Chem.* **1997** *272* 28455.
(269) Lopes, H.; Besson, S. p.; Moura, I.; Moura, J. J. *JBIC, J. Biol. Inorg. Chem.* **2001**, *6*, 55.
(270) Moenne-Loccoz, P. *Nat. Prod. Rep.* **2007**, *24*, 610.

(271) Shiro, Y.; Sugimoto, H.; Tosha, T.; Nagano, S.; Hino, T. *Philos. Trans. R. Soc., B* **2012** *367* 1195.

(272) Hino, T.; Matsumoto, Y.; Nagano, S.; Sugimoto, H.; Fukumori, Y.; Murata, T.; Iwata, S.; Shiro, Y. *Science* **2010** *330* 1666.

(273) Hille, R. *Chem. Rev.* **1996**, *96*, 2757.

(274) Hille, R. *Trends Biochem. Sci.* **2002**, *27*, 360.

(275) Kay, C. J.; Solomonson, L. P.; Barber, M. J. *Biochemistry* **1990**, *29*, 10823.

(276) Campbell, W. H.; Kinghorn, J. R. *Trends Biochem. Sci.* **1990**, *15*, 315.

(277) Chen, K.; Bonagura, C. A.; Tilley, G. J.; McEvoy, J. P.; Jung, Y.-S.; Armstrong, F. A.; Stout, C. D.; Burgess, B. K. *Nat. Struct. Biol.* **2002**, *9*, 188.

(278) Cunane, L. M.; Chen, Z.-W.; Shamala, N.; Mathews, F. S.; Cronin, C. n. N.; McIntire, W. S. *J. Mol. Biol.* **2000**, *295*, 357.

(279) Chen, L.; Durley, R.; Mathews, F.; Davidson, V. *Science* **1994**, *264*, 86.

(280) Nitschke, W.; Rutherford, A. W. *Trends Biochem. Sci.* **1991**, *16*, 241.

(281) Shen, J. R.; Ikeuchi, M.; Inoue, Y. *J. Biol. Chem.* **1997**, *272*, 17821.

(282) Kerfeld, C. A.; Krogmann, D. W. *Annu. Rev. Plant Biol.* **1998**, *49*, 397.

(283) Ferreira, K. N.; Iverson, T. M.; Maghlaoui, K.; Barber, J.; Iwata, S. *Science* **2004**, *303*, 1831.

(284) Goussias, C.; Boussac, A.; Rutherford, A. W. *Philos. Trans. R. Soc., B* **2002** *357* 1369.

(285) Alam, J.; Sprinkle, J.; Hermodson, M.; Krogmann, D. *Biochim. Biophys. Acta, Bioenerg.* **1984**, *766*, 317.

(286) Holton, R. W.; Myers, J. *Science* **1963**, *142*, 234.

(287) Navarro, J. A.; Hervás, M.; De la Cerda B.; M.A., D. l. R. *Arch. Biochem. Biophys.* **1995**, *318*, 46.

(288) Roncel, M.; Boussac, A.; Zurita, J. L.; Bottin, H.; Sugiura, M.; Kirilovsky, D.; Ortega, J. M. *JBIC, J. Biol. Inorg. Chem.* **2003**, *8*, 206.

(289) Vrettos, J. S.; Reifler, M. J.; Kievit, O.; Lakshmi, K.; de Paula, J. C.; Brudvig, G. W. *JBIC, J. Biol. Inorg. Chem.* **2001**, *6*, 708.

(290) Roncel, M.; Kirilovsky, D.; Guerrero, F.; Serrano, A.; Ortega, J. M. *Biochim. Biophys. Acta, Bioenerg.* **2012**, *1817*, 1152.

(291) Chitnis, P. R.; Xu, Q.; Chitnis, V. P.; Nechushtai, R. *Photosynth. Res.* **1995**, *44*, 23.

(292) Ho, K.; Krogmann, D. *Biochim. Biophys. Acta, Bioenerg.* **1984**, *766*, 310.

(293) Navarro, J.; Hervás, M.; De la Rosa, M. *JBIC, J. Biol. Inorg. Chem.* **1997**, *2*, 11.

(294) De la Rosa, M. A.; Navarro, J.; Díaz-Quintana, A.; De la Cerda, B.; Molina-Heredia, F. P.; Balme, A.; Murdoch, P. d. S.; Díaz-Moreno, I.; Durán, R.; Hervás, M. *Bioelectrochemistry* **2002**, *55*, 41.

(295) Malakhov, M. P.; Malakhova, O. A.; Murata, N. *FEBS Lett.* **1999**, *444*, 281.

(296) Molina-Heredia, F. P.; Balme, A.; Hervás, M.; Navarro, J.; De la Rosa, M. A. *FEBS Lett.* **2002**, *517*, 50.

(297) Leys, D.; Backers, K.; Meyer, T. E.; Hagen, W. R.; Cusanovich, M. A.; Van Beeumen, J. J. *J. Biol. Chem.* **2000**, *275*, 16050.

(298) Blakemore, R.; Maratea, D.; Wolfe, R. *J. Bacteriol.* **1979**, *140*, 720.

(299) Richardson, D. J. *Microbiology* **2000**, *146*, 551.

(300) Czjzek, M.; Arnoux, P.; Haser, R.; Shepard, W. *Acta Crystallogr., Sect. D: Biol. Crystallogr.* **2001**, *57*, 670.

(301) Dantas, J. M.; Saraiva, I. H.; Morgado, L.; Silva, M. A.; Schiffer, M.; Salgueiro, C. A.; Louro, R. O. *Dalton Trans.* **2011**, *40*, 12713.

(302) Morgado, L.; Bruix, M.; Pessanha, M.; Londer, Y. Y.; Salgueiro, C. A. *Biophys. J.* **2010**, *99*, 293.

(303) Pokkuluri, P.; Londer, Y.; Yang, X.; Duke, N.; Erickson, J.; Orshonsky, V.; Johnson, G.; Schiffer, M. *Biochim. Biophys. Acta, Bioenerg.* **2010**, *1797*, 222.

(304) Dahl, C.; Engels, S.; Pott-Sperling, A. S.; Schulte, A.; Sander, J.; Lubbe, Y.; Deuster, O.; Brune, D. C. *J. Bacteriol.* **2005**, *187*, 1392.

(305) Roldάn, M. D.; Sears, H. J.; Cheesman, M. R.; Ferguson, S. J.; Thomson, A. J.; Berks, B. C.; Richardson, D. J. *J. Biol. Chem.* **1998**, *273*, 28785.

(306) Dobbin, P.; Butt, J.; Powell, A.; Reid, G.; Richardson, D. *Biochem. J* **1999**, *342*, 439.

(307) Igarashi, N.; Moriyama, H.; Fujiwara, T.; Fukumori, Y.; Tanaka, N. *Nat. Struct. Mol. Biol.* **1997**, *4*, 276.

(308) Einsle, O.; Messerschmidt, A.; Stach, P.; Bourenkov, G. P.; Bartunik, H. D.; Huber, R.; Kroneck, P. M. *Nature* **1999**, *400*, 476.

(309) Kemp, G.; Clarke, T.; Marritt, S.; Lockwood, C.; Poock, S.; Hemmings, A.; Richardson, D.; Cheesman, M.; Butt, J. *Biochem. J* **2010**, *431*, 73.

(310) Bamford, V.; Dobbin, P. S.; Richardson, D. J.; Hemmings, A. M. *Nat. Struct. Mol. Biol.* **1999**, *6*, 1104.

(311) Leys, D.; Tsapin, A. S.; Nealson, K. H.; Meyer, T. E.; Cusanovich, M. A.; Van Beeumen, J. J. *Nat. Struct. Mol. Biol.* **1999**, *6*, 1113.

(312) Taylor, P.; Pealing, S. L.; Reid, G. A.; Chapman, S. K.; Walkinshaw, M. D. *Nat. Struct. Mol. Biol.* **1999**, *6*, 1108.

(313) Field, S. J.; Dobbin, P. S.; Cheesman, M. R.; Watmough, N. J.; Thomson, A. J.; Richardson, D. J. *J. Biol. Chem.* **2000**, *275*, 8515.

(314) Simon, J. r.; Pisa, R.; Stein, T.; Eichler, R.; Klimmek, O.; Gross, R. *Eur. J. Biochem.* **2001**, *268*, 5776.

(315) Bewley, K.; FirerSherwood, M.; Mock, J.; Ando, N.; Drennan, C.; Elliott, S. *Biochem. Soc. Trans.* **2012**, *40*, 1268.

(316) Clarke, T. A.; Edwards, M. J.; Gates, A. J.; Hall, A.; White, G. F.; Bradley, J.; Reardon, C. L.; Shi, L.; Beliaev, A. S.; Marshall, M. J.; Wang, Z.; Watmough, N. J.; Fredrickson, J. K.; Zachara, J. M.; Butt, J. N.; Richardson, D. J. *Proc. Natl. Acad. Sci. U. S. A.* **2011**, *108*, 9384.

(317) Gralnick, J. A.; Vali, H.; Lies, D. P.; Newman, D. K. *Proc. Natl. Acad. Sci. U. S. A.* **2006**, *103*, 4669.

(318) Lovley, D. R. *Annu. Rev. Microbiol.* **1993**, *47*, 263.

(319) Myers, C. R.; Myers, J. M. *J. Bacteriol.* **1997**, *179*, 1143.

(320) Myers, C. R.; Myers, J. M. *Biochim. Biophys. Acta* **1997**, *1326*, 307.

(321) Myers, C. R.; Nealson, K. H. *Science* **1988**, *240*, 1319.

(322) Nealson, K. H. *Prokaryotes.*; Springer: Berlin, 2006.

(323) Schwalb, C.; Chapman, S. K.; Reid, G. A. *Biochemistry* **2003**, *42*, 9491.

(324) Shi, L.; Richardson, D. J.; Wang, Z.; Kerisit, S. N.; Rosso, K. M.; Zachara, J. M.; Fredrickson, J. K. *Environ. Microbiol. Rep.* **2009**, *1*, 220.

(325) Myers, J. M.; Myers, C. R. *J. Bacteriol.* **2000**, *182*, 67.

(326) Dohnalkova, A. C.; Marshall, M. J.; Arey, B. W.; Williams, K. H.; Buck, E. C.; Fredrickson, J. K. *Appl. Environ. Microbiol.* **2011** *77* 1254.

(327) Firer-Sherwood, M.; Pulcu, G. S.; Elliott, S. J. *JBIC, J. Biol. Inorg. Chem.* **2008**, *13*, 849.

(328) Hartshorne, R. S.; Reardon, C. L.; Ross, D.; Nuester, J.; Clarke, T. A.; Gates, A. J.; Mills, P. C.; Fredrickson, J. K.; Zachara, J. M.; Shi, L.; Beliaev, A. S.; Marshall, M. J.; Tien, M.; Brantley, S.; Butt, J. N.; Richardson, D. J. *Proc. Natl. Acad. Sci. U. S. A.* **2009** *106* 22169.

(329) Pitts, K. E.; Dobbin, P. S.; Reyes-Ramirez, F.; Thomson, A. J.; Richardson, D. J.; Seward, H. E. *J. Biol. Chem.* **2003**, *278*, 27758.

(330) Firer-Sherwood, M. A.; Ando, N.; Drennan, C. L.; Elliott, S. J. *J. Phys. Chem. B* **2011**, *115*, 11208.

(331) Fonseca, B. M.; Paquete, C. M.; Neto, S. E.; Pacheco, I.; Soares, C. M.; Louro, R. O. *Biochem. J.* **2013**, *449*, 101.

(332) Coursolle, D.; Gralnick, J. A. *Mol. Microbiol.* **2010**, *77*, 995.

(333) Shi, L.; Squier, T. C.; Zachara, J. M.; Fredrickson, J. K. *Mol. Microbiol.* **2007**, *65*, 12.

(334) Breuer, M.; Zarzycki, P.; Blumberger, J.; Rosso, K. M. *J. Am. Chem. Soc.* **2012**, *134*, 9868.

(335) Breuer, M.; Zarzycki, P.; Shi, L.; Clarke, T. A.; Edwards, M. J.; Butt, J. N.; Richardson, D. J.; Fredrickson, J. K.; Zachara, J. M.; Blumberger, J.; Rosso, K. M. *Biochem. Soc. Trans.* **2012**, *40*, 1198.

(336) Beliaev, A. S.; Saffarini, D. A. *J. Bacteriol.* **1998**, *180*, 6292.

(337) Ma, J. G.; Zhang, J.; Franco, R.; Jia, S. L.; Moura, I.; Moura, J. J.; Kroneck, P. M.; Shelnutt, J. A. *Biochemistry* **1998**, *37*, 12431.

(338) Pieulle, L.; Haladjian, J.; Bonicel, J.; Hatchikian, E. C. *Biochim. Biophys. Acta* **1996**, *1273*, 51.

(339) Coutinho, I. B.; Xavier, A. V. *Methods Enzymol.* **1994**, *243*, 119.

(340) Louro, R. O.; Catarino, T.; LeGall, J.; Turner, D. L.; Xavier, A. V. *ChemBioChem* **2001**, *2*, 831.

(341) Martel, P. J.; Soares, C. M.; Baptista, A. M.; Fuxreiter, M.; Naray-Szabo, G.; Louro, R. O.; Carrondo, M. A. *J. Biol. Inorg. Chem.* **1999**, *4*, 73.

(342) Park, J. S.; Ohmura, T.; Kano, K.; Sagara, T.; Niki, K.; Kyogoku, Y.; Akutsu, H. *Biochim. Biophys. Acta* **1996**, *1293*, 45.

(343) Brennan, L.; Turner, D. L.; Messias, A. C.; Teodoro, M. L.; LeGall, J.; Santos, H.; Xavier, A. V. *J. Mol. Biol.* **2000**, *298*, 61.

(344) Harada, E.; Fukuoka, Y.; Ohmura, T.; Fukunishi, A.; Kawai, G.; Fujiwara, T.; Akutsu, H. *J. Mol. Biol.* **2002**, *319*, 767.

(345) Salgueiro, C. A.; da Costa, P. N.; Turner, D. L.; Messias, A. C.; van Dongen, W. M.; Saraiva, L. M.; Xavier, A. V. *Biochemistry* **2001**, *40*, 9709.

(346) Matias, P. M.; Pereira, I. A.; Soares, C. M.; Carrondo, M. A. *Prog. Biophys. Mol. Biol.* **2005**, *89*, 292.

(347) Norager, S.; Legrand, P.; Pieulle, L.; Hatchikian, C.; Roth, M. *J. Mol. Biol.* **1999**, *290*, 881.

(348) Pieulle, L.; Morelli, X.; Gallice, P.; Lojou, E.; Barbier, P.; Czjzek, M.; Bianco, P.; Guerlesquin, F.; Hatchikian, E. C. *J. Mol. Biol.* **2005**, *354*, 73.

(349) Quintas, P. O.; Oliveira, M. S.; Catarino, T.; Turner, D. L. *Biochim. Biophys. Acta* **2013**, *1827*, 502.

(350) Lederer, F. *Biochimie* **1994**, *76*, 674.

(351) Qian, W.; Wang, Y.-H.; Wang, W.-H.; Yao, P.; Zhuang, J.-H.; Xie, Y.; Huang, Z.-X. *J. Electroanal. Chem.* **2002**, *535*, 85.

(352) Schenkman, J. B.; Jansson, I. *Pharmacol. Ther.* **2003**, *97*, 139.

(353) Vergeres, G.; Waskell, L. *Biochimie* **1995**, *77*, 604.

(354) Hultquist, D. E.; Passon, P. G. *Nat. New Biol.* **1971**, *229*, 252.

(355) Sannes, L. J.; Hultquist, D. E. *Biochim. Biophys. Acta* **1978**, *544*, 547.

(356) Strittmatter, P.; Spatz, L.; Corcoran, D.; Rogers, M. J.; Setlow, B.; Redline, R. *Proc. Natl. Acad. Sci. U. S. A.* **1974**, *71*, 4565.

(357) Parthasarathy, S.; Altuve, A.; Terzyan, S.; Zhang, X.; Kuczera, K.; Rivera, M.; Benson, D. R. *Biochemistry* **2011**, *50*, 5544.

(358) Altuve, A.; Silchenko, S.; Lee, K. H.; Kuczera, K.; Terzyan, S.; Zhang, X.; Benson, D. R.; Rivera, M. *Biochemistry* **2001**, *40*, 9469.

(359) Borgese, N.; D'Arrigo, A.; De Silvestris, M.; Pietrini, G. *FEBS Lett.* **1993**, *325*, 70.

(360) Fukushima, K.; Sato, R. *J. Biochem.* **1973**, *74*, 161.

(361) Kuroda, R.; Ikenoue, T.; Honsho, M.; Tsujimoto, S.; Mitoma, J. Y.; Ito, A. *J. Biol. Chem.* **1998**, *273*, 31097.

(362) Mitoma, J.; Ito, A. *EMBO J.* **1992**, *11*, 4197.

(363) Rivera, M.; Wells, M. A.; Walker, F. A. *Biochemistry* **1994**, *33*, 2161.

(364) Ito, A.; Hayashi, S.; Yoshida, T. *Biochem. Biophys. Res. Commun.* **1981**, *101*, 591.

(365) Nishino, H.; Ito, A. *J. Biochem.* **1986**, *100*, 1523.

(366) Durley, R. C.; Mathews, F. S. *Acta Crystallogr. D Biol. Crystallogr.* **1996**, *52*, 65.

(367) Alam, S.; Yee, J.; Couture, M.; Takayama, S. J.; Tseng, W. H.; Mauk, A. G.; Rafferty, S. *Metallomics* **2012**, *4*, 1255.

(368) La Mar, G. N.; Burns, P. D.; Jackson, J. T.; Smith, K. M.; Langry, K. C.; Strittmatter, P. *J. Biol. Chem.* **1981**, *256*, 6075.

(369) Kababya, S.; Nelson, J.; Calle, C.; Neese, F.; Goldfarb, D. *J. Am. Chem. Soc.* **2006**, *128*, 2017.

(370) Keller, R.; Groudinsky, O.; Wuthrich, K. *Biochim. Biophys. Acta* **1976**, *427*, 497.

(371) Keller, R. M.; Wuthrich, K. *Biochim. Biophys. Acta* **1972**, *285*, 326.

(372) Keller, R. M.; Wuthrich, K. *Biochim. Biophys. Acta* **1980**, *621*, 204.

(373) McLachlan, S. J.; La Mar, G. N.; Burns, P. D.; Smith, K. M.; Langry, K. C. *Biochim. Biophys. Acta* **1986**, *874*, 274.

(374) Lee, K. B.; La Mar, G. N.; Kehres, L. A.; Fujinari, E. M.; Smith, K. M.; Pochapsky, T. C.; Sligar, S. G. *Biochemistry* **1990**, *29*, 9623.

(375) Rivera, M.; Barillas-Mury, C.; Christensen, K. A.; Little, J. W.; Wells, M. A.; Walker, F. A. *Biochemistry* **1992**, *31*, 12233.

(376) Lee, K.; La Mar, G. N.; Pandey, R. K.; Rezzano, I. N.; Mansfield, K. E.; Smith, K. M.; Pochapsky, T. C.; Sligar, S. G. *Biochemistry* **1991**, *30*, 1878.

(377) Guiles, R. D.; Basus, V. J.; Kuntz, I. D.; Waskell, L. *Biochemistry* **1992**, *31*, 11365.

(378) Lee, K. B.; La Mar, G. N.; Mansfield, K. E.; Smith, K. M.; Pochapsky, T. C.; Sligar, S. G. *Biochim. Biophys. Acta* **1993**, *1202*, 189.

(379) McLachlan, S. J.; La Mar, G. N.; Lee, K. B. *Biochim. Biophys. Acta* **1988**, *957*, 430.

(380) Veitch, N. C.; Whitford, D.; Williams, R. J. *FEBS Lett.* **1990**, *269*, 297.

(381) Arnesano, F.; Banci, L.; Bertini, I.; Faraone-Mennella, J.; Rosato, A.; Barker, P. D.; Fersht, A. R. *Biochemistry* **1999**, *38*, 8657.

(382) Hamada, K.; Bethge, P. H.; Mathews, F. S. *J. Mol. Biol.* **1995**, *247*, 947.

(383) Wittung-Stafshede, P.; Gray, H. B.; Winkler, J. R. *J. Am. Chem. Soc.* **1997**, *119*, 9562.

(384) Bixler, J.; Bakker, G.; McLendon, G. *J. Am. Chem. Soc.* **1992**, *114*, 6938.

(385) Pascher, T.; Chesick, J. P.; Winkler, J. R.; Gray, H. B. *Science* **1996**, *271*, 1558.

(386) Tezcan, F. A.; Winkler, J. R.; Gray, H. B. *J. Am. Chem. Soc.* **1998**, *120*, 13383.

(387) Winkler, J. R.; Wittung-Stafshede, P.; Leckner, J.; Malmstrom, B. G.; Gray, H. B. *Proc. Natl. Acad. Sci. U. S. A.* **1997**, *94*, 4246.

(388) Wittung-Stafshede, P.; Lee, J. C.; Winkler, J. R.; Gray, H. B. *Proc. Natl. Acad. Sci. U. S. A.* **1999**, *96*, 6587.

(389) Choma, C. T.; Lear, J. D.; Nelson, M. J.; Dutton, P. L.; Robertson, D. E.; DeGrado, W. F. *J. Am. Chem. Soc.* **1994**, *116*, 856.

(390) DeGrado, W. F.; Regan, L.; Ho, S. P. *Cold Spring Harbor Symp. Quant. Biol.* **1987**, *52*, 521.

(391) Regan, L.; DeGrado, W. F. *Science* **1988**, *241*, 976.
(392) DeGrado, W. F.; Wasserman, Z. R.; Lear, J. D. *Science* **1989**, *243*, 622.
(393) Robertson, D. E.; Farid, R. S.; Moser, C. C.; Urbauer, J. L.; Mulholland, S. E.; Pidikiti, R.; Lear, J. D.; Wand, A. J.; DeGrado, W. F.; Dutton, P. L. *Nature* **1994**, *368*, 425.
(394) Kalsbeck, W. A.; Robertson, D. E.; Pandey, R. K.; Smith, K. M.; Dutton, P. L.; Bocian, D. F. *Biochemistry* **1996**, *35*, 3429.
(395) Shifman, J. M.; Gibney, B. R.; Sharp, R. E.; Dutton, P. L. *Biochemistry* **2000**, *39*, 14813.
(396) Ishida, M.; Dohmae, N.; Shiro, Y.; Oku, T.; Iizuka, T.; Isogai, Y. *Biochemistry* **2004**, *43*, 9823.
(397) Gibney, B. R.; Rabanal, F.; Skalicky, J. J.; Wand, A. J.; Dutton, P. L. *J. Am. Chem. Soc.* **1997**, *119*, 2323.
(398) Gibney, B. R.; Rabanal, F.; Reddy, K. S.; Dutton, P. L. *Biochemistry* **1998**, *37*, 4635.
(399) Chen, X.; Discher, B. M.; Pilloud, D. L.; Gibney, B. R.; Moser, C. C.; Dutton, P. L. *J. Phys. Chem. B* **2001**, *106*, 617.
(400) Privett, H. K.; Reedy, C. J.; Kennedy, M. L.; Gibney, B. R. *J. Am. Chem. Soc.* **2002**, *124*, 6828.
(401) Gibney, B. R.; Isogai, Y.; Rabanal, F.; Reddy, K. S.; Grosset, A. M.; Moser, C. C.; Dutton, P. L. *Biochemistry* **2000**, *39*, 11041.
(402) Reddi, A. R.; Reedy, C. J.; Mui, S.; Gibney, B. R. *Biochemistry* **2007**, *46*, 291.
(403) Huang, S. S.; Koder, R. L.; Lewis, M.; Wand, A. J.; Dutton, P. L. *Proc. Natl. Acad. Sci. U. S. A.* **2004**, *101*, 5536.
(404) Discher, B. M.; Noy, D.; Strzalka, J.; Ye, S. X.; Moser, C. C.; Lear, J. D.; Blasie, J. K.; Dutton, P. L. *Biochemistry* **2005**, *44*, 12329.
(405) Ghirlanda, G.; Osyczka, A.; Liu, W.; Antolovich, M.; Smith, K. M.; Dutton, P. L.; Wand, A. J.; DeGrado, W. F. *J. Am. Chem. Soc.* **2004**, *126*, 8141.
(406) Farid, T. A.; Kodali, G.; Solomon, L. A.; Lichtenstein, B. R.; Sheehan, M. M.; Fry, B. A.; Bialas, C.; Ennist, N. M.; Siedlecki, J. A.; Zhao, Z.; Stetz, M. A.; Valentine, K. G.; Anderson, J. L. R.; Wand, A. J.; Discher, B. M.; Moser, C. C.; Dutton, P. L. *Nat. Chem. Biol.* **2013**, *9*, 826.
(407) Costanzo, L.; Geremia, S.; Randaccio, L.; Nastri, F.; Maglio, O.; Lombardi, A.; Pavone, V. *JBIC, J. Biol. Inorg. Chem.* **2004**, *9*, 1017.
(408) Bender, G. M.; Lehmann, A.; Zou, H.; Cheng, H.; Fry, H. C.; Engel, D.; Therien, M. J.; Blasie, J. K.; Roder, H.; Saven, J. G.; DeGrado, W. F. *J. Am. Chem. Soc.* **2007**, *129*, 10732.
(409) Korendovych, I. V.; Senes, A.; Kim, Y. H.; Lear, J. D.; Fry, H. C.; Therien, M. J.; Blasie, J. K.; Walker, F. A.; DeGrado, W. F. *J. Am. Chem. Soc.* **2010**, *132*, 15516.
(410) Anderson, J. L. R.; Armstrong, C. T.; Kodali, G.; Lichtenstein, B. R.; Watkins, D. W.; Mancini, J. A.; Boyle, A. L.; Farid, T. A.; Crump, M. P.; Moser, C. C.; Dutton, P. L. *Chem. Sci.* **2014**.
(411) Jiang, X.; Pistor, E.; Farid, R. S.; Farid, H. *Protein Sci.* **2000**, *9*, 403.
(412) Xu, Z.; Farid, R. S. *Protein Sci.* **2001**, *10*, 236.
(413) Hecht, M. H.; Vogel, K. M.; Spiro, T. G.; Rojas, N. R. L.; Kamtekar, S.; Simons, C. T.; McLean, J. E.; Farid, R. S. *Protein Sci.* **1997**, *6*, 2512.
(414) Wei, Y. N.; Liu, T.; Sazinsky, S. L.; Moffet, D. A.; Pelczer, I.; Hecht, M. H. *Protein Sci.* **2003**, *12*, 92.
(415) Moffet, D. A.; Foley, J.; Hecht, M. H. *Biophys. Chem.* **2003**, *105*, 231.
(416) Das, A.; Trammell, S. A.; Hecht, M. H. *Biophys. Chem.* **2006**, *123*, 102.
(417) Rau, H. K.; Haehnel, W. *J. Am. Chem. Soc.* **1998**, *120*, 468.
(418) Rau, H. K.; DeJonge, N.; Haehnel, W. *Angew. Chem., Int. Ed.* **2000**, *39*, 250.

(419) Albrecht, T.; Li, W. W.; Ulstrup, J.; Haehnel, W.; Hildebrandt, P. *ChemPhysChem* **2005**, *6*, 961.

(420) Albrecht, T.; Li, W.-W.; Haehnel, W.; Hildebrandt, P.; Ulstrup, J. *Bioelectrochemistry* **2006**, *69*, 193.

(421) Benson, D. R.; Hart, B. R.; Zhu, X.; Doughty, M. B. *J. Am. Chem. Soc.* **1995**, *117*, 8502.

(422) Arnold, P. A.; Benson, D. R.; Brink, D. J.; Hendrich, M. P.; Jas, G. S.; Kennedy, M. L.; Petasis, D. T.; Wang, M. *Inorg. Chem.* **1997**, *36*, 5306.

(423) Liu, D.; Williamson, D. A.; Kennedy, M. L.; Williams, T. D.; Morton, M. M.; Benson, D. R. *J. Am. Chem. Soc.* **1999**, *121*, 11798.

(424) Liu, D.; Lee, K.-H.; R. Benson, D. *Chem. Commun.* **1999**, 1205.

(425) Cowley, A. B.; Kennedy, M. L.; Silchenko, S.; Lukat-Rodgers, G. S.; Rodgers, K. R.; Benson, D. R. *Inorg. Chem.* **2006**, *45*, 9985.

(426) Nastri, F.; Lombardi, A.; Morelli, G.; Maglio, O.; Dauria, G.; Pedone, C.; Pavone, V. *Chem. - Eur. J.* **1997**, *3*, 340.

(427) D'Auria, M.; Racioppi, R. *Tetrahedron* **1997**, *53*, 17307.

(428) Lombardi, A.; Nastri, F.; Sanseverino, M.; Maglio, O.; Pedone, C.; Pavone, V. *Inorg. Chim. Acta* **1998**, *276*, 301.

(429) Lombardi, A.; Nastri, F.; Marasco, D.; Maglio, O.; De Sanctis, G.; Sinibaldi, F.; Santucci, R.; Coletta, M.; Pavone, V. *Chem. - Eur. J.* **2003**, *9*, 5643.

(430) Arnold, P. A.; Shelton, W. R.; Benson, D. R. *J. Am. Chem. Soc.* **1997**, *119*, 3181.

(431) Huffman, D. L.; Rosenblatt, M. M.; Suslick, K. S. *J. Am. Chem. Soc.* **1998**, *120*, 6183.

(432) Huffman, D. L.; Suslick, K. S. *Inorg. Chem.* **2000**, *39*, 5418.

(433) Rosenblatt, M. M.; Huffman, D. L.; Wang, X.; Remmer, H. A.; Suslick, K. S. *J. Am. Chem. Soc.* **2002**, *124*, 12394.

(434) Rosenblatt, M. M.; Wang, J.; Suslick, K. S. *Proc. Natl. Acad. Sci. U. S. A.* **2003**, *100*, 13140.

(435) Isogai, Y.; Ota, M.; Fujisawa, T.; Izuno, H.; Mukai, M.; Nakamura, H.; Iizuka, T.; Nishikawa, K. *Biochemistry* **1999**, *38*, 7431.

(436) Isogai, Y.; Ishii, A.; Fujisawa, T.; Ota, M.; Nishikawa, K. *Biochemistry* **2000**, *39*, 5683.

(437) Isogai, Y.; Ishida, M. *Biochemistry* **2009**, *48*, 8136.

(438) Qin, J.; La Mar, G. N.; Dou, Y.; Admiraal, S. J.; Ikeda-Saito, M. *J. Biol. Chem.* **1994**, *269*, 1083.

(439) Lloyd, E.; Hildebrand, D. P.; Tu, K. M.; Mauk, A. G. *J. Am. Chem. Soc.* **1995**, *117*, 6434.

(440) Dou, Y.; Admiraal, S. J.; Ikeda-Saito, M.; Krzywda, S.; Wilkinson, A. J.; Li, T.; Olson, J. S.; Prince, R. C.; Pickering, I. J.; George, G. N. *J. Biol. Chem.* **1995**, *270*, 15993.

(441) Shinde, S.; Cordova, J. M.; Woodrum, B. W.; Ghirlanda, G. *JBIC, J. Biol. Inorg. Chem.* **2012**, *17*, 557.

(442) Wilson, J. R.; Caruana, D. J.; Gilardi, G. *Chem. Commun.* **2003**, 356.

(443) Di Nardo, G.; Di Venere, A.; Mei, G.; Sadeghi, S. J.; Wilson, J. R.; Gilardi, G. *JBIC, J. Biol. Inorg. Chem.* **2009**, *14*, 497.

(444) Cordova, J. M.; Noack, P. L.; Hilcove, S. A.; Lear, J. D.; Ghirlanda, G. *J. Am. Chem. Soc.* **2007**, *129*, 512.

(445) Ibrahim, S. M.; Nakajima, H.; Ohta, T.; Ramanathan, K.; Takatani, N.; Naruta, Y.; Watanabe, Y. *Biochemistry* **2011**, *50*, 9826.

(446) Tomlinson, E. J.; Ferguson, S. J. *J. Biol. Chem.* **2000**, *275*, 32530.

(447) Tomlinson, E. J.; Ferguson, S. J. *Proc. Natl. Acad. Sci. U. S. A.* **2000**, *97*, 5156.

(448) Barker, P. D.; Ferrer, J. C.; Mylrajan, M.; Loehr, T. M.; Feng, R.; Konishi, Y.; Funk, W. D.; MacGillivray, R. T.; Mauk, A. G. *Proc. Natl. Acad. Sci. U. S. A.* **1993**, *90*, 6542.

(449) Barker, P. D.; Nerou, E. P.; Freund, S. M.; Fearnley, I. M. *Biochemistry* **1995**, *34*, 15191.
(450) Wain, R.; Redfield, C.; Ferguson, S. J.; Smith, L. J. *J. Biol. Chem.* **2004**, *279*, 15177.
(451) Arnesano, F.; Banci, L.; Bertini, I.; Ciofi-Baffoni, S.; Woodyear, T. L.; Johnson, C. M.; Barker, P. D. *Biochemistry* **2000**, *39*, 1499.
(452) Watt, G. D.; Frankel, R. B.; Papaefthymiou, G. C.; Spartalian, K.; Stiefel, E. I. *Biochemistry* **1986**, *25*, 4330.
(453) Lember, R.; Barrett, J. *Cytochromes*; Academic Press: London, 1973.
(454) Barker, P. D.; Ferguson, S. J. *Structure* **1999**, *7*, R281.
(455) Allen, J. W. A.; Barker, P. D.; Daltrop, O.; Stevens, J. M.; Tomlinson, E. J.; Sinha, N.; Sambongi, Y.; Ferguson, S. J. *Dalton Trans.* **2005**, *0*, 3410.
(456) Bowman, S. E. J.; Bren, K. L. *Nat. Prod. Rep.* **2008**, *25*, 1118.
(457) Zheng, Z.; Gunner, M. R. *Proteins: Struct., Funct., Bioinf.* **2009**, *75*, 719.
(458) Contreras-Zentella, M.; Mendoza, G.; Membrillo-Hernández, J.; Escamilla, J. E. *J. Biol. Chem.* **2003**, *278*, 31473.
(459) Zhuang, J.; Amoroso, J. H.; Kinloch, R.; Dawson, J. H.; Baldwin, M. J.; Gibney, B. R. *Inorg. Chem.* **2006**, *45*, 4685.
(460) Zhuang, J.; Reddi, A. R.; Wang, Z.; Khodaverdian, B.; Hegg, E. L.; Gibney, B. R. *Biochemistry* **2006**, *45*, 12530.
(461) Raphael, A. L.; Gray, H. B. *Proteins: Struct., Funct., Bioinf.* **1989**, *6*, 338.
(462) Hay, S.; Wydrzynski, T. *Biochemistry* **2004**, *44*, 431.
(463) Miller, G. T.; Zhang, B.; Hardman, J. K.; Timkovich, R. *Biochemistry* **2000**, *39*, 9010.
(464) Sligar, S. G.; Egeberg, K. D.; Sage, J. T.; Morikis, D.; Champion, P. M. *J. Am. Chem. Soc.* **1987**, *109*, 7896.
(465) Barker, P. D.; Nerou, E. P.; Cheesman, M. R.; Thomson, A. J.; de Oliveira, P.; Hill, H. A. O. *Biochemistry* **1996**, *35*, 13618.
(466) Barker, P. D.; Freund, S. M. *Biochemistry* **1996**, *35*, 13627.
(467) Cheesman, M. R.; Kadir, F. H.; al-Basseet, J.; al-Massad, F.; Farrar, J.; Greenwood, C.; Thomson, A. J.; Moore, G. R. *Biochem. J.* **1992**, *286 (Pt 2)*, 361.
(468) Kassner, R. J. *Proc. Natl. Acad. Sci. U. S. A.* **1972**, *69*, 2263.
(469) Churg, A. K.; Warshel, A. *Biochemistry* **1986**, *25*, 1675.
(470) Battistuzzi, G.; Borsari, M.; Cowan, J. A.; Ranieri, A.; Sola, M. *J. Am. Chem. Soc.* **2002**, *124*, 5315.
(471) Stellwagen, E. *Nature* **1978**, *275*, 73.
(472) Paoli, M.; Marles-Wright, J.; Smith, A. *DNA Cell Biol.* **2002**, *21*, 271.
(473) Warshel, A.; Papazyan, A.; Muegge, I. *JBIC, J. Biol. Inorg. Chem.* **1997**, *2*, 143.
(474) Bowman, S. E. J.; Bren, K. L. *Inorg. Chem.* **2010**, *49*, 7890.
(475) Banci, L.; Bertini, I.; Turano, P.; Tien, M.; Kirk, T. K. *Proc. Natl. Acad. Sci. U. S. A.* **1991**, *88*, 6956.
(476) Berghuis, A. M.; Guillemette, J. G.; Smith, M.; Brayer, G. D. *J. Mol. Biol.* **1994**, *235*, 1326.
(477) Ye, T.; Kaur, R.; Wen, X.; Bren, K. L.; Elliott, S. J. *Inorg. Chem.* **2005**, *44*, 8999.
(478) Ozawa, K.; Takayama, Y.; Yasukawa, F.; Ohmura, T.; Cusanovich, M. A.; Tomimoto, Y.; Ogata, H.; Higuchi, Y.; Akutsu, H. *Biophys. J.* **2003**, *85*, 3367.
(479) Worrall, J. A. R.; Schlarb-Ridley, B. G.; Reda, T.; Marcaida, M. J.; Moorlen, R. J.; Wastl, J.; Hirst, J.; Bendall, D. S.; Luisi, B. F.; Howe, C. J. *J. Am. Chem. Soc.* **2007**, *129*, 9468.
(480) Lett, C. M.; Guillemette, J. G. *Biochem. J.* **2002**, *362*, 281.
(481) Varadarajan, R.; Zewert, T.; Gray, H.; Boxer, S. *Science* **1989**, *243*, 69.

(482) Springs, S. L.; Bass, S. E.; Bowman, G.; Nodelman, I.; Schutt, C. E.; McLendon, G. L. *Biochemistry* **2002**, *41*, 4321.

(483) Tai, H.; Mikami, S.-i.; Irie, K.; Watanabe, N.; Shinohara, N.; Yamamoto, Y. *Biochemistry* **2009**, *49*, 42.

(484) Takayama, Y.; Taketa-Sato, M.; Komori, H.; Morita, K.; Kang, S.-J.; Higuchi, Y.; Akutsu, H. *Bull. Chem. Soc. Jpn.* **2011**, *84*, 1096.

(485) Moore, G. R. *FEBS Lett.* **1983**, *161*, 171.

(486) Mikami, S.-i.; Tai, H.; Yamamoto, Y. *Biochemistry* **2009**, *48*, 8062.

(487) Tai, H.; Udagawa, T.; Mikami, S.-i.; Sugimoto, A.; Yamamoto, Y. *J. Inorg. Biochem.* **2012**, *108*, 182.

(488) Louro, R. O.; Catarino, T.; Salgueiro, C. A.; LeGall, J.; Xavier, A. V. *JBIC, J. Biol. Inorg. Chem.* **1996**, *1*, 34.

(489) Matsuno, T.; Morishita, N.; Yamazaki, K.; Inoue, N.; Sato, Y.; Ichise, N.; Hara, I.; Hoshino, T.; Matsuyama, H.; Yoshimune, K.; Yumoto, I. *J. Biosci. Bioeng.* **2007**, *103*, 247.

(490) Shibamoto, T.; Kato, Y.; Watanabe, T. *FEBS Lett.* **2008**, *582*, 1490.

(491) Moore, G. R.; Pettigrew, G. W.; Pitt, R. C.; Williams, R. J. P. *Biochim. Biophys. Acta, Bioenerg.* **1980**, *590*, 261.

(492) Takayama, S. J.; Mikami, S.; Terui, N.; Mita, H.; Hasegawa, J.; Sambongi, Y.; Yamamoto, Y. *Biochemistry* **2005**, *44*, 5488.

(493) Pettigrew, G. W.; Bartsch, R. G.; Meyer, T. E.; Kamen, M. D. *Biochim. Biophys. Acta* **1978**, *503*, 509.

(494) Shifman, J. M.; Moser, C. C.; Kalsbeck, W. A.; Bocian, D. F.; Dutton, P. L. *Biochemistry* **1998**, *37*, 16815.

(495) Reid, L. S.; Mauk, M. R.; Mauk, A. G. *J. Am. Chem. Soc.* **1984**, *106*, 2182.

(496) Hunter, C. L.; Lloyd, E.; Eltis, L. D.; Rafferty, S. P.; Lee, H.; Smith, M.; Mauk, A. G. *Biochemistry* **1997**, *36*, 1010.

(497) Chapman, S. K.; Daff, S.; Munro, A. W. In *Metal Sites in Proteins and Models*; Hill, H. A. O., Sadler, P. J., Thomson, A. J., Eds.; Springer Berlin Heidelberg: 1997; Vol. 88, p 39.

(498) Fan, K.; Akutsu, H.; Kyogoku, Y.; Niki, K. *Biochemistry* **1990**, *29*, 2257.

(499) Santos, H.; Moura, J. J. G.; Moura, I.; Legall, J.; Xavier, A. V. *Eur. J. Biochem.* **1984**, *141*, 283.

(500) Coletta, M.; Catarino, T.; Legall, J.; Xavier, A. V. *Eur. J. Biochem.* **1991**, *202*, 1101.

(501) Correia, I. J.; Paquete, C. M.; Coelho, A.; Almeida, C. C.; Catarino, T.; Louro, R. O.; Frazão, C.; Saraiva, L. M.; Carrondo, M. A.; Turner, D. L.; Xavier , A. V. *J. Biol. Chem.* **2004**, *279*, 52227.

(502) Louro, R. O. *JBIC, J. Biol. Inorg. Chem.* **2007**, *12*, 1.

(503) Teixeira, V. H.; Soares, C. M.; Baptista, A. M. *JBIC, J. Biol. Inorg. Chem.* **2002**, *7*, 200.

(504) Louro, R. O.; Catarino, T.; Turner, D. L.; Piçarra-Pereira, M. A.; Pacheco, I.; LeGall, J.; Xavier, A. V. *Biochemistry* **1998**, *37*, 15808.

(505) Yoshikawa, S.; Muramoto, K.; Shinzawa-Itoh, K. *Annu. Rev. Biophys.* **2011**, *40*, 205.

(506) Michel, H. *Biochemistry* **1999**, *38*, 15129.

(507) Kaila, V. R. I.; Verkhovsky, M. I.; Wikström, M. *Chem. Rev.* **2010**, *110*, 7062.

(508) Senge, M. O. *Chem. Commun.* **2006**, *0*, 243.

(509) Roder, B.; Buchner, M.; Ruckmann, I.; Senge, M. O. *Photochem. Photobiol. Sci.* **2010**, *9*, 1152.

(510) Jentzen, W.; Ma, J.-G.; Shelnutt, J. A. *Biophys. J.* **1998**, *74*, 753.

(511) Senge, M. O. *J. Photochem. Photobiol., B* **1992**, *16*, 3.

(512) Hobbs, J.; Shelnutt, J. *J. Protein Chem.* **1995**, *14*, 19.

(513) Olea, C.; Kuriyan, J.; Marletta, M. A. *J. Am. Chem. Soc.* **2010**, *132*, 12794.
(514) Can, M.; Zoppellaro, G.; Andersson, K. K.; Bren, K. L. *Inorg. Chem.* **2011**, *50*, 12018.
(515) A. Shelnutt, J.; Song, X.-Z.; Ma, J.-G.; Jia, S.-L.; Jentzen, W.; J. Medforth, C. *Chem. Soc. Rev.* **1998**, *27*, 31.
(516) Ma, J.-G.; Laberge, M.; Song, X.-Z.; Jentzen, W.; Jia, S.-L.; Zhang, J.; Vanderkooi, J. M.; Shelnutt, J. A. *Biochemistry* **1998**, *37*, 5118.
(517) Patra, R.; Chaudhary, A.; Ghosh, S. K.; Rath, S. P. *Inorg. Chem.* **2008**, *47*, 8324.
(518) Ravikanth, M.; Chandrashekar, T. K. In *Coordination Chemistry*; Springer Berlin Heidelberg: 1995; Vol. 82, p 105.
(519) MacGowan, S. A.; Senge, M. O. *Inorg. Chem.* **2013**, *52*, 1228.
(520) Imlay, J. A. *Mol. Microbiol.* **2006**, *59*, 1073.
(521) Johnson, D. C.; Dean, D. R.; Smith, A. D.; Johnson, M. K. *Annu. Rev. Biochem.* **2005**, *74*, 247.
(522) Dos, S., Patricia C.; Dean, D. R. *Proc. Natl. Acad. Sci. U. S. A.* **2008**, *105*, 11589.
(523) Beinert, H.; Meyer, J.; Lill, R.; Elsevier Ltd.: 2004; Vol. 2, p 482.
(524) Lill, R. *Nature* **2009**, *460*, 831.
(525) Flint, D. H.; Allen, R. M. *Chem. Rev.* **1996**, *96*, 2315.
(526) Bian, S.; Cowan, J. A. *Coord. Chem. Rev.* **1999**, *190-192*, 1049.
(527) Broderick, J. B.; Elsevier Ltd.: 2004; Vol. 8, p 739.
(528) Cammack, R. *Adv. Inorg. Chem.* **1992**, *38*, 281.
(529) Beinert, H.; Holm, R. H.; Munck, E. *Science* **1997**, *277*, 653.
(530) Py, B.; Moreau, P. L.; Barras, F. *Curr. Opin. Microbiol.* **2011**, *14*, 218.
(531) Beinert, H.; Kiley, P. J. *Curr. Opin. Chem. Biol.* **1999**, *3*, 152.
(532) Brzoska, K.; Meczynska, S.; Kruszewski, M. *Acta Biochim. Pol.* **2006**, *53*, 685.
(533) Rouault, T. A.; Klausner, R. D. *Trends Biochem. Sci.* **1996**, *21*, 174.
(534) Lukianova, O. A.; David, S. S. *Curr. Opin. Chem. Biol.* **2005**, *9*, 145.
(535) *Eur. J. Biochem.* **1978**, *35*, 1.
(536) Beinert, H.; Kennedy, M. C. *Eur. J. Biochem.* **1989**, *186*, 5.
(537) Bill, E. *Hyperfine Interact.* **2012**, *205*, 139.
(538) Orme-Johnson, W. H. *Annu. Rev. Biochem.* **1973**, *42*, 159.
(539) Tsibris, J. C. M.; Woody, R. W. *Coord. Chem. Rev.* **1970**, *5*, 417.
(540) Sticht, H.; Rosch, P. *Prog. Biophys. Mol. Biol.* **1998**, *70*, 95.
(541) Balk, J.; Lill, R. *ChemBioChem* **2004**, *5*, 1044.
(542) Noodleman, L.; Lovell, T.; Liu, T.; Himo, F.; Torres, R. A. *Curr. Opin. Chem. Biol.* **2002**, *6*, 259.
(543) Beinert, H. *JBIC, J. Biol. Inorg. Chem.* **2000**, *5*, 409.
(544) Hong, J.-S.; Rabinowitz, J. C. *Biochem. Biophys. Res. Commun.* **1967**, *29*, 246.
(545) Malkin, R.; Rabinowitz, J. C. *Biochem. Biophys. Res. Commun.* **1966**, *23*, 822.
(546) Bayer, E.; Eckstein, H.; Hagenmaier, H.; Josef, D.; Koch, J.; Krauss, P.; Roeder, A.; Schretzmann, P. *Eur. J. Biochem.* **1969**, *8*, 33.
(547) Rouault, T. A. *Dis. Models & Mech.* **2012**, *5*, 155.
(548) Frazzon, J.; Fick, J. R.; Dean, D. R. *Biochem. Soc. Trans.* **2002**, *30*, 680.
(549) Py, B.; Barras, F. *Nat. Rev. Microbiol.* **2010**, *8*, 436.
(550) Peters, J. W.; Broderick, J. B. *Annu. Rev. Biochem.* **2012**, *81*, 429.
(551) Bandyopadhyay, S.; Chandramouli, K.; Johnson, M. K. *Biochem. Soc. Trans.* **2008**, *36*, 1112.
(552) Ayala-Castro, C.; Saini, A.; Outten, F. W. *Microbiol. Mol. Biol. Rev.* **2008**, *72*, 110.

(553) Roche, B.; Aussel, L.; Ezraty, B.; Mandin, P.; Py, B.; Barras, F. *Biochim. Biophys. Acta* **2013**, *1827* 455.

(554) Lill, R.; Mu¨hlenhoff, U. *Trends Biochem. Sci.* **2005**, *30*, 133.

(555) Day, M. W.; Hsu, B. T.; Joshua-Tor, L.; Park, J. B.; Zhou, Z. H.; Adams, M. W. W.; Rees, D. C. *Protein Sci.* **1992**, *1*, 1494.

(556) Dauter, Z.; Wilson, K. S.; Sieker, L. C.; Moulis, J.-M.; Meyer, J. *Proc. Natl. Acad. Sci. U. S. A.* **1996**, *93*, 8836.

(557) LeGall, J.; Liu, M. Y.; Gomes, C. M.; Braga, V.; Pacheco, I.; Regalla, M.; Xavier, A. V.; Teixeira, M. *FEBS Lett.* **1998**, *429*, 295.

(558) Hiller, R.; Zhou, Z. H.; Adams, M. W. W.; Englander, S. W. *Proc. Natl. Acad. Sci. U. S. A.* **1997**, *94*, 11329.

(559) Vondrasek, J.; Bendova, L.; Klusak, V.; Hobza, P. *J. Am. Chem. Soc.* **2005**, *127*, 2615.

(560) Riley, K. E.; Merz, K. M., Jr. *J. Phys. Chem. B* **2006**, *110*, 15650.

(561) Sieker, L. C.; Stenkamp, R. E.; LeGall, J. *Methods Enzymol.* **1994**, *243*, 203.

(562) Xiao, Z.; Lavery, M. J.; Ayhan, M.; Scrofani, S. D. B.; Wilce, M. C. J.; Guss, J. M.; Tregloan, P. A.; George, G. N.; Wedd, A. G. *J. Am. Chem. Soc.* **1998**, *120*, 4135.

(563) Westler, W. M.; Lin, I. J.; Perczel, A.; Weinhold, F.; Markley, J. L. *J. Am. Chem. Soc.* **2011**, *133*, 1310.

(564) Bertini, I.; Luchinat, C. *Nature* **2011**, *470*, 469.

(565) Zartler, E. R.; Jenney, F. E., Jr.; Terrell, M.; Eidsness, M. K.; Adams, M. W. W.; Prestegard, J. H. *Biochemistry* **2001**, *40*, 7279.

(566) Min, T.; Ergenekan, C. E.; Eidsness, M. K.; Ichiye, T.; Kang, C. *Protein Sci.* **2001**, *10*, 613.

(567) Park, I. Y.; Youn, B.; Harley, J. L.; Eidsness, M. K.; Smith, E.; Ichiye, T.; Kang, C. *JBIC, J. Biol. Inorg. Chem.* **2004**, *9*, 423.

(568) Kennepohl, P.; Solomon, E. I. *Inorg. Chem.* **2003**, *42*, 696.

(569) Lee, H. J.; Basran, J.; Scrutton, N. S. *Biochemistry* **1998**, *37*, 15513.

(570) Perry, A.; Tambyrajah, W.; Grossmann, J. G.; Lian, L.-Y.; Scrutton, N. S. *Biochemistry* **2004**, *43*, 3167.

(571) Lode, E. T.; Coon, M. J. *J. Biol. Chem.* **1971**, *246*, 791.

(572) Adman, E. T.; Sieker, L. C.; Jensen, L. H. *J. Mol. Biol.* **1991**, *217*, 337.

(573) Van Beilen, J. B.; Neuenschwander, M.; Smits, T. H. M.; Roth, C.; Balada, S. B.; Witholt, B. *J. Bacteriol.* **2002**, *184*, 1722.

(574) Bau, R.; Rees, D. C.; Kurtz, D. M., Jr.; Scott, R. A.; Huang, H.; Adams, M. W. W.; Eidsness, M. K. *JBIC, J. Biol. Inorg. Chem.* **1998**, *3*, 484.

(575) Hageluekent, G.; Wiehlmannt, L.; Adams, T. M.; Kolmar, H.; Heinz, D. W.; Tuemmler, B.; Schubert, W.-D. *Proc. Natl. Acad. Sci. U. S. A.* **2007**, *104*, 12276.

(576) Page, C. C.; Moser, C. C.; Chen, X.; Dutton, P. L. *Nature* **1999**, *402*, 47.

(577) Santos, H.; Fareleira, P.; Xavier, A. V.; Chen, L.; Liu, M. Y.; LeGall, J. *Biochem. Biophys. Res. Commun.* **1993**, *195*, 551.

(578) Victor, B. L.; Vicente, J. B.; Rodrigues, R.; Oliveira, S.; Rodrigues-Pousada, C.; Frazao, C.; Gomes, C. M.; Teixeira, M.; Soares, C. M. *JBIC, J. Biol. Inorg. Chem.* **2003**, *8*, 475.

(579) Gomes, C. M.; Silva, G.; Oliveira, S.; LeGall, J.; Liu, M.-Y.; Xavier, A. V.; Rodrigues-Pousada, C.; Teixeira, M. *J. Biol. Chem.* **1997**, *272*, 22502.

(580) Frazao, C.; Silva, G.; Gomes, C. M.; Matias, P.; Coelho, R.; Sieker, L.; Macedo, S.; Liu, M. Y.; Oliveira, S.; Teixeira, M.; Xavier, A. V.; Rodrigues-Pousada, C.; Carrondo, M. A.; Le Gall, J. *Nat. Struct. Biol.* **2000**, *7*, 1041.

(581) Fareleira, P.; Santos, B. S.; Antonio, C.; Moradas-Ferreira, P.; LeGall, J.; Xavier, A. V.; Santos, H. *Microbiology* **2003**, *149*, 1513.
(582) Jenney, F. E., Jr.; Verhagen, M. F. J. M.; Cui, X.; Adams, M. W. W. *Science* **1999**, *286*, 306.
(583) Coulter, E. D.; Kurtz, D. M., Jr. *Arch. Biochem. Biophys.* **2001**, *394*, 76.
(584) Yoon, K.-S.; Hille, R.; Hemann, C.; Tabita, F. R. *J. Biol. Chem.* **1999**, *274*, 29772.
(585) Shimizu, F.; Ogata, M.; Yagi, T.; Wakabayashi, S.; Matsubara, H. *Biochimie* **1989**, *71*, 1171.
(586) Wastl, J.; Duin, E. C.; Iuzzolino, L.; Dorner, W.; Link, T.; Hoffmann, S.; Sticht, H.; Dau, H.; Lingelbach, K.; Maier, U.-G. *J. Biol. Chem.* **2000**, *275*, 30058.
(587) Gaillard, J.; Zhuang-Jackson, H.; Moulis, J.-M. *Eur. J. Biochem.* **1996**, *238*, 346.
(588) Holm, R. H.; Kennepohl, P.; Solomon, E. I. *Chem. Rev.* **1996**, *96*, 2239.
(589) Meyer, J.; Moulis, J.-M. *Handb. Metalloproteins* **2001**, *1*, 505.
(590) Xiao, Z.; Wedd, A. G. *Mod. Coord. Chem.* **2002**, 288.
(591) Swartz, P. D.; Beck, B. W.; Ichiye, T. *Biophys. J.* **1996**, *71*, 2958.
(592) Swartz, P. D.; Ichiye, T. *Biophys. J.* **1997**, *73*, 2733.
(593) Tan, M.-L.; Kang, C.; Ichiye, T. *Proteins Struct., Funct., Bioinf.* **2006**, *62*, 708.
(594) Sulpizi, M.; Raugei, S.; VandeVondele, J.; Carloni, P.; Sprik, M. *J. Phys. Chem. B* **2007**, *111*, 3969.
(595) Gamiz-Hernandez, A. P.; Kieseritzky, G.; Ishikita, H.; Knapp, E. W. *J. Chem. Theory Comput.* **2011**, *7*, 742.
(596) Rose, K.; Shadle, S. E.; Eidsness, M. K.; Kurtz, D. M., Jr.; Scott, R. A.; Hedman, B.; Hodgson, K. O.; Solomon, E. I. *J. Am. Chem. Soc.* **1998**, *120*, 10743.
(597) Swartz, P. D.; Ichiye, T. *Biochemistry* **1996**, *35*, 13772.
(598) Gilles de Pelichy, L. D.; Smith, E. T. *Biochemistry* **1999**, *38*, 7874.
(599) Sundararajan, M.; Hillier, I. H.; Burton, N. A. *J. Phys. Chem. A* **2006**, *110*, 785.
(600) Sun, N.; Dey, A.; Xiao, Z.; Wedd, A. G.; Hodgson, K. O.; Hedman, B.; Solomon, E. I. *J. Am. Chem. Soc.* **2010**, *132*, 12639.
(601) Kuemmerle, R.; Zhuang-Jackson, H.; Gaillard, J.; Moulis, J.-M. *Biochemistry* **1997**, *36*, 15983.
(602) Eidsness, M. K.; Burden, A. E.; Richie, K. A.; Kurtz, D. M., Jr.; Scott, R. A.; Smith, E. T.; Ichiye, T.; Beard, B.; Min, T.; Kang, C. *Biochemistry* **1999**, *38*, 14803.
(603) Yoo, S. J.; Meyer, J.; Achim, C.; Peterson, J.; Hendrich, M. P.; Munck, E. *JBIC, J. Biol. Inorg. Chem.* **2000**, *5*, 475.
(604) Ayhan, M.; Xiao, Z.; Lavery, M. J.; Hamer, A. M.; Nugent, K. W.; Scrofani, S. D. B.; Guss, M.; Wedd, A. G. *Inorg. Chem.* **1996**, *35*, 5902.
(605) Xiao, Z.; Maher, M. J.; Cross, M.; Bond, C. S.; Guss, J. M.; Wedd, A. G. *JBIC, J. Biol. Inorg. Chem.* **2000**, *5*, 75.
(606) Ayhan, M.; Xiao, Z.; Lavery, M. J.; Hammer, A. M.; Scrofani, S. D. B.; Wedd, A. G. *ACS Symp. Ser.* **1996**, *653*, 40.
(607) Mukherjee, M. *Acta Crystallogr., Sect. D Biol. Crystallogr.* **1999**, *D55*, 820.
(608) Lin, I. J.; Gebel, E. B.; Machonkin, T. E.; Westler, W. M.; Markley, J. L. *J. Am. Chem. Soc.* **2003**, *125*, 1464.
(609) Park, I. Y.; Eidsness, M. K.; Lin, I. J.; Gebel, E. B.; Youn, B.; Harley, J. L.; Machonkin, T. E.; Frederick, R. O.; Markley, J. L.; Smith, E. T.; Ichiye, T.; Kang, C. *Proteins Struct., Funct., Bioinf.* **2004**, *57*, 618.
(610) Lin, I. J.; Gebel, E. B.; Machonkin, T. E.; Westler, W. M.; Markley, J. L. *Proc. Natl. Acad. Sci. U. S. A.* **2005**, *102*, 14581.

(611) Zeng, Q.; Smith, E. T.; Kurtz, D. M., Jr.; Scott, R. A. *Inorg. Chim. Acta* **1996**, *242*, 245.
(612) Zheng, H.; Kellog, S. J.; Erickson, A. E.; Dubauskie, N. A.; Smith, E. T. *JBIC, J. Biol. Inorg. Chem.* **2003**, *8*, 12.
(613) Low, D. W.; Hill, M. G. *J. Am. Chem. Soc.* **1998**, *120*, 11536.
(614) Xiao, Y.; Wang, H.; George, S. J.; Smith, M. C.; Adams, M. W. W.; Jenney, F. E., Jr.; Sturhahn, W.; Alp, E. E.; Zhao, J.; Yoda, Y.; Dey, A.; Solomon, E. I.; Cramer, S. P. *J. Am. Chem. Soc.* **2005**, *127*, 14596.
(615) Cheney, B. V.; Schulz, M. W.; Cheney, J. *Biochim. Biophys. Acta, Protein Struct. Mol. Enzymol.* **1989**, *996*, 116.
(616) Reid, K. S. C.; Lindley, P. F.; Thornton, J. M. *FEBS Lett.* **1985**, *190*, 209.
(617) Adman, E.; Watenpaugh, K. D.; Jensen, L. H. *Proc. Natl. Acad. Sci. U. S. A.* **1975**, *72*, 4854.
(618) Backes, G.; Mino, Y.; Loehr, T. M.; Meyer, T. E.; Cusanovich, M. A.; Sweeney, W. V.; Adman, E. T.; Sanders-Loehr, J. *J. Am. Chem. Soc.* **1991**, *113*, 2055.
(619) Okamura, T.-A.; Takamizawa, S.; Ueyama, N.; Nakamura, A. *Inorg. Chem.* **1998**, *37*, 18.
(620) Atherton, N. M.; Garbett, K.; Gillard, R. D.; Mason, R.; Mayhew, S. J.; Peel, J. L.; Stangroom, J. E. *Nature* **1966**, *212*, 590.
(621) Zawadzke, L. E.; Berg, J. M. *J. Am. Chem. Soc.* **1992**, *114*, 4002.
(622) Eidsness, M. K.; Richie, K. A.; Burden, A. E.; Kurtz, D. M., Jr.; Scott, R. A. *Biochemistry* **1997**, *36*, 10406.
(623) Vrajmasu, V. V.; Bominaar, E. L.; Meyer, J.; Muenck, E. *Inorg. Chem.* **2002**, *41*, 6358.
(624) Barra, A. L.; Hassan, A. K.; Janoschka, A.; Schmidt, C. L.; Schunemann, V. *Appl. Magn. Reson.* **2006**, *30*, 385.
(625) Rao, K. K.; Evans, M. C. W.; Cammack, R.; Hall, D. O.; Thompson, C. L.; Jackson, P. J.; Johnson, C. E. *Biochem. J.* **1972**, *129*, 1063.
(626) Zheng, P.; Li, H. *J. Am. Chem. Soc.* **2011**, *133*, 6791.
(627) Zheng, P.; Takayama, S.-i. J.; Mauk, A. G.; Li, H. *J. Am. Chem. Soc.* **2012**, *134*, 4124.
(628) Bergmann, U.; Sturhahn, W.; Linn, D. E., Jr.; Jenney, F. E., Jr.; Adams, M. W. W.; Rupnik, K.; Hales, B. J.; Alp, E. E.; Mayse, A.; Cramer, S. P. *J. Am. Chem. Soc.* **2003**, *125*, 4016.
(629) Wilkens, S. J.; Xia, B.; Weinhold, F.; Markley, J. L.; Westler, W. M. *J. Am. Chem. Soc.* **1998**, *120*, 4806.
(630) Xia, B.; Wilkens, S. J.; Westler, W. M.; Markley, J. L. *J. Am. Chem. Soc.* **1998**, *120*, 4893.
(631) Volkman, B. F.; Wilkens, S. J.; Lee, A. L.; Xia, B.; Westler, W. M.; Beger, R.; Markley, J. L. *J. Am. Chem. Soc.* **1999**, *121*, 4677.
(632) Wasserfallen, A.; Ragettli, S.; Jouanneau, Y.; Leisinger, T. *Eur. J. Biochem.* **1998**, *254*, 325.
(633) Gardner, A. M.; Helmick, R. A.; Gardner, P. R. *J. Biol. Chem.* **2002**, *277*, 8172.
(634) Drake Harold, L.; Daniel Steven, L. *Res. Microbiol.* **2004**, *155*, 869.
(635) Gomes, C. M.; Vicente, J. B.; Wasserfallen, A.; Teixeira, M. *Biochemistry* **2000**, *39*, 16230.
(636) Vicente, J. B.; Teixeira, M. *J. Biol. Chem.* **2005**, *280*, 34599.
(637) Vicente, J. B.; Scandurra, F. M.; Rodrigues, J. V.; Brunori, M.; Sarti, P.; Teixeira, M.; Giuffre, A. *FEBS Journal* **2007**, *274*, 677.
(638) Silaghi-Dumitrescu, R.; Coulter, E. D.; Das, A.; Ljungdahl, L. G.; Jameson, G. N. L.; Huynh, B. H.; Kurtz, D. M., Jr. *Biochemistry* **2003**, *42*, 2806.
(639) Zanello, P. *Coord. Chem. Rev.* **2013**, *257*, 1777.
(640) van Beilen, J. B.; Wubbolts, M. G.; Witholt, B. *Biodegradation* **1994**, *5*, 161.
(641) Lee, H. J.; Lian, L.-Y.; Scrutton, N. S. *Biochem. J.* **1997**, *328*, 131.
(642) Moura, J. J. G.; Goodfellow, B. J.; Romao, M. J.; Rusnak, F.; Moura, I. *Comments Inorg. Chem.* **1996**, *19*, 47.

(643) Archer, M.; Huber, R.; Tavares, P.; Moura, I.; Moura, J. J. G.; Carrondo, M. A.; Sieker, L. C.; LeGall, J.; Romao, M. J. *J. Mol. Biol.* **1995**, *251*, 690.

(644) Hoff, A. J.; Editor *Advanced EPR. Applications in Biology and Biochemistry*, 1989, 813-838.

(645) Moura, I.; Huynh, B. H.; Hausinger, R. P.; Le Gall, J.; Xavier, A. V.; Munck, E. *J. Biol. Chem.* **1980**, *255*, 2493.

(646) Yu, L.; Kennedy, M.; Czaja, C.; Tavares, P.; Moura, J. J. G.; Moura, I.; Rusnak, F. *Biochem. Biophys. Res. Commun.* **1997**, *231*, 679.

(647) Tavares, P.; Ravi, N.; Moura, J. J. G.; LeGall, J.; Huang, Y.-H.; Crouse, B. R.; Johnson, M. K.; Huynh, B. H.; Moura, I. *J. Biol. Chem.* **1994**, *269*, 10504.

(648) Auchere, F.; Pauleta, S. R.; Tavares, P.; Moura, I.; Moura, J. J. G. *JBIC, J. Biol. Inorg. Chem.* **2006**, *11*, 433.

(649) Rodrigues, J. V.; Saraiva, L. M.; Abreu, I. A.; Teixeira, M.; Cabelli, D. E. *JBIC, J. Biol. Inorg. Chem.* **2007**, *12*, 248.

(650) Riebe, O.; Fischer, R.-J.; Bahl, H. *FEBS Lett.* **2007**, *581*, 5605.

(651) Devreese, B.; Tavares, P.; Lampreia, J.; Van Damme, N.; Le Gall, J.; Moura, J. J. G.; Van Beeumen, J.; Moura, I. *FEBS Lett.* **1996**, *385*, 138.

(652) Coelho, A. V.; Matias, P.; Fulop, V.; Thompson, A.; Gonzalez, A.; Carrondo, M. A. *JBIC, J. Biol. Inorg. Chem.* **1997**, *2*, 680.

(653) Verhagen, M. F. J. M.; Voorhorst, W. G. B.; Kolkman, J. A.; Wolbert, R. B. G.; Hagen, W. R. *FEBS Lett.* **1993**, *336*, 13.

(654) Cordas, C. M.; Raleiras, P.; Auchere, F.; Moura, I.; Moura, J. J. G. *Eur. Biophys. J.* **2012**, *41*, 209.

(655) Ascenso, C.; Rusnak, F.; Cabrito, I.; Lima, M. J.; Naylor, S.; Moura, I.; Moura, J. J. G. *JBIC, J. Biol. Inorg. Chem.* **2000**, *5*, 720.

(656) Berthomieu, C.; Dupeyrat, F.; Fontecave, M.; Vermeglio, A.; Niviere, V. *Biochemistry* **2002**, *41*, 10360.

(657) Emerson, J. P.; Cabelli, D. E.; Kurtz, D. M., Jr. *Proc. Natl. Acad. Sci. U. S. A.* **2003**, *100*, 3802.

(658) Abreu, I. A.; Saraiva, L. M.; Carita, J.; Huber, H.; Stetter, K. O.; Cabelli, D.; Teixeira, M. *Mol. Microbiol.* **2000**, *38*, 322.

(659) Weinberg, M. V.; Jenney, F. E., Jr.; Cui, X.; Adams, M. W. W. *J. Bacteriol.* **2004**, *186*, 7888.

(660) deMare, F.; Kurtz, D. M., Jr.; Nordlund, P. *Nat. Struct. Biol.* **1996**, *3*, 539.

(661) Jin, S.; Kurtz, D. M., Jr.; Liu, Z.-J.; Rose, J.; Wang, B.-C. *J. Am. Chem. Soc.* **2002**, *124*, 9845.

(662) LeGall, J.; Prickril, B. C.; Moura, I.; Xavier, A. V.; Moura, J. J. G.; Huynh Boi, H. *Biochemistry* **1988**, *27*, 1636.

(663) Pierik, A. J.; Wolbert, R. B. G.; Portier, G. L.; Verhagen, M. F. J. M.; Hagen, W. R. *Eur. J. Biochem.* **1993**, *212*, 237.

(664) Luo, Y.; Ergenekan, C. E.; Fischer, J. T.; Tan, M.-L.; Ichiye, T. *Biophys. J.* **2010**, *98*, 560.

(665) Jin, S.; Kurtz, D. M., Jr.; Liu, Z.-J.; Rose, J.; Wang, B.-C. *Biochemistry* **2004**, *43*, 3204.

(666) Pinto, A. F.; Todorovic, S.; Hildebrandt, P.; Yamazaki, M.; Amano, F.; Igimi, S.; Romao, C. V.; Teixeira, M. *JBIC, J. Biol. Inorg. Chem.* **2011**, *16*, 501.

(667) Lumppio, H. L.; Shenvi, N. V.; Garg, R. P.; Summers, A. O.; Kurtz, D. M., Jr. *J. Bacteriol.* **1997**, *179*, 4607.

(668) Coulter, E. D.; Shenvi, N. V.; Kurtz, D. M., Jr. *Biochem. Biophys. Res. Commun.* **1999**, *255*, 317.

(669) Matsubara, H.; Saeki, K. *Adv. Inorg. Chem.* **1992**, *38*, 223.

(670) Shethna, Y. I.; Wilson, P. W.; Hansen, R. E.; Beinert, H. *Proc. Natl. Acad. Sci. U. S. A.* **1964**, *52*, 1263.
(671) Massey, V. *J. Biol. Chem.* **1957**, *229*, 763.
(672) Yoch, D. C.; Valentine, R. C. *Annu. Rev. Microbiol.* **1972**, *26*, 139.
(673) Bruschi, M.; Guerlesquin, F. *FEMS Microbiol. Rev.* **1988**, *54*, 155.
(674) Sieker, L. C.; Adman, E. T. In *Encyclopedia of Inorganic and Bioinorganic Chemistry*; John Wiley & Sons, Ltd: 2011.
(675) Valentine, R. C. *Bacteriological Reviews* **1964**, *28*, 497.
(676) Lovenberg, W.; Buchanan, B. B.; Rabinowitz, J. C. *J. Biol. Chem.* **1963**, *238*, 3899.
(677) Binda, C.; Aliverti, A. In *Encyclopedia of Inorganic and Bioinorganic Chemistry*; John Wiley & Sons, Ltd: 2011.
(678) Hurley, J. K.; Weber-Main, A. M.; Hodges, A. E.; Stankovich, M. T.; Benning, M. M.; Holden, H. M.; Cheng, H.; Xia, B.; Markley, J. L.; Genzor, C.; Gomez-Moreno, C.; Hafezi, R.; Tollin, G. *Biochemistry* **1997**, *36*, 15109.
(679) De, P., Antonio R.; Jelesarov, I.; Ackermann, F.; Koppenol, W. H.; Hirasawa, M.; Knaff, D. B.; Bosshard, H. R. *Protein Sci.* **1993**, *2*, 1126.
(680) De, P., A. R.; Schuermann, P.; Bosshard, H. R. *FEBS Lett.* **1994**, *337*, 217.
(681) Muller, J. J.; Muller, A.; Rottmann, M.; Bernhardt, R.; Heinemann, U. *J. Mol. Biol.* **1999**, *294*, 501.
(682) Zanetti, G.; Pandini, V.; Elsevier Ltd.: 2004; Vol. 2, p 104.
(683) Fukuyama, K. *Photosynth. Res.* **2004**, *81*, 289.
(684) Holden, H. M.; Jacobson, B. L.; Hurley, J. K.; Tollin, G.; Oh, B. H.; Skjeldal, L.; Chae, Y. K.; Cheng, H.; Xia, B.; Markley, J. L. *J. Bioenerg. Biomembr.* **1994**, *26*, 67.
(685) Morales, R.; Chron, M.-H.; Hudry-Clergeon, G.; Petillot, Y.; Norager, S.; Medina, M.; Frey, M. *Biochemistry* **1999**, *38*, 15764.
(686) Bes, M. T.; Parisini, E.; Inda, L. A.; Saraiva, L. M.; Peleato, M. L.; Sheldrick, G. M. *Structure (London, U. K.)* **1999**, *7*, 1201.
(687) *Non heme iron proteins, role in energy conversion*; Hardy, R.; Knight Jr, E.; McDonald, C.; D'Eustachio, A., Eds.; Antonio press: Ohio, 1965.
(688) Meyer, J.; Moulis, J. M.; Lutz, M. *Biochem. Biophys. Res. Commun.* **1984**, *119*, 828.
(689) Meyer, J.; LA Andrade, S.; Einsle, O. In *Encyclopedia of Inorganic and Bioinorganic Chemistry*; John Wiley & Sons: 2011.
(690) Golinelli, M.-P.; Akin, L. A.; Crouse, B. R.; Johnson, M. K.; Meyer, J. *Biochemistry* **1996**, *35*, 8995.
(691) Golinelli, M.-P.; Chatelet, C.; Duin, E. C.; Johnson, M. K.; Meyer, J. *Biochemistry* **1998**, *37*, 10429.
(692) Meyer, J. *FEBS Lett.* **2001**, *509*, 1.
(693) Yeh, A. P.; Chatelet, C.; Soltis, S. M.; Kuhn, P.; Meyer, J.; Rees, D. C. *J. Mol. Biol.* **2000**, *300*, 587.
(694) Hase, T.; Schuermann, P.; Knaff, D. B. In *Photosystem I*; Goldbeck, J. H., Ed.; Springer: 2004.
(695) Hurley, J. K.; Medina, M.; Gomez-Moreno, C.; tollin, G. *Arch. Biochem. Biophys.* **1994**, *312*, 480.
(696) Hurley, J. K.; Schmeits, J. L.; Genzor, C.; Gomez-Moreno, C.; Tollin, G. *Arch. Biochem. Biophys.* **1996**, *333*, 243.
(697) Hurley, J. K.; Salamon, Z.; Meyer, T. E.; Fitch, J. C.; Cusanovich, M. A.; Markley, J. L.; Cheng, H.; Xia, B.; Chae, Y. K. *Biochemistry* **1993**, *32*, 9346.

(698) Hurley, J. K.; Tollin, G.; Medina, M.; Gomez-Moreno, C. *Adv. Photosynth. Respir.* **2006**, *24*, 455.

(699) Kimata-Ariga, Y.; Kubota-Kawai, H.; Lee, Y.-H.; Muraki, N.; Ikegami, T.; Kurisu, G.; Hase, T. *Biochem. Biophys. Res. Commun.* **2013**, *434*, 867.

(700) Dai, S.; Schwendtmayer, C.; Schurmann, P.; Ramaswamy, S.; Eklund, H. *Science* **2000**, *287*, 655.

(701) Schmitz, S.; Navarro, F.; Kutzki, C. K.; Florencio, F. J.; Boehme, H. *Biochim. Biophys. Acta, Bioenerg.* **1996**, *1277*, 135.

(702) Garcia-Sanchez, M. I.; Gotor, C.; Jacquot, E.-P.; Stein, M.; Suzuki, A.; Vega, J. M. *Eur. J. Biochem.* **1997**, *250*, 364.

(703) Akashi, T.; Matsumura, T.; Ideguchi, T.; Iwakiri, K.-I.; Kawakatsu, T.; Taniguchi, I.; Hase, T. *J. Biol. Chem.* **1999**, *274*, 29399.

(704) Hase, T.; Schurmann, P.; Knaff, D. B. *Adv. Photosynth. Respir.* **2006**, *24*, 477.

(705) Antonkine, M. L.; Koay, M. S.; Epel, B.; Breitenstein, C.; Gopta, O.; Gaertner, W.; Bill, E.; Lubitz, W. *Biochim. Biophys. Acta, Bioenerg.* **2009**, *1787*, 995.

(706) Ewen, K. M.; Kleser, M.; Bernhardt, R. *Biochim. Biophys. Acta, Proteins Proteomics* **2011**, *1814*, 111.

(707) Vickery, L. E. *Steroids* **1997**, *62*, 124.

(708) Ziegler, G. A.; Vonrhein, C.; Hanukoglu, I.; Schulz, G. E. *J. Mol. Biol.* **1999**, *289*, 981.

(709) Muller, J. J.; Lapko, A.; Bourenkov, G.; Ruckpaul, K.; Heinemann, U. *J. Biol. Chem.* **2001**, *276*, 2786.

(710) Chatelet, C.; Meyer, J. *Biochim. Biophys. Acta, Protein Struct. Mol. Enzymol.* **2001**, *1549*, 32.

(711) Skjeldal, L.; Markley, J. L.; Coghlan, V. M.; Vickery, L. E. *Biochemistry* **1991**, *30*, 9078.

(712) Lambeth, J. D.; Kamin, H. *J. Biol. Chem.* **1979**, *254*, 2766.

(713) Salamon, Z.; Gleason, F. K.; Tollin, G. *Arch. Biochem. Biophys.* **1992**, *299*, 193.

(714) Vidakovis, M.; Fraczkiewicz, G.; Germanas, J. P. *J. Biol. Chem.* **1996**, *271*.

(715) Agarwall, A.; Li, D.; Cowan, J. A. *Proc. Natl. Acad. Sci. U. S. A.* **1995**, *92*, 9440.

(716) Duff, J. L. C.; Breton, J. L. J.; Butt, J. N.; Armstrong, F. A.; Thomson, A. J. *J. Am. Chem. Soc.* **1996**, *118*, 8593.

(717) Nakamura, A.; Ueyama, N. *ACS Symp. Ser.* **1988**, *372*, 292.

(718) Chen, K.; Tilley, G. J.; Sridhar, V.; Prasad, G. S.; Stout, C. D.; Armstrong, F. A.; Burgess, B. K. *J. Biol. Chem.* **1999**, *274*, 36479.

(719) Langen, R.; Jensen, G. M.; Jacob, U.; Stephens, P. J.; Warshel, A. *J. Biol. Chem.* **1992**, *267*, 25625.

(720) Meyer, J.; Andrade, S. L.; Einsle, O. In *Handbook of Metalloproteins*; John Wiley & Sons, Ltd: 2006.

(721) Werth, M. T.; Cecchini, G.; Manodori, A.; Ackrell, B. A. C.; Schroder, I.; Gunsalus, R. P.; Johnson, M. K. *Proc. Natl. Acad. Sci. U. S. A.* **1990**, *87*, 8965.

(722) Hollocher, T. C.; Solomon, F.; Ragland, T. E. *J. Biol. Chem.* **1966**, *241*, 3452.

(723) Dervartanian, D. V.; Orme-Johnson, W. H.; Hansen, R. E.; Beinert, H.; Tsai, R. L.; Tsibris, J. C. M.; Bartholomaus, R. C.; Gunsalus, I. C. *Biochem. Biophys. Res. Commun.* **1967**, *26*, 569.

(724) Crouse, B. R.; Meyer, J.; Johnson, M. K. *J. Am. Chem. Soc.* **1995**, *117*, 9612.

(725) Fu, W.; Drozdzewski, P. M.; Davies, M. D.; Sligar, S. G.; Johnson, M. K. *J. Biol. Chem.* **1992**, *267*, 15502.

(726) Dunham, W. R.; Palmer, G.; Sands, R. H.; Bearden, A. J. *Biochim. Biophys. Acta* **1971**, *253*, 373.

(727) Cheng, H.; Markley, J. L. *Annu. Rev. Biophys. Biomol. Struct.* **1995**, *24*, 209.
(728) Meyer, J.; Clay, M. D.; Johnson, M. K.; Stubna, A.; Muenck, E.; Higgins, C.; Wittung-Stafshede, P. *Biochemistry* **2002**, *41*, 3096.
(729) Otaka, E.; Ooi, T. *J. Mol. Evol.* **1987**, *26*, 257.
(730) Gaillard, J.; Quinkal, I.; Moulis, J. M. *Biochemistry* **1993**, *32*, 9881.
(731) Dauter, Z.; Wilson, K. S.; Sieker, L. C.; Meyer, J.; Moulis, J.-M. *Biochemistry* **1997**, *36*, 16065.
(732) Mulholland, S. E.; Gibney, B. R.; Rabanal, F.; Dutton, P. L. *Biochemistry* **1999**, *38*, 10442.
(733) Bott, A. W. *Curr. Sep.* **1999**, *18*, 47.
(734) Hannan, J. P.; Busch, J. L. H.; Breton, J.; James, R.; Thomson, A. J.; Moore, G. R.; Davy, S. L. *JBIC, J. Biol. Inorg. Chem.* **2000**, *5*, 432.
(735) Busch, J. L.; Breton, J. L.; Bartlett, B. M.; Armstrong, F. A.; James, R.; Thomson, A. J. *Biochem. J.* **1997**, *323*, 95.
(736) Macedo, A. L.; Rodrigues, P.; Goodfellow, B. J. *Coord. Chem. Rev.* **1999**, *190-192*, 871.
(737) Stout, C. D. In *Encyclopedia of Inorganic and Bioinorganic Chemistry*; John Wiley & Sons, Ltd: 2011.
(738) Quinkal, I.; Kyritsis, P.; Kohzuma, T.; Im, S.-C.; Sykes, A. G.; Moulis, J.-M. *Biochim. Biophys. Acta, Protein Struct. Mol. Enzymol.* **1996**, *1295*, 201.
(739) Fish, A.; Danieli, T.; Ohad, I.; Nechushtai, R.; Livnah, O. *J. Mol. Biol.* **2005**, *350*, 599.
(740) Bertini, I. In *Biological inorganic chemistry, structure and reactivity*; Univeresity Science books: 2007, p 244.
(741) O'Keefe, D. P.; Gibson, K. J.; Emptage, M. H.; Lenstra, R.; Romesser, J. A.; Litle, P. J.; Omer, C. A. *Biochemistry* **1991**, *30*, 447.
(742) Farrar, J. A.; Lappalainen, P.; Zumft, W. G.; Saraste, M.; Thomson, A. J. *Eur. J. Biochem.* **1995**, *232*, 294.
(743) Kyritsis, P.; Hatzfeld, O. M.; Link, T. A.; Moulis, J.-M. *J. Biol. Chem.* **1998**, *273*, 15404.
(744) Kyritsis, P.; Huber, J. G.; Quinkal, I.; Gaillard, J.; Moulis, J.-M. *Biochemistry* **1997**, *36*, 7839.
(745) Breton, J. L.; Duff, J. L. C.; Butt, J. N.; Armstrong, F. A.; George, S. J.; Petillot, Y.; Forest, E.; Schaefer, G.; Thomson, A. J. *Eur. J. Biochem.* **1995**, *233*, 937.
(746) Shen, B.; Martin, L. L.; Butt, J. N.; Armstrong, F. A.; Stout, C. D.; Jensen, G. M.; Stephens, P. J.; La, M., Gerd N.; Gorst, C. M.; Burgess, B. K. *J. Biol. Chem.* **1993**, *268*, 25928.
(747) Camba, R.; Armstrong, F. A. *Biochemistry* **2000**, *39*, 10587.
(748) Brereton, P. S.; Maher, M. J.; Tregloan, P. A.; Wedd, A. G. *Biochim. Biophys. Acta, Protein Struct. Mol. Enzymol.* **1999**, *1429*, 307.
(749) Shen, W. H.; Choe, S. Y.; Eisenberg, D.; Collier, R. J. *J. Biol. Chem.* **1994**, *269*, 29077.
(750) Iismaa, S. E.; Vazquez, A. E.; Jensen, G. M.; Stephens, P. J.; Butt, J. N.; Armstrong, F. A.; Burgess, B. K. *J. Biol. Chem.* **1991**, *266*, 21563.
(751) Moulis, J. M.; Meyer, J.; Lutz, M. *Biochemistry* **1984**, *23*, 6605.
(752) Jensen, G. M.; Warshel, A.; Stephens, P. J. *Biochemistry* **1994**, *33*, 10911.
(753) Kyritsis, P.; Kuemmerle, R.; Huber, J. G.; Gaillard, J.; Guigliarelli, B.; Popescu, C.; Muenck, E.; Moulis, J.-M. *Biochemistry* **1999**, *38*, 6335.
(754) Sweeney, W. V.; Rabinowitz, J. C. *Annu. Rev. Biochem.* **1980**, *49*, 139.
(755) Busse, S. C.; La, M., Gerd N.; Yu, L. P.; Howard, J. B.; Smith, E. T.; Zhou, Z. H.; Adams, M. W. W. *Biochemistry* **1992**, *31*, 11952.
(756) Kummerle, R.; Kyritsis, P.; Gaillard, J.; Moulis, J.-M. *J. Inorg. Biochem.* **2000**, *79*, 83.

(757) Wildegger, G.; Bentrop, D.; Ejchart, A.; Alber, M.; Hage, A.; Sterner, R.; Roesch, P. *Eur. J. Biochem.* **1995**, *229*, 658.

(758) Loehr, T. M. *J. Raman Spectrosc.* **1992**, *23*, 531.

(759) Mitra, D.; Pelmenschikov, V.; Guo, Y.; Case, D. A.; Wang, H.; Dong, W.; Tan, M.-L.; Ichiye, T.; Jenney, F. E.; Adams, M. W. W.; Yoda, Y.; Zhao, J.; Cramer, S. P. *Biochemistry* **2011**, *50*, 5220.

(760) Hagedoorn, P. L.; Chen, T.; Schroeder, I.; Piersma, S. R.; de, V., Simon; Hagen, W. R. *JBIC, J. Biol. Inorg. Chem.* **2005**, *10*, 259.

(761) Duderstadt, R. E.; Brereton, P. S.; Adams, M. W. W.; Johnson, M. K. *FEBS Lett.* **1999**, *454*, 21.

(762) Pereira, M. M.; Jones, K. L.; Campos, M. G.; Melo, A. M. P.; Saraiva, L. M.; Louro, R. O.; Wittung-Stafshede, P.; Teixeira, M. *Biochim. Biophys. Acta, Proteins Proteomics* **2002**, *1601*, 1.

(763) Lin, Y.-H.; Huang, H.-E.; Chen, Y.-R.; Liao, P.-L.; Chen, C.-L.; Feng, T.-Y. *Phytopathology* **2011**, *101*, 741.

(764) Klipp, W.; Reilander, H.; Schluter, A.; Krey, R.; Puhler, A. *Mol. Gen. Genet.* **1989**, *216*, 293.

(765) Masepohl, B.; Kutsche, M.; Riedel, K. U.; Schmehl, M.; Klipp, W.; Puehler, A. *Mol. Gen. Genet.* **1992**, *233*, 33.

(766) Sjoblom, S.; Harjunpaa, H.; Brader, G.; Palva, E. T. *Mol. Plant-Microbe Interact.* **2008**, *21*, 967.

(767) Huang, H.-E.; Ger, M.-J.; Chen, C.-Y.; Yip, M.-K.; Chung, M.-C.; Feng, T.-Y. *Plant Sci. (Amsterdam, Neth.)* **2006**, *171*, 17.

(768) Kwon, D.-H.; El-Zaatari, F. A. K.; Kato, M.; Osato, M. S.; Reddy, R.; Yamaoka, Y.; Graham, D. Y. *Antimicrob. Agents Chemother.* **2000**, *44*, 2133.

(769) Yip, M.-K.; Huang, H.-E.; Ger, M.-J.; Chiu, S.-H.; Tsai, Y.-C.; Lin, C.-I.; Feng, T.-Y. *Plant Cell Rep.* **2007**, *26*, 449.

(770) Rieske, J. S.; MacLennan, D. H.; Coleman, R. *Biochem. Biophys. Commun.* **1964**, *15*, 388.

(771) Schneider, D.; Schmidt, C. L. *Biochim. Biophys. Acta, Bioenerg.* **2005**, *1710*, 1.

(772) Harnisch, U.; Weiss, H.; Sebald, W. *Eur. J. Biochem.* **1985**, *149*, 95.

(773) Link, T. A. *Adv. Inorg. Chem.* **1999**, *47*, 83.

(774) Iwata, S.; Saynovits, M.; Link, T. A.; Michel, H. *Structure (London, U. K.)* **1996**, *4*, 567.

(775) Graham, L. A.; Trumpower, B. L. *J. Biol. Chem.* **1991**, *266*, 22485.

(776) Davidson, E.; Ohnishi, T.; Atta-Asafo-Adjei, E.; Daldal, F. *Biochemistry* **1992**, *31*, 3342.

(777) Schmidt, C. L.; Anemuller, S.; Schafer, G. *FEBS Lett.* **1996**, *388*, 43.

(778) Fee, J. A.; Findling, K. L.; Yoshida, T.; Hille, R.; Tarr, G. E.; Hearshen, D. O.; Dunham, W. R.; Day, E. P.; Kent, T. A.; Munck, E. *J. Biol. Chem.* **1984**, *259*, 124.

(779) Gatti, D. L.; Meinhardt, S. W.; Onishi, T.; Tzagoloff, A. *J. Mol. Biol.* **1989**, *205*, 421.

(780) Brown, E. N.; Friemann, R.; Karlsson, A.; Parales, J. V.; Couture, M. M.-J.; Eltis, L. D.; Ramaswamy, S. *JBIC, J. Biol. Inorg. Chem.* **2008**, *13*, 1301.

(781) Denke, E.; Merbitz-Zahradnik, T.; Hatzfeld, O. M.; Snyder, C. H.; Link, T. A.; Trumpower, B. L. *J. Biol. Chem.* **1998**, *273*, 9085.

(782) Lebrun, E.; Santini, J. M.; Brugna, M.; Ducluzeau, A.-L.; Ouchane, S.; Schoepp-Cothenet, B.; Baymann, F.; Nitschke, W. *Mol. Biol. Evol.* **2006**, *23*, 1180.

(783) Botelho, H. M.; Leal, S. S.; Veith, A.; Prosinecki, V.; Bauer, C.; Frohlich, R.; Kletzin, A.; Gomes, C. M. *JBIC, J. Biol. Inorg. Chem.* **2010**, *15*, 271.

(784) Bonisch, H.; Schmidt, C. L.; Schafer, G.; Ladenstein, R. *J. Mol. Biol.* **2002**, *319*, 791.

(785) Kauppi, B.; Lee, K.; Carredano, E.; Parales, R. E.; Gibson, D. T.; Eklund, H.; Ramaswamy, S. *Structure (London, U. K.)* **1998**, *6*, 571.

(786) Schmidt, C. L. *J. Bioenerg. Biomembr.* **2004**, *36*, 107.
(787) Link, T. A. *FEBS Lett.* **1997**, *412*, 257.
(788) Mason, J. R.; Cammack, R. *Annu. Rev. Microbiol.* **1992**, *46*, 277.
(789) Parales, R. E.; Parales, J. V.; Gibson, D. T. *J. Bacteriol.* **1999**, *181*, 1831.
(790) Tarasev, M.; Pinto, A.; Kim, D.; Elliott, S. J.; Ballou, D. P. *Biochemistry* **2006**, *45*, 10208.
(791) Pinto, A.; Tarasev, M.; Ballou, D. P. *Biochemistry* **2006**, *45*, 9032.
(792) Martins, B. M.; Svetlitchnaia, T.; Dobbek, H. *Structure (Cambridge, MA, U. S.)* **2005**, *13*, 817.
(793) Ferraro, D. J.; Gakhar, L.; Ramaswamy, S. *Biochem. Biophys. Res. Commun.* **2005**, *338*, 175.
(794) Snyder, C. H.; Merbitz-Zahradnik, T.; Link, T. A.; Trumpower, B. L. *J. Bioenerg. Biomembr.* **1999**, *31*, 235.
(795) Kletzin, A.; Ferreira, A. S.; Hechler, T.; Bandeiras, T. M.; Teixeira, M.; Gomes, C. M. *FEBS Lett.* **2005**, *579*, 1020.
(796) Ugulava, N. B.; Crofts, A. R. *FEBS Lett.* **1998**, *440*, 409.
(797) Verhagen, M. F. J. M.; Link, T. A.; Hagen, W. R. *FEBS Lett.* **1995**, *361*, 75.
(798) Link, T. A.; Hagen, W. R.; Pierik, A. J.; Assmann, C.; Von, J., Gebhard. *Eur. J. Biochem.* **1992**, *208*, 685.
(799) Couture, M. M.-J.; Auger, M.; Rosell, F.; Mauk, A. G.; Boubour, E.; Lennox, R. B.; Eltis, L. D. *Biochim. Biophys. Acta, Protein Struct. Mol. Enzymol.* **1999**, *1433*, 159.
(800) Kuznetsov, A. M.; Zueva, E. M.; Masliy, A. N.; Krishtalik, L. I. *Biochim. Biophys. Acta* **2010**, *1797*, 347.
(801) Brugna, M.; Albouy, D.; Nitschke, W. *J. Bacteriol.* **1998**, *180*, 3719.
(802) Anemueller, S.; Schmidt, C. L.; Schaefer, G.; Bill, E.; Trautwein, A. X.; Teixeira, M. *Biochem. Biophys. Res. Commun.* **1994**, *202*, 252.
(803) Albers, A.; Bayer, T.; Demeshko, S.; Dechert, S.; Meyer, F. *Chem. - Eur. J.* **2013**, *19*, 10101.
(804) Konkle, M. E.; Muellner, S. K.; Schwander, A. L.; Dicus, M. M.; Pokhrel, R.; Britt, R. D.; Taylor, A. B.; Hunsicker-Wang, L. M. *Biochemistry* **2009**, *48*, 9848.
(805) Matsuura, K.; Bowyer, J. R.; Ohnishi, T.; Dutton, P. L. *J. Biol. Chem.* **1983**, *258*, 1571.
(806) Von, J., G.; Ohnishi, T. *FEBS Lett.* **1985**, *185*, 311.
(807) Konkle, M. E.; Elsenheimer, K. N.; Hakala, K.; Robicheaux, J. C.; Weintraub, S. T.; Hunsicker-Wang, L. M. *Biochemistry* **2010**, *49*, 7272.
(808) Zu, Y.; Couture, M. M.-J.; Kolling, D. R. J.; Crofts, A. R.; Eltis, L. D.; Fee, J. A.; Hirst, J. *Biochemistry* **2003**, *42*, 12400.
(809) Link, T. A.; Hatzfeld, O. M.; Unalkat, P.; Shergill, J. K.; Cammack, R.; Mason, J. R. *Biochemistry* **1996**, *35*, 7546.
(810) Colbert, C. L.; Couture, M. M.; Eltis, L. D.; Bolin, J. T. *Structure* **2000**, *8*, 1267.
(811) Lhee, S., University of Illinois at Urbana-Champaign, 2007.
(812) Klingen, A. R.; Ullmann, G. M. *Biochemistry* **2004**, *43*, 12383.
(813) Dikanov, S. A.; Kolling, D. J.; Endeward, B.; Samoilova, R. I.; Prisner, T. F.; Nair, S. K.; Crofts, A. R. *J. Biol. Chem.* **2006**, *281*, 27416.
(814) Lhee, S.; Kolling, D. R. J.; Nair, S. K.; Dikanov, S. A.; Crofts, A. R. *J. Biol. Chem.* **2010**, *285*, 9233.
(815) Schroter, T.; Hatzfeld, O. M.; Gemeinhardt, S.; Korn, M.; Friedrich, T.; Ludwig, B.; Link, T. A. *Eur. J. Biochem.* **1998**, *255*, 100.
(816) Brasseur, G.; Sled, V.; Liebl, U.; Ohnishi, T.; Daldal, F. *Biochemistry* **1997**, *36*, 11685.

(817) Leggate, E. J.; Hirst, J. *Biochemistry* **2005**, *44*, 7048.
(818) Cooley, J. W.; Roberts, A. G.; Bowman, M. K.; Kramer, D. M.; Daldal, F. *Biochemistry* **2004**, *43*, 2217.
(819) Merbitz-Zahradnik, T.; Zwicker, K.; Nett, J. H.; Link, T. A.; Trumpower, B. L. *Biochemistry* **2003**, *42*, 13637.
(820) Zu, Y.; Fee, J. A.; Hirst, J. *Biochemistry* **2002**, *41*, 14054.
(821) Unalkat, P.; Hatzfeld, O.; Link, T. A.; Tan, H.-M.; Cammack, R.; Mason, J. R. *J. Inorg. Biochem.* **1995**, *59*, 528.
(822) Beharry, Z. M.; Eby, D. M.; Coulter, E. D.; Viswanathan, R.; Neidle, E. L.; Phillips, R. S.; Kurtz, D. M., Jr. *Biochemistry* **2003**, *42*, 13625.
(823) Brugna, M.; Nitschke, W.; Asso, M.; Guigliarelli, B.; Lemesle-Meunier, D.; Schmidt, C. *J. Biol. Chem.* **1999**, *274*, 16766.
(824) Iwasaki, T.; Kounosu, A.; Kolling, D. R. J.; Lhee, S.; Crofts, A. R.; Dikanov, S. A.; Uchiyama, T.; Kumasaka, T.; Ishikawa, H.; Kono, M.; Imai, T.; Urushiyama, A. *Protein Sci.* **2006**, *15*, 2019.
(825) Wilson, D. F.; Erecinska, M.; Brocklehurst, E. S. *Arch. Biochem. Biophys.* **1972**, *151*, 180.
(826) Link, T. A.; Hatzfeld, O. M.; Saynovits, M. In *Bioinorganic Chemistry*; Trautwein, A. X., Ed.; Wiley-VCH: 1997, p 312.
(827) Link, T. A.; Saynovits, M.; Assmann, C.; Iwata, S.; Ohnishi, T.; Von, J., Gebhard. *Eur. J. Biochem.* **1996**, *237*, 71.
(828) Bertrand, P.; Guigliarelli, B.; Gayda, J. P.; Beardwood, P.; Gibson, J. F. *Biochim. Biophys. Acta, Protein Struct. Mol. Enzymol.* **1985**, *831*, 261.
(829) T'sai, A. L.; Palmer, G. *Biochim. Biophys. Acta* **1983**, *722*, 349.
(830) Hatzfeld, O.,M. Ph.D Thesis. Frankfurt, 1998.
(831) Prince, R. C.; Lindsay, J. G.; Dutton, P. L. *FEBS Lett.* **1975**, *51*, 108.
(832) Sharp, R. E.; Palmitessa, A.; Gibney, B. R.; Moser, C. C.; Daldal, F.; Dutton, P. L. *FEBS Lett.* **1998**, *431*, 423.
(833) Evans, M. C. W.; Lord, A. V.; Reeves, S. G. *Biochem. J.* **1974**, *138*, 177.
(834) Nitschke, W.; Joliot, P.; Liebl, U.; Rutherford, A. W.; Hauska, G.; Mueller, A.; Riedel, A. *Biochim. Biophys. Acta, Bioenerg.* **1992**, *1102*, 266.
(835) Zhang, H.; Carrell, C. J.; Huang, D.; Sled, V.; Ohnishi, T.; Smith, J. L.; Cramer, W. A. *J. Biol. Chem.* **1996**, *271*, 31360.
(836) Holton, B.; Wu, X.; Tsapin, A. I.; Kramer, D. M.; Malkin, R.; Kallas, T. *Biochemistry* **1996**, *35*, 15485.
(837) Liebl, U.; Pezennec, S.; Riedel, A.; Kellner, E.; Nitschke, W. *J. Biol. Chem.* **1992**, *267*, 14068.
(838) Lewis, R. J.; Prince, R. C.; Dutton, P. L.; Knaff, D. B.; Krulwich, T. A. *J. Biol. Chem.* **1981**, *256*, 10543.
(839) Liebl, U.; Rutherford, A. W.; Nitschke, W. *FEBS Lett.* **1990**, *261*, 427.
(840) Riedel, A.; Kellner, E.; Grodzitzki, D.; Liebl, U.; Hauska, G.; Mueller, A.; Rutherford, A. W.; Nitschke, W. *Biochim. Biophys. Acta, Bioenerg.* **1993**, *1183*, 263.
(841) Kuila, D.; Fee, J. A. *J. Biol. Chem.* **1986**, *261*, 2768.
(842) Schmidt, C. L.; Hatzfeld, O. M.; Petersen, A.; Link, T. A.; Schaefer, G. *Biochem. Biophys. Res. Commun.* **1997**, *234*, 283.
(843) Geary, P. J.; Saboowalla, F.; Patil, D.; Cammack, R. *Biochem. J.* **1984**, *217*, 667.
(844) Bertrand, P.; Gayda, J. P. *Biochim. Biophys. Acta, Protein Struct.* **1979**, *579*, 107.
(845) Shergill, J. K.; Joannou, C. L.; Mason, J. R.; Cammack, R. *Biochemistry* **1995**, *34*, 16533.

(846) Rosche, B.; Fetzner, S.; Lingens, F.; Nitschke, W.; Riedel, A. *Biochim. Biophys. Acta, Protein Struct. Mol. Enzymol.* **1995**, *1252*, 177.

(847) Tsang, H. T.; Batie, C. J.; Ballou, D. P.; Penner-Hahn, J. E. *Biochemistry* **1989**, *28*, 7233.

(848) Kuila, D.; Schoonover, J. R.; Dyer, R. B.; Batie, C. J.; Ballou, D. P.; Fee, J. A.; Woodruff, W. H. *Biochim. Biophys. Acta, Bioenerg.* **1992**, *1140*, 175.

(849) Iwasaki, T.; Kounosu, A.; Kolling, D. R. J.; Crofts, A. R.; Dikanov, S. A.; Jin, A.; Imai, T.; Urushiyama, A. *J. Am. Chem. Soc.* **2004**, *126*, 4788.

(850) Rotsaert, F. A. J.; Pikus, J. D.; Fox, B. G.; Markley, J. L.; Sanders-Loehr, J. *JBIC, J. Biol. Inorg. Chem.* **2003**, *8*, 318.

(851) Cosper, N. J.; Eby, D. M.; Kounosu, A.; Kurosawa, N.; Neidle, E. L.; Kurtz, D. M., Jr.; Iwasaki, T.; Scott, R. A. *Protein Sci.* **2002**, *11*, 2969.

(852) Tiago, d. O. F.; Bominaar, E. L.; Hirst, J.; Fee, J. A.; Munck, E. *J. Am. Chem. Soc.* **2004**, *126*, 5338.

(853) Cline, J. F.; Hoffman, B. M.; Mims, W. B.; LaHaie, E.; Ballou, D. P.; Fee, J. A. *J. Biol. Chem.* **1985**, *260*, 3251.

(854) Britt, R. D.; Sauer, K.; Klein, M. P.; Knaff, D. B.; Kriauciunas, A.; Yu, C. A.; Yu, L.; Malkin, R. *Biochemistry* **1991**, *30*, 1892.

(855) Gurbiel, R. J.; Ohnishi, T.; Robertson, D. E.; Daldal, F.; Hoffman, B. M. *Biochemistry* **1991**, *30*, 11579.

(856) Gurbiel, R. J.; Doan, P. E.; Gassner, G. T.; Macke, T. J.; Case, D. A.; Ohnishi, T.; Fee, J. A.; Ballou, D. P.; Hoffman, B. M. *Biochemistry* **1996**, *35*, 7834.

(857) Shergill, J. K.; Cammack, R. *Biochim. Biophys. Acta, Bioenerg.* **1994**, *1185*, 35.

(858) Dikanov, S. A.; Xun, L.; Karpiel, A. B.; Tyryshkin, A. M.; Bowman, M. K. *J. Am. Chem. Soc.* **1996**, *118*, 8408.

(859) Kolling, D. R. J.; Samoilova, R. I.; Shubin, A. A.; Crofts, A. R.; Dikanov, S. A. *J. Phys. Chem. A* **2009**, *113*, 653.

(860) Neese, F.; Kappl, R.; Huttermann, J.; Zumft, W. G.; Kroneck, P. M. H. *JBIC, J. Biol. Inorg. Chem.* **1998**, *3*, 53.

(861) Holz, R. C.; Small, F. J.; Ensign, S. A. *Biochemistry* **1997**, *36*, 14690.

(862) de, V., S.; Cherepanov, A.; Berg, A.; Canters, G. W. *Inorg. Chim. Acta* **1998**, *275-276*, 493.

(863) Xia, B.; Pikus, J. D.; Xia, W.; McClay, K.; Steffan, R. J.; Chae, Y. K.; Westler, W. M.; Markley, J. L.; Fox, B. G. *Biochemistry* **1999**, *38*, 727.

(864) Hsueh, K.-L.; Westler, W. M.; Markley, J. L. *J. Am. Chem. Soc.* **2010**, *132*, 7908.

(865) Hsueh, K.-L.; Tonelli, M.; Cai, K.; Westler, W. M.; Markley, J. L. *Biochemistry* **2013**, *52*, 2862.

(866) Leggate, E. J.; Bill, E.; Essigke, T.; Ullmann, G. M.; Hirst, J. *Proc. Natl. Acad. Sci. U. S. A.* **2004**, *101*, 10913.

(867) Zhu, J.; Egawa, T.; Yeh, S.-R.; Yu, L.; Yu, C.-A. *Proc. Natl. Acad. Sci. U. S. A.* **2007**, *104*, 4864.

(868) Hori, K. *J. Biochem.* **1961**, *50*, 481.

(869) Dus, K.; De, K., Henk; Sletten, K.; Bartsch, R. G. *Biochim. Biophys. Acta, Protein Struct.* **1967**, *140*, 291.

(870) Parisini, E.; Capozzi, F.; Lubini, P.; Lamzin, V.; Luchinat, C.; Sheldrick, G. M. *Acta Crystallogr., Sect. D: Biol. Crystallogr.* **1999**, *D55*, 1773.

(871) Kim, J. D.; Rodriguez-Granillo, A.; Case, D. A.; Nanda, V.; Falkowski, P. G. *PLoS Computational Biology* **2012**, *8*, e1002463.

(872) Carter Jr, C. W. In *Handbook of metalloproteins*; John Wiley & Sons, Ltd: 2006.

(873) Cowan, J. A.; Lui, S. M. *Adv. Inorg. Chem.* **1998**, *45*, 313.
(874) Cavazza, C.; Guigliarelli, B.; Bertrand, P.; Bruschi, M. *FEMS Microbiol. Lett.* **1995**, *130*, 193.
(875) Bian, S.; Hemann, C. F.; Hille, R.; Cowan, J. A. *Biochemistry* **1996**, *35*, 14544.
(876) Soriano, A.; Li, D.; Bian, S.; Agarwal, A.; Cowan, J. A. *Biochemistry* **1996**, *35*, 12479.
(877) Iwagami, S. G.; Creagh, A. L.; Haynes, C. A.; Borsari, M.; Felli, I. C.; Piccioli, M.; Eltis, L. D. *Protein Sci.* **1995**, *4*, 2562.
(878) Kusano, T.; Takeshima, T.; Sugawara, K.; Inoue, C.; Shiratori, T.; Yano, T.; Fukumori, Y.; Yamanaka, T. *J. Biol. Chem.* **1992**, *267*, 11242.
(879) Pereira, M. M.; Antunes, A. M.; Nunes, O. C.; da, C., Milton S.; Teixeira, M. *FEBS Lett.* **1994**, *352*, 327.
(880) Fukumori, Y.; Yamanaka, T. *Curr. Microbiol.* **1979**, *3*, 117.
(881) Lieutaud, C.; Alric, J.; Bauzan, M.; Nitschke, W.; Schoepp-Cothenet, B. *Proc. Natl. Acad. Sci. U. S. A.* **2005**, *102*, 3260.
(882) Hochkoeppler, A.; Kofod, P.; Ferro, G.; Ciurli, S. *Arch. Biochem. Biophys.* **1995**, *322*, 313.
(883) Ciurli, S.; Musiani, F. *Photosynth. Res.* **2005**, *85*, 115.
(884) Banci, L.; Bertini, I.; Briganti, F.; Luchinat, C.; Scozzafava, A.; Oliver, M. V. *Inorg. Chem.* **1991**, *30*, 4517.
(885) Heering, H. A.; Bulsink, Y. B. M.; Hagen, W. R.; Meyer, T. E. *Biochemistry* **1995**, *34*, 14675.
(886) Heering, H. A.; Bulsink, Y. B. M.; Hagen, W. R.; Meyer, T. E. *Eur. J. Biochem.* **1995**, *232*, 811.
(887) Ichiye, T. *AIP Conf. Proc.* **1999**, *492*.
(888) Hill, R. B.; bracken, C.; DeGrado, W. F.; Palmer, A. G. I. *J. Am. Chem. Soc.* **2000**, *122*, 11610.
(889) Dey, A.; Roche, C. L.; Walters, M. A.; Hodgson, K. O.; Hedman, B.; Solomon, E. I. *Inorg. Chem.* **2005**, *44*, 8349.
(890) Banci, L.; Bertini, I.; Ciurli, S.; Luchinat, C.; Pierattelli, R. *Inorg. Chim. Acta* **1995**, *240*, 251.
(891) Bertini, I.; Borsari, M.; Bosi, M.; Eltis, L. D.; Felli, I. C.; Luchinat, C.; Piccioli, M. *JBIC, J. Biol. Inorg. Chem.* **1996**, *1*, 257.
(892) Benning, M. M.; Meyer, T. E.; Rayment, I.; Holden, H. M. *Biochemistry* **1994**, *33*, 2476.
(893) Sticht, H.; Wildegger, G.; Bentrop, D.; Darimont, B.; Sterner, R.; Rosch, P. *Eur. J. Biochem.* **1996**, *237*, 726.
(894) Agarwal, A.; Li, D.; Cowan, J. A. *J. Am. Chem. Soc.* **1995**, *118*, 927.
(895) Dilg, A. W. E.; Mincione, G.; Achterhold, K.; Iakovleva, O.; Mentler, M.; Luchinat, C.; Bertini, I.; Parak, F. G. *JBIC, J. Biol. Inorg. Chem.* **1999**, *4*, 727.
(896) Luchinat, C.; Capozzi, F.; Borsari, M.; Battistuzzi, G.; Sola, M. *Biochem. Biophys. Res. Commun.* **1994**, *203*, 436.
(897) Perrin, B. S.; Ichiye, T. *Biochemistry* **2013**, *52*, 3022.
(898) Glaser, T.; Bertini, I.; Moura, J. J. G.; Hedman, B.; Hodgson, K. O.; Solomon, E. I. *J. Am. Chem. Soc.* **2001**, *123*, 4859.
(899) Niu, S.; Ichiye, T. *J. Am. Chem. Soc.* **2009**, *131*, 5724.
(900) Dey, A.; Glaser, T.; Couture, M. M.-J.; Eltis, L. D.; Holm, R. H.; Hedman, B.; Hodgson, K. O.; Solomon, E. I. *J. Am. Chem. Soc.* **2004**, *126*, 8320.
(901) Dey, A.; Jenney, F. E., Jr.; Adams, M. W. W.; Babini, E.; Takahashi, Y.; Fukuyama, K.; Hodgson, K. O.; Hedman, B.; Solomon, E. I. *Science* **2007**, *318*, 1464.

(902) Kerfeld, C. A.; Chan, C.; Hirasawa, M.; Kleis-SanFrancisco, S.; Yeates, T. O.; Knaff, D. B. *Biochemistry* **1996**, *35*, 7812.

(903) Moulis, J. M.; Scherrer, N.; Gagnon, J.; Forest, E.; Petillot, Y.; Garcia, D. *Arch. Biochem. Biophys.* **1993**, *305*, 186.

(904) Ciszewska, H.; Bagyinka, C.; Tigyi, G.; Kovacs, K. L. *Acta Biochim. Biophys. Hung.* **1989**, *24*, 361.

(905) Zorin, N. A.; Gogotov, I. N. *Biokhimiya (Moscow)* **1983**, *48*, 1181.

(906) Tedro, S. M.; Meyer, T. E.; Bartsch, R. G.; Kamen, M. D. *J. Biol. Chem.* **1981**, *256*, 731.

(907) Ciszewska, H.; Bagyinka, C.; Kovacs, K. L. In *Biokonvers. Soln. Energ., Mater. Mezhdunar. Simp* 1984.

(908) Wermter, U.; Fischer, U. *Z. Naturforsch., C: J. Biosci.* **1983**, *38C*, 968.

(909) Bartsch, R. G. *Methods Enzymol.* **1978**, *53*, 329.

(910) Sola, M.; Cowan, J. A.; Gray, H. B. *Biochemistry* **1989**, *28*, 5261.

(911) Tedro, S. M.; Meyer, T. E.; Kamen, M. D. *J. Biol. Chem.* **1974**, *249*, 1182.

(912) Tedro, S. M.; Meyer, T. E.; Kamen, M. D. *Arch. Biochem. Biophys.* **1985**, *241*, 656.

(913) Bhattacharyya, A. K.; Meyer, T. E.; Cusanovich, M. A.; Tollin, G. *Biochemistry* **1987**, *26*, 758.

(914) Meyer, T. E. *Methods Enzymol.* **1994**, *243*, 435.

(915) Hochkoeppler, A.; Zannoni, D.; Ciurli, S.; Meyer, T. E.; Cusanovich, M. A.; Tollin, G. *Proc. Natl. Acad. Sci. U. S. A.* **1996**, *93*, 6998.

(916) Hochkoeppler, A.; Kofod, P.; Zannoni, D. *FEBS Lett.* **1995**, *375*, 197.

(917) Ambler, R. P.; Meyer, T. E.; Kamen, M. D. *Arch. Biochem. Biophys.* **1993**, *306*, 215.

(918) Meyer, T. E.; Cannac, V.; Fitch, J.; Bartsch, R. G.; Tollin, D.; Tollin, G.; Cusanovich, M. A. *Biochim. Biophys. Acta, Bioenerg.* **1990**, *1017*, 125.

(919) Rayment, I.; Wesenberg, G.; Meyer, T. E.; Cusanovich, M. A.; Holden, H. M. *J. Mol. Biol.* **1992**, *228*, 672.

(920) Schoepp, B.; Parot, P.; Menin, L.; Gaillard, J.; Richaud, P.; Vermeglio, A. *Biochemistry* **1995**, *34*, 11736.

(921) Tedro, S. M.; Meyer, T. E.; Kamen, M. D. *J. Biol. Chem.* **1977**, *252*, 7826.

(922) Breiter, D. R.; Meyer, T. E.; Rayment, I.; Holden, H. M. *J. Biol. Chem.* **1991**, *266*, 18660.

(923) Stombaugh, N. A.; Sundquist, J. E.; Burris, R. H.; Orme-Johnson, W. H. *Biochemistry* **1976**, *15*, 2633.

(924) Fukuyama, K.; Matsubara, H.; Tsukihara, T.; Katsube, Y. *J. Mol. Biol.* **1989**, *210*, 383.

(925) Sweeney, W. V.; Rabinowitz, J. C.; Yoch, D. C. *J. Biol. Chem.* **1975**, *250*, 7842.

(926) Przysiecki, C. T.; Meyer, T. E.; Cusanovich, M. A. *Biochemistry* **1985**, *24*, 2542.

(927) Bertini, I.; Capozzi, F.; Luchinat, C.; Piccioli, M. *Eur. J. Biochem.* **1993**, *212*, 69.

(928) Banci, L.; Bertini, I.; Ferretti, S.; Luchinat, C.; Piccioli, M. *J. Mol. Struct.* **1993**, *292*, 207.

(929) Bertini, I.; Capozzi, F.; Luchinat, C.; Piccioli, M.; Vicens, O., Margarita. *Inorg. Chim. Acta* **1992**, *198-200*, 483.

(930) Ciurli, S.; Cremonini, A.; Kofod, P.; Luchinat, C. *Eur. J. Biochem.* **1996**, *236*, 405.

(931) Bertini, I.; Capozzi, F.; Luchinat, C. *ACS Symp. Ser.* **2003**, *858*, 272.

(932) Gaillard, J.; Albrand, J. P.; Moulis, J. M.; Wemmer, D. E. *Biochemistry* **1992**, *31*, 5632.

(933) Bertini, I.; Donaire, A.; Felli, I. C.; Luchinat, C.; Rosato, A. *Inorg. Chem.* **1997**, *36*, 4798.

(934) Priem, A. H.; Klaassen, A. A. K.; Reijerse, E. J.; Meyer, T. E.; Luchinat, C.; Capozzi, F.; Dunham, W. R.; Hagen, W. R. *JBIC, J. Biol. Inorg. Chem.* **2005**, *10*, 417.

(935) Anderson, R. E.; Anger, G.; Petersson, L.; Ehrenberg, A.; Cammack, R.; Hall, D. O.; Mullinger, R.; Rao, K. K. *Biochim. Biophys. Acta, Bioenerg.* **1975**, *376*, 63.

(936) Antanaitis, B. C.; Moss, T. H. *Biochim. Biophys. Acta, Protein Struct.* **1975**, *405*, 262.

(937) Dilg, A. W. E.; Grantner, K.; Iakovleva, O.; Parak, F. G.; Babini, E.; Bertini, I.; Capozzi, F.; Luchinat, C.; Meyer-Klaucke, W. *JBIC, J. Biol. Inorg. Chem.* **2002**, *7*, 691.

(938) Bentrop, D.; Bertini, I.; Iacoviello, R.; Luchinat, C.; Niikura, Y.; Piccioli, M.; Presenti, C.; Rosato, A. *Biochemistry* **1999**, *38*, 4669.

(939) Teixeira, M.; Moura, I.; Xavier, A. V.; Moura, J. J. G.; LeGall, J.; DerVartanian, D. V.; Peck, H. D., Jr.; Huynh Boi, H. *J. Biol. Chem.* **1989**, *264*, 16435.

(940) Volbeda, A.; Charon, M.-H.; Piras, C.; Hatchikian, E. C.; Frey, M.; Fontecilla-Camps, J. C. *Nature* **1995**, *373*, 580.

(941) Montet, Y.; Amara, P.; Volbeda, A.; Vernede, X.; Hatchikian, E. C.; Field, M. J.; Frey, M.; Fontecilla-Camps, J. C. *Nat. Struct. Biol.* **1997**, *4*, 523.

(942) Garcin, E.; Vernede, X.; Hatchikian, E. C.; Volbeda, A.; Frey, M.; Fontecilla-Camps, J. C. *Structure (London, U. K.)* **1999**, *7*, 557.

(943) Marques, M. C.; Coelho, R.; De Lacey, A. L.; Pereira, I. A. C.; Matias, P. M. *J. Mol. Biol.* **2010**, *396*, 893.

(944) Rousset, M.; Montet, Y.; Guigliarelli, B.; Forget, N.; Asso, M.; Bertrand, P.; Fontecilla-Camps, J. C.; Hatchikian, E. C. *Proc. Natl. Acad. Sci. U. S. A.* **1998**, *95*, 11625.

(945) Pelmenschikov, V.; Kaupp, M. *J. Am. Chem. Soc.* **2013**, *135*, 11809.

(946) Grubel, K.; Holland, P. L. *Angew. Chem., Int. Ed.* **2012**, *51*, 3308.

(947) Ludwig, M.; Cracknell, J. A.; Vincent, K. A.; Armstrong, F. A.; Lenz, O. *J. Biol. Chem.* **2009**, *284*, 465.

(948) Fritsch, J.; Scheerer, P.; Frielingsdorf, S.; Kroschinsky, S.; Friedrich, B.; Lenz, O.; Spahn, C. M. T. *Nature* **2011**, *479*, 249.

(949) Shomura, Y.; Yoon, K.-S.; Nishihara, H.; Higuchi, Y. *Nature* **2011**, *479*, 253.

(950) Pandelia, M.-E.; Nitschke, W.; Infossi, P.; Giudici-Orticoni, M.-T.; Bill, E.; Lubitz, W. *Proc. Natl. Acad. Sci. U. S. A.* **2011**, *108*, 6097.

(951) Goris, T.; Wait, A. F.; Saggu, M.; Fritsch, J.; Heidary, N.; Stein, M.; Zebger, I.; Lendzian, F.; Armstrong, F. A.; Friedrich, B.; Lenz, O. *Nat. Chem. Biol.* **2011**, *7*, 310.

(952) Pandelia, M.-E.; Fourmond, V.; Tron-Infossi, P.; Lojou, E.; Bertrand, P.; Leger, C.; Giudici-Orticoni, M.-T.; Lubitz, W. *J. Am. Chem. Soc.* **2010**, *132*, 6991.

(953) Lukey, M. J.; Roessler, M. M.; Parkin, A.; Evans, R. M.; Davies, R. A.; Lenz, O.; Friedrich, B.; Sargent, F.; Armstrong, F. A. *J. Am. Chem. Soc.* **2011**, *133*, 16881.

(954) Vignais, P. M.; Billoud, B.; Meyer, J. *FEMS Microbiol. Rev.* **2001**, *25*, 455.

(955) Dubini, A.; Mus, F.; Seibert, M.; Grossman, A. R.; Posewitz, M. C. *J. Biol. Chem.* **2009**, *284*, 7201.

(956) Mulder, D. W.; Shepard, E. M.; Meuser, J. E.; Joshi, N.; King, P. W.; Posewitz, M. C.; Broderick, J. B.; Peters, J. W. *Structure (Cambridge, MA, U. S.)* **2011**, *19*, 1038.

(957) Nicolet, Y.; Piras, C.; Legrand, P.; Hatchikian, C. E.; Fontecilla-Camps, J. C. *Structure (London, U. K.)* **1999**, *7*, 13.

(958) Peters, J. W.; Lanzilotta, W. N.; Lemon, B. J.; Seefeldt, L. C. *Science* **1998**, *282*, 1853.

(959) Georgiadis, M. M.; Komiya, H.; Chakrabarti, P.; Woo, D.; Kornuc, J. J.; Rees, D. C. *Science* **1992**, *257*, 1653.

(960) Smith, B. E. *Adv. Inorg. Chem.* **1999**, *47*, 159.

(961) Watt, G. D.; Reddy, K. R. N. *J. Inorg. Biochem.* **1994**, *53*, 281.

(962) Angove, H. C.; Yoo, S. J.; Munck, E.; Burgess, B. K. *J. Biol. Chem.* **1998**, *273*, 26330.

(963) Strop, P.; Takahara, P. M.; Chiu, H.-J.; Angove, H. C.; Burgess, B. K.; Rees, D. C. *Biochemistry* **2001**, *40*, 651.

(964) Lindahl, P. A.; Boon Keng, T.; Orme-Johnson, W. H. *Inorg. Chem.* **1987**, *26*, 3912.
(965) Schindelin, H.; Kisker, C.; Schlessman, J. L.; Howard, J. B.; Rees, D. C. *Nature* **1997**, *387*, 370.
(966) Jang, S. B.; Seefeldt, L. C.; Peters, J. W. *Biochemistry* **2000**, *39*, 14745.
(967) Jeong, M. S.; Jang, S. B. *Mol. Cells* **2004**, *18*, 374.
(968) Jang, S. B.; Seefeldt, L. C.; Peters, J. W. *Biochemistry* **2000**, *39*, 641.
(969) Sen, S.; Krishnakumar, A.; McClead, J.; Johnson, M. K.; Seefeldt, L. C.; Szilagyi, R. K.; Peters, J. W. *J. Inorg. Biochem.* **2006**, *100*, 1041.
(970) Tezcan, F. A.; Kaiser, J. T.; Mustafi, D.; Walton, M. Y.; Howard, J. B.; Rees, D. C. *Science* **2005**, *309*, 1377.
(971) Sen, S.; Igarashi, R.; Smith, A.; Johnson, M. K.; Seefeldt, L. C.; Peters, J. W. *Biochemistry* **2004**, *43*, 1787.
(972) Peters, J. W.; Stowell, M. H. B.; Soltis, S. M.; Finnegan, M. G.; Johnson, M. K.; Rees, D. C. *Biochemistry* **1997**, *36*, 1181.
(973) Surerus, K. K.; Hendrich, M. P.; Christie, P. D.; Rottgardt, D.; Orme-Johnson, W. H.; Munck, E. *J. Am. Chem. Soc.* **1992**, *114*, 8579.
(974) Pierik, A. J.; Wassink, H.; Haaker, H.; Hagen, W. R. *Eur. J. Biochem.* **1993**, *212*, 51.
(975) Huber, R.; Hof, P.; Duarte, R. O.; Moura, J. J. G.; Moura, I.; Liu, M.-Y.; LeGall, J.; Hille, R.; Archer, M.; Romao, M. J. *Proc. Natl. Acad. Sci. U. S. A.* **1996**, *93*, 8846.
(976) Rebelo, J. M.; Dias, J. M.; Huber, R.; Moura, J. J. G.; Romao, M. J. *JBIC, J. Biol. Inorg. Chem.* **2001**, *6*, 791.
(977) Coelho, C.; Mahro, M.; Trincao, J.; Carvalho, A. T. P.; Ramos, M. J.; Terao, M.; Garattini, E.; Leimkuehler, S.; Romao, M. J. *J. Biol. Chem.* **2012**, *287*, 40690.
(978) Turner, N.; Barata, B.; Bray, R. C.; Deistung, J.; Le Gall, J.; Moura, J. J. G. *Biochem. J.* **1987**, *243*, 755.
(979) Bray, R. C.; Turner, N. A.; Le Gall, J.; Barata, B. A. S.; Moura, J. J. G. *Biochem. J.* **1991**, *280*, 817.
(980) Moura, J. J. G.; Xavier, A. V.; Hatchikian, E. C.; Le Gall, J. *FEBS Lett.* **1978**, *89*, 177.
(981) Moura, I.; Pereira, A. S.; Tavares, P.; Moura, J. J. G. *Adv. Inorg. Chem.* **1999**, *47*, 361.
(982) Barata, B. A. S.; Liang, J.; Moura, I.; Legall, J.; Moura, J. J. G.; Huynh Boi, H. *Eur. J. Biochem.* **1992**, *204*, 773.
(983) Dobbek, H.; Gremer, L.; Meyer, O.; Huber, R. *Proc. Natl. Acad. Sci. U. S. A.* **1999**, *96*, 8884.
(984) Meyer, O.; Gremer, L.; Ferner, R.; Ferner, M.; Dobbek, H.; Gnida, M.; Meyer-Klaucke, W.; Huber, R. *Biol. Chem.* **2000**, *381*, 865.
(985) Ferry, J. G. *Annu. Rev. Microbiol.* **1995**, *49*, 305.
(986) Ragsdale, S. W.; Kumar, M. *Chem. Rev.* **1996**, *96*, 2515.
(987) Ermler, U.; Grabarse, W.; Shima, S.; Goubeaud, M.; Thauer, R. K. *Curr. Opin. Struct. Biol.* **1998**, *8*, 749.
(988) Dobbek, H.; Svetlitchnyi, V.; Gremer, L.; Huber, R.; Meyer, O. *Science* **2001**, *293*, 1281.
(989) Drennan, C. L.; Heo, J.; Sintchak, M. D.; Schreiter, E.; Ludden, P. W. *Proc. Natl. Acad. Sci. U. S. A.* **2001**, *98*, 11973.
(990) Kung, Y.; Drennan, C. L. *Curr. Opin. Chem. Biol.* **2011**, *15*, 276.
(991) Gong, W.; Hao, B.; Wei, Z.; Ferguson, D. J., Jr.; Tallant, T.; Krzycki, J. A.; Chan, M. K. *Proc. Natl. Acad. Sci. U. S. A.* **2008**, *105*, 9558.
(992) Arendsen, A. F.; Hadden, J.; Card, G.; McAlpine, A. S.; Bailey, S.; Zaitsev, V.; Duke, E. H. M.; Lindley, P. F.; Krockel, M.; Trautwein, A. X.; Feiters, M. C.; Charnock, J. M.; Garner, C. D.; Marritt, S.

J.; Thomson, A. J.; Kooter, I. M.; Johnson, M. K.; Van Den Berg, W. A. M.; Van Dongen, W. M. A. M.; Hagen, W. R. *JBIC, J. Biol. Inorg. Chem.* **1998**, *3*, 81.

(993) Cooper, S. J.; Garner, C. D.; Hagen, W. R.; Lindley, P. F.; Bailey, S. *Biochemistry* **2000**, *39*, 15044.

(994) Van den Berg, W. A. M.; Hagen, W. R.; Van Dongen, W. M. A. M. *Eur. J. Biochem.* **2000**, *267*, 666.

(995) Aragao, D.; Mitchell, E. P.; Frazao, C. F.; Carrondo, M. A.; Lindley, P. F. *Acta Crystallogr., Sect. D Biol. Crystallogr.* **2008**, *64*, 665.

(996) Aragao, D.; Macedo, S.; Mitchell, E. P.; Romao, C. V.; Liu, M. Y.; Frazao, C.; Saraiva, L. M.; Xavier, A. V.; LeGall, J.; van Dongen, W. M. A. M.; Hagen, W. R.; Teixeira, M.; Carrondo, M. A.; Lindley, P. *JBIC, J. Biol. Inorg. Chem.* **2003**, *8*, 540.

(997) Kanatzidis, M. G.; Hagen, W. R.; Dunham, W. R.; Lester, R. K.; Coucouvanis, D. K. *J. Am. Chem. Soc.* **1985**, *107*, 953.

(998) Stokkermans, J. P. W. G.; Houba, P. H. J.; Pierik, A. J.; Hagen, W. R.; Van Dongen, W. M. A. M.; Veeger, C. *Eur. J. Biochem.* **1992**, *210*, 983.

(999) Arendsen, A. F.; Lindley, P. F. *Adv. Inorg. Chem.* **1999**, *47*, 219.

(1000) Crane, B. R.; Siegel, L. M.; Getzoff, E. D. *Science* **1995**, *270*, 59.

(1001) Crane, B. R.; Getzoff, E. D. *Curr. Opin. Struct. Biol.* **1996**, *6*, 744.

(1002) Nakayama, M.; Akashi, T.; Hase, T. *J. Inorg. Biochem.* **2000**, *82*, 27.

(1003) Wessels, J. G. H. *Adv. Microb. Physiol.* **1997**, *38*, 1.

(1004) Moreno-Vivian, C.; Cabello, P.; Martinez-Luque, M.; Blasco, R.; Castillo, F. *J. Bacteriol.* **1999**, *181*, 6573.

(1005) Richardson, D. J.; Berks, B. C.; Russell, D. A.; Spiro, S.; Taylor, C. J. *Cell. Mol. Life Sci.* **2001**, *58*, 165.

(1006) Hirasawa, M.; Tollin, G.; Salamon, Z.; Knaff, D. B. *Biochim. Biophys. Acta, Bioenerg.* **1994**, *1185*, 336.

(1007) Swamy, U.; Wang, M.; Tripathy, J. N.; Kim, S.-K.; Hirasawa, M.; Knaff, D. B.; Allen, J. P. *Biochemistry* **2005**, *44*, 16054.

(1008) Setif, P.; Hirasawa, M.; Cassan, N.; Lagoutte, B.; Tripathy, J. N.; Knaff, D. B. *Biochemistry* **2009**, *48*, 2828.

(1009) Peck, H. D., Jr.; LeGall, J. *Philos. Trans. R. Soc., B* **1982**, *298*, 443.

(1010) Stroupe, M. E.; Getzoff, E. D. *Handb. Metalloproteins* **2001**, *1*, 471.

(1011) Kopriva, S.; Koprivova, A. *J. Exp. Bot.* **2004**, *55*, 1775.

(1012) Krueger, R. J.; Siegel, L. M. *Biochemistry* **1982**, *21*, 2892.

(1013) Janick, P. A.; Rueger, D. C.; Krueger, R. J.; Barber, M. J.; Siegel, L. M. *Biochemistry* **1983**, *22*, 396.

(1014) Hirasawa, M.; Nakayama, M.; Hase, T.; Knaff, D. B. *Biochim. Biophys. Acta, Bioenerg.* **2004**, *1608*, 140.

(1015) Zeghouf, M.; Fontecave, M.; Coves, J. *J. Biol. Chem.* **2000**, *275*, 37651.

(1016) Molitor, M.; Dahl, C.; Molitor, I.; Schafer, U.; Speich, N.; Huber, R.; Deutzmann, R.; Truper, H. G. *Microbiology (Reading, U. K.)* **1998**, *144*, 529.

(1017) Schiffer, A.; Parey, K.; Warkentin, E.; Diederichs, K.; Huber, H.; Stetter, K. O.; Kroneck, P. M. H.; Ermler, U. *J. Mol. Biol.* **2008**, *379*, 1063.

(1018) Oliveira, T. F.; Vonrhein, C.; Matias, P. M.; Venceslau, S. S.; Pereira, I. A. C.; Archer, M. *J. Biol. Chem.* **2008**, *283*, 34141.

(1019) Hsieh, Y.-C.; Liu, M.-Y.; Wang, V. C. C.; Chiang, Y.-L.; Liu, E.-H.; Wu, W.-g.; Chan, S. I.; Chen, C.-J. *Mol. Microbiol.* **2010**, *78*, 1101.

(1020) Oliveira Tania, F.; Franklin, E.; Afonso Jose, P.; Khan Amir, R.; Oldham Neil, J.; Pereira Ines, A. C.; Archer, M. *Front. Microbiol.* **2011**, *2*, 71.

(1021) Saraste, M. *Science* **1999**, *283*, 1488.

(1022) Sun, F.; Zhou, Q.; Pang, X.; Xu, Y.; Rao, Z. *Curr. Opin. Struct. Biol.* **2013**, Ahead of Print.

(1023) Baradaran, R.; Berrisford, J. M.; Minhas, G. S.; Sazanov, L. A. *Nature* **2013**, *494*, 443.

(1024) Sun, F.; Huo, X.; Zhai, Y.; Wang, A.; Xu, J.; Su, D.; Bartlam, M.; Rao, Z. *Cell* **2005**, *121*, 1043.

(1025) Yankovskaya, V.; Horsefield, R.; Toernroth, S.; Luna-Chavez, C.; Miyoshi, H.; Leger, C.; Byrne, B.; Cecchini, G.; Iwata, S. *Science* **2003**, *299*, 700.

(1026) Iwata, S.; Lee, J. W.; Okada, K.; Lee, J. K.; Iwata, M.; Rasmussen, B.; Link, T. A.; Ramaswamy, S.; Jap, B. K. *Science* **1998**, *281*, 64.

(1027) Lange, C.; Hunte, C. *Proc. Natl. Acad. Sci. U. S. A.* **2002**, *99*, 2800.

(1028) Xia, D.; Yu, C.-A.; Kim, H.; Xia, J.-Z.; Kachurin, A. M.; Zhang, L.; Yu, L.; Deisenhofer, J. *Science* **1997**, *277*, 60.

(1029) Zhang, Z.; Huang, L.; Shulmeister, V. M.; Chi, Y.-I.; Kim, K. K.; Hung, L.-W.; Crofts, A. R.; Berry, E. A.; Kim, S.-H. *Nature* **1998**, *392*, 677.

(1030) Tsukihara, T.; Aoyama, H.; Yamashita, E.; Tomizaki, T.; Yamaguchi, H.; Shinzawa-Itoh, K.; Nakashima, R.; Yaono, R.; Yoshikawa, S. *Science* **1995**, *269*, 1069.

(1031) Tsukihara, T.; Aoyama, H.; Yamashita, E.; Tomizaki, T.; Yamaguchi, H.; Shinzawa-Itoh, K.; Nakashima, R.; Yaono, R.; Yoshikawa, S. *Science* **1996**, *272*, 1136.

(1032) Abrahams, J. P.; Leslie, A. G. W.; Lutter, R.; Walker, J. E. *Nature* **1994**, *370*, 621.

(1033) Sazanov, L. A.; Hinchliffe, P. *Science* **2006**, *311*, 1430.

(1034) Efremov, R. G.; Baradaran, R.; Sazanov, L. A. *Nature* **2010**, *465*, 441.

(1035) Efremov, R. G.; Sazanov, L. A. *Nature* **2011**, *476*, 414.

(1036) Hunte, C.; Zickermann, V.; Brandt, U. *Science* **2010**, *329*, 448.

(1037) Carroll, J.; Fearnley, I. M.; Skehel, J. M.; Shannon, R. J.; Hirst, J.; Walker, J. E. *J. Biol. Chem.* **2006**, *281*, 32724.

(1038) Sazanov, L. A.; Carroll, J.; Holt, P.; Toime, L.; Fearnley, I. M. *J. Biol. Chem.* **2003**, *278*, 19483.

(1039) Yagi, T.; Matsuno-Yagi, A. *Biochemistry* **2003**, *42*, 2266.

(1040) Sazanov, L. A. *Biochemistry* **2007**, *46*, 2275.

(1041) Huang, L.-s.; Sun, G.; Cobessi, D.; Wang, A. C.; Shen, J. T.; Tung, E. Y.; Anderson, V. E.; Berry, E. A. *J. Biol. Chem.* **2006**, *281*, 5965.

(1042) Cheng, V. W. T.; Ma, E.; Zhao, Z.; Rothery, R. A.; Weiner, J. H. *J. Biol. Chem.* **2006**, *281*, 27662.

(1043) Cecchini, G.; Sices, H.; Schroeder, I.; Gunsalus, R. P. *J. Bacteriol.* **1995**, *177*, 4587.

(1044) Haegerhaell, C.; Sled, V.; Hederstedt, L.; Ohnishi, T. *Biochim. Biophys. Acta, Bioenerg.* **1995**, *1229*, 356.

(1045) Manodori, A.; Cecchini, G.; Schroder, I.; Gunsalus, R. P.; Werth, M. T.; Johnson, M. K. *Biochemistry* **1992**, *31*, 2703.

(1046) Haegerhaell, C. *Biochim. Biophys. Acta, Bioenerg.* **1997**, *1320*, 107.

(1047) Janssen, S.; Schafer, G.; Anemuller, S.; Moll, R. *J. Bacteriol.* **1997**, *179*, 5560.

(1048) Yu, L.; Xu, J. X.; Haley, P. E.; Yu, C. A. *J. Biol. Chem.* **1987**, *262*, 1137.

(1049) Iverson, T. M.; Luna-Chavez, C.; Cecchini, G.; Rees, D. C. *Science* **1999**, *284*, 1961.

(1050) Lancaster, C. R. D.; Kroger, A.; Auer, M.; Michel, H. *Nature* **1999**, *402*, 377.

(1051) Nanda, V.; Rosenblatt, M. M.; Osyczka, A.; Kono, H.; Getahun, Z.; Dutton, P. L.; Saven, J. G.; DeGrado, W. F. *J. Am. Chem. Soc.* **2005**, *127*, 5804.

(1052) Ogino, H.; Inomata, S.; Tobita, H. *Chem. Rev.* **1998**, *98*, 2093.
(1053) Rao, P. V.; Holm, R. H. *Chem. Rev.* **2004**, *104*, 527.
(1054) Saouma, C. T.; Kaminsky, W.; Mayer, J. M. *J. Am. Chem. Soc.* **2012**, *134*, 7293.
(1055) Mouesca, J.-M.; Lamotte, B. *Coord. Chem. Rev.* **1998**, *178-180*, 1573.
(1056) Anand, B. N. *Resonance* **1998**, *3*, 52.
(1057) Holm, R. H.; Elsevier Ltd.: 2004; Vol. 8, p 61.
(1058) Gibney, B. R. *Chemtracts* **2003**, *16*, 263.
(1059) Kennedy, M. L.; Gibney, B. R. *J. Am. Chem. Soc.* **2002**, *124*, 6826.
(1060) Coldren, C. D.; Hellinga, H. W.; Caradonna, J. P. *Proc. Natl. Acad. Sci. U. S. A.* **1997**, *94*, 6635.
(1061) Gibney, B. R.; Mulholland, S. E.; Rabanal, F.; Dutton, P. L. *Proc. Natl. Acad. Sci. U. S. A.* **1996**, *93*, 15041.
(1062) Grzyb, J.; Xu, F.; Nanda, V.; Luczkowska, R.; Reijerse, E.; Lubitz, W.; Noy, D. *Biochim. Biophys. Acta, Bioenerg.* **2012**, *1817*, 1256.
(1063) Grzyb, J.; Xu, F.; Weiner, L.; Reijerse, E. J.; Lubitz, W.; Nanda, V.; Noy, D. *Biochim. Biophys. Acta, Bioenerg.* **2010**, *1797*, 406.
(1064) Ryle, M. J.; Lanzilotta, W. N.; Seefeldt, L. C.; Scarrow, R. C.; Jensen, G. M. *J. Biol. Chem.* **1996**, *271*, 1551.
(1065) Anderson, G. L.; Howard, J. B. *Biochemistry* **1984**, *23*, 2118.
(1066) Fu, W. G.; Morgan, T. V.; Mortenson, L. E.; Johnson, M. K. *FEBS Lett.* **1991**, *284*, 165.
(1067) Mulliez, E.; Ollagnier-De, C., S.; Meier, C.; Cremonini, M.; Luchinat, C.; Trautwein, A. X.; Fontecave, M. *JBIC, J. Biol. Inorg. Chem.* **1999**, *4*, 614.
(1068) Yang, J.; Naik, S. G.; Ortillo, D. O.; Garcia-Serres, R.; Li, M.; Broderick, W. E.; Huynh, B. H.; Broderick, J. B. *Biochemistry* **2009**, *48*, 9234.
(1069) Zhang, B.; Crack, J. C.; Subramanian, S.; Green, J.; Thomson, A. J.; Le, B., Nick E.; Johnson, M. K. *Proc. Natl. Acad. Sci. U. S. A.* **2012**, *109*, 15734.
(1070) Nicolet, Y.; Rohac, R.; Martin, L.; Fontecilla-Camps, J. C. *Proc. Natl. Acad. Sci. U. S. A.* **2013**, *110*, 7188.
(1071) Crack, J. C.; Green, J.; Le Brun, N. E.; Thomson, A. J. *J. Biol. Chem.* **2006**, *281*, 18909.
(1072) Khoroshilova, N.; Popescu, C.; Munck, E.; Beinert, H.; Kiley, P. J. *Proc. Natl. Acad. Sci. U. S. A.* **1997**, *94*, 6087.
(1073) Jervis, A. J.; Crack, J. C.; White, G.; Artymiuk, P. J.; Cheesman, M. R.; Thomson, A. J.; Le Brun, N. E.; Green, J. *Proc. Natl. Acad. Sci. U. S. A.* **2009**, *106*, 4659.
(1074) Crack, J. C.; Gaskell, A. A.; Green, J.; Cheesman, M. R.; Le Brun, N. E.; Thomson, A. J. *J. Am. Chem. Soc.* **2008**, *130*, 1749.
(1075) Kent, T. A.; Emptage, M. H.; Merkle, H.; Kennedy, M. C.; Beinert, H.; Muenck, E. *J. Biol. Chem.* **1985**, *260*, 6871.
(1076) Kent, T. A.; Dreyer, J. L.; Kennedy, M. C.; Boi, H. H.; Emptage, M. H.; Beinert, H.; Muenck, E. *Proc. Natl. Acad. Sci. U. S. A.* **1982**, *79*, 1096.
(1077) Kennedy, M. C.; Kent, T. A.; Emptage, M.; Merkle, H.; Beinert, H.; Munck, E. *J. Biol. Chem.* **1984**, *259*, 14463.
(1078) Guergova-Kuras, M.; Kuras, R.; Ugulava, N.; Hadad, I.; Crofts, A. R. *Biochemistry* **2000**, *39*, 7436.
(1079) Moura, J. J. G.; Moura, I.; Kent, T. A.; Lipscomb, J. D.; Huynh, B. H.; LeGall, J.; Xavier, A. V.; Munck, E. *J. Biol. Chem.* **1982**, *257*, 6259.
(1080) Krebs, C.; Henshaw, T. F.; Cheek, J.; Huynh, B. H.; Broderick, J. B. *J. Am. Chem. Soc.* **2000**, *122*, 12497.

(1081) Bingemann, R.; Klein, A. *Eur. J. Biochem.* **2000**, *267*, 6612.
(1082) Hannan, J. P.; Busch, J. L. H.; James, R.; Thomson, A. J.; Moore, G. R.; Davy, S. L. *FEBS Lett.* **2000**, *468*, 161.
(1083) Finnegan, M. G.; Conover, R. C.; Park, J.-B.; Zhou, Z. H.; Adams, M. W. W.; Johnson, M. K. *Inorg. Chem.* **1995**, *34*, 5358.
(1084) Butt, J. N.; Sucheta, A.; Armstrong, F. A.; Breton, J.; Thomson, A. J.; Hatchikian, E. C. *J. Am. Chem. Soc.* **1991**, *113*, 8948.
(1085) Duee, E. D.; Fanchon, E.; Vicat, J.; Sieker, L. C.; Meyer, J.; Moulis, J.-M. *J. Mol. Biol.* **1994**, *243*, 683.
(1086) Stout, C. D.; Stura, E. A.; Mcree, D. E. *J. Mol. Biol.* **1998**, *278*, 629.
(1087) Cheng, H.; Xia, B.; Reed, G. H.; Markley, J. L. *Biochemistry* **1994**, *33*, 3155.
(1088) Marshall, N. M.; Garner, D. K.; Wilson, T. D.; Gao, Y.-G.; Robinson, H.; Nilges, M. J.; Lu, Y. *Nature* **2009**, *462*, 113.
(1089) Shoji, M.; Isobe, H.; Takano, Y.; Kitagawa, Y.; Yamanaka, S.; Okumura, M.; Yamaguchi, K. *J. Quantum Chem.* **2007**, *107*, 3250.
(1090) Underwood, E. J. *Trace Elements in Human and Animal Nutrition*; 4th ed.; Academic Press: New York, 1977.
(1091) Williams, R. J. P. In *Proceedings of the 5th international congress on biochemistry*; PAE, D., Ed.; Pergamon Press, Oxford: 1963; Vol. IV, p 133.
(1092) Williams, R. J. P. *Inorg. Chim. Acta. Rev.* **1971**, *5*, 137.
(1093) Malmstrom, B. G.; Vanngard, T. *J. Mol. Biol.* **1960**, *2*, 118.
(1094) Solomon, E. I.; Hare, J. W.; Gray, H. B. *Proc. Natl. Acad. Sci. U. S. A.* **1976**, *73*, 1389.
(1095) Solomon, E. I. *Inorg. Chem.* **2006**, *45*, 8012.
(1096) Colman, P. M.; Freeman, H. C.; Guss, J. M.; Murata, M.; Norris, V. A.; Ramshaw, J. A. M.; Venkatappa, M. P. *Nature* **1978**, *272*, 319.
(1097) Beinert, H. *Eur. J. Biochem.* **1997**, *245*, 521.
(1098) Beinert, H.; Griffiths, D. E.; Wharton, D. C.; Sands, R. H. *J. Biol. Chem.* **1962**, *237*, 2337.
(1099) Beinert, H.; Palmer, G. *J. Biol. Chem.* **1964**, *239*, 1221.
(1100) Beinert, H.; Palmer, G. *Adv. Enzymol. Relat. Areas Mol. Biol.* **1965**, *27*, 105.
(1101) Greenwood, C.; Hill, B. C.; Barber, D.; Eglinton, D. G.; Thomson, A. J. *Biochem. J.* **1983**, *215*, 303.
(1102) Thomson, A. J.; Greenwood, C.; Peterson, J.; Barrett, C. P. *J. Inorg. Biochem.* **1986**, *28*, 195.
(1103) Gibson, Q. H.; Greenwood, C. *Biochem. J.* **1963**, *86*, 541.
(1104) Gibson, Q. H.; Greenwood, C. *J. Biol. Chem.* **1965**, *240*, 2694.
(1105) Buse, G.; Steffens, G. C. *J. Bioenerg. Biomembr.* **1991**, *23*, 269.
(1106) Steffens, G. C.; Soulimane, T.; Wolff, G.; Buse, G. *Eur. J. Biochem.* **1993**, *213*, 1149.
(1107) Andrew, C. R.; Fraczkiewicz, R.; Czernuszewicz, R. S.; Lappalainen, P.; Saraste, M.; Sanders-Loehr, J. *J. Am. Chem. Soc.* **1996**, *118*, 10436.
(1108) Blackburn, N. J.; Barr, M. E.; Woodruff, W. H.; van der Ooost, J.; de Vries, S. *Biochemistry* **1994**, *33*, 10401.
(1109) Iwata, S.; Ostermeier, C.; Ludwig, B.; Michel, H. *Nature* **1995**, *376*, 660.
(1110) Malkin, R.; Malmstro.Bg *Adv. Enzymol. Relat. Subj. Biochem.* **1970**, *33*, 177.
(1111) Fee, J. A. *Struct. Bonding (Berlin, Ger.)* **1975**, *33*, 1.
(1112) Neese, F.; Zumft, W. G.; Antholine, W. E.; Kroneck, P. M. H. *J. Am. Chem. Soc.* **1996**, *118*, 8692.

(1113) Gamelin, D. R.; Randall, D. W.; Hay, M. T.; Houser, R. P.; Mulder, T. C.; Canters, G. W.; de, V. S.; Tolman, W. B.; Lu, Y.; Solomon, E. I. *J. Am. Chem. Soc.* **1998**, *120*, 5246.

(1114) Farrar, J. A.; Neese, F.; Lappalainen, P.; Kroneck, P. M. H.; Saraste, M.; Zumft, W. G.; Thomson, A. J. *J. Am. Chem. Soc.* **1996**, *118*, 11501.

(1115) Olsson, M. H.; Ryde, U. *J. Am. Chem. Soc.* **2001**, *123*, 7866.

(1116) Adman, E. In *Metalloproteins*; Macmillan: 1985; Vol. 1, p 1.

(1117) Prigge, S. T.; Kolhekar, A. S.; Eipper, B. A.; Mains, R. E.; Amzel, L. M. *Science* **1997**, *278*, 1300.

(1118) Gray, H. B.; Solomon, E. I. In *Copper proteins*; Spiro, T. G., Ed.; Wiley, New York: 1981; Vol. 3, p 1.

(1119) Hart, P. J.; Nersissian, A. M.; George, S. D. In *Encyclopedia of Inorganic Chemistry*; John Wiley & Sons, Ltd: 2006.

(1120) Smeekens, S.; De, G. M.; Van, B. J.; Weisbeek, P. *Nature* **1985**, *317*, 456.

(1121) Sutherland, I. W.; Wilkinson, J. F. *J. Gen. Microbiol.* **1963**, *30*, 105.

(1122) Pascher, T.; Karlsson, B. G.; Nordling, M.; Malmstroem, B. G.; Vaenngaard, T. *Eur. J. Biochem.* **1993**, *212*, 289.

(1123) Tobari, J.; Harada, Y. *Biochem. Biophys. Res. Commun.* **1981**, *101*, 502.

(1124) van Houwelingen, T.; Canters, G. W.; Stobbelaar, G.; Duine, J. A.; Frank, J., Jr.; Tsugita, A. *Eur. J. Biochem.* **1985**, *153*, 75.

(1125) Katoh, S. *Nature* **1960**, *186*, 533.

(1126) Katoh, S.; Shiratori, I.; Takamiya, A. *J. Biochem.* **1962**, *51*, 32.

(1127) Iwasaki, H.; Matsubara, T. *J. Biochem.* **1973**, *73*, 659.

(1128) Sakurai, T.; Ikeda, O.; Suzuki, S. *Inorg. Chem.* **1990**, *29*, 4715.

(1129) Cobley, J. G.; Haddock, B. A. *FEBS Lett.* **1975**, *60*, 29.

(1130) Lappin, A. G.; Lewis, C. A.; Ingledew, W. J. *Inorg. Chem.* **1985**, *24*, 1446.

(1131) McManus, J. D.; Brune, D. C.; Han, J.; Sanders-Loehr, J.; Meyer, T. E.; Cusanovich, M. A.; Tollin, G.; Blankenship, R. E. *J. Biol. Chem.* **1992**, *267*, 6531.

(1132) Markossian, K. A.; Aikazyan, V. T.; Nalbandyan, R. M. *Biochim. Biophys. Acta* **1974**, *359*, 47.

(1133) Battistuzzi, G.; Borsari, M.; Loschi, L.; Righi, F.; Sola, M. *J. Am. Chem. Soc.* **1999**, *121*, 501.

(1134) Scharf, B.; Engelhard, M. *Biochemistry* **1993**, *32*, 12894.

(1135) Komorowski, L.; Schafer, G. *FEBS Lett.* **2001**, *487*, 351.

(1136) Arciero, D. M.; Hooper, A. B.; Rosenzweig, A. C. *Biochemistry* **2001**, *40*, 5674.

(1137) Arciero, D. M.; Pierce, B. S.; Hendrich, M. P.; Hooper, A. B. *Biochemistry* **2002**, *41*, 1703.

(1138) Peisach, J.; Levine, W. G.; Blumberg, W. E. *J. Biol. Chem.* **1967**, *242*, 2847.

(1139) Nersissian, A. M.; Immoos, C.; Hill, M. G.; Hart, P. J.; Williams, G.; Herrmann, R. G.; Valentine, J. S. *Protein Sci.* **1998**, *7*, 1915.

(1140) Nersissian, A. M.; Valentine, J. S. *unpublished*.

(1141) Malmstrom, B. G.; Reinhammar, B.; Vanngard, T. *Biochim. Biophys. Acta* **1968**, *156*, 67.

(1142) Xu, F.; Shin, W.; Brown, S. H.; Wahleithner, J. A.; Sundaram, U. M.; Solomon, E. I. *Biochim. Biophys. Acta* **1996**, *1292*, 303.

(1143) Ducros, V.; Brzozowski, A. M.; Wilson, K. S.; Brown, S. H.; Ostergaard, P.; Schneider, P.; Yaver, D. S.; Pedersen, A. H.; Davies, G. J. *Nat. Struct. Biol.* **1998**, *5*, 310.

(1144) Reinhammar, B. R. M. *Biochim. Biophys. Acta, Bioenerg.* **1972**, *275*, 245.

(1145) Reinhammar, B. R.; Vanngard, T. I. *Eur. J. Biochem.* **1971**, *18*, 463.

(1146) Kroneck Peter M, H.; Armstrong Fraser, A.; Merkle, H.; Marchesini, A. In *Ascorbic Acid: Chemistry, Metabolism, and Uses*; AMERICAN CHEMICAL SOCIETY: 1982; Vol. 200, p 223.

(1147) Holmberg, C. G.; Laurell, C. B. *Acta Chem. Scand.* **1948**, *2*, 550.
(1148) Machonkin, T. E.; Zhang, H. H.; Hedman, B.; Hodgson, K. O.; Solomon, E. I. *Biochemistry* **1998**, *37*, 9570.
(1149) Machonkin, T. E.; Solomon, E. I. *J. Am. Chem. Soc.* **2000**, *122*, 12547.
(1150) Vulpe, C. D.; Kuo, Y.-M.; Murphy, T. L.; Cowley, L.; Askwith, C.; Libina, N.; Gitschier, J.; Anderson, G. J. *Nat. Genet.* **1999**, *21*, 195.
(1151) Askwith, C.; Eide, D.; Van Ho, A.; Bernard, P. S.; Li, L.; Davis-Kaplan, S.; Sipe, D. M.; Kaplan, J. *Cell* **1994**, *76*, 403.
(1152) Machonkin, T. E.; Quintanar, L.; Palmer, A. E.; Hassett, R.; Severance, S.; Kosman, D. J.; Solomon, E. I. *J. Am. Chem. Soc.* **2001**, *123*, 5507.
(1153) Masuko, M.; Iwasaki, H.; Sakurai, T.; Suzuki, S.; Nakahara, A. *J. Biochem.* **1984**, *96*, 447.
(1154) De Rienzo, F.; Gabdoulline, R. R.; Menziani, M. C.; Wade, R. C. *Protein Sci.* **2000**, *9*, 1439.
(1155) Wittung, P.; Källebring, B.; Malmström, B. G. *FEBS Lett.* **1994**, *349*, 286.
(1156) Valentine, J. S.; Doucette, P. A.; Zittin Potter, S. *Annu. Rev. Biochem.* **2005**, *74*, 563.
(1157) Stevens, F. J. *J. Mol. Recognit.* **2008**, *21*, 20.
(1158) Hasnain, S. S.; Hodgson, K. O. *J. Synchrotron Radiat.* **1999**, *6*, 852.
(1159) Tullius, T. D.; Frank, P.; Hodgson, K. O. *Proc. Natl. Acad. Sci. U. S. A.* **1978**, *75*, 4069.
(1160) Nar, H.; Messerschmidt, A.; Huber, R.; Vandekamp, M.; Canters, G. W. *J. Mol. Biol.* **1991**, *221*, 765.
(1161) Walter, R. L.; Ealick, S. E.; Friedman, A. M.; Blake, R. C.; Proctor, P.; Shoham, M. *J. Mol. Biol.* **1996**, *263*, 730.
(1162) Guss, J. M.; Bartunik, H. D.; Freeman, H. C. *Acta Crystallogr., Sect. B: Struct. Sci.* **1992**, *48*, 790.
(1163) Guss, J. M.; Harrowell, P. R.; Murata, M.; Norris, V. A.; Freeman, H. C. *J. Mol. Biol.* **1986**, *192*, 361.
(1164) Cunane, L. M.; Chen, Z. W.; Durley, R. C. E.; Mathews, F. S. *Acta Crystallogr., Sect. D: Biol. Crystallogr.* **1996**, *52*, 676.
(1165) Zhu, Z. Y.; Cunane, L. M.; Chen, Z. W.; Durley, R. C. E.; Mathews, F. S.; Davidson, V. L. *Biochemistry* **1998**, *37*, 17128.
(1166) Guss, J. M.; Merritt, E. A.; Phizackerley, R. P.; Freeman, H. C. *J. Mol. Biol.* **1996**, *262*, 686.
(1167) Hart, P. J.; Nersissian, A. M.; Herrmann, R. G.; Nalbandyan, R. M.; Valentine, J. S.; Eisenberg, D. *Protein Sci.* **1996**, *5*, 2175.
(1168) Malmström, B. G. In *Oxidases and Related Redox Systems*; King, T. E., Mason, H. S., Morrison, M., Eds. New York, 1964, p 207.
(1169) Gray, H. B.; Malmstroem, B. G. *Comments Inorg. Chem.* **1983**, *2*, 203.
(1170) Vallee, B. L.; Williams, R. J. *Proc. Natl. Acad. Sci. U. S. A.* **1968**, *59*, 498.
(1171) Penner-Hahn, J. E.; Murata, M.; Hodgson, K. O.; Freeman, H. C. *Inorg. Chem.* **1989**, *28*, 1826.
(1172) Carugo, O.; Carugo, K. D. *Trends Biochem. Sci.* **2005**, *30*, 213.
(1173) Orville, A. M.; Lountos, G. T.; Finnegan, S.; Gadda, G.; Prabhakar, R. *Biochemistry* **2009**, *48*, 720.
(1174) Nar, H.; Messerschmidt, A.; Huber, R.; Van, d. K. M.; Canters, G. W. *FEBS Lett.* **1992**, *306*, 119.
(1175) Shepard, W. E. B.; Kingston, R. L.; Anderson, B. F.; Baker, E. N. *Acta Crystallogr., Sect. D: Biol. Crystallogr.* **1993**, *D49*, 331.
(1176) Garrett, T. P. J.; Clingeleffer, D. J.; Guss, J. M.; Rogers, S. J.; Freeman, H. C. *J. Biol. Chem.* **1984**, *259*, 2822.

(1177) Petratos, K.; Papadovasilaki, M.; Dauter, Z. *FEBS Lett.* **1995**, *368*, 432.

(1178) Durley, R.; Chen, L.; Scott Mathews, F.; Lim, L. W.; Davidson, V. L. *Protein Sci.* **1993**, *2*, 739.

(1179) McMillin, D. R.; Holwerda, R. A.; Gray, H. B. *Proc. Nat. Acad. Sci. U. S. A.* **1974**, *71*, 1339.

(1180) Engeseth, H. R.; McMillin, D. R.; Otvos, J. D. *J. Biol. Chem.* **1984**, *259*, 4822.

(1181) Church, W. B.; Guss, J. M.; Potter, J. J.; Freeman, H. C. *J. Biol. Chem.* **1986**, *261*, 234.

(1182) Baker, E. N.; Anderson, B. F.; Blackwell, K. E.; Kingston, R. L.; Norris, G. E.; Shepard, W. E. B. *J. Inorg. Biochem.* **1991**, *43*, 162.

(1183) Nar, H.; Huber, R.; Messerschmidt, A.; Filippou, A. C.; Barth, M.; Jaquinod, M.; Van, d. K. M.; Canters, G. W. *Eur. J. Biochem.* **1992**, *205*, 1123.

(1184) Gewirth, A. A.; Solomon, E. I. *J. Am. Chem. Soc.* **1988**, *110*, 3811.

(1185) Solomon, E. I.; Penfield, K. W.; Gewirth, A. A.; Lowery, M. D.; Shadle, S. E.; Guckert, J. A.; LaCroix, L. B. *Inorg. Chim. Acta* **1996**, *243*, 67.

(1186) LaCroix, L. B.; Randall, D. W.; Nersissian, A. M.; Hoitink, C. W. G.; Canters, G. W.; Valentine, J. S.; Solomon, E. I. *J. Am. Chem. Soc.* **1998**, *120*, 9621.

(1187) Shadle, S. E.; Penner-Hahn, J. E.; Schugar, H. J.; Hedman, B.; Hodgson, K. O.; Solomon, E. I. *J. Am. Chem. Soc.* **1993**, *115*, 767.

(1188) Wood, P. M.; Bendall, D. S. *Biochim. Biophys. Acta, Bioenerg.* **1975**, *387*, 115.

(1189) Haehnel, W. *Annu. Rev. Plant Physiol.* **1984**, *35*, 659.

(1190) Hervas, M.; Navarro, J. A.; Diaz, A.; Bottin, H.; De la Rosa, M. A. *Biochemistry* **1995**, *34*, 11321.

(1191) Sigfridsson, K. *Photosynth. Res.* **1998**, *57*, 1.

(1192) Hope, A. B. *Biochim. Biophys. Acta, Bioenerg.* **2000**, *1456*, 5.

(1193) Tobari, J.; Harada, Y. *Biochem. Biophys. Res. Commun.* **1981**, *101*, 502.

(1194) Gray, K. A.; Davidson, V. L.; Knaff, D. B. *J. Biol. Chem.* **1988**, *263*, 13987.

(1195) van Spanning, R. J.; Wansell, C. W.; Reijnders, W. N.; Oltmann, L. F.; Stouthamer, A. H. *FEBS Lett.* **1990**, *275*, 217.

(1196) Chen, L.; Durley, R.; Poliks, B. J.; Hamada, K.; Chen, Z.; Mathews, F. S.; Davidson, V. L.; Satow, Y.; Huizinga, E. *Biochemistry* **1992**, *31*, 4959.

(1197) Brooks, H. B.; Davidson, V. L. *J. Am. Chem. Soc.* **1994**, *116*, 11201.

(1198) Dennison, C.; Canters, G. W.; Vries, S. D.; Vijgenboom, E.; Spanning, R. J. V. In *Adv. Inorg. Chem.*; Sykes, A. G., Ed.; Academic Press: 1998; Vol. Volume 45, p 351.

(1199) Davidson, V. L.; Sun, D. P. *J. Am. Chem. Soc.* **2003**, *125*, 3224.

(1200) Meschi, F.; Wiertz, F.; Klauss, L.; Cavalieri, C.; Blok, A.; Ludwig, B.; Heering, H. A.; Merli, A.; Rossi, G. L.; Ubbink, M. *J. Am. Chem. Soc.* **2010**, *132*, 14537.

(1201) Giudici-Orticoni, M.-T.; Guerlesquin, F.; Bruschi, M.; Nitschke, W. *J. Biol. Chem.* **1999**, *274*, 30365.

(1202) Appia-Ayme, C.; Guiliani, N.; Ratouchniak, J.; Bonnefoy, V. *Appl. Environ. Microbiol.* **1999**, *65*, 4781.

(1203) Kakutani, T.; Watanabe, H.; Arima, K.; Beppu, T. *J. Biochem.* **1981**, *89*, 463.

(1204) Kohzuma, T.; Takase, S.; Shidara, S.; Suzuki, S. *Chem. Lett.* **1993**, 149.

(1205) Moir, J. W. B.; Baratta, D.; Richardson, D. J.; Ferguson, S. J. *Eur. J. Biochem.* **1993**, *212*, 377.

(1206) Kukimoto, M.; Nishiyama, M.; Ohnuki, T.; Turley, S.; Adman, E. T.; Horinouchi, S.; Beppu, T. *Protein Eng.* **1995**, *8*, 153.

(1207) Kukimoto, M.; Nishiyama, M.; Tanokura, M.; Adman, E. T.; Horinouchi, S. *J. Biol. Chem.* **1996**, *271*, 13680.

(1208) Sukumar, N.; Chen, Z.-w.; Ferrari, D.; Merli, A.; Rossi, G. L.; Bellamy, H. D.; Chistoserdov, A.; Davidson, V. L.; Mathews, F. S. *Biochemistry* **2006**, *45*, 13500.

(1209) Edwards, S. L.; Davidson, V. L.; Hyun, Y.-L.; Wingfield, P. T. *J. Biol. Chem.* **1995**, *270*, 4293.

(1210) Hyun, Y.-L.; Davidson, V. L. *Biochemistry* **1995**, *34*, 12249.

(1211) Ubbink, M.; Ejdebäck, M.; Karlsson, B. G.; Bendall, D. S. *Structure* **1998**, *6*, 323.

(1212) Crowley, P. B.; Otting, G.; Schlarb-Ridley, B. G.; Canters, G. W.; Ubbink, M. *J. Am. Chem. Soc.* **2001**, *123*, 10444.

(1213) Sykes, A. G. In *Long-Range Electron Transfer in Biology*; Springer Berlin Heidelberg: 1991; Vol. 75, p 175.

(1214) He, S.; Modi, S.; Bendall, D. S.; Gray, J. C. *EMBO J.* **1991**, *10*, 4011.

(1215) Schlarb-Ridley, B. G.; Bendall, D. S.; Howe, C. J. *Biochemistry* **2003**, *42*, 4057.

(1216) Sato, K.; Kohzuma, T.; Dennison, C. *J. Am. Chem. Soc.* **2004**, *126*, 3028.

(1217) Crowley, P. B.; Hunter, D. M.; Sato, K.; McFarlane, W.; Dennison, C. *Biochem. J.* **2004**, *378*, 45.

(1218) Takayama, S. J.; Irie, K.; Tai, H. L.; Kawahara, T.; Hirota, S.; Takabe, T.; Alcaraz, L. A.; Donaire, A.; Yamamoto, Y. *JBIC, J. Biol. Inorg. Chem.* **2009**, *14*, 821.

(1219) Sykes, A. G. *Chem. Soc. Rev.* **1985**, *14*, 283.

(1220) Newton, M. D. *Chem. Rev.* **1991**, *91*, 767.

(1221) Lowery, M. D.; Guckert, J. A.; Gebhard, M. S.; Solomon, E. I. *J. Am. Chem. Soc.* **1993**, *115*, 3012.

(1222) Regan, J. J.; Di Bilio, A. J.; Langen, R.; Skov, L. K.; Winkler, J. R.; Gray, H. B.; Onuchic, J. N. *Chem. Biol.* **1995**, *2*, 489.

(1223) Holwerda, R. A.; Wherland, S.; Gray, H. B. *Annu. Rev. Biophys. Bioeng.* **1976**, *5*, 363.

(1224) Suzuki, S.; Kataoka, K.; Yamaguchi, K.; Inoue, T.; Kai, Y. *Coord. Chem. Rev.* **1999**, *190–192*, 245.

(1225) Rorabacher, D. B. *Chem. Rev.* **2004**, *104*, 651.

(1226) Gray, H. B.; Winkler, J. R. *Biochim. Biophys. Acta, Bioenerg.* **2010**, *1797*, 1563.

(1227) Modi, S.; He, S.; Gray, J. C.; Bendall, D. S. *Biochim. Biophys. Acta, Bioenerg.* **1992**, *1101*, 64.

(1228) Meyer, T. E.; Zhao, Z. G.; Cusanovich, M. A.; Tollin, G. *Biochemistry* **1993**, *32*, 4552.

(1229) Kannt, A.; Young, S.; Bendall, D. S. *Biochim. Biophys. Acta, Bioenerg.* **1996**, *1277*, 115.

(1230) Nordling, M.; Sigfridsson, K.; Young, S.; Lundberg, L. G.; Hansson, Ö. *FEBS Lett.* **1991**, *291*, 327.

(1231) Haehnel, W.; Jansen, T.; Gause, K.; Klosgen, R. B.; Stahl, B.; Michl, D.; Huvermann, B.; Karas, M.; Herrmann, R. G. *EMBO J.* **1994**, *13*, 1028.

(1232) Brooks, H. B.; Davidson, V. L. *Biochemistry* **1994**, *33*, 5696.

(1233) Davidson, V. L.; Jones, L. H. *Biochemistry* **1996**, *35*, 8120.

(1234) Kataoka, K.; Kondo, A.; Yamaguchi, K.; Suzuki, S. *J. Inorg. Biochem.* **2000**, *82*, 79.

(1235) Kataoka, K.; Yamaguchi, K.; Sakai, S.; Takagi, K.; Suzuki, S. *Biochem. Biophys. Res. Commun.* **2003**, *303*, 519.

(1236) Kataoka, K.; Yamaguchi, K.; Kobayashi, M.; Mori, T.; Bokui, N.; Suzuki, S. *J. Biol. Chem.* **2004**, *279*, 53374.

(1237) Davidson, V. L. *Acc. Chem. Res.* **1999**, *33*, 87.

(1238) Adams, G. E.; Fielden, E. M.; Michael, B. D. *Fast processes in Radiation Chemistry and Biology*; John Wiley & Sons, Inc., New York, 1975.

(1239) Farver, O.; Pecht, I. *Proc. Natl. Acad. Sci. U. S. A.* **1989**, *86*, 6968.

(1240) Marcus, R. A.; Sutin, N. *Biochim. Biophys. Acta, Rev. Bioenerg.* **1985**, *811*, 265.

(1241) Dahlin, S.; Reinhammar, B.; Wilson, M. T. *Biochem. J.* **1984**, *218*, 609.
(1242) Armstrong, F. A.; Driscoll, P. C.; Hill, H. A. O. *FEBS Lett.* **1985**, *190*, 242.
(1243) Lommen, A.; Canters, G. W. *J. Biol. Chem.* **1990**, *265*, 2768.
(1244) Kyritsis, P.; Dennison, C.; Ingledew, W. J.; McFarlane, W.; Sykes, A. G. *Inorg. Chem.* **1995**, *34*, 5370.
(1245) Hunter, D. M.; McFarlane, W.; Sykes, A. G.; Dennison, C. *Inorg. Chem.* **2001**, *40*, 354.
(1246) Dennison, C.; Lawler, A. T.; Kohzuma, T. *Biochemistry* **2002**, *41*, 552.
(1247) Sato, K.; Dennison, C. *Biochemistry* **2002**, *41*, 120.
(1248) Sato, K.; Kohzuma, T.; Dennison, C. *J. Am. Chem. Soc.* **2003**, *125*, 2101.
(1249) Sato, K.; Crowley, P. B.; Dennison, C. *J. Biol. Chem.* **2005**, *280*, 19281.
(1250) Sola, M.; Cowan, J. A.; Gray, H. B. *J. Am. Chem. Soc.* **1989**, *111*, 6627.
(1251) Concar, D. W.; Whitford, D.; Pielak, G. J.; Williams, R. J. P. *J. Am. Chem. Soc.* **1991**, *113*, 2401.
(1252) Ubbink, M.; Canters, G. W. *Biochemistry* **1993**, *32*, 13893.
(1253) Dennison, C.; Kohzuma, T. *Inorg. Chem.* **1999**, *38*, 1491.
(1254) Xu, F.; Berka, R. M.; Wahleithner, J. A.; Nelson, B. A.; Shuster, J. R.; Brown, S. H.; Palmer, A. E.; Solomon, E. I. *Biochem. J.* **1998**, *334*, 63.
(1255) Yaver, D. S.; Xu, F.; Golightly, E. J.; Brown, K. M.; Brown, S. H.; Rey, M. W.; Schneider, P.; Halkier, T.; Mondorf, K.; Dalboge, H. *Appl. Environ. Microbiol.* **1996**, *62*, 834.
(1256) Xu, F.; Palmer, A. E.; Yaver, D. S.; Berka, R. M.; Gambetta, G. A.; Brown, S. H.; Solomon, E. I. *J. Biol. Chem.* **1999**, *274*, 12372.
(1257) Romero, A.; Hoitink, C. W. G.; Nar, H.; Huber, R.; Messerschmidt, A.; Canters, G. W. *J. Mol. Biol.* **1993**, *229*, 1007.
(1258) Olesen, K.; Veselov, A.; Zhao, Y.; Wang, Y.; Danner, B.; Scholes, C. P.; Shapleigh, J. P. *Biochemistry* **1998**, *37*, 6086.
(1259) Hall, J. F.; Kanbi, L. D.; Strange, R. W.; Hasnain, S. S. *Biochemistry* **1999**, *38*, 12675.
(1260) Kataoka, K.; Nakai, M.; Yamaguchi, K.; Suzuki, S. *Biochem. Biophys. Res. Commun.* **1998**, *250*, 409.
(1261) Diederix, R. E. M.; Canters, G. W.; Dennison, C. *Biochemistry* **2000**, *39*, 9551.
(1262) Solomon, E. I.; Sundaram, U. M.; Machonkin, T. E. *Chem. Rev.* **1996**, *96*, 2563.
(1263) Sakurai, T.; Kataoka, K. *Cell. Mol. Life Sci.* **2007**, *64*, 2642.
(1264) Quintanar, L.; Stoj, C.; Taylor, A. B.; Hart, P. J.; Kosman, D. J.; Solomon, E. I. *Acc. Chem. Res.* **2007**, *40*, 445.
(1265) Lawton, T. J.; Rosenzweig, A. C. In *Encyclopedia of Inorganic and Bioinorganic Chemistry*; John Wiley & Sons, Ltd: 2011.
(1266) Sakurai, T.; Kataoka, K. In *Copper-Oxygen Chemistry*; John Wiley & Sons, Inc.: 2011, p 131.
(1267) Wasser, I. M.; de Vries, S.; Moënne-Loccoz, P.; Schröder, I.; Karlin, K. D. *Chem. Rev.* **2002**, *102*, 1201.
(1268) Hong, G.; Ivnitski, D. M.; Johnson, G. R.; Atanassov, P.; Pachter, R. *J. Am. Chem. Soc.* **2011**, *133*, 4802.
(1269) Whittaker, M.; Bergmann, D.; Arciero, D.; Hooper, A. B. *Biochim. Biophys. Acta, Bioenerg.* **2000**, *1459*, 346.
(1270) Lieberman, R. L.; Arciero, D. M.; Hooper, A. B.; Rosenzweig, A. C. *Biochemistry* **2001**, *40*, 5674.
(1271) Basumallick, L.; Sarangi, R.; DeBeer George, S.; Elmore, B.; Hooper, A. B.; Hedman, B.; Hodgson, K. O.; Solomon, E. I. *J. Am. Chem. Soc.* **2005**, *127*, 3531.

(1272) Dawson, P. E.; Kent, S. B. H. *Annu. Rev. Biochem.* **2000**, *69*, 923.
(1273) Muir, T. W. *Annu. Rev. Biochem.* **2003**, *72*, 249.
(1274) Liu, C. C.; Schultz, P. G. *Annu. Rev. Biochem.* **2010**, *79*, 413.
(1275) Karlsson, B. G.; Aasa, R.; Malmstroem, B. G.; Lundberg, L. G. *FEBS Lett.* **1989**, *253*, 99.
(1276) Karlsson, B. G.; Nordling, M.; Pascher, T.; Tsai, L.-C.; Sjolin, L.; Lundberg, L. G. *Protein Eng.* **1991**, *4*, 343.
(1277) Kroes, S. J.; Hoitink, C. W. G.; Andrew, C. R.; Sanders-Loehr, J.; Messerschmid, A.; Hagen, W. R.; Canters, G. W. *Eur. J. Biochem.* **1996**, *240*, 342.
(1278) Murphy, L. M.; Strange, R. W.; Karlsson, B. G.; Lundberg, L. G.; Pascher, T.; Reinhammar, B.; Hasnain, S. S. *Biochemistry* **1993**, *32*, 1965.
(1279) Hough, M. A.; Ellis, M. J.; Antonyuk, S.; Strange, R. W.; Sawers, G.; Eady, R. R.; Samar, H. S. *J. Mol. Biol.* **2005**, *350*, 300.
(1280) DeBeer George, S.; Basumallick, L.; Szilagyi, R. K.; Randall, D. W.; Hill, M. G.; Nersissian, A. M.; Valentine, J. S.; Hedman, B.; Hodgson, K. O.; Solomon, E. I. *J. Am. Chem. Soc.* **2003**, *125*, 11314.
(1281) Harrison, M. D.; Dennison, C. *Proteins: Struct., Funct., Bioinf.* **2004**, *55*, 426.
(1282) Frank, P.; Licht, A.; Tullius, T. D.; Hodgson, K. O.; Pecht, I. *J. Biol. Chem.* **1985**, *260*, 5518.
(1283) LaCroix, L. B.; Shadle, S. E.; Wang, Y.; Averill, B. A.; Hedman, B.; Hodgson, K. O.; Solomon, E. I. *J. Am. Chem. Soc.* **1996**, *118*, 7755.
(1284) Berry, S. M.; Ralle, M.; Low, D. W.; Blackburn, N. J.; Lu, Y. *J. Am. Chem. Soc.* **2003**, *125*, 8760.
(1285) Garner, D. K.; Vaughan, M. D.; Hwang, H. J.; Savelieff, M. G.; Berry, S. M.; Honek, J. F.; Lu, Y. *J. Am. Chem. Soc.* **2006**, *128*, 15608.
(1286) Yanagisawa, S.; Dennison, C. *J. Am. Chem. Soc.* **2005**, *127*, 16453.
(1287) Messerschmidt, A.; Prade, L.; Kroes, S. J.; Sanders-Loehr, J.; Huber, R.; Canters, G. W. *Proc. Natl. Acad. Sci. U. S. A.* **1998**, *95*, 3443.
(1288) van Gestel, M.; Canters, G. W.; Krupka, H.; Messerschmid, A.; de Waal, E. C.; Warmerdam, G. C. M.; Groenen, E. J. J. *J. Am. Chem. Soc.* **2000**, *122*, 2322.
(1289) Karlsson, B. G.; Tsai, L. C.; Nar, H.; SandersLoehr, J.; Bonander, N.; Langer, V.; Sjolin, L. *Biochemistry* **1997**, *36*, 4089.
(1290) Strange, R. W.; Murphy, L. M.; Karlsson, B. G.; Reinhammar, B.; Hasnain, S. S. *Biochemistry* **1996**, *35*, 16391.
(1291) Webb, M. A.; Kiser, C. N.; Richards, J. H.; Di Bilio, A. J.; Gray, H. B.; Winkler, J. R.; Loppnow, G. R. *J. Phys. Chem. B* **2000**, *104*, 10915.
(1292) Basumallick, L.; Szilagyi, R. K.; Zhao, Y.; Shapleigh, J. P.; Scholes, C. P.; Solomon, E. I. *J. Am. Chem. Soc.* **2003**, *125*, 14784.
(1293) Clark, K. M.; Yu, Y.; Marshall, N. M.; Sieracki, N. A.; Nilges, M. J.; Blackburn, N. J.; van der Donk, W. A.; Lu, Y. *J. Am. Chem. Soc.* **2010**, *132*, 10093.
(1294) Den Blaauwen, T.; Van de Kamp, M.; Canters, G. W. *J. Am. Chem. Soc.* **1991**, *113*, 5050.
(1295) van Pouderoyen, G.; Andrew, C. R.; Loehr, T. M.; Sanders-Loehr, J.; Mazumdar, S.; Hill, H. A.; Canters, G. W. *Biochemistry* **1996**, *35*, 1397.
(1296) Den Blaauwen, T.; Canters, G. W. *J. Am. Chem. Soc.* **1993**, *115*, 1121.
(1297) Jeuken, L. J. C.; van Vliet, P.; Verbeet, M. P.; Camba, R.; McEvoy, J. P.; Armstrong, F. A.; Canters, G. W. *J. Am. Chem. Soc.* **2000**, *122*, 12186.
(1298) Gorren, A. C. F.; denBlaauwen, T.; Canters, G. W.; Hopper, D. J.; Duine, J. A. *FEBS Lett.* **1996**, *381*, 140.
(1299) Alagaratnam, S.; Meeuwenoord, N. J.; Navarro, J. A.; Hervas, M.; De la Rosa, M. A.; Hoffmann, M.; Einsle, O.; Ubbink, M.; Canters, G. W. *FEBS J.* **2011**, *278*, 1506.

(1300) Canters, G. W.; Kolczak, U.; Armstrong, F.; Jeuken, L. J.; Camba, R.; Sola, M. *Faraday Discuss.* **2000**, 205.

(1301) Berry, S. M.; Gieselman, M. D.; Nilges, M. J.; van der Donk, W. A.; Lu, Y. *J. Am. Chem. Soc.* **2002**, *124*, 2084.

(1302) Ralle, M.; Berry, S. M.; Nilges, M. J.; Gieselman, M. D.; van der Donk, W. A.; Lu, Y.; Blackburn, N. J. *J. Am. Chem. Soc.* **2004**, *126*, 7244.

(1303) Sarangi, R.; Gorelsky, S. I.; Basumallick, L.; Hwang, H. J.; Pratt, R. C.; Stack, T. D. P.; Lu, Y.; Hodgson, K. O.; Hedman, B.; Solomon, E. I. *J. Am. Chem. Soc.* **2008**, *130*, 3866.

(1304) Mizoguchi, T. J.; Di Bilio, A. J.; Gray, H. B.; Richards, J. H. *J. Am. Chem. Soc.* **1992**, *114*, 10076.

(1305) Piccioli, M.; Luchinat, C.; Mizoguchi, T. J.; Ramirez, B. E.; Gray, H. B.; Richards, J. H. *Inorg. Chem.* **1995**, *34*, 737.

(1306) Faham, S.; Mizoguchi, T. J.; Adman, E. T.; Gray, H. B.; Richards, J. H.; Rees, D. C. *JBIC, J. Biol. Inorg. Chem.* **1997**, *2*, 464.

(1307) DeBeer, S.; Kiser, C. N.; Mines, G. A.; Richards, J. H.; Gray, H. B.; Solomon, E. I.; Hedman, B.; Hodgson, K. O. *Inorg. Chem.* **1999**, *38*, 433.

(1308) Lancaster, K. M.; George, S. D.; Yokoyama, K.; Richards, J. H.; Gray, H. B. *Nat. Chem.* **2009**, *1*, 711.

(1309) Lancaster, K. M.; Yokoyama, K.; Richards, J. H.; Winkler, J. R.; Gray, H. B. *Inorg. Chem.* **2009**, *48*, 1278.

(1310) Lancaster, K. M.; Sproules, S.; Palmer, J. H.; Richards, J. H.; Gray, H. B. *J. Am. Chem. Soc.* **2010**, *132*, 14590.

(1311) Lancaster, K. M.; Farver, O.; Wherland, S.; Crane, E. J., III; Richards, J. H.; Pecht, I.; Gray, H. B. *J. Am. Chem. Soc.* **2011**, *133*, 4865.

(1312) Kanbi, L. D.; Antonyuk, S.; Hough, M. A.; Hall, J. F.; Dodd, F. E.; Hasnain, S. S. *J. Mol. Biol.* **2002**, *320*, 263.

(1313) Libeu, C. A. P.; Kukimoto, M.; Nishiyama, M.; Horinouchi, S.; Adman, E. T. *Biochemistry* **1997**, *36*, 13160.

(1314) Botuyan, M. V.; ToyPalmer, A.; Chung, J.; Blake, R. C.; Beroza, P.; Case, D. A.; Dyson, H. J. *J. Mol. Biol.* **1996**, *263*, 752.

(1315) Lowery, M. D.; Solomon, E. I. *Inorg. Chim. Acta* **1992**, *198*, 233.

(1316) Hadt, R. G.; Sun, N.; Marshall, N. M.; Hodgson, K. O.; Hedman, B.; Lu, Y.; Solomon, E. I. *J. Am. Chem. Soc.* **2012**, *134*, 16701.

(1317) Farver, O.; Marshall, N. M.; Wherland, S.; Lu, Y.; Pecht, I. *Proc. Natl. Acad. Sci. U. S. A.* **2013**, *110*, 10536.

(1318) Dennison, C.; Vijgenboom, E.; de Vries, S.; van der Oost, J.; Canters, G. W. *FEBS Lett.* **1995**, *365*, 92.

(1319) Hay, M.; Richards, J. H.; Lu, Y. *Proc. Natl. Acad. Sci. U. S. A.* **1996**, *93*, 461.

(1320) Berry, S. M.; Bladholm, E. L.; Mostad, E. J.; Schenewerk, A. R. *JBIC, J. Biol. Inorg. Chem.* **2011**, *16*, 473.

(1321) Dennison, C.; Vijgenboom, E.; Hagen, W. R.; Canters, G. W. *J. Am. Chem. Soc.* **1996**, *118*, 7406.

(1322) Buning, C.; Canters, G. W.; Comba, P.; Dennison, C.; Jeuken, L.; Melter, M.; Sanders-Loehr, J. *J. Am. Chem. Soc.* **1999**, *122*, 204.

(1323) Remenyi, R.; Jeuken, L. J.; Comba, P.; Canters, G. W. *JBIC, J. Biol. Inorg. Chem.* **2001**, *6*, 23.

(1324) Battistuzzi, G.; Borsari, M.; Canters, G. W.; di Rocco, G.; de Waal, E.; Arendsen, Y.; Leonardi, A.; Ranieri, A.; Sola, M. *Biochemistry* **2005**, *44*, 9944.

(1325) Yanagisawa, S.; Dennison, C. *J. Am. Chem. Soc.* **2003**, *125*, 4974.

(1326) Yanagisawa, S.; Dennison, C. *J. Am. Chem. Soc.* **2004**, *126*, 15711.

(1327) Li, C.; Banfield, M. J.; Dennison, C. *J. Am. Chem. Soc.* **2007**, *129*, 709.

(1328) Wikstrom, M. *Biochim. Biophys. Acta, Bioenerg.* **2004**, *1655*, 241.

(1329) Brown, K.; Tegoni, M.; Prudencio, M.; Pereira, A. S.; Besson, S.; Moura, J.; Moura, I.; Cambillau, C. *Nat. Struct. Mol. Biol.* **2000**, *7*, 191.

(1330) Haltia, T.; Brown, K.; Tegoni, M.; Cambillau, C.; Saraste, M.; Mattila, K.; Djinovic-Carugo, K. *Biochem. J.* **2003**, *369*, 77.

(1331) Komorowski, L.; Anemuller, S.; Schafer, G. *J. Bioenerg. Biomembr.* **2001**, *33*, 27.

(1332) Suharti; Heering, H. A.; de Vries, S. *Biochemistry* **2004**, *43*, 13487.

(1333) Suharti; Strampraad, M. J.; Schröder, I.; de Vries, S. *Biochemistry* **2001**, *40*, 2632.

(1334) Ryden, L. G.; Hunt, L. T. *J. Mol. Evol.* **1993**, *36*, 41.

(1335) Abolmaali, B.; Taylor, H. V.; Weser, U. *Struct. Bonding (Berlin, Ger.)* **1998**, *91*, 91.

(1336) Blair, D. F.; Ellis, W. R., Jr.; Wang, H.; Gray, H. B.; Chan, S. I. *J. Biol. Chem.* **1986**, *261*, 11524.

(1337) Immoos, C.; Hill, M. G.; Sanders, D.; Fee, J. A.; Slutter, S. E.; Richards, J. H.; Gray, H. B. *JBIC, J. Biol. Inorg. Chem.* **1996**, *1*, 529.

(1338) Ghosh, S. K.; Saha, S. K.; Ghosh, M. C.; Bose, R. N.; Reed, J. W.; Gould, E. S. *Inorg. Chem.* **1992**, *31*, 3358.

(1339) Lappalainen, P.; Aasa, R.; Malmstrom, B. G.; Saraste, M. *J. Biol. Chem.* **1993**, *268*, 26416.

(1340) Farver, O.; Chen, Y.; Fee, J. A.; Pecht, I. *FEBS Lett.* **2006**, *580*, 3417.

(1341) Slutter, C. E.; Langen, R.; Sanders, D.; Lawrence, S. M.; Wittung, P.; Di Bilio, A. J.; Hill, M. G.; Fee, J. A.; Richards, J. H.; et, a. *Inorg. Chim. Acta* **1996**, *243*, 141.

(1342) Slutter, C. E.; Sanders, D.; Wittung, P.; Malmstrom, B. G.; Aasa, R.; Richards, J. H.; Gray, H. B.; Fee, J. A. *Biochemistry* **1996**, *35*, 3387.

(1343) Fujita, K.; Nakamura, N.; Ohno, H.; Leigh, B. S.; Niki, K.; Gray, H. B.; Richards, J. H. *J. Am. Chem. Soc.* **2004**, *126*, 13954.

(1344) Blackburn, N. J.; de Vries, S.; Barr, M. E.; Houser, R. P.; Tolman, W. B.; Sanders, D.; Fee, J. A. *J. Am. Chem. Soc.* **1997**, *119*, 6135.

(1345) von Wachenfeldt, C.; de Vries, S.; van der Oost, J. *FEBS Lett.* **1994**, *340*, 109.

(1346) Riester, J.; Zumft, W. G.; Kroneck, P. M. H. *Eur. J. Biochem.* **1989**, *178*, 751.

(1347) Hulse, C. L.; Averill, B. A. *Biochem. Biophys. Res. Commun.* **1990**, *166*, 729.

(1348) Kelly, M.; Lappalainen, P.; Talbo, G.; Haltia, T.; van, d. O. J.; Saraste, M. *J. Biol. Chem.* **1993**, *268*, 16781.

(1349) Wilmanns, M.; Lappalainen, P.; Kelly, M.; Sauer-Eriksson, E.; Saraste, M. *Proc. Natl. Acad. Sci. U. S. A.* **1995**, *92*, 11955.

(1350) Hay, M. T.; Ang, M. C.; Gamelin, D. R.; Solomon, E. I.; Antholine, W. E.; Ralle, M.; Blackburn, N. J.; Massey, P. D.; Wang, X.; Kwon, A. H.; Lu, Y. *Inorg. Chem.* **1998**, *37*, 191.

(1351) Prudencio, M.; Pereira, A. S.; Tavares, P.; Besson, S.; Cabrito, I.; Brown, K.; Samyn, B.; Devreese, B.; Van, B. J.; Rusnak, F.; Fauque, G.; Moura, J. J.; Tegoni, M.; Cambillau, C.; Moura, I. *Biochemistry* **2000**, *39*, 3899.

(1352) Paumann, M.; Lubura, B.; Regelsberger, G.; Feichtinger, M.; Koellensberger, G.; Jakopitsch, C.; Furtmueller, P. G.; Peschek, G. A.; Obinger, C. *J. Biol. Chem.* **2004**, *279*, 10293.

(1353) Larsson, S.; Kaellebring, B.; Wittung, P.; Malmstroem, B. G. *Proc. Natl. Acad. Sci.* **1995**, *92*, 7167.

(1354) Henkel, G.; Mueller, A.; Weissgraeber, S.; Buse, G.; Soulimane, T.; Steffens, G. C. M.; Nolting, H.-F. *Angew. Chem., Int. Ed.* **1995**, *34*, 1488.

(1355) Froncisz, W.; Scholes, C. P.; Hyde, J. S.; Wei, Y. H.; King, T. E.; Shaw, R. W.; Beiner, H. *J. Biol. Chem.* **1979**, *254*, 7482.

(1356) Hoffman, B. M.; Roberts, J. E.; Swanson, M.; Speck, S. H.; Margoliash, E. *Proc. Natl. Acad. Sci.* **1980**, *77*, 1452.

(1357) Slutter, C. E.; Gromov, I.; Richards, J. H.; Pecht, I.; Goldfarb, D. *J. Am. Chem. Soc.* **1999**, *121*, 5077.

(1358) Lappalainen, P.; Watmough, N. J.; Greenwood, C.; Saraste, M. *Biochemistry* **1995**, *34*, 5824.

(1359) Williams, P. A.; Blackburn, N. J.; Sanders, D.; Bellamy, H.; Stura, E. A.; Fee, J. A.; McRee, D. E. *Nat. Struct. Biol.* **1999**, *6*, 509.

(1360) Song, A.; Li, L.; Yu, T.; Chen, S.; Huang, Z. *Protein Eng.* **2003**, *16*, 435.

(1361) Maneg, O.; Ludwig, B.; Malatesta, F. *J. Biol. Chem.* **2003**, *278*, 46734.

(1362) van der Oost, J.; Lappalainen, P.; Musacchio, A.; Warne, A.; Lemieux, L.; Rumbley, J.; Gennis, R. B.; Aasa, R.; Pascher, T.; Malmstrom, B. G.; et al. *EMBO J.* **1992**, *11*, 3209.

(1363) Jones, L. H.; Liu, A.; Davidson, V. L. *J. Biol. Chem.* **2003**, *278*, 47269.

(1364) Andrew, C. R.; Lappalainen, P.; Saraste, M.; Hay, M. T.; Lu, Y.; Dennison, C.; Canters, G. W.; Fee, J. A.; Nakamura, N.; Sanders-Loehr, J. *J. Am. Chem. Soc.* **1995**, *117*, 10759.

(1365) Savelieff, M. G.; Lu, Y. *JBIC, J. Biol. Inorg. Chem.* **2010**, *15*, 461.

(1366) DeBeer, G. S.; Metz, M.; Szilagyi, R. K.; Wang, H.; Cramer, S. P.; Lu, Y.; Tolman, W. B.; Hedman, B.; Hodgson, K. O.; Solomon, E. I. *J. Am. Chem. Soc.* **2001**, *123*, 5757.

(1367) Robinson, H.; Ang, M. C.; Gao, Y. G.; Hay, M. T.; Lu, Y.; Wang, A. H. *Biochemistry* **1999**, *38*, 5677.

(1368) Zickermann, V.; Verkhovsky, M.; Morgan, J.; Wikstroem, M.; Anemueller, S.; Bill, E.; Steffens, G. C. M.; Ludwig, B. *Eur. J. Biochem.* **1995**, *234*, 686.

(1369) Zhen, Y.; Schmidt, B.; Kang, U. G.; Antholine, W.; Ferguson-Miller, S. *Biochemistry* **2002**, *41*, 2288.

(1370) Wang, K.; Geren, L.; Zhen, Y.; Ma, L.; Ferguson-Miller, S.; Durham, B.; Millett, F. *Biochemistry* **2002**, *41*, 2298.

(1371) Slutter, C. E.; Gromov, I.; Epel, B.; Pecht, I.; Richards, J. H.; Goldfarb, D. *J. Am. Chem. Soc.* **2001**, *123*, 5325.

(1372) Fernandez, C. O.; Cricco, J. A.; Slutter, C. E.; Richards, J. H.; Gray, H. B.; Vila, A. J. *J. Am. Chem. Soc.* **2001**, *123*, 11678.

(1373) Blackburn, N. J.; Ralle, M.; Gomez, E.; Hill, M. G.; Pastuszyn, A.; Sanders, D.; Fee, J. A. *Biochemistry* **1999**, *38*, 7075.

(1374) Hwang, H. J.; Berry, S. M.; Nilges, M. J.; Lu, Y. *J. Am. Chem. Soc.* **2005**, *127*, 7274.

(1375) Ledesma, G. N.; Murgida, D. H.; Ly, H. K.; Wackerbarth, H.; Ulstrup, J.; Costa-Filho, A. J.; Vila, A. J. *J. Am. Chem. Soc.* **2007**, *129*, 11884.

(1376) Alvarez-Paggi, D.; Abriata, L. A.; Murgida, D. H.; Vila, A. J. *Chem. Commun.* **2013**, *49*, 5381.

(1377) Wang, X.; Berry, S. M.; Xia, Y.; Lu, Y. *J. Am. Chem. Soc.* **1999**, *121*, 7449.

(1378) Berry, S. M.; Wang, X.; Lu, Y. *J. Inorg. Biochem.* **2000**, *78*, 89.

(1379) Lukoyanov, D.; Berry, S. M.; Lu, Y.; Antholine, W. E.; Scholes, C. P. *Biophys. J.* **2002**, *82*, 2758.

(1380) Xie, X.; Gorelsky, S. I.; Sarangi, R.; Garner, D. K.; Hwang, H. J.; Hodgson, K. O.; Hedman, B.; Lu, Y.; Solomon, E. I. *J. Am. Chem. Soc.* **2008**, *130*, 5194.

(1381) Zickermann, V.; Wittershagen, A.; Kolbesen, B. O.; Ludwig, B. *Biochemistry* **1997**, *36*, 3232.
(1382) Charnock, J. M.; Dreusch, A.; Korner, H.; Neese, F.; Nelson, J.; Kannt, A.; Michel, H.; Garner, C. D.; Kroneck, P. M.; Zumft, W. G. *Eur. J. Biochem.* **2000**, *267*, 1368.
(1383) Hwang, H. J.; Nagraj, N.; Lu, Y. *Inorg. Chem.* **2006**, *45*, 102.
(1384) Savelieff, M. G.; Lu, Y. *Inorg. Chim. Acta* **2008**, *361*, 1087.
(1385) New, S. Y.; Marshall, N. M.; Hor, T. S. A.; Xue, F.; Lu, Y. *Chem. Commun.* **2012**, *48*, 4217.
(1386) Pan, L. P.; Hibdon, S.; Liu, R. Q.; Durham, B.; Millett, F. *Biochemistry* **1993**, *32*, 8492.
(1387) Farver, O.; Einarsdottir, O.; Pecht, I. *Eur. J. Biochem.* **2000**, *267*, 950.
(1388) Farver, O.; Lu, Y.; Ang, M. C.; Pecht, I. *Proc. Natl. Acad. Sci.* **1999**, *96*, 899.
(1389) Farver, O.; Hwang, H. J.; Lu, Y.; Pecht, I. *J. Phys. Chem. B* **2007**, *111*, 6690.
(1390) Hwang, H. J.; Lu, Y. *Proc. Natl. Acad. Sci. U. S. A.* **2004**, *101*, 12842.
(1391) Kim, B.-E.; Nevitt, T.; Thiele, D. J. *Nat. Chem. Biol.* **2008**, *4*, 176.
(1392) Leary, S. C.; Winge, D. R.; Cobine, P. A. *Biochim. Biophys. Acta, Mol. Cell Res.* **2009**, *1793*, 146.
(1393) Boal, A. K.; Rosenzweig, A. C. *Chem. Rev.* **2009**, *109*, 4760.
(1394) Banci, L.; Bertini, I.; Cantini, F.; Ciofi-Baffoni, S. *Cell. Mol. Life Sci.* **2010**, *67*, 2563.
(1395) Banci, L.; Bertini, I.; McGreevy, K. S.; Rosato, A. *Nat. Prod. Rep.* **2010**, *27*, 695.
(1396) Robinson, N. J.; Winge, D. R. *Annu. Rev. Biochem.* **2010**, *79*, 537.
(1397) Bertini, I.; Cavallaro, G.; McGreevy, K. S. *Coord. Chem. Rev.* **2010**, *254*, 506.
(1398) Banci, L.; Bertini, I.; Cavallaro, G.; Ciofi-Baffoni, S. *FEBS Journal* **2011**, *278*, 2244.
(1399) Richter, O. M. H.; Ludwig, B. *Rev. Physiol., Biochem. Pharmacol.* **2003**, *147*, 47.
(1400) Ostermeier, C.; Iwata, S.; Ludwig, B.; Michel, H. *Nat. Struct. Biol.* **1995**, *2*, 842.
(1401) Soulimane, T.; Buse, G.; Bourenkov, G. P.; Bartunik, H. D.; Huber, R.; Than, M. E. *EMBO J.* **2000**, *19*, 1766.
(1402) Zumft, W. G. *Microbiol. Mol. Biol. Rev.* **1997**, *61*, 533.
(1403) Zumft, W. G.; Kroneck, P. M. H. *Adv. Microb. Physiol.* **2007**, *52*, 107.
(1404) Wunsch, P.; Herb, M.; Wieland, H.; Schiek, U. M.; Zumft, W. G. *J. Bacteriol.* **2003**, *185*, 887.
(1405) Zumft, W. G. *J. Mol. Microbiol. Biotechnol.* **2005**, *10*, 154.
(1406) Wang, X.; Ang, M. C.; Lu, Y. *J. Am. Chem. Soc.* **1999**, *121*, 2947.
(1407) Cavallini, D.; De, M. C.; Dupre, S.; Rotilio, G. *Arch. Biochem. Biophys.* **1969**, *130*, 354.
(1408) Cavallini, D.; De, M. C.; Dupre, S. *Arch. Biochem. Biophys.* **1968**, *124*, 18.
(1409) Pecci, L.; Montefoschi, G.; Musci, G.; Cavallini, D. *Amino Acids* **1997**, *13*, 355.
(1410) Savelieff, M. G.; Wilson, T. D.; Elias, Y.; Nilges, M. J.; Garner, D. K.; Lu, Y. *Proc. Natl. Acad. Sci. U. S. A.* **2008**, *105*, 7919.
(1411) Wilson, T. D.; Savelieff, M. G.; Nilges, M. J.; Marshall, N. M.; Lu, Y. *J. Am. Chem. Soc.* **2011**, *133*, 20778.
(1412) Belle, C.; Rammal, W.; Pierre, J.-L. *J. Inorg. Biochem.* **2005**, *99*, 1929.
(1413) Harding, C.; McKee, V.; Nelson, J. *J. Am. Chem. Soc.* **1991**, *113*, 9684.
(1414) Barr, M. E.; Smith, P. H.; Antholine, W. E.; Spencer, B. *J. Chem. Soc., Chem. Commun.* **1993**, 1649.
(1415) Harding, C.; Nelson, J.; Symons, M. C. R.; Wyatt, J. *J. Chem. Soc., Chem. Commun.* **1994**, 2499.
(1416) Houser, R. P.; Young, V. G., Jr.; Tolman, W. B. *J. Am. Chem. Soc.* **1996**, *118*, 2101.
(1417) LeCloux, D. D.; Davydov, R.; Lippard, S. J. *J. Am. Chem. Soc.* **1998**, *120*, 6810.
(1418) Houser, R. P.; Tolman, W. B. *Inorg. Chem.* **1995**, *34*, 1632.

(1419) Miskowski, V. M.; Franzen, S.; Shreve, A. P.; Ondrias, M. R.; Wallace-Williams, S. E.; Barr, M. E.; Woodruff, W. H. *Inorg. Chem.* **1999**, *38*, 2546.

(1420) He, C.; Lippard, S. J. *Inorg. Chem.* **2000**, *39*, 5225.

(1421) Franzen, S.; Miskowski, V. M.; Shreve, A. P.; Wallace-Williams, S. E.; Woodruff, W. H.; Ondrias, M. R.; Barr, M. E.; Moore, L.; Boxer, S. G. *Inorg. Chem.* **2001**, *40*, 6375.

(1422) Gupta, R.; Zhang, Z. H.; Powell, D.; Hendrich, M. P.; Borovik, A. S. *Inorg. Chem.* **2002**, *41*, 5100.

(1423) Harkins, S. B.; Peters, J. C. *J. Am. Chem. Soc.* **2004**, *126*, 2885.

(1424) Zhao, Q.; Wang, X.; Liu, Y.; Fang, R. *Chem. Lett.* **2004**, *33*, 138.

(1425) Wen, Y.-H.; Cheng, J.-K.; Zhang, J.; Li, Z.-J.; Kang, Y.; Yao, Y.-G. *Inorg. Chem. Commun.* **2004**, *7*, 1120.

(1426) Patel, D. V.; Mihalcik, D. J.; Kreisel, K. A.; Yap, G. P. A.; Zakharov, L. N.; Kassel, W. S.; Rheingold, A. L.; Rabinovich, D. *Dalton Trans.* **2005**, 2410.

(1427) Feng, Y.; Han, Z.; Peng, J.; Hao, X. *J. Mol. Struct.* **2005**, *734*, 171.

(1428) Jiang, X.; Bollinger, J. C.; Baik, M.-H.; Lee, D. *Chem. Commun.* **2005**, 1043.

(1429) Gennari, M.; Pécaut, J.; DeBeer, S.; Neese, F.; Collomb, M.-N.; Duboc, C. *Angew. Chem., Int. Ed.* **2011**, *50*, 5662.

(1430) Li, H.; Webb, S. P.; Ivanic, J.; Jensen, J. H. *J. Am. Chem. Soc.* **2004**, *126*, 8010.

(1431) Garcia-Horsman, J. A.; Barquera, B.; Rumbley, J.; Ma, J.; Gennis, R. B. *J. Bacteriol.* **1994**, *176*, 5587.

(1432) Pereira, M. M.; Santana, M.; Teixeira, M. *Biochim. Biophys. Acta, Bioenerg.* **2001**, *1505*, 185.

(1433) Capaldi, R. A. *Annu. Rev. Biochem.* **1990**, *59*, 569.

(1434) Ferguson-Miller, S.; Brautigan, D.; Margoliash, E. *J. Biol. Chem.* **1978**, *253*, 149.

(1435) Berry, E. A.; Trumpower, B. L. *J. Biol. Chem.* **1985**, *260*, 2458.

(1436) Fergusonmiller, S.; Brautigan, D. L.; Margoliash, E. *J. Biol. Chem.* **1976**, *251*, 1104.

(1437) Fee, J. A.; Kuila, D.; Mather, M. W.; Yoshida, T. *Biochim. Biophys. Acta* **1986**, *853*, 153.

(1438) Sone, N.; Yokoi, F.; Fu, T.; Ohta, S.; Metso, T.; Raitio, M.; Saraste, M. *J. Biochem.* **1988**, *103*, 606.

(1439) Capaldi, R. A.; Darleyusmar, V.; Fuller, S.; Millett, F. *FEBS Lett.* **1982**, *138*, 1.

(1440) Rieder, R.; Bosshard, H. R. *J. Biol. Chem.* **1980**, *255*, 4732.

(1441) Staudenmayer, N.; Ng, S.; Smith, M. B.; Millett, F. *Biochemistry* **1977**, *16*, 600.

(1442) Osheroff, N.; Borden, D.; Koppenol, W. H.; Margoliash, E. *J. Biol. Chem.* **1980**, *255*, 1689.

(1443) Speck, S. H.; Dye, D.; Margoliash, E. *Proc. Natl. Acad. Sci. U. S. A. Biol. Sci.* **1984**, *81*, 347.

(1444) Antalis, T. M.; Palmer, G. *J. Biol. Chem.* **1982**, *257*, 6194.

(1445) Greenwood, C.; Brittain, T.; Wilson, M.; Brunori, M. *Biochem. J.* **1976**, *157*, 591.

(1446) Veerman, E. C. I.; Wilms, J.; Casteleijn, G.; Vangelder, B. F. *Biochim. Biophys. Acta* **1980**, *590*, 117.

(1447) Sarti, P.; Antonini, G.; Malatesta, F.; Vallone, B.; Brunori, M. *Ann. N. Y. Acad. Sci.* **1988**, *550*, 161.

(1448) Wilson, M. T.; Peterson, J.; Antonini, E.; Brunori, M.; Colosimo, A.; Wyman, J. *Proc. Natl. Acad. Sci. U. S. A. Biol. Sci.* **1981**, *78*, 7115.

(1449) Nilsson, T.; Copeland, R. A.; Smith, P. A.; Chan, S. I. *Biochemistry* **1988**, *27*, 8254.

(1450) Nilsson, T.; Gelles, J.; Li, P. M.; Chan, S. I. *Biochemistry* **1988**, *27*, 296.

(1451) Kornblatt, J. A.; Luu, H. A. *Eur. J. Biochem.* **1986**, *159*, 407.

(1452) Michel, B.; Bosshard, H. R. *J. Biol. Chem.* **1984**, *259*, 85.

(1453) Copeland, R. A.; Smith, P. A.; Chan, S. I. *Biochemistry* **1987**, *26*, 7311.

(1454) Jensen, P.; Wilson, M. T.; Aasa, R.; Malmstrom, B. G. *Biochem. J.* **1984**, *224*, 829.

(1455) Jones, M. G.; Bickar, D.; Wilson, M. T.; Brunori, M.; Colosimo, A.; Sarti, P. *Biochem. J.* **1984**, *220*, 57.

(1456) Scholes, C. P.; Malmstrom, B. G. *FEBS Lett.* **1986**, *198*, 125.

(1457) Galinato, M. G. I.; Kleingardner, J. G.; Bowman, S. E. J.; Alp, E. E.; Zhao, J.; Bren, K. L.; Lehnert, N. *Proc. Natl. Acad. Sci. U. S. A.* **2012**, *109*, 8896.

(1458) Sakamoto, K.; Kamiya, M.; Imai, M.; Shinzawa-Itoh, K.; Uchida, T.; Kawano, K.; Yoshikawa, S.; Ishimori, K. *Proc. Natl. Acad. Sci. U. S. A.* **2011**, *108*, 12271.

(1459) Rasmussen, T.; Berks, B. C.; Sanders-Loehr, J.; Dooley, D. M.; Zumft, W. G.; Thomson, A. J. *Biochemistry* **2000**, *39*, 12753.

(1460) Simon, J. r.; Einsle, O.; Kroneck, P. M.; Zumft, W. G. *FEBS Lett.* **2004**, *569*, 7.

(1461) Crofts, A. R. *Annu. Rev. Physiol.* **2004**, *66*, 689.

(1462) Hunte, C.; Koepke, J.; Lange, C.; Rossmanith, T.; Michel, H. *Structure* **2000**, *8*, 669.

(1463) Xia, D.; Yu, C. A.; Kim, H.; Xian, J. Z.; Kachurin, A. M.; Zhang, L.; Yu, L.; Deisenhofer, J. *Science* **1997**, *277*, 60.

(1464) Hunter, C. N.; Daldal, F. *The Purple Phototrophic Bacteria*; Springer: Dordrecht, The Netherlands, 2009.

(1465) Kokhan, O.; Wraight, C. A.; Tajkhorshid, E. *Biophys. J.* **2010**, *99*, 2647.

(1466) Koppenol, W. H.; Rush, J. D.; Mills, J. D.; Margoliash, E. *Mol. Biol. Evol.* **1991**, *8*, 545.

(1467) Tiede, D. M.; Vashishta, A. C.; Gunner, M. R. *Biochemistry* **1993**, *32*, 4515.

(1468) Sarewicz, M.; Borek, A.; Daldal, F.; Froncisz, W.; Osyczka, A. *J. Biol. Chem.* **2008**, *283*, 24826.

(1469) Sarewicz, M.; Szytula, S.; Dutka, M.; Osyczka, A.; Froncisz, W. *Eur. Biophys. J. Biophys. Lett.* **2008**, *37*, 483.

(1470) Sarewicz, M.; Pietras, R.; Froncisz, W.; Osyczka, A. *Metallomics* **2011**, *3*, 404.

(1471) Sadoski, R. C.; Engstrom, G.; Tian, H.; Zhang, L.; Yu, C.-A.; Yu, L.; Durham, B.; Millett, F. *Biochemistry* **2000**, *39*, 4231.

(1472) Gurung, B.; Yu, L.; Xia, D.; Yu, C.-A. *J. Biol. Chem.* **2005**, *280*, 24895.

(1473) Cramer, W. A.; Soriano, G. M.; Ponomarev, M.; Huang, D.; Zhang, H.; Martinez, S. E.; Smith, J. L. *Annu. Rev. Plant Physiol. Plant Mol. Biol.* **1996**, *47*, 477.

(1474) Kallas, T. *Photosynthesis: Plastid Biology, Energy Conversion and Carbon Assimilation, Advances in Photosynthesis and Respiration.*, 2012; Vol. 34.

(1475) Baniulis, D.; Yamashita, E.; Zhang, H.; Hasan, S. S.; Cramer, W. A. *Photochem. Photobiol.* **2008**, *84*, 1349.

(1476) Cramer, W. A.; Yamashita, E.; Baniulis, D.; Hassan, S. S. In *Handbook of Metalloproteins,*; Messerschmidt, A., Ed.; John Wiley: Chichester, 2011.

(1477) Kallas, T. In *Photosynthesis: Plastid Biology, Energy Conversion and Carbon Assimilation*; Eaton-Rye, J. J., Tripathy, B. C., Sharkey, T. D., Eds.; Springer: London, 2012; Vol. 34, p 501.

(1478) Baniulis, D.; Yamashita, E.; Whitelegge, J. P.; Zatsman, A. I.; Hendrich, M. P.; Hasan, S. S.; Ryan, C. M.; Cramer, W. A.; *J. Biol. Chem.* **2009**, *284*, 9861.

(1479) Kurisu, G.; Zhang, H.; Smith, J. L.; Cramer, W. A. *Science* **2003**, *302*, 1009.

(1480) Yamashita, E.; Zhang, H.; Cramer, W. *J. Mol. Biol.* **2007**, *370*, 39.

(1481) Yan, J.; Kurisu, G.; Cramer, W. A. *Proc. Natl. Acad. Sci. U. S. A.* **2006**, *103*, 69.

(1482) Crofts, A. R.; Meinhardt, S.; Jones, K. R.; Snozzi, M. *Biochim. Biophys. Acta, Bioenerg.* **1983**, *723*, 202.

(1483) Mitchell, P. *J. Theor. Biol.* **1976**, *62*, 327.

(1484) Carrell, C. J.; Schlarb, B. G.; Bendall, D. S.; Howe, C. J.; Cramer, W. A.; Smith, J. L. *Biochemistry* **1999**, *38*, 9590.

(1485) Martinez, S. E.; Huang, D.; Ponomarev, M.; Cramer, W. A.; Smith, J. L. *Protein Sci.* **1996**, *5*, 1081.

(1486) Ponamarev, M. V.; Cramer, W. A. *Biochemistry* **1998**, *37*, 17199.

(1487) Williamson, D. A.; Benson, D. R. *Chem. Commun.* **1998**, *0*, 961.

(1488) Kennedy, M. L.; Silchenko, S.; Houndonougbo, N.; Gibney, B. R.; Dutton, P. L.; Rodgers, K. R.; Benson, D. R. *J. Am. Chem. Soc.* **2001**, *123*, 4635.

(1489) De, V., Catherine; Ouyang, Y.; Finazzi, G.; Wollman, F.-A.; Kallas, T. *J. Biol. Chem.* **2004**, *279*, 44621.

(1490) Jormakka, M.; Byrne, B.; Iwata, S. *Curr. Opin. Struct. Biol.* **2003**, *13*, 418.

(1491) Boyington, J. C.; Gladyshev, V. N.; Khangulov, S. V.; Stadtman, T. C.; Sun, P. D. *Science* **1997**, *275*, 1305.

(1492) Jormakka, M.; Tornroth, S.; Byrne, B.; Iwata, S. *Science* **2002**, *295*, 1863.

(1493) Raaijmakers, H.; Macieira, S.; Dias, J. M.; Teixeira, S.; Bursakov, S.; Huber, R.; Moura, J. J. G.; Moura, I.; Romao, M. J. *Structure (Cambridge, MA, U. S.)* **2002**, *10*, 1261.

(1494) Berks, B. C.; Page, M. D.; Richardson, D. J.; Reilly, A.; Cavil, A.; Outen, F.; Ferguson, S. J. *Mol. Microbiol.* **1995**, *15*, 319.

(1495) Costa, C.; Teixeira, M.; LeGall, J.; Moura, J. J. G.; Moura, I. *JBIC, J. Biol. Inorg. Chem.* **1997**, *2*, 198.

(1496) Almendra, M. J.; Gavel, O.; Duarte, R. O.; Caldeira, J.; Bursakov, S. A.; Costa, C.; Moura, I.; Moura, J. J. G. *J. Inorg. Biochem.* **1997**, *67*, 16.

(1497) Jormakka, M.; Richardson, D.; Byrne, B.; Iwata, S. *Structure (Cambridge, MA, U. S.)* **2004**, *12*, 95.

(1498) Bertero, M. G.; Rothery, R. A.; Palak, M.; Hou, C.; Lim, D.; Blasco, F.; Weiner, J. H.; Strynadka, N. C. J. *Nat. Struct. Biol.* **2003**, *10*, 681.

(1499) Arnoux, P.; Sabaty, M.; Alric, J.; Frangioni, B.; Guigliarelli, B.; Adriano, J.-M.; Pignol, D. *Nat. Struct. Biol.* **2003**, *10*, 928.

(1500) Dias, J.; Than, M.; Humm, A.; Bourenkov, G. P.; Bartunik, H. D.; Bursakov, S.; Calvete, J.; Caldeira, J.; Carneiro, C.; Moura, J. J.; Moura, I.; Romao, M. J. *Structure (London, U. K.)* **1999**, *7*, 65.

(1501) Najmudin, S.; Gonzalez, P. J.; Trincao, J.; Coelho, C.; Mukhopadhyay, A.; Cerqueira, N. M. F. S. A.; Romao, C. C.; Moura, I.; Moura, J. J. G.; Brondino, C. D.; Romao, M. J. *JBIC, J. Biol. Inorg. Chem.* **2008**, *13*, 737.

(1502) Jepson, B. J. N.; Mohan, S.; Clarke, T. A.; Gates, A. J.; Cole, J. A.; Butler, C. S.; Butt, J. N.; Hemmings, A. M.; Richardson, D. J. *J. Biol. Chem.* **2007**, *282*, 6425.

(1503) Schindelin, H.; Kisker, C.; Hilton, J.; Rajagopalan, K. V.; Rees, D. C. *Science* **1996**, *272*, 1615.

(1504) Coelho, C.; Gonzalez, P. J.; Moura, J. G.; Moura, I.; Trincao, J.; Romao, M. J. *J. Mol. Biol.* **2011**, *408*, 932.

(1505) Gonzalez, P. J.; Correia, C.; Moura, I.; Brondino, C. D.; Moura, J. J. G. *J. Inorg. Biochem.* **2006**, *100*, 1015.

(1506) Dauter, Z.; Wilson, K. S.; Sieker, L. C.; Meyer, J.; Moulis, J. M. *Biochemistry* **1997**, *36*, 16065.

(1507) Van de Kamp, M.; Floris, R.; Hali, F. C.; Canters, G. W. *J. Am. Chem. Soc.* **1990**, *112*, 907.

(1508) Berghuis, A. M.; Brayer, G. D. *J. Mol. Biol.* **1992**, *223*, 959.